THE UNIVERSITY OF
WARWICK

Library Declaration and Deposit Agreement

1. STUDENT DETAILS

Please complete the following:

Full name: JACOPO BAGLIERI

University ID number: 0867707

2. THESIS DEPOSIT

2.1 I understand that under my registration at the University, I am required to deposit my thesis with the University in BOTH hard copy and in digital format. The digital version should normally be saved as a single pdf file.

2.2 The hard copy will be housed in the University Library. The digital version will be deposited in the University's Institutional Repository (WRAP). Unless otherwise indicated (see 2.3 below) this will be made openly accessible on the Internet and will be supplied to the British Library to be made available online via its Electronic Theses Online Service (EThOS) service.
[At present, theses submitted for a Master's degree by Research (MA, MSc, LLM, MS or MMedSci) are not being deposited in WRAP and not being made available via EthOS. This may change in future.]

2.3 In exceptional circumstances, the Chair of the Board of Graduate Studies may grant permission for an embargo to be placed on public access to the hard copy thesis for a limited period. It is also possible to apply separately for an embargo on the digital version. (Further information is available in the *Guide to Examinations for Higher Degrees by Research.*)

2.4 *If you are depositing a thesis for a Master's degree by Research, please complete section (a) below. For all other research degrees, please complete both sections (a) and (b) below:*

(a) Hard Copy

I hereby deposit a hard copy of my thesis in the University Library to be made publicly available to readers (please delete as appropriate) [redacted] immediately OR after an embargo period of ..... months/years as agreed by the Chair of the Board of Graduate Studies.

I agree that my thesis may be photocopied. YES / [redacted] *(Please delete as appropriate)*

(b) Digital Copy

I hereby deposit a digital copy of my thesis to be held in WRAP and made available via EThOS.

Please choose one of the following options:

EITHER My thesis can be made publicly available online. YES / [redacted] *(Please delete as appropriate)*

OR My thesis can be made publicly available only after.....[date] (Please give date)
YES / NO *(Please delete as appropriate)*

OR My full thesis cannot be made publicly available online but I am submitting a separately identified additional, abridged version that can be made available online.
YES / NO *(Please delete as appropriate)*

OR My thesis cannot be made publicly available online. YES / NO *(Please delete as appropriate)*

3. GRANTING OF NON-EXCLUSIVE RIGHTS

Whether I deposit my Work personally or through an assistant or other agent, I agree to the following:

Rights granted to the University of Warwick and the British Library and the user of the thesis through this agreement are non-exclusive. I retain all rights in the thesis in its present version or future versions. I agree that the institutional repository administrators and the British Library or their agents may, without changing content, digitise and migrate the thesis to any medium or format for the purpose of future preservation and accessibility.

4. DECLARATIONS

(a) I DECLARE THAT:

- I am the author and owner of the copyright in the thesis and/or I have the authority of the authors and owners of the copyright in the thesis to make this agreement. Reproduction of any part of this thesis for teaching or in academic or other forms of publication is subject to the normal limitations on the use of copyrighted materials and to the proper and full acknowledgement of its source.
- The digital version of the thesis I am supplying is the same version as the final, hard-bound copy submitted in completion of my degree, once any minor corrections have been completed.
- I have exercised reasonable care to ensure that the thesis is original, and does not to the best of my knowledge break any UK law or other Intellectual Property Right, or contain any confidential material.
- I understand that, through the medium of the Internet, files will be available to automated agents, and may be searched and copied by, for example, text mining and plagiarism detection software.

(b) IF I HAVE AGREED (in Section 2 above) TO MAKE MY THESIS PUBLICLY AVAILABLE DIGITALLY, I ALSO DECLARE THAT:

- I grant the University of Warwick and the British Library a licence to make available on the Internet the thesis in digitised format through the Institutional Repository and through the British Library via the EThOS service.
- If my thesis does include any substantial subsidiary material owned by third-party copyright holders, I have sought and obtained permission to include it in any version of my thesis available in digital format and that this permission encompasses the rights that I have granted to the University of Warwick and to the British Library.

5. LEGAL INFRINGEMENTS

I understand that neither the University of Warwick nor the British Library have any obligation to take legal action on behalf of myself, or other rights holders, in the event of infringement of intellectual property rights, breach of contract or of any other right, in the thesis.

Please sign this agreement and return it to the Graduate School Office when you submit your thesis.

Student's signature:  Date: 22/07/2012

Assembly and Mechanism of Bacterial Twin-arginine Translocation Systems

Jacopo Baglieri

A thesis submitted for the degree of Doctor of Philosophy

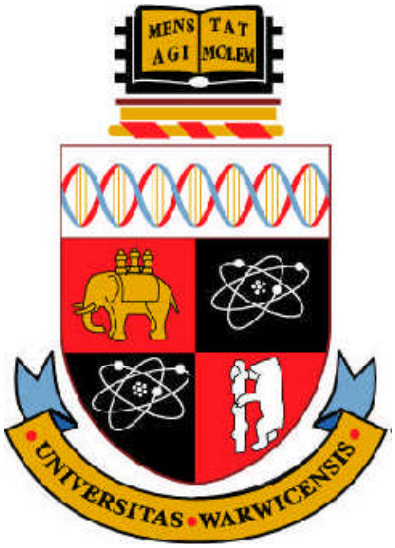

University of Warwick

School of Life Sciences

July 2012

Table of contents

Table of contents	**i**
List of figures	**viii**
List of tables	**xi**
Acknowledgements	**xii**
Declaration	**xiii**
Summary	**xiv**
List of abbreviations	**xv**
List of amino acids	**xvi**

Chapter 1 Introduction: Protein translocation in bacteria **1**

1.1 Bacterial protein translocation 2

1.2 The General Secretory (Sec) pathway 4

1.2.1 The Sec pathway in bacteria 4

1.2.2 The Sec pathway in chloroplasts 7

1.3 The Signal Recognition Particle (SRP) 9

1.4 The Twin-arginine translocation (Tat) pathway 11

1.4.1 The role of the Tat pathway 12

1.4.2 The Tat signal peptides 15

1.4.3 Proofreading and quality control of Tat substrates 17

1.4.4 The Tat pathway components 18

1.4.5 The TatE subunit 23

1.4.6 Tat complexes organization 24

1.4.7 The Tat pathway mechanism of translocation 26

1.4.8 The Tat pathway in Gram-positive bacteria 28

1.4.9 The Tat pathway in chloroplasts 29

1.5 Aims and objectives of this study 31

Chapter 2 Materials and Methods 33

2.1 Suppliers of materials 34

2.2 Growth and storage of *E. coli* cultures 36

2.2.1 Strains of *E. coli* used 36

2.2.2 Standard growth conditions 36

2.2.3 Antibiotic supplements 37

2.2.4 Storage of *E. coli* cells 37

2.3 Preparation and transformation of competent cells 37

2.3.1 Preparation of competent *E. coli* cells 37

2.3.2 Preparation of plasmid DNA from *E. coli* cells 37

2.3.3 Transformation of competent *E. coli* cells with plasmid DNA 38

2.3.4 Bacterial plasmids used in this work 38

2.3.5 Affinity tag used 39

2.4 DNA manipulation and cloning techniques 39

2.4.1 Preparation of Genome DNA from *E. coli* cells 39

2.4.2 Primers used for the construct generated 39

2.4.3 Site-directed *in vitro* mutagenesis of plasmid DNA 40

2.4.4 Primers used for the mutagenesis of *tatA-strep* 40

2.4.5 PCR 41

2.4.6 Agarose gel electrophoresis 41

2.4.7 Purification of DNA by gel extraction 41

2.4.8 Restriction endonuclease digestion of DNA 42

2.4.9 Ligation of DNA fragments 42

2.4.10 Determination of DNA concentration 42

2.4.11 Sequencing of plasmid DNA 42

2.4.12 Sequencing primers used in this study 43

2.5 Protein preparation 43

2.5.1 Induction of plasmids 43

2.5.2 Fractionation of *E. coli* cells 44

2.5.3 Isolation and solubilisation of *E. coli* membranes for protein purification and gel filtration chromatography 44

2.6 Protein chromatography methods 45

2.6.1 Q-Sepharose anion exchange chromatography 45

2.6.2 Streptactin™-Sepharose affinity chromatography 45

2.6.3 Superdex™-200 gel filtration chromatography 46

2.6.4 Gel filtration chromatography: estimation of mass of protein complexes 46

2.6.5 Determining the concentration of purified proteins 47

2.7 Protein electrophoresis 47

2.7.1 SDS polyacrylamide gel electrophoresis (SDS-PAGE) 47

2.7.2 Native gel electrophoresis (N-PAGE) 47

2.7.3 Blue-native polyacrylamide gel electrophoresis (BN-PAGE) 48

2.8 Protein detection 49

2.8.1 Protein detection by Western blotting 49

2.8.2 Detection of proteins by immunoblotting 49

2.8.3 Silver staining 51

2.8.4 TMAO reductase (TorA) activity assays 51

2.9 Confocal microscopy 52

2.10 Triton X-114 to separate membrane and soluble proteins 52

2.11 Trichloroacetic acid (TCA) precipitation 53

2.12 Protease accessibility experiments 53

2.13 Co-immunoprecipitation experiments 53

2.14 Single-particle electron microscopy 54

2.15 Specialist software used in this study 54

Chapter 3 Purification and characterization of *Escherichia coli* TatE complexes 56

3.1 Introduction 57

3.2 Results 60

3.2.1 Translocation of TMAO reductase by overexpressed TatE 60

3.2.2 Translocation of the cell wall amidases AmiA and AmiC by overexpressed TatE 61

3.2.3 Anion exchange and affinity chromatography of TatE complexes 62

3.2.4 Anion exchange and affinity chromatography of TatA complexes 64

3.2.5 Gel filtration chromatography of TatE and TatA complexes 64

3.2.6 Gel filtration chromatography of TatE complexes using different detergents 67

3.2.7 Blue-native polyacrylamide gel electrophoresis (BN-PAGE) of purified TatE complexes 69

3.2.8 Blue-native polyacrylamide gel electrophoresis of solubilised membranes expressing TatE 70

3.2.9 Electron microscopy of TatE complexes 71

3.2.10 Topological orientation of TatE 74

3.3 Discussion 77

Chapter 4 Characterization of soluble TatE and TatA complexes 81

4.1 Introduction 82

4.2 Results 84

4.2.1 Purification of TatE complexes from cytosolic fractions 84

4.2.2 Purification of TatA complexes from cytosolic fractions 86

4.2.3 Separation of TatE and TatA proteins into soluble and insoluble fractions using the detergent Triton X-114 87

4.2.4 Blue-native polyacrylamide gel electrophoresis (BN-PAGE) of cytosolic TatE and TatA complexes 90

4.3 Discussion 92

Chapter 5 Study of the TatE subunit interactions with the other Tat components 94

5.1 Introduction 95

5.2 Results 97

5.2.1 Influence of the TatABC subunits on TatE stability in *E. coli* 97

5.2.2 TatE is not stable in *ΔtatABCDE* cells 98

5.2.3 TatE does not appear to interact with the TatB and TatC subunits 99

5.2.4 Study of the interaction between the TatE and TatA subunits 102

5.2.5 Blue-native polyacrylamide gel electrophoresis (BN-PAGE) of TatAE mixed complexes 105

5.3 Discussion 107

Chapter 6 The TatAc protein of *Bacillus subtilis* forms active Tat systems with TatCd and TatCy 110

6.1 Introduction 111

6.2 Results 115

6.2.1 TMAO reductase translocation by *B. subtilis* TatAc in *E. coli* strains 115

6.2.2 Translocation of ssDmsA-GFP, ssAmiA-GFP and ssMdoD-GFP in *ΔtatAE* cells expressing TatAc 117

6.2.3 Blue-native polyacrylamide gel electrophoresis (BN-PAGE) of TatAc complex 120

6.2.4 Translocation of TMAO reductase by TatAcCd and TatAcCy mixed translocases 121

6.2.5 Translocation of the cell wall amidases, AmiA and AmiC by TatAcCd and TatAcCy 123

6.2.6 Blue-native polyacrylamide gel electrophoresis (BN-PAGE) of TatAcCd and TatAcCy complexes 125

6.2.7 Affinity and gel filtration chromatography of TatAc, TatAcCd and TatAcCy complexes 126

6.3 Discussion 130

Chapter 7 Final Discussion **134**

7.1 An alternative model of Tat-dependent transport in *E. coli* 136

7.2 TatE is present in the cytoplasm and forms TatAE mixed complexes in the membrane 138

7.3 The *B. subtilis* TatAcCd and TatAcCy mixed translocases are active in *E. coli* 141

Chapter 8 References **143**

Appendix A. Co-immunoprecipitation images **165**

Appendix B. Published work **167**

List of figures

Figure 1.1 Schematics of Gram-negative, Gram-positive and cyanobacteria cells 3

Figure 1.2 Protein translocation by the *E. coli* Sec pathway 7

Figure 1.3 Overview of membrane protein insertion directed by bacterial SRP 11

Figure 1.4.1 The Tat signal peptide 17

Figure 1.4.2 Chromosomal organisation of the *tat* genes in *E. coli* 19

Figure 1.4.3 Predicted structure and topological arrangement of the *E. coli* Tat components 23

Figure 1.4.4 Proposed mechanism of Tat translocation in *E. coli* 29

Figure 3.1.1 Predicted secondary structure elements of the *E. coli* TatE (A) and TatA protein (B) 58

Figure 3.1.2 Sequence alignment of *E. coli* TatE and TatA 59

Figure 3.2.1 Translocation of TMAO reductase by overexpressed TatE 61

Figure 3.2.2 Overexpressed TatE can complement the filamentous phenotype of *E. coli ΔtatAE* cells 62

Figure 3.2.3 Anion exchange and affinity chromatography of TatE complexes 63

Figure 3.2.4 Anion exchange and affinity chromatography of TatA complexes 64

Figure 3.2.5 Gel filtration chromatography of TatE and TatA complexes 66

Figure 3.2.6 Gel filtration chromatography of TatE in different detergents 68

Figure 3.2.7 BN-PAGE of purified TatE and TatA complexes 70

Figure 3.2.8 BN-PAGE of TatE and TatABC complexes 71

Figure 3.2.9 Micrographs of class averages of TatE complexes 72

Figure 3.2.10 Three-dimensional density maps of TatE complex assemblies 73

Figure 3.2.11 Micrographs of multi-ringed TatE complex structures 74

Figure 3.2.12 Topological organization of TatE probed by protease accessibility assay 76

Figure 3.3 Alternative models for Tat-dependent translocation 80

Figure 4.2.1 Purification of TatE complexes from the cytoplasm 85

Figure 4.2.2 Localization of *E. coli* TatC 86

Figure 4.2.3 Purification of TatA complexes from the cytoplasm 87

Figure 4.2.4 Separation of a membrane protein using Triton X-114 88

Figure 4.2.5 Determination of cytosolic TatE and TatA solubility by Triton X-114 phase separation 89

Figure 4.2.6 BN-PAGE of cytosolic TatE and TatA complexes 91

Figure 5.2.1 Expression and stability of TatE proteins in different backgrounds 97

Figure 5.2.2 TatE time course experiment in *E. coli ΔtatAE* and *ΔtatABCDE* cells 99

Figure 5.2.3 Co-immunoprecipitation experiments 101

Figure 5.2.4 Traslocation of TMAO reductase by simultaneous overexpression of TatE and TatA 103

Figure 5.2.5 Co-purification of TatE and TatA by affinity chromatography 104

Figure 5.2.6 BN-PAGE of TatAE mixed complexes 106

Figure 6.1 Sequence alignment of *B. subtilis* TatAd, TatAy and TatAc 114

Figure 6.2.1 Traslocation of TMAO reductase by expression of *B. subtilis* TatAc in *E. coli* strain 116

Figure 6.2.2 Translocation of DmsA-GFP, AmiA-GFP and MdoD-GFP in *ΔtatAE* cells expressing TatAc 119

Figure 6.2.3 BN-PAGE of TatAc complexes 121

Figure 6.2.4 Traslocation of TMAO reductase by expression of *B. subtilis* TatAcCd and TatAcCy in *E. coli* 123

Figure 6.2.5 *B. subtilis* TatAcCd and TatAcCy facilitate AmiA and AmiC export in *E. coli* 124

Figure 6.2.6 BN-PAGE of TatAcCd and TatAcCy complexes 126

Figure 6.2.7 Affinity chromatography of *B. subtilis* TatAc, TatAcCd and TatAcCy 127

Figure 6.2.8 Gel filtration chromatography of *B. subtilis* TatAc, TatAcCd and TatAcCy complexes 129

List of tables

Table 2.2.1	Strains of *E. coli* used in this work	36
Table 2.3.4	List of plasmids used in this work	38
Table 2.4.2	DNA primers used for the preparation of the pBAD-E-Strep construct	40
Table 2.4.4	DNA primers used for site-directed mutagenesis of pBAD-A-Strep	40
Table 2.4.12	Sequencing primers used in this study	43
Table 2.8.2	Antibodies used for immunodetection	50

Acknowledgements

I would like to thank Professor Colin Robinson for giving me the opportunity to carry out the work presented in this thesis, and also for supervision and guidance throughout my research and in the preparation of this manuscript.

I am immensely grateful to Dr. James Barnett for invaluable discussions as well as critical reading of this manuscript.

I would like to thank Professor Jan Maarten van Dijl and Carmine Monteferrante for the gift of constructs for the overexpression of the *B. subtilis* Tat proteins, without which part of this work would not have been possible.

I would also like to thank Professor Gunner von Heijne for the gift of the leader peptidase expression plasmid and of the anti-leader peptidase antiserum.

Many thanks go to Daniel Beck and Professor Corinne Smith for providing the single particle images and the three-dimensional models presented in chapter 3.

I would like to thank all past and present members of the Robinson's Lab for all the help, advice and encouragement during the course of this work. In particular I thank Anna Albiniak (precious advices on confocal microscopy work, chapter 3), Nishi Vasisht, Daniel Beck, Roshani Patel and Dr. Cristina Matos.

At last, I am particularly thankful to my parents for their support and love throughout my life and for always being fully behind me in whatever I have chosen to do.

Declaration

The work presented in this thesis is original, and was conducted by the author, unless otherwise stated, under the supervision of Professor Colin Robinson (University of Warwick).

None of the work presented in this thesis has been submitted previously for another degree.

This research was funded by the CEU Transys ITN (Marie Curie Initial Training Network, Project: 215524).

Single-particle electron microscopy was performed by Daniel Beck (University of Warwick).

Carmine Monteferrante, University of Groningen, performed work contributing to chapter 6.

Several of the plasmid constructs used in this study were provided by others as indicated in the text.

Part of this work has been published in the following journal articles:

Baglieri, J., Beck, D., Vasisht, N., Smith, C. J. and Robinson, C. (2012). Structure of TatA paralog, TatE, suggests a structurally homogeneous form of Tat protein translocase that transports folded proteins of differing diameter. *J. Biol. Chem.* **287**, 7335-7344.

Monteferrante, C. G., Baglieri, J., Robinson, C. and van Dijl, J. M. (2012). The third TatA subunit TatAc of *Bacillus subtilis* can form active twin-arginine translocases with the TatCd and TatCy subunits. *Appl. Environ. Microbiol*. **78**, 4999-5001.

Albiniak, A. M., Baglieri, J. and Robinson, C. (2012). Targeting of lumenal proteins across the thylakoid membrane. *J. Exp. Bot.* **63**, 1689-1698.

Summary

The bacterial twin-arginine translocation (Tat) pathway is able to export pre-folded cofactor containing proteins across the cytoplasmic membrane. Tat substrates bear cleavable N-terminal signal peptides that are characterized by the presence of a critical and highly conserved twin-arginine motif which lends the Tat pathway its name.

In *Escherichia coli* and many other Gram-negative bacteria, three integral membrane proteins: TatA, TatB and TatC are essential for Tat-dependent translocation. In contrast *Bacillus subtilis* possesses a simpler TatAC system which lacks the TatB component. In *E. coli* the TatA protein assembles into homo-oligomeric complexes that vary considerably in size. The TatA proteins found in *B. subtilis* do not exhibit the same degree of heterogeneity and this suggested mechanistic differences between the Tat pathways of Gram-negative and Gram-positive bacteria. How the Tat system works is still poorly understood, and the work presented in this thesis sought to gain insights into the assembly and mechanism of *E. coli* and *B. subtilis* Tat pathways. This work focused on the study of two previously uncharacterized components: the *E. coli* TatA paralog TatE subunit and *B. subtilis* TatAc subunit.

In this thesis the purification and characterization of *E. coli* TatE complexes is reported. Using analytical gel filtration chromatography, blue-native gel-electrophoresis (BN-PAGE) and single-particle analysis of purified TatE complexes, it was found that the TatE complexes are more discrete than the highly heterogeneous TatA complexes. This finding, together with the ability of TatE to support the translocation of the 90-kDa TorA protein, suggested alternative translocation models in which single TatE complexes do not contribute the bulk of the translocation channel, similar to the *B. subtilis* model.

In addition, co-purification and BN-PAGE experiments demonstrated for the first time that TatE interacts with TatA to form TatAE mixed complexes in the membrane, and reveals a completely novel form of Tat complex that might be functionally significant.

A soluble population of TatE was also identified in *E. coli* cell extracts, and phase separation experiments using Triton X-114 suggested it may be mis-localized.

In a separate set of studies, the ability of the *B. subtilis* TatAc protein to form active translocases in combination with the *B. subtilis* TatCd or TatCy proteins was investigated for the first time. The TatAcCd and TatAcCy mixed translocases were able to translocate several *E. coli* Tat substrates including, TorA, AmiA and AmiC. Finally BN-PAGE and gel filtration chromatography showed that the TatAcCd and TatAcCy complexes were significantly smaller than the previously described *E. coli* TatABC substrate-binding complex.

List of abbreviations

AmiA	N-acetylmuramoyl-L-alanine amidase A
AmiC	N-acetylmuramoyl-L-alanine amidase C
APH	Amphipathic Helix
APS	Ammonium persulphate
ATP	Adenosine 5′- triphosphate
BN-PAGE	Blue-native PAGE
BSA	Bovine serum albumin
C-	Carboxy terminus
C	Cytoplasmic fraction
DDM	*n*-Dodecyl-*ß*-D-maltoside
DHFR	Dihydrofolate reductase
dH_2O	Distilled water
DMSO	Dimethyl sulphoxide
DmsA	Dimethyl sulphoxide reductase
dNTP	Deoxynucleotide 5′- triphosphate
E	Elution fraction
ECL™	Chemiluminescence
EDTA	Ethylenediaminetetraacetic acid
EM	Electron microscopy
FeS	Iron-sulfur
FT	Flow through fraction
GFP	Green fluorescent protein
GTP	Guanidine 5′- triphosphate
HRP	Horseradish peroxidise
IMPs	Inner membrane proteins
IMVs	Inverted inner membrane vesicles
IPTG	Isopropyl β-D-1-thiogalactopyranoside
kDa	kilo Dalton
LB	Luria-Bertani medium
M	Membrane fraction

MdoD	Glucans biosynthesis protein D
N-	Amino terminus
OD	Optical density
P	Periplasmic fraction
PAGE	Polyacrylamide gel electrophoresis
PBS(-T)	Phosphate buffered saline (0.01% Tween 20)
PCR	Polymerase chain reaction
PMF	Proton motive force
PVDF	Polyvinylidene fluoride
RNA	Ribonucleic acid
rpm	Revolutions per minute
SDS	Sodium dodecyl sulphate
Sec	General secretory pathway
SRP	Signal recognition particle
strep	*Strep*-II^{TM} tag
Tat	Twin-arginine translocation
TCA	Trichloroacetic acid
TEMED	N,N,N′,N′ Tetramethylethylenediamine
TM	Transmembrane span
TMAO	Trimethylamine-*N*-oxide
TorA	Trimethylamine-*N*-oxide reductase
UV	Ultraviolet
v/v	Volume per volume
W	Wash fraction
WT	Wild type
w/v	Weight per volume
YFP	Yellow fluorescent protein
Δ	Delta (gene deletion)

List of amino acids

Amino acid	Single letter code	3 letter code
Alanine	A	Ala
Asparagine or Aspartic acid	B	Asx
Cysteine	C	Cys
Aspartic acid	D	Asp
Glutamic acid	E	Glu
Phenylalanine	F	Phe
Glycine	G	Gly
Histidine	H	His
Isoleucine	I	Ile
Lysine	K	Lys
Leucine	L	Leu
Methionine	M	Met
Asparagine	N	Asn
Proline	P	Pro
Glutamine	Q	Gln
Arginine	R	Arg
Serine	S	Ser
Threonine	T	Thr
Valine	V	Val
Tryptophan	W	Trp
Tyrosine	Y	Tyr
Glutamine or Glutamic acid	Z	Glx

Chapter 1.

Introduction:
Protein Translocation in Bacteria

1.1 Bacterial protein translocation

The translocation of proteins from one compartment to another is an essential feature of cellular life. The proper functioning of extra-cytoplasmic proteins requires their export to, and productive folding in, the correct cellular compartment. Bacteria are prokaryotes and they are broadly classified into two separate groups: Gram-positive and Gram-negative (Figure 1.1A). The names originate from the reaction of cells to the Gram stain, a test long-employed for the classification of bacterial species. Those that retain Gram-stain are classified as Gram-positive bacteria whilst those that do not are classified as Gram-negative bacteria. Gram-positive bacteria possess a thick cell wall containing many layers of peptidoglycan and teichoic acid. In contrast, Gram-negative bacteria have a relatively thin cell wall consisting of a few layers of peptidoglycan surrounded by a second lipid membrane containing lipopolysaccharides and lipoproteins. Therefore Gram-negative cells typically have four compartments: the cytoplasm, the cytoplasmic (inner) membrane, the periplasm and the outer membrane. In bacteria up to 20% of all of the proteins synthesised in the cytoplasm are destined for translocation across the cytoplasmic membrane (Pugsley, 1993). The functions of the secreted proteins include biogenesis of organelles, such as Pili and Flagella; nutrient acquisition; virulence; and efflux of drugs and other toxins. Export of these proteins to the Gram-negative bacterial surface involves transport across the inner membrane, periplasm and outer membrane of the cell envelope. The majority of proteins are translocated across the inner membrane by the General secretory (Sec) pathway. Specialised pathways to export proteins to the outer membrane also exist, reviewed in Kostakioti *et al*. (2005). Other secretion systems have evolved that secrete proteins in a single process across both membranes (Saier, 2006). Although the Sec pathway appears to be the major translocation system, a small number of substrates use the Twin-arginine translocation (Tat) pathway instead. Interestingly the Gram-negative cyanobacteria, in addition to the typical features of Gram-negative, posses a network of internal thylakoid membranes (Figure 1.1B) that are the site of both photosynthesis and respiration (Peschek, 1996). Cynobacteria are therefore considered to be the progenitors of plant chloroplasts (De Marais *et al*., 2000). Homologues of the Sec and Tat translocation pathways have been identified in cyanobacteria (Aldridge *et*

al., 2008; Fulda *et al.*, 2000; Nakai *et al.*, 1993; Nakai *et al.*, 1994; Srivastava *et al.*, 2005) and there is good evidence that the Tat pathway operates in both cytoplasmic and thylakoid membranes of cyanobacteria (Spence *et al.*, 2003). For a review of the Tat export pathway in cyanobacteria see Barnett *et al.* (2011b).

This thesis focuses on translocation of proteins across the cytoplasmic membrane by the Tat pathway in *Escherichia coli* and *Bacillus subtilis*, reviewing the assembly and mechanism underlying this system.

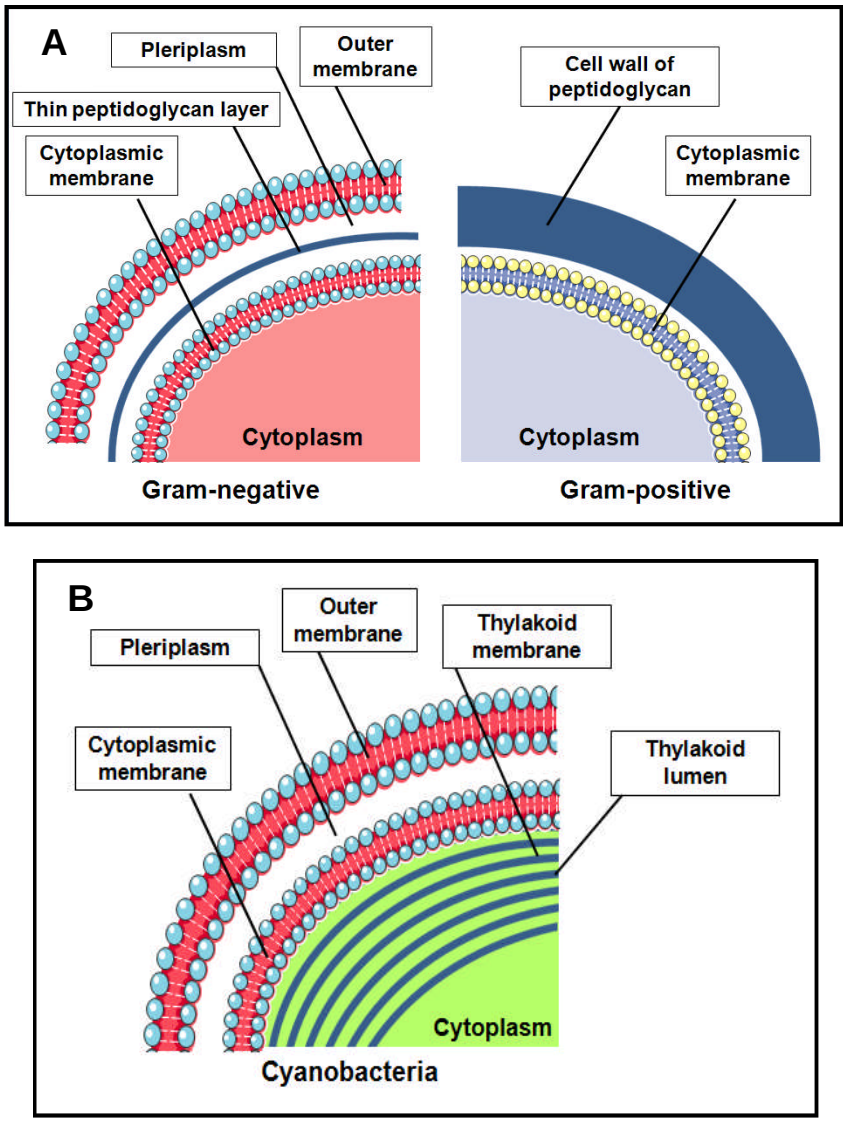

Figure 1.1 Schematics of Gram-negative, Gram-positive and cyanobacterial cells

A Gram-negative bacteria have four compartments: the cytoplasm, the cytoplasmic (inner) membrane, the periplasm and the outer membrane. Gram-positive bacteria have a single membrane surrounded by a much thicker cell wall layer of peptidoglycan and co-anionic polymer.

B. Cyanobacteria possess a network of internal thylakoid membranes.

1.2 The General Secretory (Sec) pathway

Sec systems are evolutionarily conserved protein translocation machineries that are present in the eukaryotic endoplasmic reticulum (Osborne *et al*., 2005), the archaeal plasma membrane (Bolhuis, 2004), the cytoplasmic membrane of both Gram-negative and Gram-positive bacteria (Driessen and Nouwen, 2008), the eubacterial plasma membrane (Dalbey and Chen, 2004; Veenendaal *et al*., 2004; Vrontou and Economou, 2004), and the thylakoid membranes of plant and algal chloroplasts. Components of the Sec pathway have also been identified in cyanobacteria (Nakai *et al*., 1994; Nakai *et al*., 1993). A common mechanistic feature of all Sec systems is that the substrates are transported in an unfolded conformation through a protein-conducting channel. Proteins which are destined to be exported by the Sec pathway are synthesised with a signal peptide which is recognised by protein targeting components and then directed for export. The signal peptide is on average 24 amino acids long (Cristóbal *et al*., 1999) and has a tripartite structure, composed of a positively charged N-terminal region (N-region), a hydrophobic core (H-region) and a polar C-terminal region (C-region) which normally contains a signal peptidase cleavage site.

1.2.1 The Sec pathway in bacteria

In bacteria, the majority of extracellular proteins are exported by the Sec pathway. It also operates in the insertion of membrane proteins into the bacterial cytoplasmic membrane, reviewed in Xie and Dalbey (2008).

In *E. coli*, the Sec translocon consists minimally of SecA, SecE, SecG and SecY (Akimaru *et al*., 1991). SecY is a 48 kDa protein with 10 transmembrane (TM) spans (Akiyama and Ito, 1987) which has its N- and C- termini located on the cytoplasmic side of the membrane, whilst the SecE and SecG proteins are ~ 15 kDa and have 3 and 2 TM spans respectively (Nishiyama *et al*., 1994; Schatz *et al*., 1989). The Sec core components consist of the integral membrane proteins SecY and SecE which are tightly bound to one another (Brundage *et al*., 1990) and are thought

to form the key parts of Sec protein conducting channel. SecG, which is located peripherally in the complex (Hanada *et al*., 1994; Nishiyama *et al*., 1994), is also part of the well-characterised SecYEG translocon.

A SecDFYajC hetero-trimeric ancillary complex is found associated with the SecYEG complex in the membrane. Cells lacking SecDF show a reduced level of export activity (Duong and Wickner, 1997) and its precise function was rather unclear (Nouwen *et al*., 2005). Nevertheless a recent work has suggested that SecDF may function as a membrane-integrated chaperone which is powered by proton motive force and is involved in an ATP-independent protein translocation (Tsukazaki *et al*., 2011).

A SecYEG dimer has been proposed to form a translocation channel that is ~ 4 Å at its most constricted point and ~ 20-25 Å at its widest (Berg *et al*., 2004; Breyton *et al*., 2002; Mitra *et al*., 2005). The structure of the SecYEG complex presents a cavity at the periplasmic face of the membrane which is covered by a periplasmic loop of SecY. It is thought that when the translocation starts the loop of SecY is displaced resulting in the formation of an aqueous channel across the membrane (Harris and Silhavy, 1999).

SecA is a 102 kDa hydrophilic protein. It has been found both within the cytoplasm and in the membrane where it is associated with SecYEG (Cabelli *et al*., 1991; Chun and Randall, 1994). Recently it has been suggested that a single copy of the SecYEG complex is sufficient both for SecA binding and for preprotein translocation (Kedrov *et al*., 2011). Six SecA crystal structures have been published, five of them are dimeric (Hunt *et al*., 2002; Papanikolau *et al*., 2007; Sharma *et al*., 2003; Vassylyev *et al*., 2006; Zimmer and Rapoport, 2009), and one is monomeric (Osborne *et al*., 2004). The protomers of each dimer all have a similar structure, but surprisingly the position of each protomer relative to one another is unique (Sardis and Economou, 2010).

The signal peptide of some preprotein substrates bind post-translationally to the chaperone SecB, a secretion dedicated chaperone that is present in many Gram-negative bacteria but is absent in Gram-positive bacteria (Müller *et al*., 2000; van

Wely *et al*., 2001). SecB keeps the substrate in a largely unfolded conformation in the cytoplasm. SecB then binds to SecA, the unfolded preprotein is transferred to SecA, and SecB disassociates. However, not all secretory proteins depend on SecB. These preproteins are targeted to the Sec translocase by SecA or by general cytosolic chaperones such as GroEL and/or DnaK, which can substitute partially for SecB under certain conditions (Bochkareva *et al*., 1998; Lecker *et al*., 1989).

SecA, through a cycle of ATP binding hydrolysis and release, drives the translocation of the precursor trough the SecYEG pore (Dalbey and Chen, 2004). The proton motive force (PMF) takes part to the transport process, stimulating insertion of the preprotein (van Dalen *et al*., 1999) and driving translocation (Driessen, 1992). After completion of translocation the signal peptide of the preprotein is cleaved off by the signal peptidase SPase I (Paetzel *et al*., 2002), and the mature protein folds in the periplasm.

Figure 1.2 shows the current model of Sec-dependent translocation in *E. coli.*

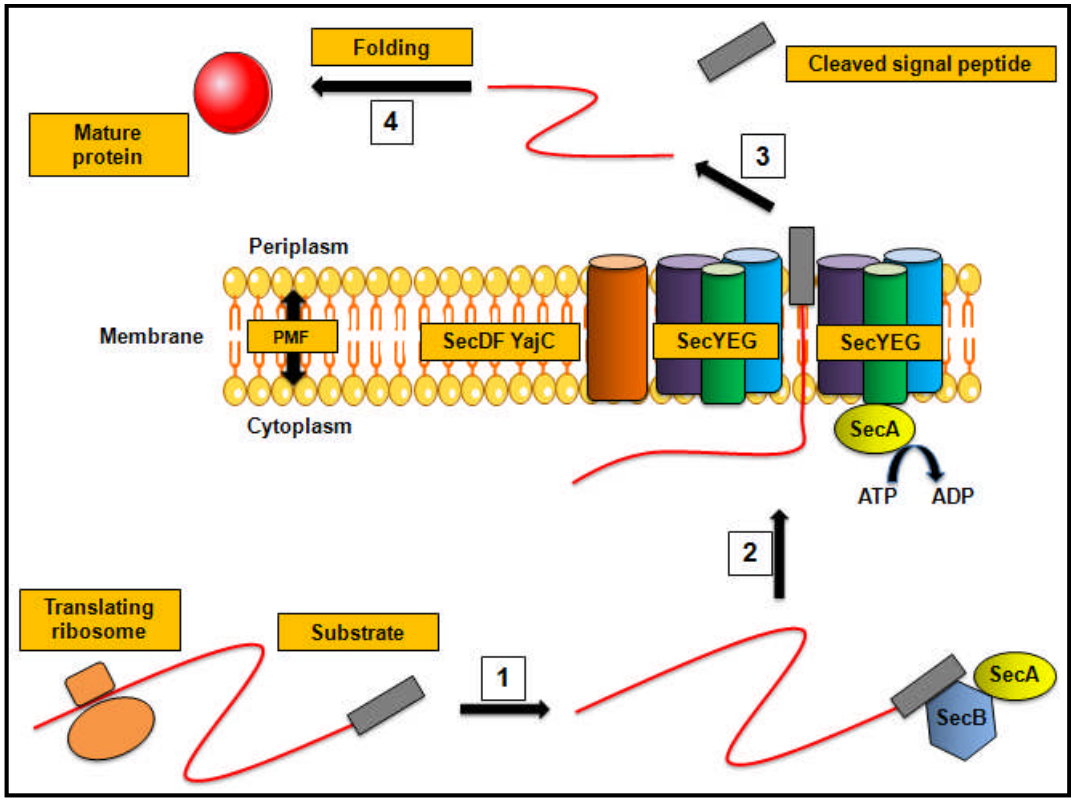

Figure 1.2 Protein translocation by the *E. coli* Sec pathway
Following protein synthesis, substrate proteins are bound by the SecB chaperone (**1**). The substrate is targeted to the SecYEG complex through the interactions of SecB with the SecYEG associated SecA protein. The signal peptide of the substrate binds to SecA triggering the release of SecB. The substrate is then translocated through the SecYEG pore in a mechanism that is driven by ATP hydrolysis by SecA (**2**). After translocation, the signal peptide (represented as a grey rectangle) is removed by processing peptidases (**3**) and the protein is able to fold (**4**).

1.2.2 The Sec pathway in chloroplasts

Chloroplasts are organelles which are the site of photosynthesis and important biochemical reactions in plant cells. They possess an envelope and an internal thylakoid membrane system. Overall they have three compartments: the intermembrane space, stroma and thylakoid lumen. The majority of chloroplast proteins are made in the cytosol and transported into chloroplasts by two translocases namely the TOC/TIC complex which are located in the outer and inner envelope membrane of chloroplasts respectively (Jarvis and Robinson, 2004). Both Tat and

Sec pathways operate at the thylakoid membrane where they translocate luminal proteins from the stroma.

In bacteria, much work has been performed in order to characterize the Sec pathway, whereas, in chloroplasts, our knowledge of the cpSec pathway is limited, with current models being mainly based on homology to the bacterial Sec pathway. In chloroplasts, homologues of SecA (cpSecA), SecY (cpSecY) and SecE (cpSecE) have been identified (Laidler *et al*., 1995; Nakai *et al*., 1994; Roy and Barkan, 1998; Schuenemann *et al*., 1999; Yuan *et al*., 1994), but several components of the bacterial Sec pathway (SecB, SecG and SecD/F) have not been identified in chloroplasts. Studies show that thylakoid cpSecA/cpSecYE works similarly to the *E. coli* system (Haward *et al*., 1997).

As in bacteria, the translocation step across thylakoid membranes is dependent on ATP and it is inhibited by the SecA inhibitor azide (Hulford *et al*., 1994; Yuan *et al*., 1994). Moreover antibodies against cpSecY prevent cpSecA-dependent protein translocation, suggesting that, as the bacterial counterparts, cpSecY and cpSecA work in concert (Mori *et al*., 1999).

Interestingly it has been shown that cpSecA ATPase activity is stimulated by Sec-dependent thylakoid signal peptides, but not by *E. coli* signal peptides, and that stimulation of cpSecA ATPase activity exhibits specific lipid requirements that differ from those of *E. coli* SecA (Sun *et al*., 2007).

Recently it has been shown that cpSecA is essential for photosynthetic development in *Arabidopsis*, because its absence can lead to severe defects in chloroplast sub-organelle structure and function (Liu *et al*., 2010). The inability of the chloroplast Sec translocon to transport dihydrofolate reductase (DHFR), in a methotrexate-stabilized folded conformation, demonstrates that the chloroplast Sec pathway, similar to bacteria, requires protein substrates to be in an unfolded state for transport (Hynds *et al*., 1998; Marques *et al*., 2004).

In chloroplasts there is no homologue of the bacterial cytosolic chaperone SecB, which is dedicated to preventing folding of Sec substrates, thus the stromal factors necessary to maintain Sec pre-proteins in an unfolded state remain unknown.

In summary, it appears that the thylakoid Sec system is something of a slimmed-down, 'minimal' Sec-type system that lacks many of the non-essential components found in *E. coli*. In general, however, the available evidence suggests that it operates by a broadly similar mechanism.

1.3 The Signal Recognition Particle (SRP)

Integral membrane proteins can be inserted into membranes during their synthesis (co-translationally) (Cross *et al*., 2009; Luirink and Sinning, 2004; Pool, 2005). The signal recognition particle (SRP) together with the Sec pathway is a key component of this process and it is one of the most extensively studied protein targeting pathways.

Remarkably, SRP is conserved in all three kingdoms of life, reviewed in Pool (2005), from bacteria, where SRP targets proteins to the inner membrane, through to eukaryotes, where SRP delivers proteins to the endoplasmic reticulum.

SRP of *Escherichia coli* consists of only two components: Ffh (fifty four homolog) and a 4.5S RNA which consists of 114 nucleotides. Whereas FtsY (filamentous temperature sensitive Y) functions as the SRP receptor. Many Gram-positive bacteria contain a 6S RNA molecule which in *Bacillus subtilis* binds an additional protein (HbsU), but its function is unknown (Grudnik *et al*., 2009). SRP in chloroplasts (cpSRP) does not contain an SRP RNA and can also act post-translationally (Schünemann, 2007). However, a novel protein (cpSRP43) is present which might replace the RNA (Stengel *et al*., 2008).

In *E. coli*, Ffh which is a 48 kDa GTPase (Phillips and Silhavy, 1992), binds with the ribosome and the signal peptide or hydrophobic TM domain of the nascent protein,

and then interacts with FtsY; a membrane protein interacting also with SecYEG (Angelini *et al.*, 2005; Bernstein *et al*., 1989). This interaction enables FtsY and the Ffh subunit of SRP to bind GTP. Upon GTP hydrolysis the ribosome and nascent chain complex are transferred to the SecYEG complex. It is thought that the SecYEG channel has a gate that allows membrane proteins to insert into the lipid bilayer exiting laterally from the channel (Duong and Wickner, 1998).

The schematic mechanism of the bacterial SRP targeting pathway is shown in Figure 1.3.

An additional mechanism has recently been discovered that allows membrane protein insertion to occur in a process dependent on the protein YidC (Samuelson *et al*., 2000). YidC has itself a membrane localization and belongs to the Oxa membrane protein family, including Alb3 in chloroplast thylakoids and Oxa1p in mitochondria (Dalbey and Kuhn, 2000). YidC associates with the transmembrane domains of inner membrane proteins (IMPs) such as Lep, FtsQ, and MtlA, upon their lateral exit from the Sec translocon (Dalbey *et al*., 2011; Wang and Dalbey, 2011). For the lipoprotein CyoA, YidC has been shown to work upstream of the Sec translocon (Celebi *et al*., 2006; du Plessis *et al*., 2006; van Bloois *et al*., 2006). For another subset of IMPs, YidC alone is sufficient for insertion and assembly of the complete protein into the inner membrane (Price and Driessen, 2010; Yuan *et al*., 2010). For a review of YidC dependent membrane protein insertion see Wang and Dalbey (2011).

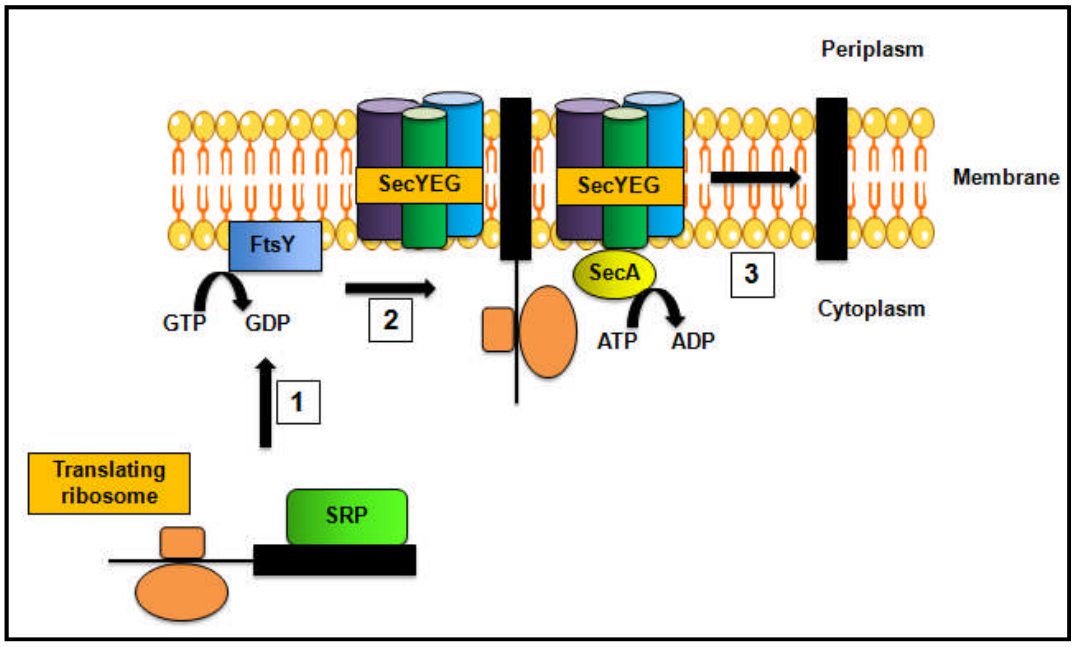

Figure 1.3 Overview of membrane protein insertion directed by bacterial SRP
Proteins bind to SRP as they exit the translating ribosome. Ribosome/substrate/SRP complexes dock with SecYEG associated FtsY proteins (**1**). Substrates pass into the SecYEG pore co-translationally (**2**) before inserting laterally into the lipid bilayer (**3**).

1.4 The Twin-arginine translocation (Tat) pathway

The Tat pathway was discovered in chloroplasts towards the beginning of the 1990s. Before this finding, the Sec pathway was thought to be solely responsible for the export of proteins across the bacterial cytoplasmic membrane.

Export *via* the Sec pathway is driven by ATP and the PMF, however a subset of thylakoid lumenal proteins did not need ATP for translocation but instead were depended on the difference in pH between the lumen of the thylakoid and the stroma (Cline *et al*., 1992; Klösgen *et al*., 1992; Mould and Robinson, 1991). This pathway was originally called the ΔpH-dependent pathway.

The first Tat component was identified after the isolation of a maize *hcf106* (high chlorophyll fluorescence 106) mutant, defective in a Sec-independent protein transport pathway (Settles *et al*., 1997; Voelker and Barkan, 1995). This was

followed by the identification of *E. coli* Tat components (Bogsch *et al*., 1998; Sargent *et al*., 1998; Weiner *et al*., 1998). Components of the Tat pathway have been identified in both Gram-positive and Gram-negative bacteria, archaea and cyanobacteria, with putative homologues also identified in plant mitochondria (Yen *et al*., 2002). No Tat homologues have, however, been found in animals or yeast.

Analysis of the signal sequences of proteins translocated via this pathway showed that the substrates bore cleavable N-terminal signal peptides containing a critical and highly conserved twin-arginine (RR) motif (Chaddock *et al*., 1995; Stanley *et al*., 2000), leading to the pathway being termed the twin-arginine translocaton pathway. Unlike the Sec pathway, where proteins are exported in an unfolded conformation, the Tat system appears to be unique in its ability to transport massive folded proteins across energy-transducing membranes, reviewed in Robinson *et al*. (2011).

Because of this peculiarity, the Tat system has attracted a great deal of commercial interest with a view to secreting complex heterologous proteins which are not compatible with the Sec pathway (Brüser, 2007; Kim *et al*., 2005). A recent study has investigated the impact of the Tat pathway overexpression on the cell culture and protein production and interestingly no adverse effects on cell integrity or downstream processing have been observed (Branston *et al*., 2012). Additionally, since the Tat system is involved in bacterial pathogenesis (De Buck *et al*., 2008), but is absent from mammalian cells, it may represent an important new target for novel antimicrobial compounds (Ochsner *et al*., 2002).

1.4.1 The role of the Tat pathway

The Tat system is vital for many bacterial processes, including energy metabolism, anaerobic growth, formation of the cell envelope, biofilm formation, heavy metal resistance, nitrogen-fixing symbiosis, and bacterial pathogenesis (Berks *et al*., 2005). Its physiological role is to allow the cell to complete the maturation of periplasmic proteins in the cytoplasm before they are exported (Berks *et al*., 2003).

There is evidence that the Tat transporter only tolerates folded protein substrates. This has been demonstrated for the *E. coli* Tat system using an *in vivo* assay based on the reporter protein alkaline phosphatase (PhoA) (DeLisa *et al*., 2003). Further evidence for the export of folded proteins comes from the Tat ability to export the two subunits of the nickel-containing hydrogenase 2 only when they both bind their cofactors (Rodrigue *et al*., 1999).

The Tat system has been also shown to be capable of transporting heterologous substrates that are known to be tightly folded prior to transport. These include jellyfish green fluorescent protein (GFP) (Santini *et al*., 2001; Thomas *et al*., 2001) and *c*-type cytochromes (Sanders *et al*., 2001) in studies with bacteria, and methotrexate-bound dihydrofolate reductase (Hynds *et al*., 1998) or disulfide bond-stabilised bovine pancreatic trypsin inhibitor (Clark and Theg, 1997) in studies carried out with the plant thylakoid Tat system.

In *E. coli*, around 18 of the 28 or so Tat substrates are either known or predicted to bind redox cofactors (Palmer *et al*., 2005). The stable insertion of cofactors into proteins normally requires the protein to fold around the cofactor therefore the substrate protein must be folded prior to be exported (Berks *et al*., 2003). There is no evidence to suggest these cofactors can be bound in the periplasm so it is believed the proteins must be fully or largely folded when exported. In fact if cofactor insertion is blocked the precursor protein is not transported (Santini *et al*., 1998).

It has also been shown that substitutions in the [4Fe-4S] centre of the FeS protein NrfC, which disrupt cofactor binding and folding, result in a complete block of export (Matos *et al*., 2008). Thus proteins which bind cofactors in the cytoplasm prior to transport must use the Tat rather than Sec pathway (Berks *et al*., 2003).

Interestingly, a more recent work has shown that in *Synechocystis* the Tat pathway has an important role in preventing the aberrant binding of metal ions by apo-proteins (Tottey *et al*., 2008) confirming the importance of the Tat system in the biosynthesis of non cytoplasmic metalloproteins.

Proteins binding iron-sulfur clusters are the most common substrates of the Tat pathway. Examples of other cofactor-containing Tat substrates include trimethyl *N*-oxide reductase (TorA), and dimethyl sulfoxide reductase (DmsA) which contain molybdopterin cofactors and are important for the anaerobic respiration (Méjean *et al*., 1994; Weiner *et al*, 1988). In fact the Tat pathway has been shown to be essential for anaerobic growth (Jack *et al*., 2001). Other Tat substrates which contain cofactors are copper containing proteins and hydrogenases which can be split into two broad classes based on cofactor content: the [Fe] hydrohenases and the [NiFe] hydrogenases (Berks *et al*., 2003).

While the bacterial Tat pathway was initially identified as a pathway dedicated to the export of proteins binding complex cofactors, now it has been estimated that *E. coli* K-12 strains contain nine proteins with putative Tat signal peptides which do not contain complex cofactors (Berks *et al*., 2000; Ize *et al*., 2003; Stanley *et al*., 2001; Stanley *et al*., 2000). Probably these proteins are targeted through the Tat system because they fold too rapidly or stably to be transported by the Sec apparatus. Two Tat substrates which do not contain cofactors are the cell wall amidases AmiA and AmiC. Their mis-localization results in a cell division phenotype with cells growing as long filamentous chains (Bernhardt and de Boer, 2003; Ize *et al*., 2003). This phenotype renders the cell vulnerable to adverse environmental conditions (Stanley *et al*., 2001). These results highlight that the Tat pathway is required for the cell wall biogenesis.

The Tat system is also required for bacteria to successfully interact with host organisms during symbiotic nitrogen fixation (Meloni *et al*., 2003) and in bacterial infections of animal and plants (Ding and Christie, 2003; Ochsner *et al*., 2002; Pradel *et al*., 2003). Examples include, *Pseudomanas aeruginosa* (Ochsner *et al*., 2002), *Yersinia pseudotuberculosis,* (Lavander *et al*., 2006), *Agrobacterium tumefaciens* (Dilks *et al*., 2003; Yen *et al*., 2002) as well as some strains of *E. coli*. However, to date only the Tat substrate phospholipase C protein has been confirmed to be directly involved in virulence (De Buck *et al*., 2005; McDonough *et al*., 2005; Saint-Joanis *et al*., 2006; Voulhoux *et al*., 2001). Interestingly, given that there are no Tat homologues in mammalian cells, the Tat pathway of human pathogens could be exploited as a potential target for the development of novel antimicrobial drugs.

In addition to the ability of export folded proteins across membranes, it has been shown that the *E. coli* Tat pathway can also insert proteins into the membrane (De Buck *et al*., 2007; Hatzixanthis *et al*., 2003; Summer *et al*., 2000), using a mechanism which is independent of both YidC and SecYEG (Hatzixanthis *et al*., 2003) but it is as yet unknown. In *Legionella pneumophila* and *Paracoccus dentrificans* the Tat pathway has also been found to insert the Rieske Fe/S proteins into the plasma membrane (Bachmann *et al*., 2006; De Buck *et al*., 2007).

1.4.2 The Tat signal peptides

Both Tat and Sec substrates are targeted for export by the presence of a signal sequence at their extreme N-terminus (Berks *et al*., 2000; Sargent *et al*., 2002). Signal sequences in general contain three distinct domains; a positively charged N-terminal domain (N-region), hydrophobic core domain (H-region) and C-terminal domain (C-region) that is polar and terminates in an A–Xaa–A consensus motif where Xaa is any amino acid. This motif is required for removal of the signal peptide by signal peptidase following translocation (von Heijne, 1985).

Signal sequences that target proteins to the Tat machinery (Figure 1.4.1) conform to the overall tripartite structure but have additional features that distinguish them from those present on Sec-targeted substrates. The most important of these is the presence of a consensus S-R-R-x-F-L-K motif, where the two Arginine residues are almost invariant, the other amino acids are found with a frequency exceeding 50% and x is any polar amino acids (Palmer *et al*., 2005; Berks, 1996; Stanley *et al*., 2000).

Plant Tat signal peptides have instead a shorter consensus sequence (R-R-x-x-ϕ) in comparison to the extended bacterial one; where ϕ is typically Leucine, Phenylalanine, Valine or Methionine, and x can be any amino acid (Stanley *et al*., 2000).

Mutagenesis studies have shown that while the twin-arginine motif is absolutely critical in chloroplast Tat signals (substitution of either R to K results in a complete

block in translocation (Stanley *et al*., 2000)) the twin-arginine is less critical in bacterial Tat signal peptides.

In *E. coli* substitution of both residues with Lysine completely abolishes Tat-specific export but the conservative substitution of a single Arginine usually affects only the rate of translocation (Buchanan *et al*., 2001; DeLisa *et al*., 2002; Mendel *et al*., 2008). Of the two Arginine residues, the second seems to be more important (DeLisa *et al*., 2002). Signal peptide mutations have broadly similar effects on export by both the *E. coli* and the *B. subtilis* Tat systems (Ize *et al*., 2002a; Mendel *et al*., 2008)). This suggests that Tat signal peptides have a generally similar structure in both Gram-positive and Gram-negative bacteria.

Other residues within the consensus motif have also been found to be important for translocation. For example, the hydrophilic -1 residue, relative to the twin-arginine motif (typically Serine, Threonine, Aspartate or Asparagine). When this Serine of the *E. coli* TorA and DmsA signal peptides is mutated to Alanine, a dramatic reduction in translocation activity is observed (Mendel *et al*., 2008). The residue at position +2, relative to the twin-arginine, is generally either a Phenylalanine or a Leucine. In the signal peptide of TorA, if this Phenilalanine is replaced by either Alanine or Serine there is no effect on transport, whilst substitution by Aspartic acid causes a complete block in translocation (Mendel *et al*., 2008). In contrast, the signal peptide of DmsA has a Leucine in position +2 and interestingly, if this residue is replaced by either Alanine or Aspartic acid, the Tat transport is completely blocked (Mendel *et al*., 2008). Thus these results show that an acidic residue in position +2 is not tolerated.

As well as the twin-arginine motif, Tat signal peptides also differ from Sec signal peptides in several other ways. Tat signal peptides are typically longer than their Sec counterparts, with an average length of 38 amino acids versus 23 residues for Sec signal peptides (Cristóbal *et al*., 1999). Sec signal peptides are more hydrophobic than Tat signal peptides, and increasing the hydrophobicity of Tat signal peptides can convert them into Sec signals (Cristóbal *et al*., 1999; Ize *et al*., 2002a), suggesting that this may be an important sorting determinant to prevent mis-targeting by signal peptides that are otherwise rather similar (Robinson *et al*., 2011).

Additionally, Tat signal peptides often have a basic residue in the C-region which is almost never present in Sec signals and is thought to work as a "Sec-avoidance" motif (Blaudeck *et al.*, 2003; Bogsch *et al.*, 1997).

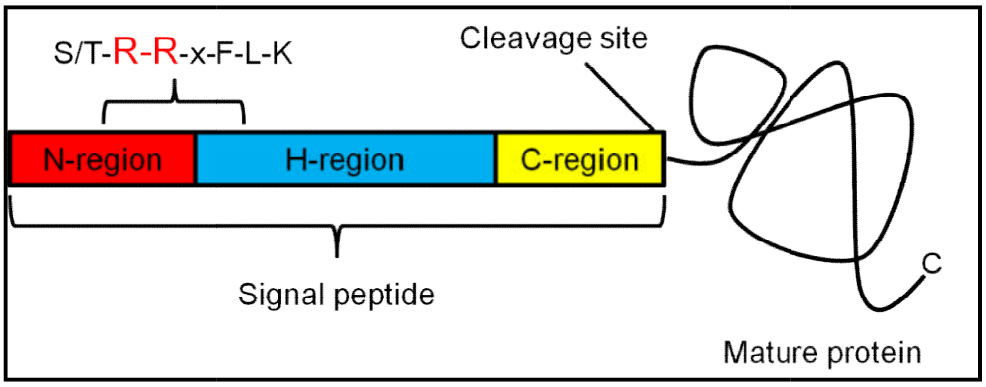

Figure 1.4.1 The Tat signal peptide
A typical tripartite structure of the Tat signal peptide is here shown: N-terminal positively charged region (N-region), hydrophobic central region (H-region), and C-terminal polar region (C-region) are indicated. The Tat consensus motif (S/T-R-R-x-F-L-K) is shown and the signal peptidase cleavage site at the A-Xaa-A motif is indicated.

1.4.3 Proofreading and quality control of Tat substrates

The Tat pathway's ability to translocate fully folded proteins is one of its most intriguing aspects. As mentioned above, the bacterial Tat pathway is able to transport cofactor-containing redox enzymes which must bind their cofactors in the cytoplasm before transport, so folding must take place before translocation (Berks, 1996; Ilbert *et al.*, 2003; Santini *et al.*, 1998). This necessitates the operation of effective proofreading systems that prevent the futile export of apo-proteins, reviewed in Sargent (2007). In support to the existence of such mechanism it has been shown that TorA and PhoA are only translocated upon cofactor insertion and correct folding (Santini *et al.*, 1998; DeLisa *et al.*, 2003).

An exciting development is the identification in *E. coli* of substrate-specific proteins that appear to be involved in this type of quality control process. These cytosolic

chaperones interact with the N-terminal signal peptides of Tat substrates preventing premature interactions with the Tat machinery before cofactor assembly and protein folding is complete. The *E. coli* TorD and DmsD accessory proteins, which have been identified as such quality-control, bind to the signal peptides and mature regions of the cofactorless precursor proteins TorA and DmsA respectively (Genest *et al*., 2006; Hatzixanthis *et al*., 2005; Jack *et al*., 2004; Ray *et al*., 2003). Recently, a surface plasmon resonance analysis has revealed that the hydrophobic core of TorA and DmsA signal sequences is responsible for the specific binding to TorD and DmsD respectively (Shanmugham *et al*., 2012). In contrast it has been shown that the cytoplasmic chaperone NapD binds the signal peptide of the periplasmic nitrate reductase (NapA) next to the twin-arginine motif (Grahl *et al*., 2012).

A general quality control mechanism, which recognises hydrophobic stretches has been hypothesized (DeLisa *et al*., 2003). This idea is supported by a study which shows that the Tat-dependent translocation could be blocked by the insertion of hydrophobic stretches (Richter *et al*., 2007).

Finally another study has suggested that incorrectly folded precursors may reach the Tat translocon, but then fail to undergo full translocation (Lim *et al*., 2009), although these results require further exploration to determine how well such unfolded substrates are generally recognised.

1.4.4 The Tat pathway components

In *E. coli*, three *tat* genes are required for translocation: two homologous, *tatA* and *tatB* genes, and *tatC* which are co-expressed alongside the *tatD* gene in an operon (Figure 1.4.2). The *tatD* gene encodes a protein with DNase activity and is thought not to function in the Tat pathway (Wexler *et al*., 2000). A fifth *tat* gene, *tatE*, is also present in *E. coli* and is expressed elsewhere in the genome. All of the *E. coli tat* genes are expressed at constitutive levels in a variety of growth conditions (Jack *et al*., 2001), but are only essential for anaerobic growth on minimal media (Santini *et al*., 1998; Sargent *et al*., 1998; Weiner *et al*., 1998).

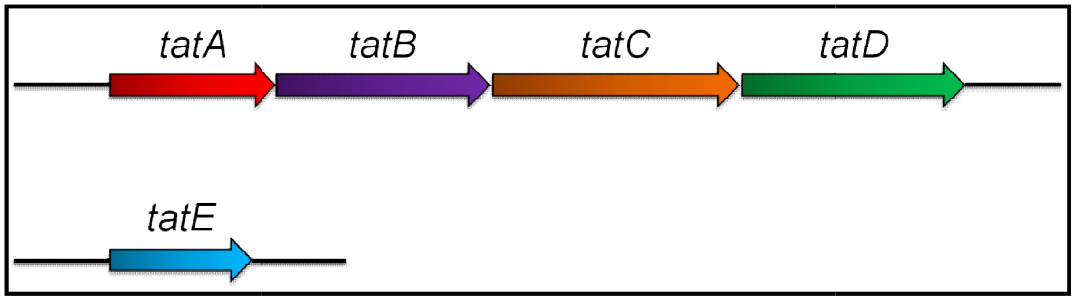

Figure 1.4.2 Chromosomal organisation of the *tat* genes in *E. coli*
tatA, *tatB* and *tatC*, which are all essential for function, are organised in an operon along with a fourth gene, *tatD*. A fifth *tat* gene, *tatE* is a gene duplication of *tatA* that is expressed elsewhere in the genome.

The *tatA* gene encodes an 82 amino acid integral membrane protein of ~ 9.5 kDa. It is predicted to have an N-terminal α-helical TM domain which protrudes into the periplasm, followed by a short 'hinge' region, an α-helical amphipathic helix (APH), that lies along the inner face of the membrane surface, and a largely unstructured C-terminal domain (Lee *et al*., 2002; Sargent *et al*., 1998; Settles *et al*., 1997) (Figure 1.4.3).

According to proteinase accessibility experiments TatA has an N-out topology (Porcelli *et al*., 2002). However another study proposed that it has an N-in topology (Chan *et al*., 2007). The same study also proposed a dual topology for the C-terminus of TatA in support of the hypothesis previously put forward in an earlier study (Gouffi *et al*., 2004). Thus these studies suggest that the C-terminal amphipathic domain of TatA may insert into the membrane during translocation.

In contrast a recent study has shown that TatA has an N-out, C-in topology in intact cells (Koch *et al*., 2012). The same study has also shown that the topology of TatA is fixed and is not affected either by the absence of other Tat components or by the overproduction of a Tat substrate, suggesting that during the Tat translocation the topological reorganization of TatA is unlikely.

TatA is found at ~ 20 times the level of TatB (Sargent *et al*., 2001) and it is thought to form the translocation pore of the Tat pathway (see below) (Gohlke *et al*., 2005; Oates *et al*., 2005). TatA tagged with yellow fluorescent protein (YFP) localises evenly around the periphery of the cell (Berthelmann and Brüser, 2004; Leake *et al*., 2008; Ray *et al*., 2005).

There is some evidence that as well as being present in the membrane TatA may be also present in the cytoplasm of some bacteria. Soluble TatA homologues have been observed in the Gram-positive bacteria *Streptomyces lividans* (De Keersmaeker *et al*., 2005) and *Bacillus subtilis* (Pop *et al*., 2003) and also in plant chloroplasts (Frielingsdorf *et al*, 2008). In *B. subtilis*, the soluble population of TatA protein is proposed to act as the initial receptor for Tat substrates, with TatA-substrate complexes targeted to membrane localised TatCd (Schreiber *et al*., 2006). Interestingly, in *E. coli* overexpression of TatA causes the formation of cytoplasmic 'tubes' (Berthelmann *et al*., 2008).

Several mutagenesis studies have been performed on the *E. coli* TatA protein in order to investigate the importance of several residues for the Tat-dependent translocation (Barrett *et al*., 2005b; Barrett *et al*., 2003; Greene *et al*., 2007; Hicks *et al*., 2003; Hicks *et al*., 2005). The majority of loss of function substitutions localise in the APH and hinge region. For example the single substitution of a phenylalanine (Phe39) and the triple substitution of three lysine residues in the APH (Lys37, Lys40, Lys41) both lead to a block of export. Moreover a cysteine scanning study shows that a glutamine in the TatA TM domain (Gln8) is also important for the Tat function (Greene *et al*, 2007).

More recently it has been shown that an acidic motif following the TatA amphipathic helix is critical for the Tat activity (Warren *et al*., 2009) It is thought the TatA TM domain is involved in interactions which drive the formation of TatA complexes (De Leeuw *et al*., 2001; Greene *et al*., 2007; Porcelli *et al*., 2002). Whereas the C-terminus of TatA appears to be non-essential for function (Lee *et al*., 2002). In a recent study, NMR and CD spectroscopy, performed on a synthetic peptide representing the amphipathic region of TatA shows that the helical structure of this amphipathic helix in TatA is dependent on the presence of a stable membrane

mimetic environment (Chan *et al*., 2011). The synthetic APH associates with negatively charged lipids while having little effect on zwitterionic bilayers.

TatA and TatB share 25% sequence identity and the two subunits have a similar secondary structure (Figure 1.4.3); TatB is, however, significantly longer. TatB is ~ 18.5 kDa and is composed of 171 amino acids. Like TatA it has a transmembrane domain with its N-terminus protruding into the periplasm, a small hinge region which follows the transmembrane span, a longer amphipathic helix and a longer C-terminus in the cytoplasm (Bolhuis *et al*., 2001).

Recently it has been demonstrated that TatB, as TatA, has an N-out, C-in topology in intact cells (Koch *et al*., 2012). Truncation analysis of the TatB C-terminal tail suggests that it is not required for translocation activity (Lee *et al*., 2002). Further truncation of the C-terminal two thirds of TatB still allows complex formation with TatC, although protein translocation is severely affected (Maldonado *et al*., 2011b). The same study showed that the membrane extrinsic domain of TatB forms parallel contacts with at least one other TatB protein (Maldonado *et al*., 2011b).

As in TatA, the TatB hinge region and amphipathic helix are crucial for transport since single amino acid substitutions in these regions affect dramatically the Tat function (Barrett *et al*., 2003; Hicks *et al*., 2003; Lee *et al*., 2006).

The localisation of TatB in the plasma membrane is a matter of controversy. In fact one study shows a TatB-GFP fusion to have, similarly to TatA, a uniform distribution around the periphery of the cell (Ray *et al*., 2005), whereas another study finds TatB to localise to the cell poles (Berthelmann and Brüser, 2004). While in *E. coli* TatB is present only in the membrane, in *Streptomyces lividans*, which is the only Gram-positive bacterium to have TatB, it is localized in the cytoplasm (De Keersmaeker *et al*., 2005). The meaning of this TatB soluble population is still unknown.

Some studies suggest that in *E. coli* TatB is not required for transport of all substrates; since TatB has been shown not to be essential for the translocation of Colicin V in *E. coli* (Ize *et al*., 2002b). In addition, a study performed in *E. coli*,

using a chimeric Tat-substrate, has demonstrated that translocation can occur in the absence of TatB (Blaudeck *et al*., 2005).

TatC is the largest of the three Tat components in *E. coli* and is the most highly conserved. It is ~ 32 kDa and is composed of 258 amino acids. TatC has 6 transmembrane α-helical domains and its N- and C-termini are both located in the cytoplasm (Behrendt *et al*., 2004) (Figure 1.4.3).

As for the other Tat components, several mutagenesis studies have been carried out on TatC (Allen *et al*., 2002; Barrett *et al*., 2005b; Buchanan, 2002; Punginelli *et al*., 2007). Two residues have been found to be important for TatC function; a Phenylalanine located in position 94 of the second TM domain (Phe94) and a Proline in the first periplasmic loop (Pro48). Phe94 has been shown to be essential for the translocase function, but not for the complex formation (Barrett *et al*., 2005a). In contrast the Pro48 resulted important also for the TatABC complex assembly (Barrett *et al*., 2005a).

Two different studies show distinct localization of TatC-GFP fusion; a polar localisation (Berthelmann and Brüser, 2004), and a uniform distribution around the plasma membrane (Ray *et al*., 2005).

TatC interacts with TatB to form the receptor complex of the Tat pathway and it is thought to be the site of signal peptide recognition (Alami *et al*., 2003; Cline and Mori, 2001). A recent study suggests that TatC forms a dimeric functional unit. Within the dimer only one functional TatC is sufficient for Tat translocation activity (Maldonado *et al*., 2011a).

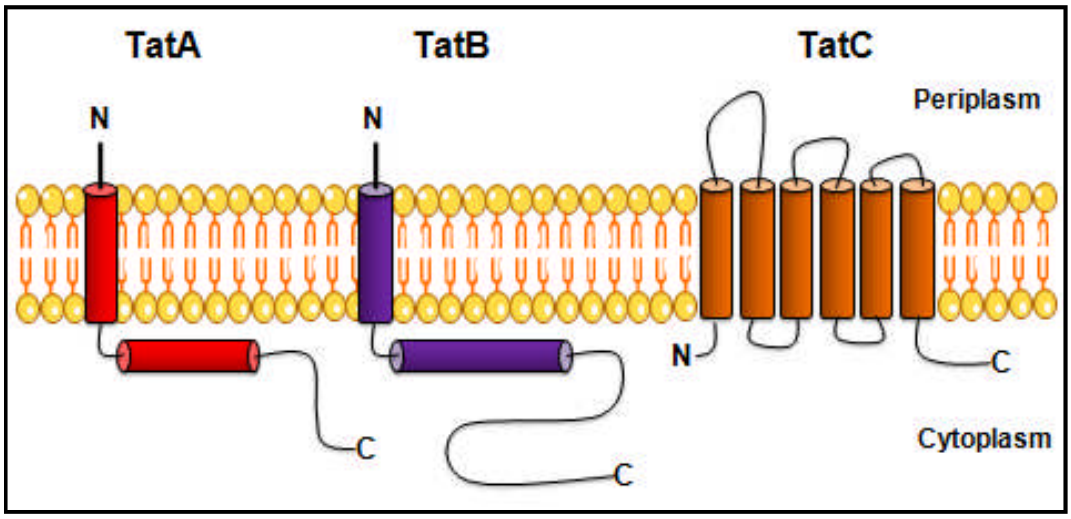

Figure 1.4.3 Predicted structure and topological arrangement of the *E. coli* Tat components
TatA and TatB are predicted to have a similar secondary structure; an N-terminal α-helical TM domain, followed by a short 'hinge' region linking the amphipathic helix that lies along the inner surface of the plasma membrane. Following the amphipathic helix is a largely unstructured C-terminal extension. TatC is a six TM domain protein with both its N- and C-termini located in the cytoplasm.

1.4.5 The TatE subunit

Although the TatABC subunits appear to form the primary translocation system, *E. coli* also contains a separate TatA paralog, TatE, that is encoded by a separate, monocistronic *tatE* gene.

The *tatE* gene is found only in enterobacteria (Yen *et al*., 2002) with the exception of the Gram-positive bacteria *Corynebacterium glutamicum* and *Corynebacterium efficiens* (Ikeda and Nakagawa, 2003). The *tatE* gene encodes a 67-amino acid predicted membrane protein that exhibits greater than 50% sequence identity with TatA (Sargent *et al*., 1998).

TatE can complement a *tatA* mutant, indicating a similar role (Sargent *et al*., 1999), but TatE is normally produced at levels that are 50-200 fold lower than those of TatA (Jack *et al*., 2001). Nevertheless, there is evidence that TatE plays a distinct role. In *E. coli*, *tatE* is induced in biofilms, and *Pseudomonas stutzeri tatE* expression is

associated with denitrification, perhaps pointing to an important role for TatE proteins under specific growth conditions, or possibly as an adaption for handling specific substrates (Beloin *et al*., 2004; Heikkilä *et al*., 2001).

Despite this, the role of TatE in the Tat pathway of *E. coli* has been largely unstudied and its precise function still remains to be determined.

1.4.6 Tat complexes organization

In *Escherichia coli* and many other Gram-negative bacteria, the minimal set of components required for Tat-dependent translocation are the three integral membrane proteins, TatA, TatB and TatC, which, as it has been discussed before, are encoded by the *tatABC* operon.

These subunits are found in two types of complex within the plasma membrane: a TatABC complex and separate TatA complexes. The TatABC complex has been purified and shown to contain equal amounts of TatB and TatC, with small and variable amounts of TatA (Bolhuis *et al.*, 2001). Its size, estimated by gel filtration, was found to be around 600 kDa, so clearly contains multiple copies of the Tat components.

According to blue-native polyacrylamide gel electrophoresis (BN-PAGE) experiments, which provide a more accurate complex size determination, the TatABC complexes run as a discrete band of 370 kDa (Oates *et al*., 2005). Electron microscopy studies has shown that the TatABC complex has an asymmetric elliptical shape with maximal dimensions up to 13 nm and a central pool of stain linking to the exterior of the complex (Oates *et al*., 2003).

The role of the TatA subunit within the TatABC complex is still debated. A study showed that the TatBC complex is unstable in the absence of TatA suggesting that TatA stabilises the TatB subunit specifically within this complex (Mangels *et al*., 2005). In contrast, more recently it has been shown that TatA has no effect on either the formation nor stability of the TatBC complex (Orriss *et al*., 2007). The authors

also suggest that TatC forms a core to the TatBC complex on to which TatB assembles.

A parallel study from another group showed different results where TatB, in absence of TatC builds up modular complexes ranging in size from about 100 to over 880 kDa, whereas TatC alone can form a 250 kDa complex which could be a scaffold that can recruit TatB to form defined TatBC complexes (Behrendt *et al*., 2007). Apart from a 370 kDa TatABC complex, also a 580 kDa TatBC-containing complex, which can bind Tat substrates, has been detected (Richter and Bruser, 2005).

The vast majority of *E. coli* TatA is found in separate TatA homo-oligomeric complexes ranging from ~ 50 kDa to over 500 kDa according to BN-PAGE experiments (Oates *et al*., 2005). Electron microscopy and random conical tilt reconstructions of purified complexes suggests that these TatA complexes may form pores of different sizes which match the varying dimensions of Tat substrates (Gohlke *et al*., 2005; Oates *et al*., 2005) and indeed the differing size classes have potential pores of correspondingly differing diameters (Gohlke *et al*., 2005). Accordingly, it is widely believed that TatA forms the bulk of the translocation pore.

Furthermore the stoichiometry of *E. coli* TatA complexes was investigated using *in vivo* single-molecule imaging of TatA-YFP at native levels of expression in *E. coli*. Confirming previous results, it was found that TatA forms complexes exhibiting a broad range of stoichiometries with an average of ~ 25 TatA subunits per complex. Moreover, it was showed that each cell contains ~ 15 mobile TatA complexes and a pool of ~ 100 TatA molecules in a more disperse state in the membrane (Leake *et al*., 2008).

Apart from the TatABC and separate TatA complexes, also TatAB have also been identified (Bolhuis *et al*., 2001; De Leeuw *et al*., 2001). The purified TatAB complex was found to have an apparent molecular mass of 600 kDa, estimated by gel filtration chromatography (Sargent *et al*., 2001). The same report shows, by means of negative stain electron microscopy, that isolated TatAB complexes form a double-layered ring structure. The role of the TatAB complexes is still debated; one hypothesis is that

they may be either an assembly or disassembly intermediate generated during translocation activity (Oates *et al*., 2005).

1.4.7 Tat pathway mechanism of translocation

It is widely accepted that the Tat system transports large proteins but the exact mechanism by which Tat substrates are translocated across the plasma membrane remains poorly understood.

Works on the thylakoid Tat pathway show that the system is dependent on the thylakoid ΔpH but not nucleoside triphosphate hydrolysis (Cline *et al*., 1992; Klösgen *et al*., 1992; Mould and Robinson, 1991). Similarly, *in vitro* assays, using inverted *E. coli* membrane vesicles (IMVs), demonstrate that the translocation of Tat substrate proteins has no requirement for ATP but is blocked if a proton motive force is not present (Alami *et al*., 2003; Alami *et al*., 2002; Yahr and Wickner, 2001). Interestingly it has been found that *E. coli* SufI could be imported into IMVs in the absence of a ΔpH and instead two electrical-potentials steps were necessary (Bageshwar and Musser, 2007). According to this result, it was observed that *in vivo* the thylakoid Tat system can be driven by Δψ (Finazzi *et al*., 2003).

The first step in the translocation process is the targeting of the substrate to the Tat translocon. TatB and TatC in the TatABC complex are believed to form the substrate-recognition component of the Tat translocase. According to site-directed cross-linking studies (Alami *et al*., 2003), the RR proximal region of the signal peptide is in close contact with TatC, whereas the hydrophobic domain and some parts of the adjacent mature domain are in close contact with TatB (Alami *et al*., 2003; Gerard and Cline, 2006). Recently, photo cross-linking studies have shown that TatB has multiple precursor-binding sites in the predicted transmembrane and amphipathic helices (Maurer *et al*., 2010) and that the cytoplasmic N-terminus and first cytoplasmic loop of TatC is the recognition site for RR signal peptides (Zoufaly *et al*., 2012).

An electron microscopic study on the TatBC complex shows that overproduction of TatBC and the SufI substrate in the absence of TatA led to the formation of distinct TatBC-SufI complexes with one or two substrate molecules bound peripherally to TatBC at adjacent positions, implying some structural or functional disparity between TatC protomers or negative cooperativity of substrate binding (Tarry *et al*., 2009).

Recently, it has been reported that multiple precursor proteins can bind to sites in a single translocase, and can be transported across membrane together by Tat system in isolated pea chloroplasts (Ma and Cline, 2010).

Substrate binding is likely to trigger the recruitment of separate TatA complexes (Alami *et al*., 2003; Alami *et al*., 2002), which could form the translocation pore, or at least contribute to it. Analysis of *E. coli* TatA using single-particle electron microscopy reveals that TatA forms ring-shaped structures of variable diameter (Gohlke *et al*., 2005), supporting a model in which TatA form a pore-like channel and furthermore raising the possibility that TatA oligomerization and recruitment might be tailored to the dimension of the protein to be translocated.

After translocation, TatA disassociates from TatABC and the system returns to a resting state. However, it should be noted that the late stages of translocation are not understood in any real detail, and very little information on the nature of the translocation pore is available. The current model of Tat dependent translocation in *E. coli* is presented in Figure 1.4.4.

Alternative models for the Tat dependent translocation, when the TatE subunit is involved, will be discussed later on in this thesis.

Surprisingly, *in vivo* studies carried out in tobacco protoplasts show that the translocation within this pathway is reversible to a significant extent, which means that a large proportion of a given substrate could be partially translocated across the thylakoid membrane, processed to the mature size, and returned to the stroma as part of a “translocation reversal” process (Di Cola and Robinson, 2005).

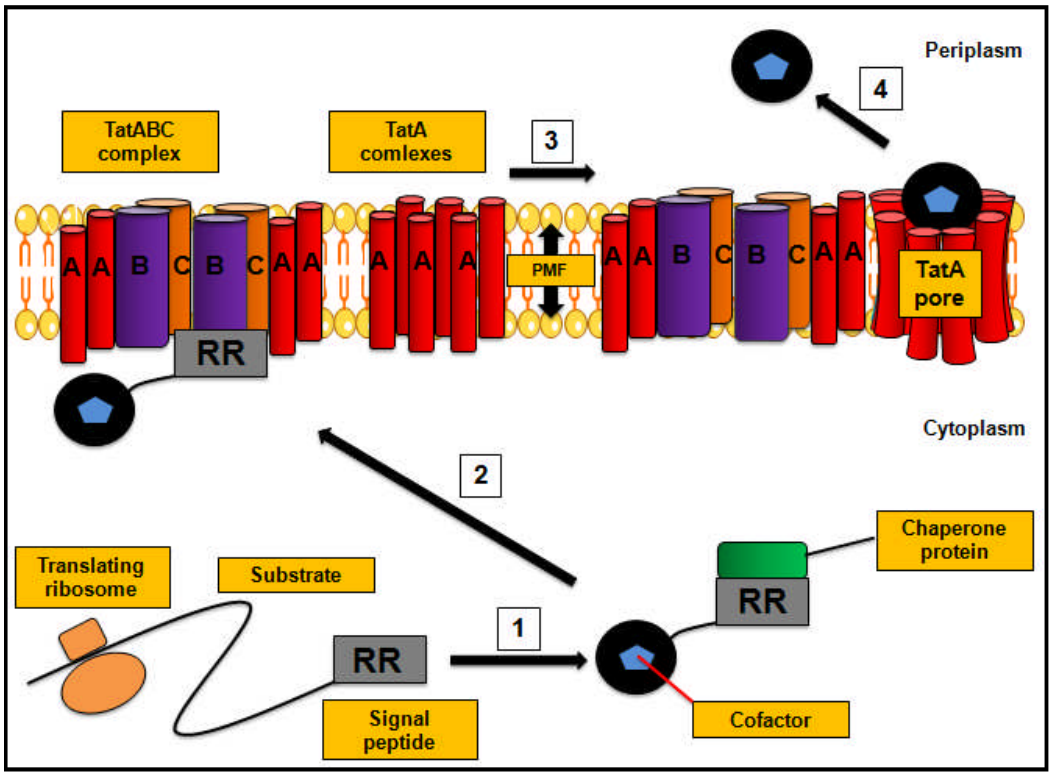

Figure 1.4.4 Proposed mechanism of Tat translocation in *E. coli*
The Tat substrate is translated at the ribosome. A substrate specific chaperone binds to the signal peptide preventing premature interaction of the substrate with the Tat machinery before cofactor insertion and correct protein folding has occurred (**1**). The signal peptide of the folded Tat substrate binds to the TatABC complex (**2**). TatA from separate complexes is recruited in a PMF dependent manner and the folded protein is translocated across the membrane, possibly through a pore formed by TatA (**3**). Upon translocation the signal peptide is cleaved and the mature protein is released into the periplasm (**4**).

1.4.8 The Tat pathway in Gram-positive bacteria

Interestingly, most Gram-positive bacteria possess a simpler "minimalist" Tat system which lacks a TatB component (Jongbloed *et al*., 2004) and contains instead a bifunctional TatA component (Jongbloed *et al*., 2006).

In *Bacillus subtilis*, two TatAC-type systems, TatAdCd and TatAyCy, operate in parallel with different substrate specificity (Jongbloed *et al*., 2006). PhoD is the only identified substrate of the TatAdCd pathway (Pop *et al*., 2002) and YwbN, a DyP-

dependent peroxidase, in contrast is translocated by the TatAyCy pathway (Jongbloed *et al*., 2004).

Again, two complexes are present at steady state: for example the TatAdCd system involves a ~ 230 kDa TatAdCd complex together with a ~ 160 kDa homo-oligomeric TatAd complex (Barnett *et al*., 2008) and the TatAyCy, is broadly similar (Barnett *et al*., 2009). These complexes therefore seem to be different to their *E. coli* counterparts in terms of size and composition, with the TatAd and TatAy complexes also appearing to lack the heterogeneity observed with the *E. coli* TatA complex. This suggests a different model for Tat-dependent protein transport to the one already described, involving a single defined translocon rather than several size variants (Barnett *et al*., 2008). However an alternative model has been presented in the literature, where a soluble population of TatA protein is proposed to act as the initial receptor for Tat substrates, with TatA-substrate complexes targeted to membrane localised TatCd (Schreiber *et al*., 2006).

The absence of any TatB component in most Gram-positive bacteria has suggested that the TatA component in these systems is bifunctional, performing the roles of both *E. coli* TatA and TatB (Jongbloed *et al*., 2006). In support to this idea recently it has been reported the presence of an N-terminal TatB-type domain within TatAd, along with a separate domain that seems to be universally conserved among TatA/TatB proteins (Barnett *et al*., 2011a).

1.4.9 The Tat pathway in chloroplasts

Like its *E. coli* counterpart, the chloroplast Tat translocase consists of three membrane proteins termed Tha4, Hcf106 and cpTatC which are homologues of the bacterial TatA, TatB and TatC respectively (Settles *et al*., 1997; Walker *et al*., 1999; Cline and Mori, 2001).

Hcf106 and Tha4 are single-spanning membrane proteins containing an N-terminal transmembrane domain followed by a short amphipathic α-helix and an unstructured

C-terminal domain. cpTatC is predicted to contain six transmembrane domains and both N- and C- termini are located in the stroma (Aldridge *et al*., 2009).

Chloroplast Tat components are organized into two complexes in the membrane. The first, Hcf106-cpTatC, is a large ~ 700 kDa complex which has been characterised by BN-PAGE analysis and co-immunoprecipitation of digitonin-solubilised thylakoid membranes (Cline and Mori, 2001). Unlike in *E. coli*, Tha4, on the other hand, has not been detected in the Hcf106-cpTatC complex at resting state, but is present as a separate homo-oligomeric complex (Dabney-Smith *et al*., 2006).

Mechanistic studies strongly suggest that substrates bind first to the Hcf106-cpTatC complex; substrates can be cross-linked to this complex under conditions that prevent full translocation (Cline and Mori, 2001; Gerard and Cline, 2006; Ma and Cline, 2000; Mori and Cline, 2002). Tha4 does cross-link to the cpTatC-Hcf106 complex in the presence of precursor protein and a thylakoid ΔpH (Mori and Cline, 2002), which suggests that the formation of the full translocon occurs under these conditions. Given the evidence that the Hcf106-cpTatC complex acts as substrate-binding unit (with the analogous TatABC complex carrying out a similar role in bacteria) it seems likely that the separate Tha4 complex, as TatA in bacteria, could form the translocation pore.

Cross-linking studies have shown that Tha4 undergoes conformational rearrangements during active protein transport, with the amphipathic helix and C-terminal tail interacting only in response to conditions leading to protein transport (Dabney-Smith *et al*., 2006). Binding of the precursor can occur in the absence of a ΔpH (Ma and Cline, 2000), but the thylakoid proton gradient induces a tighter interaction between the signal peptide and cpTatC and Hcf106 such that, during transport, the signal peptide is bound deep within the Tat receptor complex (Gerard and Cline, 2007).

1.5 Aims and objectives of this study

The overall aim of the work presented in this thesis is to gain novel insights into the assembly and mechanism of the *E. coli* and *B. subtilis* twin-arginine translocation pathways by focusing on some largely uncharacterized aspects. To achieve this goal the following questions are addressed using a number of biochemical and biophysical techniques:

1. Previous studies of Tat-dependent translocation in *E. coli* have focussed on the 3 proteins that are essential for the functioning of this system, namely TatA, TatB, and TatC. However in *E. coli* an addition TatA paralog, TatE is also constitutively expressed that can partially substitute for the function of TatA. Despite this, the TatE protein has been largely overlooked and several questions about its role remain unanswered.

- *Does the TatA paralog TatE function in Tat-dependent translocation in E. coli and can it support the translocation of a range of different substrates?*

- *Does the TatE protein assemble into homo-oligomeric complexes within the plasma membrane similar to TatA?*

- *Can we deduce anything about the possible mechanism of translocation from the biophysical characterisation of TatE?*

2. It has been reported that TatA proteins can have a dual localisation in bacteria and can be found in both membrane and soluble fractions. The functional significance of soluble TatA pools is not currently clear. It is not known if TatE shows similar behaviour in *E. coli*.

- *Does TatE have a dual localization in both membrane and cytosolic compartments in E. coli?*

- *If so, is soluble TatE functional, or is soluble TatE mis-localised?*

3. TatE is constitutively expressed in *E. coli*; it is thus reasonable to propose that it may form structural or functional interactions with one or more of the other Tat subunits. This hypothesis is tested in this study.

- *Does TatE interact with TatA, TatB, and TatC in E. coli? If so what is the nature of these interactions?*

4. In the Gram-positive bacterium *B. subtilis* two independent Tat systems operate in protein secretion. These two pathways are composed of a single TatA and TatC subunit (TatAdCd and TatAyCy). However *B. subtilis* also has a third TatA protein called TatAc and its function remains enigmatic.

- *Does TatAc function in Tat dependent translocation and can the TatAc protein form active Tat systems with both TatCd and TatCy?*

Chapter 2.

Materials and Methods

2.1 Suppliers of materials

Chemicals were obtained from the companies indicated below.

Acros (UK): Methyl viologen and Trimethylamine-*N*-oxide.

Amersham Pharmacia Biotech (UK): ECL™ detection reagents; Native protein markers for gel electrophoresis and gel filtration chromatography; Hybond™-P PVDF membrane, Q-sepharose anion exchange resin, and Superdex™-200 HR 10/30 pre packed gel filtration column.

Calbiochem (Germany): Digitonin; *n*-Dodecyl-*ß*-D-maltoside.

Fermentas (UK): Bradford reagent; GeneRuler™ 1kb DNA ladder and *EcoRI, NcoI, HindIII, PstI* restriction enzyme

Fisher Scientific (UK): Acetic acid (glacial); Acetone; Ethanol; Formaldehyde; Glycerol; Glycine; Hydrochloric acid; Magnesium sulphate; Methanol; Sodium chloride; sodium dodecyl sulphate; Sucrose, and Tris.

Fuji (Japan): Super RX film.

IBA (Germany): Biotin Blocking Buffer, Buffer E; Streptactin™ HRP-conjugate and Streptactin™ -affinity chromatography resin.

Invitrogen (USA): Anti-GFP monoclonal antibody; Proteinase K and T4 DNA ligase.

Melford (UK): Isopropyl-*ß*-D-thiogalactoside.

New England Biolabs (USA): Pre-stained broad range protein markers.

Premier International Foods (UK): Marvel milk powder.

Promega (UK): Anti-rabbit-HRP and dNTPs mix.

Qiagen (Germany): QIAprep miniprep kit, DNeasy™ blood & tissue kit and QIAprep Gel Extraction kit.

Roche applied science (UK): Complete™ protease inhibitor cocktail tablets.

Serva (Germany): Serva G Coomassie blue.

Sigma-Aldrich (UK): Aminocaproic acid; Ampicillin; L-arabinose; Avidin; Bis-Tris; *ß*-mercaptoethanol; Bovine serum albumin; C12E9; Kanamycin; Lysozyme; Protein A-Sepharose™; Silver nitrate; Sodium carbonate; Sodium dithionite; Sodium thiosulphate; Sodium molybdate; TEMED; Tricine; Triton X-100, Triton X-114; Trizma and Custom DNA primers.

Stratagene (UK): *Pfu* DNA polymerase, *DpnI* restriction enzyme and QuikChange™ site-specific mutagenesis system.

VWR (UK): 40% Acrylamide solution; Ammonium persulphate; Bromophenol blue; Calcium chloride; Disodium hydrogen phosphate; EDTA; Glucose; Magnesium chloride; Potassium chloride; Sodium dihydrogen phosphate; Sodium hydroxide pellets; Trichloroacetic acid and Tween 20.

Whatmann (UK): 3mm filter paper.

2.2 Growth and storage of *E. coli* cultures

2.2.1 Strains of *E. coli* used

All strains of *E. coli* used are given below in table 2.2.1

Strain	Genotype	Reference
MC4100	*F- ΔlacU169, araD139, rpsL150, relA1, ptsF,rbs, flbBS301*	Casadaban and Cohen, 1980
ΔtatABCDE	MC4100 *ΔtatABCDE, Ara^r*	Sargent *et al*., 1998
ΔtatAE	MC4100 *ΔtatA/E, Ara^r*	Sargent *et al*., 1998
ΔtatA	MC4100 *ΔtatA, Ara^r*	Sargent *et al*., 1998
ΔtatB	MC4100 *ΔtatB, Ara^r*	Sargent *et al*., 1998
ΔtatC	MC4100 *ΔtatC, Ara^r*	Sargent *et al*., 1998
DH5α	*supE44, ΔlacU169(80lacZΔM15), hsdR17, recA1, endA1, gyrA96, thi-1, relA1*	Sambrook *et al*., 1989

Table 2.2.1 Strains of *E. coli* used in this work

2.2.2 Standard growth conditions

E. coli were cultured using liquid Luria-Bertani (LB) media (10 g/l NaCl; 10 g/l bactotryptone; and 5 g/l yeast extract). Media was pre-warmed to 37 °C before inoculation with a bacterial colony taken from an agar plate.Unless otherwise stated liquid cultures were grown at 37 °C in a shaking incubator at 200 rpm overnight (~ 16 hours).

E. coli cells were cultured on solid media (LB + 16 g/l bacto-agar) by streaking 5 µl of liquid culture over a fresh agar plate, followed by incubation at 37 °C overnight (~ 16 hours). *E. coli* cultures were stored on LB-agar plates at 4 °C for a maximum of 6 weeks.

2.2.3 Antibiotic supplements

Ampicillin (100 μg/ml), and Kanamycin (50 μg/ml) were used in cultures carrying pBAD24 and pEXT22 plasmids respectively.

2.2.4 Storage of *E. coli* cells

Glycerol stocks of *E. coli* cultures were prepared for long-term storage by mixing 2 parts of liquid culture with 1 part of 50 % (v/v) glycerol. Cultures were frozen on dry ice and then stored -70 °C.

2.3 Preparation and transformation of competent cells

2.3.1 Preparation of competent *E. coli* cells

A 5 ml culture of *E. coli* cells was cultured overnight as described (2.2.2) and 1 ml diluted in 9 ml of fresh LB. The culture was grown until it reached an OD_{600} of ~ 0.3-0.4. Cells were pelleted by centrifugation at 4000 *g* (Beckman Jouan GR422) at 4 °C for 15 min and re-suspended in 10 ml ice-cold of solution A (10 mM MOPS pH 6.5, 10 mM rubidium chloride pH 6.5). The cells were pelleted, re-suspended in 10 ml of ice-cold solution B (10 mM MOPS pH 6.5, 10 mM rubidium chloride pH 6.5, and 50 mM $CaCl_2$ pH 6.5), and incubated at 4 °C for ~ 1 hour. Cells were collected and re-suspended in 1 ml of solution B. The cells were used within 2 days.

2.3.2 Preparation of plasmid DNA from *E. coli* cells

A 5 ml culture of *E. coli* cells was cultured overnight as described (2.2.2). Plasmid DNA was extracted from the culture using a 'Mini-prep' kit (Qiagen, Germany). The preparation was carried out exactly as instructed by the manufacturer. Plasmid DNA was recovered in 30 μl dH_2O and stored at -20°C.

2.3.3 Transformation of competent *E. coli* cells with plasmid DNA

2 µl of plasmid DNA prepared as described (2.3.2) was incubated with 100 µl of competent cells (2.3.1). Cells were incubated on ice for half an hour before being heated to 42 °C for 1 minute. Cells were then put back on ice for 5 minutes. The transformed cells were diluted with 1 ml of fresh LB and cells subsequently cultured at 37 °C with agitation at 200 rpm for exactly 1 hour. The culture was then grown on LB-agar plates (2.2.2), and transformants selected for with appropriate antibiotics (2.2.3).

2.3.4 Bacterial plasmids used in this work

Bacterial plasmids used in this work are given below in table 2.3.4.

Plasmid	Properties	Reference/source
pBAD24	Cloning Vector *araC, Amp*^{r}	Guzman *et al*., 1992
pEXT22	Cloning Vector *lacl Kan*^{r}	Dykxhoorn *et al*.,1996
pBAD-ABC-Strep	pBAD24 + *E. coli tatABC-strep*	Bolhuis *et al*.,2001
pBAD-E-Strep	pBAD24 + *E. coli tatE-strep*	Baglieri *et al*., 2012
pBAD-A-Strep	pBAD24 + *E. coli tatA-strep*	Warren *et al*., 2009
pBAD-A	pBAD24 + *E. coli tatA*	This study
pBAD-Ac-Strep	pBAD24 + *B. subtilis tatAc-strep*	Monteferrante *et al*., 2012
pBAD-AcCd-Strep	pBAD24 + *B. subtilis tatAcCd-strep*	Monteferrante *et al*., 2012
pBAD-AcCy-Strep	pBAD24 + *B. subtilis tatAcCy-strep*	Monteferrante *et al*., 2012
pBAD-ssDmsA-GFP	pBAD24 + ss-*dmsA-gfp*	Ray *et al*., 2003
pBAD-ssAmiA-GFP	pBAD24 + ss-*amiA-gfp*	Barnett *et al*., 2009
pBAD-ssMdoD-GFP	pBAD24 + *ss-mdoD-gfp*	Barnett *et al*., 2009
pBAD-Cd-Strep	pBAD24 + *B. subtilis tatCd-strep*	Monteferrante *et al*., 2012
pBAD-Cy-Strep	pBAD24 + *B. subtilis tatCy-strep*	Monteferrante *et al*., 2012
pRD8	pING1 derivative containing the *E. coli Lep* gene; Amp^r	Dalbey and Wickner 1985

Plasmid	Properties	Reference/source
pEXT-E-Strep	pEXT22 + *E. coli tatE-strep*	This study
pEXT-Ac-Strep	pEXT22 + *B. subtilis tatAc-strep*	Carmine Monteferrante (University of Groningen)

Table 2.3.4 List of plasmids used in this work

2.3.5 Affinity tag used

To facilitate protein detection and purification C-terminal tags were used where stated. The 10 amino acid *Strep*-II™ tag (IBA, Germany) was present at the C-terminus of *E. coli* TatC, TatE, TatA and *B. subtilis* TatAc, TatCd and TatCy proteins.

2.4 DNA manipulation and cloning techniques

2.4.1 Preparation of Genome DNA from *E. coli*

E. coli chromosomal DNA was isolated using a DNeasy™ blood & tissue kit. The kit was used according to the manufacturer's instructions. The extracted genome DNA was recovered in 50 μl dH_2O and used as the template of PCR.

2.4.2 Primers used for the construct generated

All primers were supplied by Invitrogen (UK). In the table below, which lists primers used and created for this study, restriction enzyme sites are underlined, the nucleotides encoding the affinity tag are shown in **bold**, and nucleotides identical to the genomic DNA are capitalized.

Construct Generated	Name of primers	Primer sequence (5' to 3')
pBAD-E-Strep	tatE_NcoI_for	ataccATGGGTGAGATTAGTATTAC
	tatEs_PstI_rev	tatccagtctgcagcctcctttat**tttttcaaactgtgggtgcgaccacgccga**CTCTTTATGAGAGAG

Table 2.4.2 DNA primers used for the preparation of the pBAD-E-Strep construct

2.4.3 Site-directed *in vitro* mutagenesis of plasmid DNA

Point mutations were introduced into *E. coli* plasmid DNA using the QuikChange™ site-specific mutagenesis system (Stratagene, USA), following the manufacturer's instructions. PCR reactions were performed using a Biometra T3 thermocycler. The PCR product was used to transform *E. coli* DH5α competent cells as described (2.3.3).

2.4.4. Primers used for the mutagenesis of *tatA-strep*

The table below lists the primers used for the site directed mutagenesis of pBAD-A-Strep in order to add a stop codone which would prevent the translation of the C-terminal *Strep*-II™ tag. Mutations are underlined.

Construct Generated	Name of primers	Primer sequence (5' to 3')
pBAD-A	STOP_for	gccacgataaagagcaggtgtaagcgtggtcgca
	STOP_rev	tgcgaccacgcttacacctgctctttatcgtggc

Table 2.4.4 DNA primers used for site-directed mutagenesis of pBAD-A-Strep

2.4.5 PCR

PCR was typically performed with 5 µl 10x enzyme buffer, 1 µl 10 mM dNTP mix, 1.5 µl, 1.25 µl of each primer (from 20 µM stock), 1 µl template DNA (0.5 ng), 1 µl *pfu turbo* DNA polymerase (5 units/µl) and dH_2O to a final volume of 50 µl.
The reactions were performed in a Biometra T3 Thermocycler with the following cycling conditions:

95°C	1 min	
95°C	30 sec	35 cycles
52°C	45 sec	
72°C	2 min	
72°C	10 min	
2°C	pause	

2.4.6 Agarose gel electrophoresis

Agarose gels were prepared by dissolving 1–2 % (w/v) agarose in TBE buffer (89 mM Tris; 89 mM H_3BO_3; 20 mM EDTA, pH 8.0). Ethidium bromide was added (0.5 µg/ml final concentration) to allow visualisation of DNA. DNA samples were prepared by adding 2 µl of loading dye (0.25 % (w/v) bromophenol blue, 40 % (w/v) sucrose).

Gels were submerged in TBE buffer and electrophoresis was performed at 100–150 V until the dye front was at least half way through the gel. DNA was visualised using a UV transilluminator and photographs of gels were taken on a gel documentation system.

2.4.7 Purification of DNA by gel extraction

DNA was excised from agarose gels and extracted using a QIAprep Gel Extraction kit (Qiagen, Germany). The kit was used according to the manufacturer's instructions and DNA was recovered in 30 µl of Elution Buffer

2.4.8 Restriction endonuclease digestion of DNA

Restriction endonuclease digestion of DNA was performed according to the enzyme manufacturer's directions. Reactions were typically incubated at 37 °C for 1–2 hours in a 37 °C water bath, before being subjected to gel electrophoresis and purified as detailed in 2.4.7.

2.4.9 Ligation of DNA fragments

Ligation reactions were performed using T4 DNA ligase (Invitrogen) according to the manufacturer's instructions. Vector and insert DNA fragments were mixed in a 1:3 ratio of their concentrations and typically incubated at room temperature for 3 hours or overnight at 4 ºC.

2.4.10 Determination of DNA concentration

The concentration of DNA was measured by NanoDrop ND1000 spectrophotometer.

2.4.11 Sequencing of plasmid DNA

Sequencing was performed by the Molecular Biology Service, University of Warwick, using Big Dye Terminator v 3.1 Chemistry and run on a 3130xl Genetic Analyser^{TM} (Applied Biosystems). Chromas 2.33 (Technelysium Pty Ltd) software was used to analyse DNA sequence.

2.4.12 Sequencing primers used in this study

Name	Sequencing Target	Primer sequence (5' to 3')	Source
BADSEQ_F	pBAD24	TATTTGCACGGCGTCACA	C. Matos (University of Warwick)
BADSEQ_R	pBAD24	AAAACTCTCAAGGATCTT	C. Matos (University of Warwick)
pEXT22SEQ_F	pEXT22	CGCTCAAGGCGCACTCCCG	C. Matos (University of Warwick)
pEXT22SEQ_R	pEXT22	CCGCGCACATTTCCCCG	C. Matos (University of Warwick)

Table 2.4.12 Sequencing primers used in this study

2.5 Protein preparation

2.5.1 Induction of plasmids

Typically, induction of pBAD24 and pEXT22 plasmids was achieved by the addition of 1 μM arabinose and 5 mM IPTG to the growth medium respectively. Under standard conditions, plasmid induction was allowed to proceed until the culture reached mid-exponential growth phase (~ 3 hours).

Where cells carried pBAD24 and pEXT22 plasmids (for example, in GFP export assays), the pBAD24 plasmid was induced first for ~ 2 hours before removal of arabinose from the growth medium and subsequent induction of the pEXT22 plasmid for ~ 2 hours.

2.5.2 Fractionation of *E. coli* cells

E. coli cells were separated into periplasm, cytoplasm, and membrane samples using the previously described lysozyme/cold osmotic shock method (Randall and Hardy,1986). Briefly, the cells from a 10 ml culture of *E. coli* were pelleted down by centrifugation before being resuspended in 0.5 ml of pre-chilled disruption buffer (100 mM Tris-acetate pH 8.2, 500 mM sucrose and 5 mM EDTA). 0.5 ml of H_2O and 40 µl of a 4 mg/ml stock of lysozyme were added simultaneously to the cell suspension. Samples were incubated in an ice bucket for 5 to 10 minutes. The resulting spheroplasts were treated with 20 µl of 1 M $MgSO_4$ and pelleted by centrifugation at 20800 *g* (14000 rpm, Eppendorf 5417R). The supernatant (the periplasmic fraction) was collected. Spheroplasts were washed using 1 ml sonication buffer (50 mM Tris-acetate pH 8.2, and 2.5 mM EDTA) that had been pre-cooled, and briefly sonicated (30 seconds at ~ 8 microns) to break the membranes. The membrane and cytoplasmic compartments were separated by ultracentrifugation at 265000 *g* (70000 rpm) for 30 minutes (using a Beckman TL100.3 rotor that had been pre-cooled to 4 °C). Membranes were solubilised in 0.5 ml sonication buffer containing 1 % (w/v) SDS unless otherwise stated and incubated at room temperature with constant rotation.

2.5.3 Isolation and solubilisation of *E. coli* membranes for protein purification and gel filtration chromatography

For purification of proteins from the membrane fraction, membranes were prepared from a 500 ml culture of *E. coli* as described above (2.5.2) but using 50 times the volume of the buffer or reagent stated (complete protease inhibitor tablets were added to disruption and sonication buffer). Membranes were solubilised, using a syringe and needle, in 5 ml of buffer (20 mM Tris-HCl pH 8.0, 150 mM NaCl), supplemented with detergent and they were incubated at 4 ºC with constant rotation overnight. Detergents used for solubilisation were: digitonin, 2 % (w/v), *n*-dodecyl-*ß*-D-maltoside 2 % (w/v) and C12E9 2 % (w/v). Insoluble material was removed by

centrifugation at 265000 *g* (70000 rpm) for 15 min (using a Beckman TL100.3 rotor) at 4°C.

2.6 Protein chromatography methods

2.6.1 Q-Sepharose anion exchange chromatography

E. coli membranes were prepared from 500 ml cultures as described (2.5.3) and solubilised in buffer containing the stated detergent. Membranes were run directly through a 5 ml anion exchange column (Q-Sepharose) that had been pre-washed with 10 ml of equilibration buffer (20 mM Tris-HCl pH 8.0, and 0.1 % detergent). The column was subjected to washing with 10 ml of equilibration buffer plus 100 mM NaCl to remove weakly bound proteins from the column. The proteins were eluted with 10 x 1 ml of elution buffer (20 mM Tris-HCl pH 8.0, 300 mM NaCl. and 0.1 % detergent). Eluted fractions were diluted in equilibration buffer (without salt) to reduce the NaCl concentration to 150 mM.

2.6.2 Streptactin^{TM}-Sepharose affinity chromatography

Streptactin^{TM}-affinity chromatography was performed with membrane proteins that had already been partially purified by anion exchange chromatography (2.6.1). Generally and unless stated otherwise a 2 ml Streptactin^{TM} -affinity column was used. Columns were pre-equilibrated in 4 ml of equilibration buffer (20 mM Tris-HCl pH8.0, 150 mM NaCl, and 0.1 % detergent) prior to use. Before application to the column samples were incubated with 1 μM avidin at 4 ºC with constant rotation overnight to prevent the nonspecific binding of biotinylated proteins to the Streptactin^{TM} resin. Following sample application the column was washed with equilibration buffer (typically using 16 ml) before elution with 10 x 0.5 ml of buffer E plus detergent (20 mM Tris-HCl, 150 mM NaCl, 0.1 % detergent, and 2.5 mM desthiobiotin).

2.6.3 Superdex^{TM}-200 gel filtration chromatography

Gel filtration chromatography was used in order to estimate the masses of protein complexes and as a final clean-up step in protein purification for further electron microscopy studies.

240 µl of the most concentrated fraction eluted from a Streptactin^{TM}-affinity column (2.6.2) was injected onto a Superdex^{TM}-200 column attached to an AKTA purifier FPLC system (Amersham bioscience UK). The column was pre-equilibrated with buffer (20 mM Trizma-HCl, 150 mM NaCl, and 0.1 % (w/v) detergent). Following sample application the protein was eluted from the column using a single column volume of the equilibration buffer. The eluted sample was collected in 0.5 ml fractions.

For analytical studies the protocol used was the same as above except detergent solubilised membranes were applied directly to the Superdex^{TM}-200 column. Membranes were prepared as described in 2.5.2.

2.6.4 Gel filtration chromatography: estimation of mass of protein complexes

In order to estimate the mass of protein complexes the Superdex^{TM}-200 gel filtration column was calibrated. To achieve this, four protein standards of known molecular mass were run through the column 2 at a time. These were albumin 66 kDa, and thyroglobin 669 kDa; and aldolase 158 kDa and ferritin 440 kDa. Elution volumes of these standards were used to prepare a calibration curve to allow the estimation of the mass of a protein complex of unknown size from its peak elution volume.

2.6.5 Determining the concentration of purified protein

The concentration of purified proteins was determined using a Bradford reagent (Fermentas, UK). The method used was exactly as recommended by the manufacturer. The data were measured spectrophotometrically (Jenway 6505 UV/Vis spectrophotometer) and compared to the standard curve.

2.7 Protein electrophoresis

2.7.1 SDS polyacrylamide gel electrophoresis (SDS-PAGE)

SDS polyacrylamide gels were cast and run on a vertical gel electrophoresis system (CBS) according to the manufacturer's instructions. Typically 0.75 mm gels were prepared with a separating gel (17.5 % v/v acrylogel solution; 375 mM Tris-HCl pH 8.8; 0.1 % (v/v) SDS; 0.02 % (w/v) APS; 0.06 % (v/v) TEMED) and a stacking gel (5 % (v/v) acrylogel solution; 125 mM Tris-HCl pH 6.8; 0.1 % (v/v) SDS; 0.6 % (w/v) APS; 0.06 % (v/v) TEMED).

Samples were prepared by mixing with SDS sample loading buffer (125 mM Tris-HCl pH 6.8, 20 % (v/v) glycerol, 4 % (v/v) SDS, 0.02 % (w/v) bromophenol blue, 5 % (v/v) β-mercaptoethanol) and boiling for 10 min. Samples to be immunoblotted with Tat antibodies were heated to 50 ºC for 10 min.

A uniform running buffer (25 mM Tris; 250 mM glycine; 0.1 % (v/v) SDS) was used for electrophoresis. Gels were run until the dye front had migrated off the gel, typically 3 hours at 35 mA or 16 hours overnight at 2 mA.

2.7.2 Native gel electrophoresis (N-PAGE)

All native gel electrophoresis was performed using the C.B.S. (USA) vertical gel system as instructed by the manufacturer. A 10 % resolving gel was used (10 % (v/v)

acrylogel; 375 mM Tris-HCl pH 8.8; 0.1 % (w/v) APS, and 0.06 % (v/v) TEMED). A 5 % stacking gel was used over the resolving gel (5 % (v/v) acrylogel; 125 mM Tris-HCl pH 6.8; 0.6 % (w/v) APS, and 0.06 % (v/v) TEMED).

Samples were prepared by mixing 1:1 with native sample loading buffer (125 mM Tris-HCl pH 6.8, 20 % (v/v) glycerol, and 0.02 % (w/v) bromophenol blue).

Electrophoresis was performed using a uniform buffer (25 mM tris and 250 mM glycine), and gels were run at 30 mA for approximately 3 hours.

2.7.3 Blue-native polyacrylamide gel electrophoresis (BN-PAGE)

The BN-PAGE protocol was based on the method of Schägger and von Jagow (1991) using the same equipment as SDS-PAGE. A 1.5 mm gradient gel was prepared by combining a 5% acrylamide solution (5 % acrylogel; 50 mM Bis-Tris-HCl pH 7.0 (at 4 ºC); 500 mM aminocaproic acid; 0.76 % (v/v) glycerol; 4 % (v/v) APS; 0.4 % (v/v) TEMED) with a 13 % acrylamide solution (13 % acrylogel; 50 mM Bis-Tris-HCl pH 7.0 (at 4 ºC); 500 mM aminocaproic acid; 5 % (v/v) glycerol; 0.35 % (w/v) APS; 0.035 % (v/v) TEMED) in a gradient maker. A stacking gel (4 % acrylogel; 50 mM Bis-Tris-HCl pH 7.0 (at 4 °C), 0.5 mM aminocaproic acid; 0.7 % APS; 0.07 % TEMED) was added.

Gradient gels were equilibrated at 4 ºC before loading samples. Typically 1 µl of sample buffer (760 mM aminocaproic acid, 50 µM Bis-Tris-HCl pH 7.0, 5 % (w/v) Serva G Coomassie blue) was added to 10 µl of solubilised membrane.

Gels were initially run at 70 V at 4 ºC with coloured cathode buffer (50 mM Tricine pH 7.0, 15 mM Bis-Tris-HCl pH 7.0 (at 4 ºC), 0.02 % (w/v) Serva G Coomassie blue) and anode buffer (50 mM Bis-Tris-HCl pH 7.0 (at 4 °C)). When the gel front had migrated half way through the gel the coloured cathode buffer was replaced with clear cathode buffer (50 mM Tricine pH 7.0, 15 mM Bis-Tris-HCl pH 7.0 (at 4 °C)) and the gel was run overnight.

After electrophoresis the gel was equilibrated for 15 min in clear cathode buffer containing 0.05 % SDS before transfer to PVDF membrane.

2.8 Protein detection

2.8.1 Protein detection by Western blotting

Western blotting was used to transfer protein from SDS-PAGE gels onto PVDF membranes and was performed using semi-dry western blotting apparatus, (Sigma, UK). The apparatus was used exactly as instructed by the manufacturer. A uniform Towbin transfer buffer was used (25 mM Tris, 192 mM glycine, and 20 % methanol) (Towbin *et al.*, 1979). Briefly, two sheets of Whatman paper soaked in transfer buffer were placed onto the positive electrode. PVDF membrane pre-soaked in methanol was placed over the Whatman paper and the gel placed on top. Finally a top layer of two sheets of Whatman paper soaked in transfer buffer was placed over the gel. The transfer of proteins was achieved using ~ 200 mA of current over a two hour period.

For transfer of proteins from blue-native (BN) gel, a different buffer was used, (50 mM Tricine pH 7.0, 15 mM Bis-Tris-HCl pH 7.0 and 0.05 % SDS). The PVDF membrane was prepared by soaking in methanol, followed by water and then the BN transfer buffer. Following the transfer of proteins from a BN-gel, the PVDF membrane was de-stained for 1 hour using 25 % methanol and 10 % acetic acid, before finally being washed with PBS-T (137 mM NaCl, 2.7 mM KCl, 10 mM Na_2PO_4 and 0.01 % Tween 20).

2.8.2 Detection of proteins by immunoblotting

After transfer, PVDF membranes to be immunoblotted with antibodies to the *Strep*-II^{TM} tag were blocked with PBS-T pH 7.4 containing 3 % BSA for at least 1 hour. The membranes were washed in PBS-T (typically 1 x 15 min, 2 x 5 min) before incubation in PBS-T with Biotin Blocking Buffer for 10 min.

The Streptactin™-horseradish peroxidase (HRP) conjugate antibody (IBA) was added directly to the biotin blocking solution according to the manufacturer's instructions and incubated, with agitation, for 2 hours.

PVDF membranes to be immunoblotted with other antibodies were blocked with PBS-T containing 5 % (w/v) dried skimmed milk powder for at least 1 hour. The membranes were washed in PBS-T before incubation with PBS-T containing the desired primary antibody for 1 hour. The membranes were washed before incubation with the secondary antibody for 1 hour.

The membranes were washed and immunoreactive bands were detected using the ECL™ (enhanced chemiluminescence) kit (Amersham Biosciences) according to the manufacturer's instructions.

X-ray films (super RX film, Fujifilm) were developed on an AGFA Curix 60 automatic developer according to the manufacturer's instructions.

Antibodies used for immunodetection are listed below in table 2.8.2.

Antibody	Concentration	Manufacturer/Source
Rabbit anti-TatA	3 in 20000	Laboratory stock (Bolhius *et al.*, 2000)
Rabbit anti-GFP	3 in 20000	Invitrogen, USA
Rabbit anti-Lep	3 in 20000	Gunner von Heijne (University of Stockholm)
Mouse anti-*Strep*-II tag HRP conjugate	1 in 10000	IBA, Germany
Anti-rabbit IgG HRP conjugate	1 in 10000	Promega, USA

Table 2.8.2 Antibodies used for immunodetection

2.8.3 Silver staining

Following SDS-PAGE (2.7.1), gels were placed in fixer (50 % acetone, 1.25 % TCA, and 0.015 % formaldehyde) and incubated for 15 minutes. Fixer was washed from the gel with H_2O and the gel incubated with 50 % acetone for 5 minutes followed by 1 minute in sodium thiosulphate solution (0.02 % (w/v)). Gels were washed with H_2O before incubation in staining solution (0.4 % formaldehyde and 0.25 % (w/v) silver nitrate). After 8 minutes the staining solution was washed from the gel with H_2O before incubation with developer solution (0.2 mM sodium carbonate, 0.004 % (w/v) sodium thiosulphate, and 0.015 % formaldehyde). Once protein bands became apparent the staining was stopped. This was achieved by incubating the gel with 1 % acetic acid. The gel was finally washed in H_2O and then dried.

2.8.4 TMAO reductase (TorA) activity assays

The presence of TMAO reductase (TorA) was detected using a protocol adapted from Silvestro *et al.* (1989). *E. coli* cell fractions were prepared as described (2.5.1) and proteins separated by native-PAGE (2.7.2).

Immediately after electrophoresis the gel was submerged in 100 mM phosphate buffer pH 6.5 that contained 0.25 % (w/v) methyl viologen. Buffer was completely saturated with N_2 before use. The gel was then stained blue by 0.1 % (w/v) sodium dithionite (that was pre-dissolved in 0.1 M NaOH). The gel was allowed to stain for around 15 minutes before being transferred into fresh phosphate buffer (completely saturated with N_2) supplemented with 40 mM TMAO until white bands were visualised. The gels were then scanned as they developed.

2.9 Confocal microscopy

Samples were prepared for imaging by adsorbing liquid culture onto 3% agar containing growth medium. The agar was placed in an in-house built sample holder and covered with a cover slip. Imaging was performed on a laser scanning confocal microscope (LSCM) (Leica DMRE) equipped with a Leica TCS SP2 confocal unit, an acousto-optical beam splitter (AOBS^{TM}) and a 100mW argon laser. For image acquisition the laser was set to 488 nm. A 63x oil immersion objective was used.

2.10 Triton X-114 to separate membrane and soluble proteins

The separation of proteins into aqueous and detergent fractions was performed as described previously in a paper by Bordier, (1981) using the detergent Triton X-114.

E. coli cell fractions were prepared (2.5.2) and both the membrane and cytosolic fractions supplemented with 1 % Triton X-114. Samples were mixed well and incubated in an ice bucket for 30 minutes. The detergent solution was allowed to undergo a phase separation into detergent and aqueous phases by incubating the samples at 30 °C for 5 minutes.

The samples were centrifuged in a bench top centrifuged at 300 *g* for 3 minutes to separate the two phases. The aqueous phase was collected and fresh Triton X-114 was added (to 1 %) before repeating the above procedure. The detergent phase was collected and re-suspended in sonication buffer 3 (2.5.2) and the above procedure again repeated. The aqueous phase was finally collected and the detergent phase collected and re-suspended in sonication buffer. As well as using cell fractions, purified proteins prepared in buffer supplemented with 1 % Triton X-114 were also used.

2.11 Trichloroacetic acid (TCA) precipitation

Protein samples were concentrated for gel electrophoresis by TCA precipitation. One volume of 100 % (v/v) TCA was added to four volumes of protein sample and incubated for 10 minutes at 4 °C. The samples were centrifuged for 5 minutes at 12100 g (13400 rpm, Eppendorf 5417R). The supernatant was removed and 200 µl ice-cold acetone was added. The sample was incubated on ice for 5 minutes before centrifugation for 5 minutes. This step was repeated for a total of two acetone washes. The supernatant was removed and samples were allowed to air dry in 95 °C heat block for 5-10 minutes. Typically samples were resuspended in 80 µl SDS sample loading buffer (2.7.1).

2.12 Protease accessibility experiments

For the protease accessibility experiments *E. coli* cells were pelleted down and spheroplasts were prepared by resuspending the cell pellet in 2.5 ml of buffer (33 mM Tris-HCl pH 8.0, 40 % sucrose, and 5 mM Na_2EDTA 0.1 mg/ml).

Cells were incubated at 4 °C for 30 minutes and then harvested at 4000 *g* (Beckman Jouan GR422) for 15 min. The resulting spheroplast pellet was resuspended in 1 ml of ice-cold buffer (33 mM Tris-HCl and 40 % sucrose). Aliquots (50 µl) of the spheroplast preparations were incubated at 25 °C for 30 minutes in the presence of 0.5 mg/ml proteinase K (Invitrogen) and or 2 % (v/v) Triton X-100.

Samples were subjected to precipitation with TCA (2.11) and then analyzed by SDS-PAGE (2.7.1) and immunoblotting (2.8.2).

2.13 Co-immunoprecipitation experiments

For the co-immunoprecipitation experiments, *E. coli* cells were fractionated (2.5.2) and membranes were solubilised in 2 % digitonin. Aliquots of samples were diluted

to 500 µl of solubilization buffer (20 mM Tris-HCl pH 8.0, 150 mM NaCl, 0.1 % digitonin).
3 µl of the appropriate antibody was added (1 in 2000 dilution) and the sample was left rotating for 3 hours at 4 °C. 10 mg of Protein-A-Sepharose™ (Sigma-Aldrich) was soaked in 500 µl of solubilisation buffer for 5 minutes.

Each sample was added to 500 µl of Protein-A-Sepharose™ and left rotating for 2 hours at 4 °C. The sample was then centrifuged at 20800 *g* (14000 rpm, Eppendorf 5417R). The supernatant was collected and the pellet was washed with solubilisation buffer three times discarding the supernatants.

The pellet was finally resuspended in 400 µl of solubilisation buffer. Aliquots of pellet and supernatant were mixed with SDS sample loading buffer (2.7.1) and then analyzed by SDS-PAGE (2.7.1) and immunoblotting (2.8.2).

2.14 Single-particle electron microscopy

Analysis was carried out by Daniel Beck, University of Warwick. Methods are detailed in Baglieri *et al*. (2012).

2.15 Specialist software used in this study

AIDA software (Fujifilm, Japan): analysis of protein band intensities after SDS-PAGE (2.7.2) and detection by ECL™ detection reagent (2.8.2)

ClustalW: alignment of protein sequences

Chromas 2.33 (Technelysium Pty Ltd)**:** analysis of DNA sequences

Clone manager: construction of plasmid maps and design of cloning strategies

PSRIPRED: Protein secondary structure prediction (Jones, 1999; McGuffin *et al*., 2000). http://bioinf.cs.ucl.ac.uk/psipred

Chapter 3.

Purification and characterization of Escherichia coli TatE complexes

3.1 Introduction

In *Escherichia coli*, the minimal set of components required for Tat-dependent translocation are three integral membrane proteins, TatA, TatB and TatC, encoded by the *tatABC* operon, with molecular masses of 10, 18 and 30 kDa respectively (Bogsch *et al*., 1998; Sargent *et al*., 1998; Weiner *et al*., 1998). At steady state these subunits are found in two types of complex within the plasma membrane: a substrate-binding TatABC complex of ~ 370 kDa, and separate TatA homo-oligomeric complexes ranging from ~ 50 kDa to over 500 kDa (Alami *et al*., 2003; Bolhuis *et al*., 2001; Oates *et al*., 2005).

There is good evidence that the TatABC complex is responsible for the initial binding of substrate molecules, and the TatBC subunits appear to be particularly important in this respect (Alami *et al*., 2003). It is also believed that TatA complexes assemble with the TatABC complex to form a transient 'supercomplex', with TatA proposed to form the translocation channel. It has been suggested that the variable size of the TatA complex could be a key feature that enables the system to generate a channel of appropriate diameter for a given substrate (Gohlke *et al*., 2005; Oates *et al*., 2005) and electron microscopy studies have shown that TatA complexes do indeed contain potential pores of widely differing diameter (Gohlke *et al*., 2005). Accordingly, TatA is generally considered to form the bulk of the translocation pore. Studies on the Tat system in thylakoids suggest a similar mechanism in which the binding of substrate to the TatBC subunits (denoted Hcf106-cpTatC in plants) initiates assembly with the separate TatA complex (Tha4 in plants) to form the active translocon (Mori and Cline, 2002).

Although the TatABC subunits appear to form the primary translocation system, *E. coli* also contains a separate TatA paralog, TatE, that is encoded by a monocistronic *tatE* gene. The *tatE* gene is found only in enterobacteria (Yen *et al*., 2002) with the exception of the Gram-positive bacteria *Corynebacterium glutamicum* and *Corynebacterium efficiens* (Ikeda and Nakagawa, 2003). The *E. coli tatE* gene encodes a 67-amino acid predicted membrane protein that exhibits greater than 50% sequence identity with TatA (Sargent *et al*., 1998).

TatE is strongly predicted to contain a single transmembrane α-helix at the amino terminus followed by a segment containing an amphiphatic α-helix similar to TatA (Figure 3.1.1). In general, the predicted secondary structural elements of TatE resemble those of *E. coli* TatA and *Bacillus subtilis* TatAd, which have been studied by solution state NMR spectroscopy (Hu *et al*., 2010; Walther *et al*., 2010).

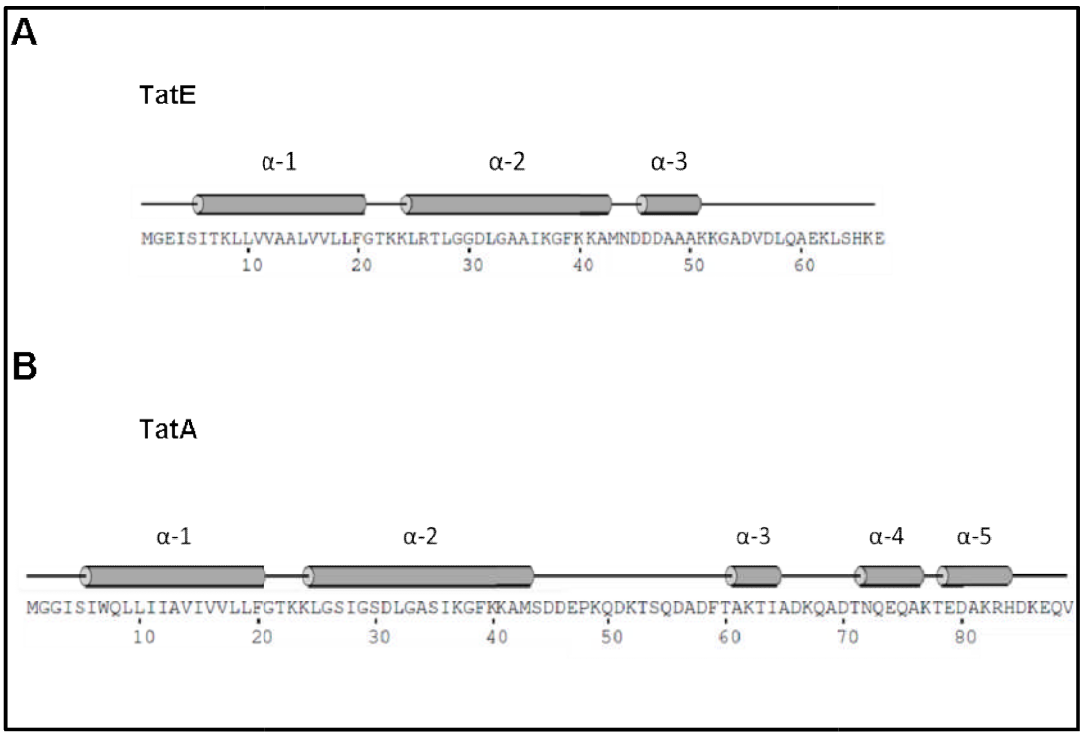

Figure 3.1.1 Predicted secondary structure elements of the *E. coli* TatE (A) and TatA protein (B)
The prediction is that of the program PSIPRED (Jones, 1999). α-helices are represented as cylinders and they are denoted as α-1, α-2, α-3, α-4 and α-5.

Figure 3.1.2 shows a sequence alignment of *E. coli* TatE and TatA, and reveals, as expected, a high degree of sequence conservation between these two proteins. Only the first 60 amino acids are shown in the figure since the conserved residues are all within this region. The TatE protein shares a completely conserved FGT motif with TatA. This motif forms a flexible hinge region between the transmembrane (TM) and amphipathic helix (APH). This region in TatA has been shown to be important for Tat activity (Greene *et al*., 2007). A Glutamine in position 8 of the TatA TM domain was also found to be important for Tat transport (Greene *et al*., 2007). In TatE this

residue is conserved substituted by Lysine. Finally TatE shares partially an acidic motif (DDD), which follows APH, with TatA. In TatA, this motif (DDE) presents a Glutamic acid residue in place of the last Aspartic acid of the TatE acidic motif. In TatA the mutations of these negatively charged amino acids to apolar uncharged residues have been shown to block the Tat activity completely (Warren *et al*., 2009).

In summary TatE shares with TatA almost all the residues which have been shown to be important for the Tat transport.

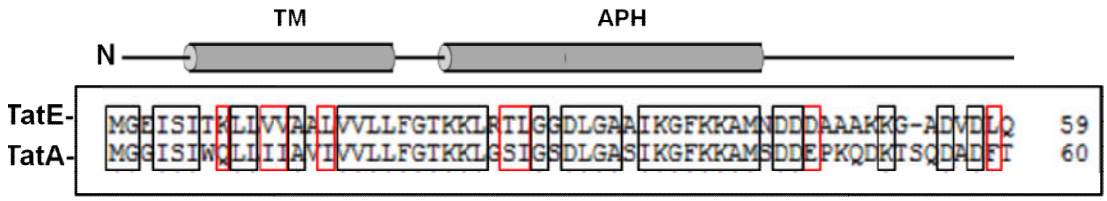

Figure 3.1.2 Sequence alignment of *E. coli* TatE and TatA
The TatE and TatA proteins were aligned using the ClustalW program. Only the first 60 amino acids are shown. Conserved residues are indicated with black boxes and conserved substitutions with red boxes. The predicted transmembrane domain (TM) and the amphipathic helix (APH) are indicated above the alignment.

Interestingly TatE and TatA are functionally interchangeable since each can complement the phenotype of *ΔtatAE* mutants (Sargent *et al*., 1998), but surprisingly *tatE* expression is between 50- and 200-fold lower than *tatA* expression (Jack *et al*., 2001).

In this chapter the purification and characterization of TatE complexes is reported for the first time and in the light of those results alternative Tat translocation models are discussed.

3.2 Results

3.2.1 Translocation of TMAO reductase by overexpressed TatE

Previous experiments performed with Tat proteins expressed at native levels have shown TatA and TatE to have overlapping functions in the Tat pathway (Sargent *et al*., 1998). In order to test whether overexpressed TatE can equally complement the previously-characterized *E. coli ΔtatAE* cells by restoring export activity, the trimethylamine-*N*-oxide (TMAO) reductase activity assay was used. TMAO reductase (TorA) is a periplasmic protein required for growth of *E. coli* on minimal TMAO and glycerol media. TorA is one of the largest Tat substrates identified in *E. coli* at ~ 90 kDa. It contains a molybdopterin cofactor that it acquires in the cytoplasm before translocation by the Tat pathway to the periplasm (Czjzek *et al*., 1998; Silvestro *et al*., 1989). TorA acts as a final electron acceptor of the respiratory chain during anaerobic growth on TMAO medium catalysing the reduction of TMAO to trimethylamine and it has been shown to be functional in the cytoplasm and periplasm, thus lending itself to analysis of the functionality of the Tat pathway (Santini *et al*., 1998). TorA can be detected using a methyl-viologen-linked reduction assay in a native polyacrylamide gel (Barrett *et al*., 2003; Hicks *et al*., 2003).

TatE was overexpressed from plasmid pBAD-E-Strep with a C-terminal *Strep*-II^{TM} tag in *E. coli ΔtatAE* cells under low oxygen conditions in order to promote the expression of TorA. Then periplasmic (P), membrane (M), and cytoplasmic (C) fractions were prepared. Samples of each were run on a 10% native polyacrylamide gel that was subsequently assayed for TorA activity as described in chapter 2.

The left-hand panel of Figure 3.2.1 shows control tests in which wild type (WT) *E. coli* MC4100 cells were fractionated into membrane, cytoplasm, and periplasm samples (lanes M, C, and P, respectively). The data show that the TorA activity was found in the periplasm as expected, with TorA activity also present in the cytoplasm as has been often observed (Bolhuis *et al*., 2001). As expected in the *E. coli ΔtatAE* double mutant, no periplasmic activity was detected since Tat export is blocked. As previously found (Sargent *et al*., 1998), TorA export proceeded in the *E. coli ΔtatA*

single mutant because TatE was able to substitute for TatA. Importantly, overexpression of TatE in *E. coli ΔtatAE* cells (*ΔtatAE* + TatE, panel) led to efficient export of TorA.

This experiment confirms that the TatE was active under these conditions and able to function effectively in the absence of TatA, in combination with TatB and TatC components expressed at native levels. The data therefore indicate that overexpressed TatE facilitates the efficient transport of TorA in the absence of TatA.

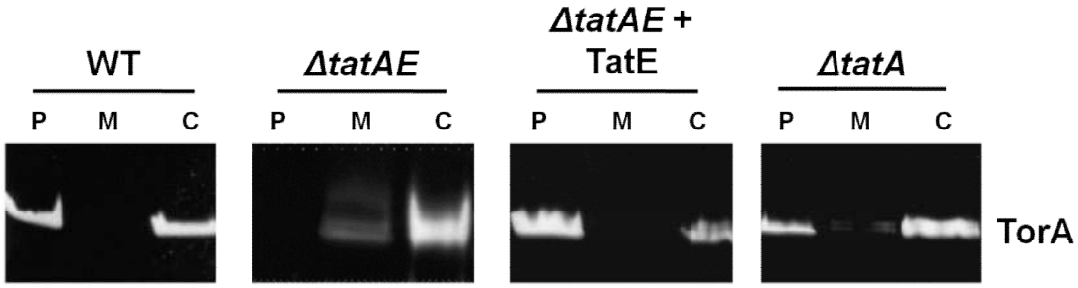

Figure 3.2.1 Translocation of TMAO reductase by overexpressed TatE
The figure shows native polyacrylamide gels stained for TMAO reductase (TorA) activity. Periplasm, membrane and cytoplasm samples (P, M, and C respectively) were prepared and analyzed from wild type (WT) *E. coli* MC4100 cells, from the *E. coli ΔtatAE* and *ΔtatA* cells and from *E. coli ΔtatAE* cells expressing *E. coli* TatE from plasmid pBAD-E-Strep (*ΔtatAE* + TatE). The mobility of active TorA is indicated.

3.2.2 Translocation of the cell wall amidases AmiA and AmiC by overexpressed TatE

E. coli amidases AmiA and AmiC are periplasmic proteins that are translocated by the Tat pathway and involved in cytokinesis (Bernhardt and de Boer, 2003). These substrates are mis-localized in an *E. coli ΔtatABCDE* strain causing a distorted cell division phenotype, such that the cells grow in long chain-like filaments (Ize *et al*., 2003).

As shown from the confocal microscopy data (Figure 3.2.2), WT *E. coli* MC4100 cells (WT panel) can be seen as single or dividing cells whilst *E. coli ΔtatAE* cells formed long chain-like filaments as expected. Overexpression of TatE in *E. coli ΔtatAE* cells restored the wild type cell division phenotype (*ΔtatAE* + TatE, panel) and the cells resembled wild type cells, indicating that AmiA and AmiC were being correctly exported by the Tat pathway.

These data, taken in conjunction with the TorA export data, show that TatE was able to effectively substitute for TatA and form an active translocon in this strain.

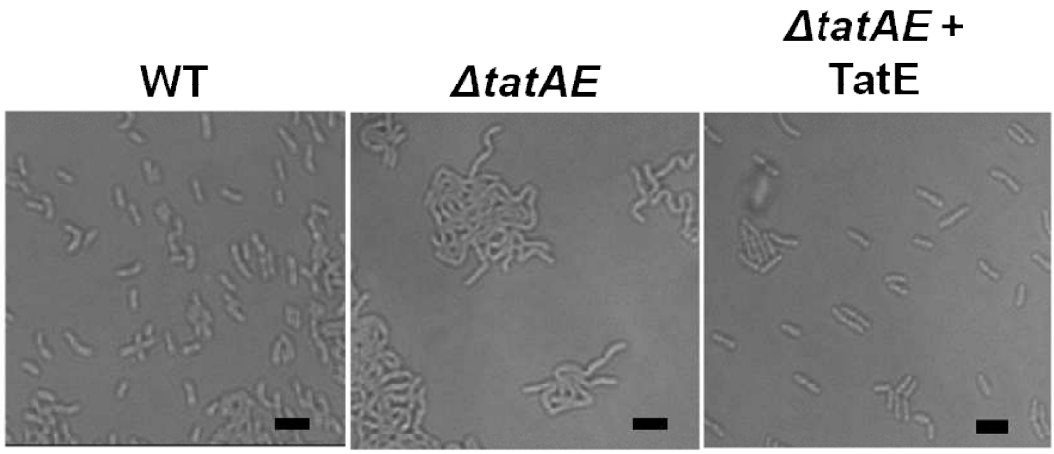

Figure 3.2.2 Overexpressed TatE can complement the filamentous phenotype of *E. coli ΔtatAE* cells
Confocal microscopy images of WT *E. coli* MC4100 cells, *E. coli ΔtatAE* cells and *E. coli ΔtatAE* cells expressing TatE from the pBAD-E-Strep plasmid (*ΔtatAE* + TatE). The scale bar is 1.5 μm.

3.2.3 Anion exchange and affinity chromatography of TatE complexes

In order to purify and study the nature of TatE complexes anion exchange and affinity chromatography were used. 500 ml of *E. coli ΔtatAE* cells expressing TatE from the plasmid pBAD-E-Strep (with a *Strep*-II^{TM} tag fused to the C-terminus of TatE) were fractionated and membranes were isolated. Total membranes were solubilised in 2 % dodecyl maltoside (DDM) and first subjected to anion exchange

chromatography using a 5 ml Q-sepharose column. Eluted protein was further purified on a 2 ml Streptactin™-affinity column. The C-terminal *Strep*-II™ tag fused to TatE binds specifically to the Streptactin™ resin. The sample was applied twice to the column in order to maximize the binding (flow through 1 and 2). The column was then subjected to washing with 16 ml of equilibration buffer before tightly bound proteins were finally eluted with 10 x 0.5 ml of buffer supplemented with desthiobiotin (a biotin derivative that competes for binding to the Streptactin™-chromatography media).

All column wash, flow through and elution fractions were resolved on SDS-PAGE gels and subsequently immunoblotted using antibodies to the *Strep*-II™ tag on TatE (Figure 3.2.3). The figure shows that a proportion of TatE was detectable in the column wash fractions (W) (Q-sepharose and Streptactin™), but most of the protein bound to the affinity column and was specifically eluted across elution fractions E5-E10.

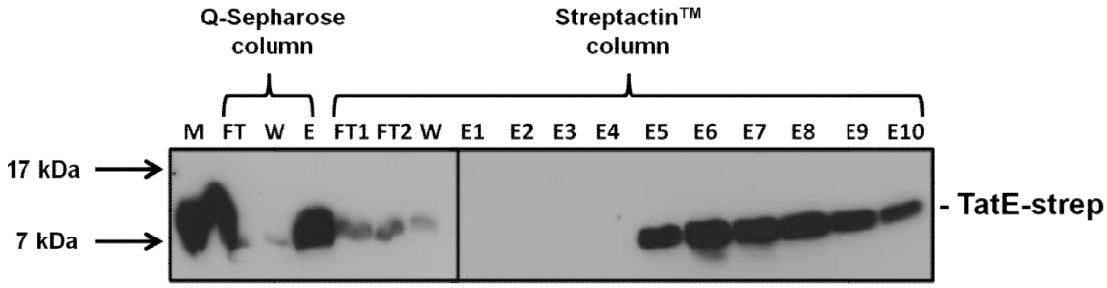

Figure 3.2.3 Anion exchange and affinity chromatography of TatE complexes
Membranes were prepared from *E. coli ΔtatAE* cells expressing *E. coli* TatE with a C-terminal *Strep*-II™ tag, solubilised in DDM and applied to a Q-sepharose anion exchange column. The Q-sepharose elution fraction was then loaded on a Streptactin™-affinity column. All column fractions were run on SDS-PAGE gels and immunoblotted using antibodies against the *Strep*-II™ tag on TatE. Whole membranes (M), column flows through (FT, FT1, and FT2), wash fractions (W), the Q-Sepharose elution fraction (E) and Streptactin™ elution fractions (E1-E10) are all indicated. Mobility of TatE-strep is indicated on the right. Molecular mass markers are indicated on the left.

3.2.4 Anion exchange and affinity chromatography of TatA complexes

For comparison, TatA complexes were also purified by anion exchange and affinity chromatography by using exactly the same protocol as used for TatE. *E. coli ΔtatAE* cells expressing TatA from the plasmid pBAD-A-Strep (with a *Strep*-II™ tag fused to the C-terminus of TatA) were used. The Figure 3.2.4 shows column wash and elution fractions immunoblotted using antibodies to the *Strep*-II™ tag on TatA.

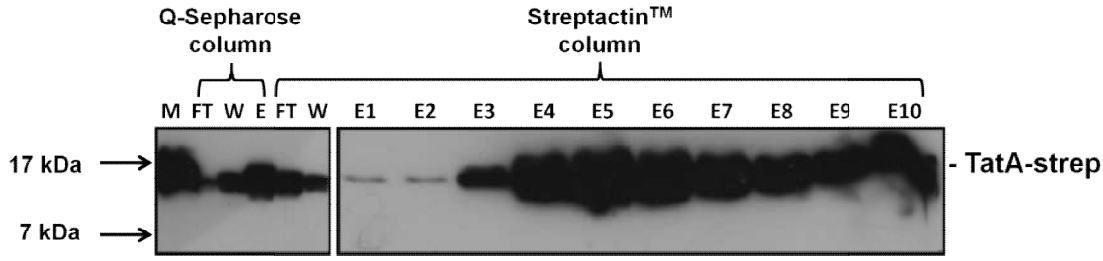

Figure 3.2.4 Anion exchange and affinity chromatography of TatA complexes
Membranes were prepared from *E. coli ΔtatAE* cells expressing *E. coli* TatA with a C-terminal *Strep*-II™ tag, solubilised in DDM and applied to a Q-sepharose anion exchange column. The Q-sepharose elution fraction was then loaded on a Streptactin™-affinity column. All column fractions were run on SDS-PAGE gels and immunoblotted using antibodies against the *Strep*-II™ tag on TatA. Whole membranes (M), column flows through (FT), wash fractions (W), the Q-Sepharose elution fraction (E) and Streptactin™ elution fractions (E1-E10) are all indicated. Mobility of TatA-strep is indicated on the right. Molecular mass markers are indicated on the left.

3.2.5 Gel filtration chromatography of TatE and TatA complexes

In order to provide an estimate of the TatE complex sizes gel filtration chromatography was used. Affinity-purified TatE was applied to a calibrated Superdex™-200 gel filtration column. The sample was eluted from the column in 0.5 ml fractions with a single column volume of equilibration buffer.

All eluted fractions were analysed by SDS-PAGE and the gels subjected to immunoblotting with *Strep*-II™ tag antibodies. As shown in Figure 3.2.5A, TatE

eluted across fractions 20-26 with a peak in fraction 23. Fraction 20 corresponded to a molecular mass of ~ 270 kDa, whereas fraction 26 of ~ 60 kDa. This represents a relatively tight peak, suggesting that TatE is quite homogeneous. In order to estimate sizes of TatE complexes the Superdex^{TM}-200 gel filtration column was calibrated using four protein standards of known molecular weight. These were thyroglobin (669 kDa), ferritin (440 kDa), aldolase (158 kDa) and albumin (66 kDa). It is important to bear in mind that the protein standards are soluble proteins and as such will not interact with the detergent molecules. Hence the size estimate based on these markers only provides an approximate guide to membrane protein complex sizes.

The purity of TatE from the 23 peak elution fraction of the gel filtration column was assessed by silver staining. The silver stain (Figure 3.2.5C) shows that TatE was the major species present but fainter higher molecular weight contaminating bands were also observed. As mentioned previously TatE eluted from the column with a peak in fraction 23 and according to the standards this gave a size estimate of ~ 130 kDa in mass on average. This result was in marked contrast to previous findings on the *E. coli* TatA complex, which was found to be very heterogeneous and present as complexes ranging in size from ~ 50 kDa to over 500 kDa (Gohlke *et al*., 2005; Oates *et al*., 2005).

To confirm this point under similar experimental conditions TatA complexes purified by Q-sepharose and Streptactin^{TM} column were subjected to gel filtration chromatography under identical conditions. *E. coli* TatA eluted across a much broader range of fractions (Figure 3.2.5B), confirming the large range of size forms for this complex. For a better visualization of the different complexes sizes, the immunoblots of the TatE and TatA complexes were further analysed by densitometry, and the intensity of the signal of each band plotted against fraction number (Figure 3.2.5D). The graph shows that TatE eluted with a sharper peak, which indicates the presence of a complex size range that is both smaller and far more homogeneous than the TatA complex.

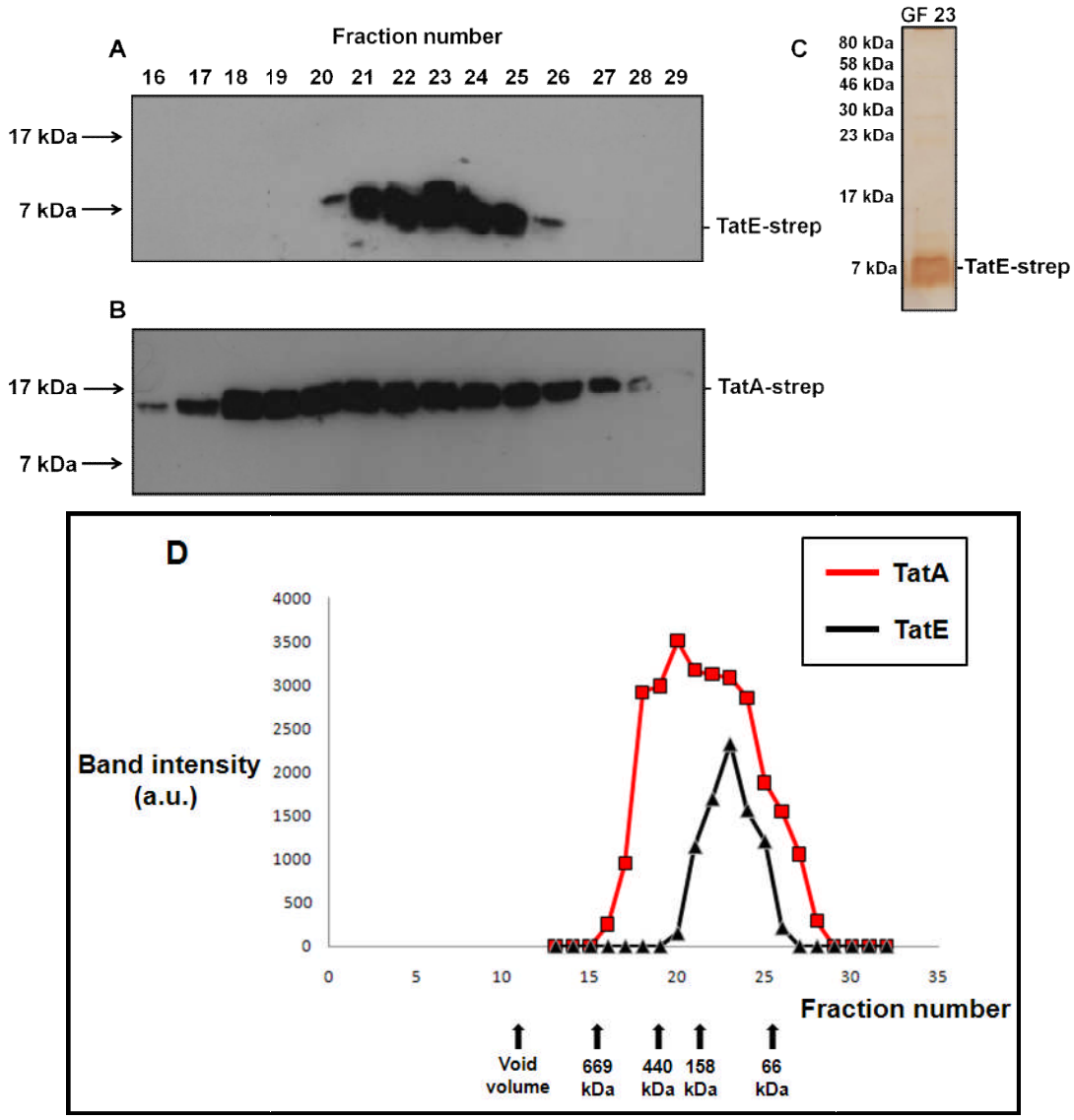

Figure 3.2.5 Gel filtration chromatography of TatE and TatA complexes
Affinity purified TatE (**A**) and TatA (**B**) complexes were applied directly to an equilibrated Superdex^{TM}-200 gel filtration column. Elution fractions were run on SDS-PAGE gels and analyzed by immunoblotting using antibodies to the *Strep*-II^{TM} tag on TatE and TatA. Mobility's of TatE-strep and TatA-strep are indicated on the right. Molecular mass markers are indicated on the left.
C. The 23 gel filtration elution fraction (GF23) was stained with silver to determine purity.
D. Immunoblots from **A** and **B** were analysed by densitometry and intensities of the bands plotted against fraction number. The elution profile of TatE is shown in black (filled triangles) and TatA in red (filled squares). The peak elution of molecular mass markers is indicated with filled triangles and their molecular masses are shown. The void volume is also indicated. (a.u., arbitrary units).

3.2.6 Gel filtration chromatography of TatE complexes using different detergents

The detergent DDM had been chosen for the purification and characterization of TatE complexes because it forms small micelle sizes, thus an accurate estimate of molecular mass can be made. In addition DDM is a relatively mild detergent that should help maintaining native protein-protein interactions and it is compatible with subsequent structural analysis methods.

In order to test if the TatE complexes exhibited the same characteristics regardless of the detergent used and the purification steps, membranes were prepared from *E. coli ΔtatAE* cells expressing TatE and solubilised in 2 % digitonin, 2 % C12E9 and 2 % DDM. Then they were applied directly to the equilibrated gel filtration column. The sample was eluted from the column in 0.5 ml fractions with a single column volume of equilibration buffer. All eluted fractions were analysed by SDS-PAGE and the gels subjected to immunoblotting with *Strep*-II^{TM} tag antibodies. The Figure 3.2.6 shows that TatE complexes eluted in a generally similar manner in all 3 cases, with similarly sharp elution peaks and a relatively small average size calculated by the protein standards. When compared with DDM- and C12E9-solubilized complexes, TatE complexes appeared to be slightly larger in digitonin (Figure 3.2.6A), but this may reflect the differing sizes of the micelles. Digitonin forms micelles with an average weight of 70 kDa, in contrast to an average micellar weight of 50 kDa observed with DDM.

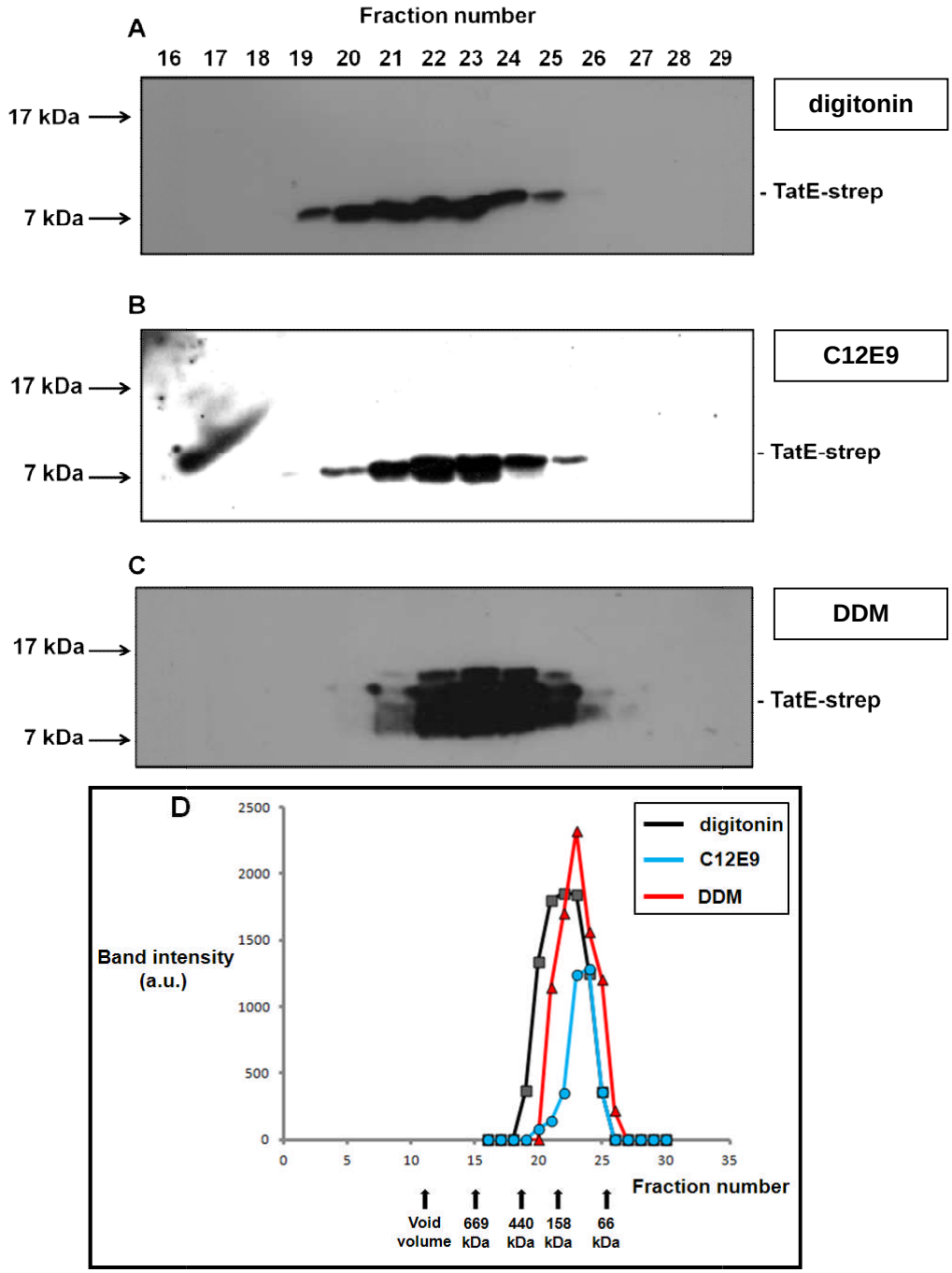

Figure 3.2.6 Gel filtration chromatography of TatE in different detergents
Membranes were prepared from *E. coli ΔtatAE* cells expressing TatE from the plasmid pBAD-E-Strep and solubilised in 2 % digitonin (**A**), 2 % C12E9 (**B**) or 2 % DDM (**C**) and subjected to gel filtration chromatography using the same detergent. Elution fractions were run on SDS-PAGE gels and analyzed by immunoblotting using antibodies to the *Strep*-II™ tag on TatE. Mobility's of TatE-strep and TatA-strep are indicated on the right. Molecular mass markers are indicated on the left.
D. Immunoblots from **A**, **B** and **C** were analysed by densitometry and intensities of the bands plotted against fraction number. The elution profile of digitonin is shown in black (filled squares), C12E9 in blue (filled circles) and DDM in red (filled triangles). The peak elution of molecular mass markers is indicated with filled triangles and their molecular masses are shown. The void volume is also indicated. (a.u., arbitrary units).

3.2.7 Blue-native polyacrylamide gel electrophoresis (BN-PAGE) of purified TatE complexes

The purified TatE complexes were further analyzed by blue-native polyacrylamide gel electrophoresis (BN-PAGE). BN-PAGE analysis has been widely used to study membrane protein complexes because it has a better resolution when compared with gel filtration chromatography, since the detergent has much less influence on the mobility of the protein complexes in the gel (Schägger *et al*., 1994; Schägger and von Jagow, 1991).

The TatE gel filtration elution fractions 20-26 from Figure 3.2.5A were loaded onto a BN-gel and the gel was subjected to immunoblotting with antibodies against the *Strep*-II™ tag on TatE. Figure 3.2.7 (left panel) shows the presence of two major bands corresponding to TatE complexes that migrated with, or close to, the 66 kDa molecular mass marker. A minor third band ran above them. The sizes of these TatE complexes were consistent with those estimated by gel filtration chromatography, where the detergent micelle contributed to the apparent size of complexes.

TatA was also analysed under identical conditions and the data are shown in Figure 3.2.7 (right panel). TatA gel filtration elution fractions 18-25 were subjected to BN-PAGE and the TatA complexes formed the characteristic ladder of bands observed in an earlier study (Oates *et al*., 2005). These bands corresponded to separate complexes with estimated sizes ranging from ~ 100 kDa to over 500 kDa.

Thus, the BN-PAGE results confirm that TatE subunits are organized as relatively small, homogeneous complexes that differ considerably from TatA complexes generated under the same conditions.

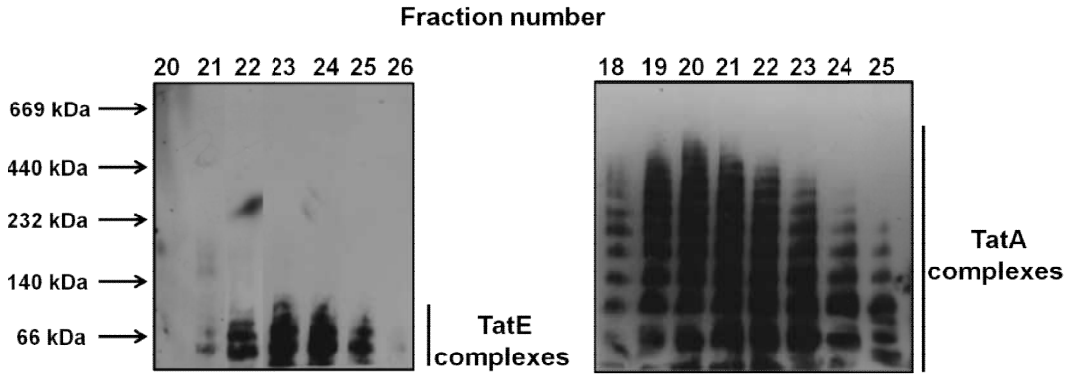

Figure 3.2.7 BN-PAGE of purified TatE and TatA complexes
TatE gel filtration elution fractions 20-26 (left panel) and TatA gel filtration elution fractions 18-25 (right panel) were subjected to BN-PAGE. The gels were immunoblotted using antibodies to the *Strep*-II^{TM} tag on the C-terminus of TatE and TatA. Mobility's of TatE and TatA complexes are indicated. Molecular mass markers are indicated on the left.

3.2.8 Blue-native polyacrylamide gel electrophoresis of solubilised membranes from cells expressing TatE

In order to rule out the possibility that the small size range of the TatE complexes is due to their dissociation during the purification process, membranes, containing TatE as above, were solubilised in digitonin and subjected to BN-PAGE without further purification.

The gel was subsequently immunoblotted using antibodies against the *Strep*-II^{TM} tag. The result in Figure 3.2.8 (TatE (*ΔtatAE*), lane) shows that TatE complexes ran as the same two primary forms observed in Figure 3.2.7 (approximately 50 kDa and 70 kDa). As a control to confirm that the gel resolved larger complexes, membranes were obtained also from *E. coli ΔtatABCDE* cells expressing *E. coli* TatABC from plasmid pBAD-ABC-Strep, with a C-terminal *Strep*-II^{TM} tag present on TatC. The blot (TatABC (*ΔtatABCDE*), lane) shows that TatC was present in the TatABC complex which has been previously described (Oates *et al*., 2005).

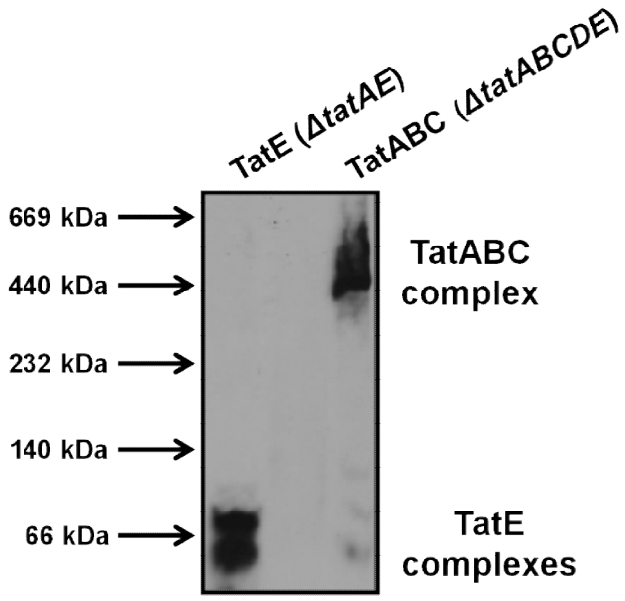

Figure 3.2.8 BN-PAGE of TatE and TatABC complexes
Membranes were prepared from *E. coli ΔtatAE* cells expressing TatE or *E. coli ΔtatABCDE* cells expressing TatABC proteins in which a *Strep*-II^{TM} tag was present on the C-terminus of TatE or TatC, respectively. The membranes were solubilised in digitonin and subjected to BN-PAGE. The gel was immunoblotted with antibodies to the *Strep*-II^{TM} tag. Mobility's of TatE and TatABC complexes are indicated on the right. Molecular mass markers are indicated on the left.

3.2.9 Electron microscopy of TatE complexes

In order to obtain more detailed structural information about TatE complexes, the gel filtration-purified TatE complexes were analyzed by electron microscopy (EM) of negatively stained samples (carried out by Daniel Beck, University of Warwick).

Electron microscopy micrographs of TatE particles were analyzed using single-particle image processing techniques and a three-dimensional reconstruction was obtained using a random conical tilt strategy. Figure 3.2.9 (courtesy of Daniel Beck) shows class averages which revealed that the TatE particles can be separated in two size classes. The complexes formed small ring-shaped structures with a maximum diameter of ~ 8 nm and a dark central area indicating the possibility of a pore or well.

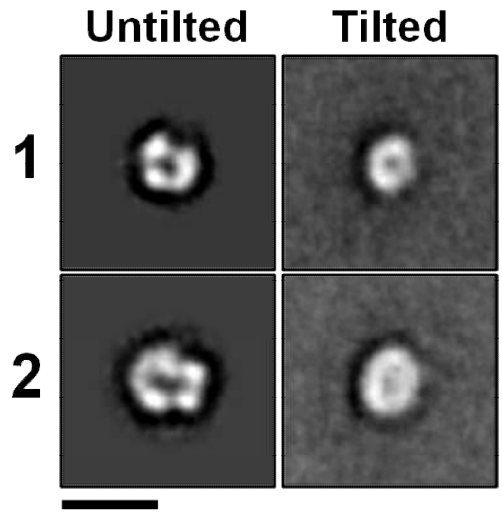

Figure 3.2.9 Micrographs of class averages of TatE complexes
Aligned class averages of the untilted particles and centered tilted particles are shown. Class 1 consists of 226 particles and class 2 contains 288. The scale bar is 10 nm. (Image provided by Daniel Beck)

Figure 3.2.10 (courtesy of Daniel Beck) shows the three-dimensional electron density map generated for both classes. The estimated resolution of the density map was ~ 29 Å. As indicated by the original images, these maps show ring-shaped structures. The dark central area observed in the micrographs was revealed to result from a central cleft or well within the ring, occluded on one side. The shape of the three-dimensional volume obtained was similar to previous structures shown for TatA complexes but much smaller in diameter (6–8 nm when compared with 9–13 nm in the case of TatA (Gohlke *et al*., 2005)). The diameter of the observed cleft for both three-dimensional volumes obtained was ~ 2.5 nm.

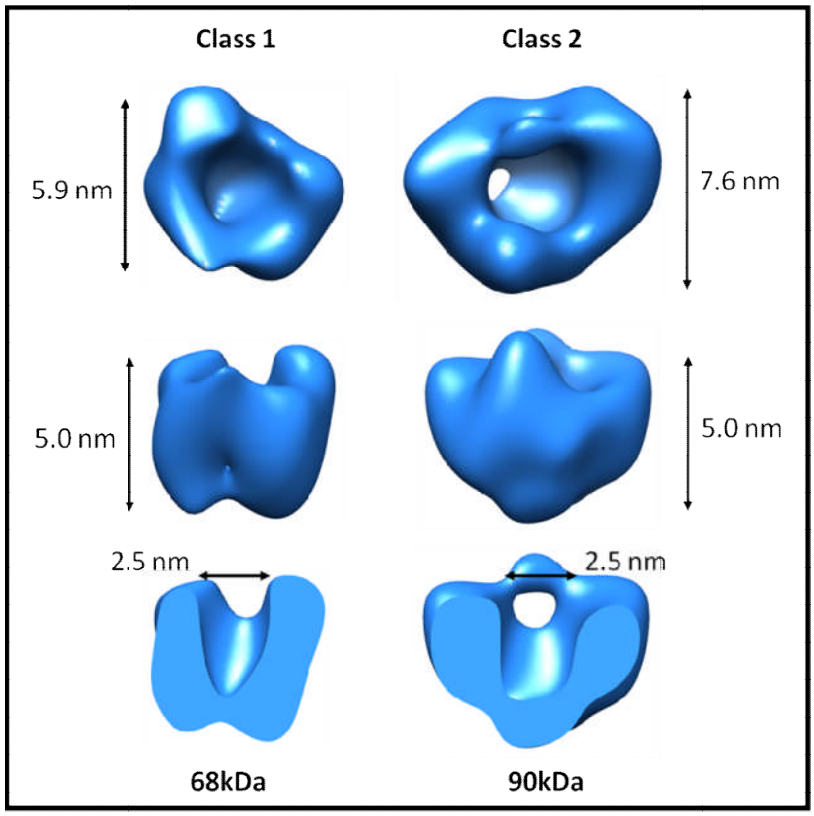

Figure 3.2.10 Three-dimensional density maps of TatE complex assemblies
The small and large TatE complexes are shown filtered to 29 Å and contoured at ~ 5 σ (S.D. above mean density). Dimensions shown from top to bottom are: complex diameter, complex height, and pore width. Molecular masses were estimated based on a protein density of 0.844 Da/Å^3. The figure was produced using the program UCSF Chimera (Image provided by Daniel Beck).

In addition to the single-ring structures described above, a number of particles contained multiple rings and appeared as potential dimers or trimers of the single-ringed structures. Figure 3.2.11 (courtesy of Daniel Beck) shows class averages of the multi-ringed TatE complex structures. These larger structures were observed across a range of samples and grids and appeared to represent a significant subset of the particles (~ 20% of the initial particle set). The majority of this set consisted of two rings with a small number showing three potential rings. As shown in Figure 3.2.11, the class average of the most homogeneous set of particles with two-ringed structures consisted in a complex of 6 by 10.5 nm. Crude size estimations based on a low resolution three-dimensional model of this class, contoured to the dimensions of

the two-dimensional average, gave a molecular mass of ~ 120 kDa. This correlates with the uppermost band seen using BN-PAGE (Figure 3.2.7) and is approximately twice the size of the single-ring structures (68–90 kDa).

The existence of multiringed forms of TatE may be relevant for the mechanism of pore formation because they show that the purified TatE complexes are capable of associating to form larger structures (see discussion). Interestingly, these larger structures still showed two small and distinct pores (Figure 3.2.11).

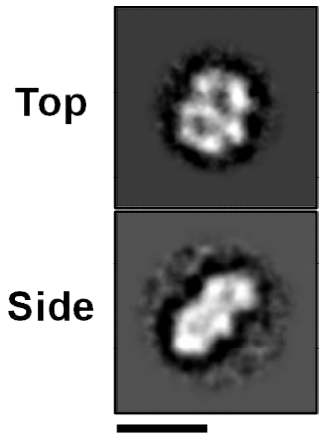

Figure 3.2.11 Micrographs of multi-ringed TatE complex structures
The most homogeneous particles were averaged to provide a top-down view (Top panel) and potential side view (Side panel). The scale bar is 10 nm. (Image provided by Daniel Beck).

3.2.10 Topological orientation of TatE

As mentioned above, the TatE three-dimensional density map shows a cylindrical ring with additional protein density forming a potential lid covering the central channel at one end only. To assess whether the lid is located at the cytoplasmic or periplasmic side of the membrane, the topological organization of TatE was attempted using protease accessibility measurements.

Spheroplasts were prepared from *E. coli ΔtatAE* cells expressing TatE from the plasmid pBAD-E-Strep and were subjected to proteinase K treatment. The fate of TatE was assessed by immunoblotting after SDS-PAGE. As shown in Figure 3.2.12, TatE was insensitive to proteinase K treatment suggesting that TatE was not accessible from the periplasmic side of the membrane. As has been shown previously (Porcelli *et al*., 2002), TatA was not accessible from the periplasmic side of the membrane either (Figure 3.2.12, centre panel). Control experiments demonstrated that permeabilization of the spheroplast membrane with the detergent Triton X-100 rendered both TatE and TatA susceptible to digestion by proteinase K. As a control for the efficacy of the proteinase K treatment, the degradation of the periplasmic loop of leader peptidase (Lep) has been tested and the data showed the appearance of characteristic degradation products when proteinase K was incubated with the spheroplasts (Porcelli *et al*., 2002).

These results suggest that the bulk of TatE was present in the cytoplasm which would place a potential lid in the TatE structure on the cytoplasmic side of the membrane. However, this point requires further analysis because the presence of a TatE periplasmic domain that is insensitive to proteinase K in the absence of Triton X-100 cannot be excluded from this experiment.

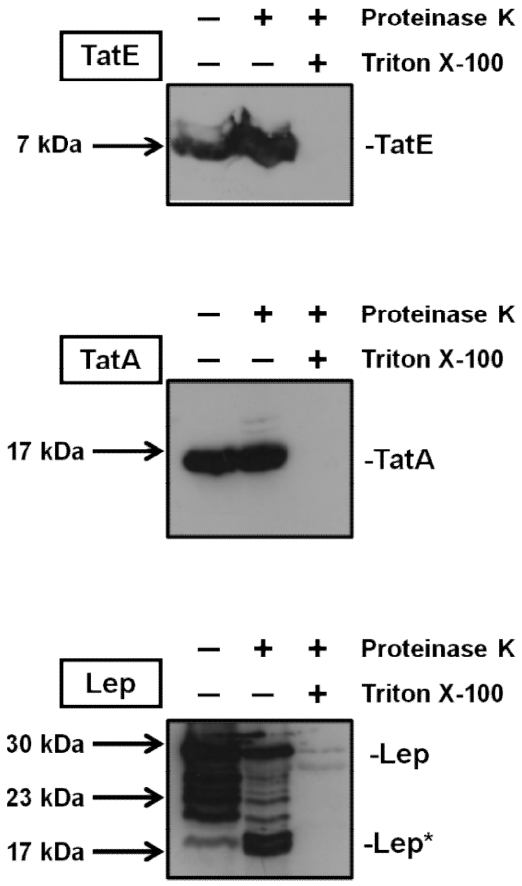

Figure 3.2.12 Topological organization of TatE probed by protease accessibility assay

Spheroplasts were prepared from *E. coli* Δ*tatAE* cells expressing TatE and TatA (from pBAD-E-Strep and pBAD-A-Strep plasmid, respectively) and leader peptidase (Lep) from pRD8 plasmid and subjected to proteinase K accessibility assay. Spheroplasts were incubated in presence of proteinase K and/or Triton X-100 where indicated. Samples were subjected to precipitation with trichloroacetic acid and run on SDS-PAGE gels followed by immunodetection using antibodies to the *Strep*-tag II™ on TatE and TatA (panels TatE and TatA) or an antiserum directed against the leader peptidase (Lep panel). Lep* indicates the characteristic degradation product formed by digestion of the periplasmic domain of membrane-embedded leader peptidase by proteinase K. Mobility's of TatE, TatA, and leader peptidase are indicated on the right. Molecular mass markers are indicated on the left.

3.3 Discussion

The mechanism of the Tat system is still poorly understood in many respects, but a series of studies indicates the possibility of distinct roles for the separate TatABC and TatA complexes that are found at the steady state. There is clear evidence that, in both plant thylakoid and *E. coli* systems, the TatABC complex has a role in substrate binding. These subunits have been shown to cross-link to *in vitro*-synthesized substrates (Alami *et al*., 2003), and a TatBC complex has been purified with one or two substrate molecules bound to it after overexpression of substrates in the absence of TatA (Tarry *et al*., 2009).

In contrast, the TatA complex appears only to become involved after this initial substrate binding step (Mori and Cline, 2002). Several lines of evidence have suggested that the TatA complex either forms the entire translocation channel, or at the very least, contributes the bulk of the channel. EM images of *E. coli* TatA complexes show the presence of potential channels (Gohlke *et al*., 2005) with a possible lid structure that could serve to seal the channel until the appropriate time. *E. coli* TatA complexes are furthermore present in a large range of sizes when purified (Gohlke *et al*., 2005; Oates *et al*., 2005), and it was suggested that this could facilitate the transport of a wide range of substrate sizes.

On the basis of these data, it has become widely accepted that the function of TatA is to generate the translocation pore for folded proteins, and this general model has been discussed in several reviews (*e.g.* Müller and Klösgen (2005)). Key factors in the above model are the size and heterogeneity of the apparent channels in the EM images. The largest class of TatA complex had a diameter of 13.5 nm and a potential channel diameter of 6.5–7 nm, large enough to accommodate the largest Tat substrates, including TorA (Golhke *et al*., 2005). The heterogeneity, on the other hand, appeared to provide a means of transporting Tat substrates of widely varying mass and shape. Thus, at the point of translocation, the full Tat translocase would exist in a series of size forms, dictated by the size of the TatA complex that was involved.

Studies on TatE complexes, reported in this chapter, were not consistent with this model. Previous studies have shown that TatE can complement the Δ*tatA* mutant (Sargent *et al*., 1999), and in this chapter, it has been confirmed that overexpressed TatE allows the efficient transport of several Tat substrates, including TorA, in the absence of TatA. However, the physicochemical/structural properties of isolated TatE complexes were very different from those of TatA complexes.

Gel filtration chromatography studies showed that TatE elutes as a more homogeneous set of complexes compared to TatA with an average size of ~ 130 kDa. However, this includes the detergent micelle, and more accurate BN-PAGE studies suggested the presence of 2–3 complex types with sizes in the 50–110-kDa range. EM analysis was used to derive three-dimensional models for the two primary TatE forms. Overall, single-ring TatE complexes were even smaller than the very smallest class of TatA complex analyzed to date (class 1 in Gohlke *et al*. (2005)), which had a diameter of 8.5–9 nm and a potential channel diameter of 3–3.5 nm. It should be emphasized that although TatE was overexpressed in this study, the pBAD vector directs only a moderate level of overexpression, and exactly the same expression system was previously used to characterize the large range of TatA complexes under essentially identical conditions (Oates *et al*., 2005). Moreover, the TatE complexes exhibited the same characteristics after purification in three different detergents. There has been no evidence for the presence of larger TatE complexes under any of these conditions, and therefore the smaller size of solubilized/purified TatE was likely to reflect the natural state of the complex.

TatE complexes resembled smaller TatA complexes in some respects, and they likewise appeared to possess a central cavity that was accessed from one side of the membrane. The N-terminal periplasmic region of TatA (and TatE) comprises only a few residues, and it is therefore highly likely that the potential lid is on the cytoplasmic face of the complex, where it may function to prevent leakage of small molecules. Proteinase K digestion studies supported this idea. Both TatE models had potential clefts or channels of 2.5 nm in diameter which are not large enough to accommodate a single TorA molecule given that, according to its crystal structure from *Shewanella massilia* (Czjzek *et al*., 1998), the narrowest diameter for TorA was estimated at about 5 nm (Wu *et al*., 2000).

Overall, from the combined biochemical/structural studies emerged that the small sizes of TatE complexes appeared to preclude a role in forming the entire translocation channel, or even the bulk thereof.

One alternative possibility is that the TatBC complex forms the primary translocation channel (Figure 3.3A) and that TatA/E serves to activate it. The size of the TatABC complex, ~ 370 kDa in *E. coli* (Oates *et al*., 2005), is such that could generate an active 'supercomplex', which may be more capable of forming a translocation channel for substrates of 90 kDa or more. Moreover, there is evidence from the thylakoid Tat system that TatC is actively involved in the actual translocation event because substrate molecules that are covalently cross-linked to TatC on the stromal side can be subsequently transported to the luminal side (Gerard and Cline, 2006).

More generally, the data are consistent with a model for Tat function that is radically different from currently favoured models. The observed heterogeneity of TatA has prompted models that involve recruitment of one variant of TatA complex, from a spectrum of size classes, to match the size of the substrate being translocated. In contrast, the observation of such a limited range of TatE forms (only two major classes) is consistent with a model in which a much more discrete form of Tat translocase is sufficiently flexible to transport a wide range of substrates (Figure 3.3B).

A second model involves a different scenario (Figure 3.3C); multiple TatE complexes bind to the TatBC complex once substrate has been bound. This would have the advantage of providing flexibility of pore size, with differing numbers of TatE complex generating translocation channels of differing diameters (the same role proposed for the variability of TatA complexes). The multi-ringed structures of TatE that have been observed would support this modular interaction of smaller rings to produce a larger superstructure. Further studies are of course required to test those models.

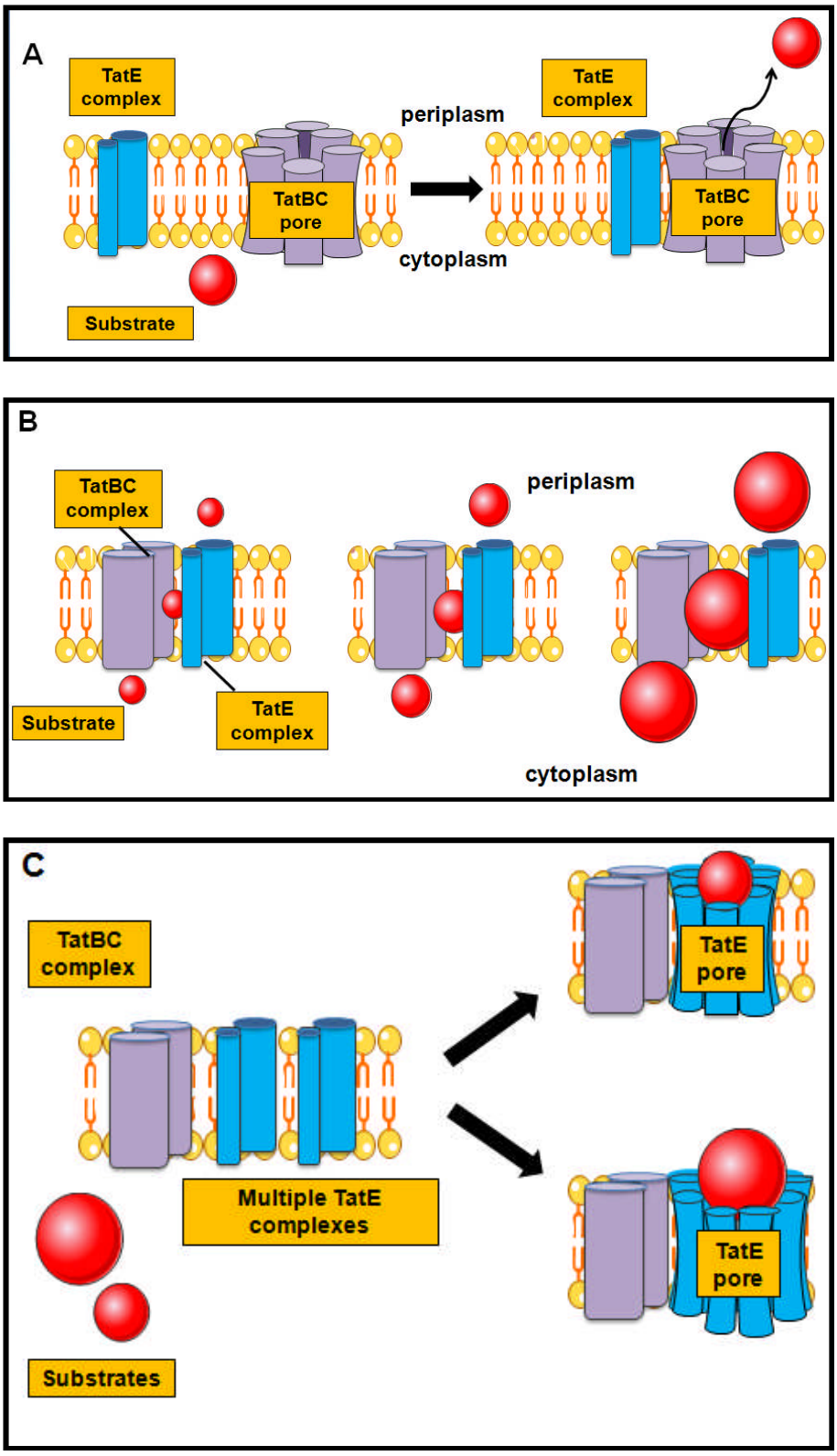

Figure 3.3 Alternative models for Tat-dependent translocation
Schematic representation of three alternative models involving either a TatBC channel (**A**) or a flexible translocon (**B**) or multiple TatE complexes forming the translocation pore (**C**). See text for detail.

Chapter 4.

Characterization of soluble TatE and TatA complexes

4.1 Introduction

The Tat system was initially discovered as a pathway that operates independently of soluble factors. This is in contrast to the Sec pathway that targets proteins to the Sec pore by soluble targeting factors, including SecB (Driessen, 2001).

In *Bacillus subtilis* however, the TatAd protein, despite having a predicted N-terminal membrane-spanning α-helical domain, was found in both the plasma membrane and the cytoplasm where it was reported to specifically interact with the twin-arginine motif of the prePhoD signal peptide (Pop *et al*., 2003). Negative contrast and freeze-fracture electron microscopy of purified soluble TatAd has suggested that this soluble population of protein forms 150-250 kDa homo-oligomeric complexes in the cytoplasm (Westermann *et al*., 2006).

The ability of soluble Tat proteins to interact with Tat substrates resulted in speculation that a soluble TatAd could recruit the preproteins to the translocase by binding to cytosolic loops of the membrane-embedded TatCd (Schreiber *et al*., 2006).

In contrast, Barnett *et al*. (2008) found by gel filtration chromatography that soluble TatAd forms large aggregates and that it was the presence of a hexa-histidine tag on the N-terminus of the TatAd protein that resulted in the lower molecular weight species observed by Westermann *et al*. (2006). Similarly, a second TatA homologue found in *B. subtilis* (TatAy), has also been found in the cytoplasm where it forms very large complexes or aggregates of ~ 5 MDa (Barnett *et al*., 2009).

Furthermore in the Gram-positive bacterium *Streptomyces lividans*, TatA and TatB are localized in both the cytoplasm and the membrane (De Keersmaeker *et al*., 2005), whereas in all other examples studied, TatB is strictly membrane localized. In the cytoplasm they are monomers as well as organized in a hetero-oligomeric complex that ranges in size from ~ 100 kDa to over 600 kDa (De Keersmaeker *et al*., 2007). The presence of soluble TatA/B homologues in Gram-positive bacteria suggested that the Tat pathway might be fundamentally different to the pathway in Gram-negative bacteria.

In *E. coli*, TatA has been found to form homo-oligomeric complexes in the membrane (Oates *et al*., 2005), nevertheless one study has questioned its strict membrane localization and suggested that TatA is capable of forming homo-multimeric tube-like structures inside the cytoplasm, which can interact with one another in the presence of TatC to form quasi-crystalline structures (Berthelmann *et al*., 2008). The Tat systems from Gram-positive and Gram-negative bacteria thus appear to be more similar than previously thought.

A soluble form of the chloroplast TatA homologue (Tha4), has also been found in the chloroplast stroma but is not required for precursor targeting to the thylakoid membrane. It does however significantly improve the efficiency of Tat-dependent transport, probably by acting as an addition pool of TatA that inserts into the membrane (Frielingsdorf *et al*., 2008).

In summary, the functional significance of soluble TatA proteins in Tat dependent translocation remains to be elucidated. In this chapter the cytosolic localization of *E. coli* TatE is investigated for the first time.

4.2 Results

4.2.1 Purification of TatE complexes from cytosolic fractions

As shown in the previous chapter TatE is found to form complexes in the membrane. The aim of this chapter is to investigate if TatE, just like *B. subtilis* TatAd and other TatA homologues, has a dual localization in the membrane and in the cytoplasm.

E. coli ΔtatAE cells expressing TatE from the plasmid pBAD-E-Strep (with a *Strep*-II™ tag fused to the C-terminus of TatE) were fractionated and the cytosolic fractions collected. No detergent was used for the purification of TatE from the cytoplasm. Samples were purified using a 2 ml Streptactin™-affinity column. The C-terminal *Strep*-II™ tag fused to TatE binds specifically to the Streptactin™ resin. After sample application the column was subjected to washing with 16 ml of equilibration buffer before tightly bound proteins were finally eluted with 10 x 0.5 ml of buffer supplemented with desthiobiotin.

All column wash and elution fractions were resolved on SDS-PAGE gels and subsequently immunoblotted using antibodies to the *Strep*-II™ tag on TatE (Figure 4.2.1). The immunoblots show that TatE was indeed detected in the cytoplasm (C) and the TatE protein was eluted from the Streptactin™ column over fractions E4-E7.

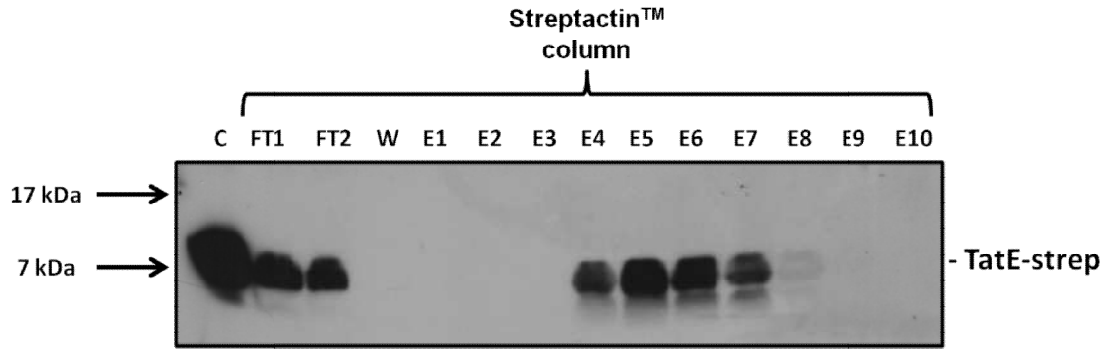

Figure 4.2.1 Purification of TatE complexes from the cytoplasm
E. coli ΔtatAE cells expressing *E. coli* TatE with a C-terminal *Strep*-II™ tag were fractionated. The cytosolic samples were purified by Streptactin™-affinity column. All column fractions were run on SDS-PAGE gel and immunoblotted using antibodies against the *Strep*-II™ tag on TatE. Cytoplasm (C), column flows through (FT1, FT2), wash fraction (W) and elution fractions (E1-E10) are all indicated. Mobility of TatE-strep is indicated on the right. Molecular mass markers are indicated on the left.

As control *E. coli ΔtatABCDE* cells expressing TatABC from the plasmid pBAD-ABC-Strep were fractionated into cytosolic and membrane samples. Cell fractions were run on SDS-PAGE gels before immunoblotting with antibodies against the *Strep*-II™ tag on TatC. The Figure 4.2.2 shows that TatC protein to localize to the membrane fraction, as expected. This result demonstrates that the fractionation was 'clean' and that the cytosolic fraction was not contaminated with membrane proteins.

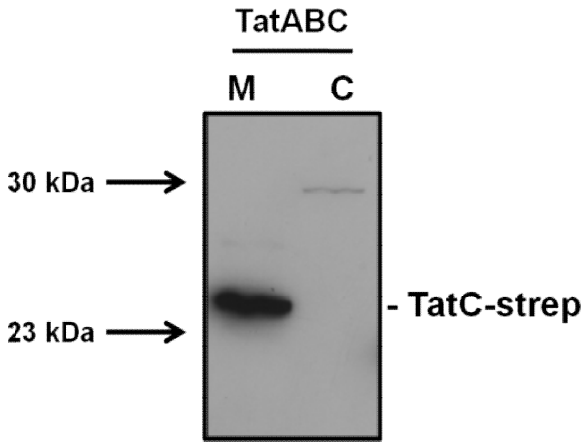

Figure 4.2.2 Localization of *E. coli* TatC
E. coli ΔtatABCDE cells expressing TatABC were fractionated into cytosolic (C) and membrane (M) samples. Cell fractions were run on SDS-PAGE gel and immunoblotted with antibodies against the *Strep*-II^{TM} tag on TatC. Mobility of TatC-strep is indicated on the right. Molecular mass markers are indicated on the left.

4.2.2 Purification of TatA complexes from cytosolic fractions

For comparison cytosolic TatA complexes were also purified by affinity chromatography. *E. coli ΔtatAE* cells expressing TatA from the plasmid pBAD-A-Strep (with a *Strep*-II^{TM} tag fused to the C-terminus of TatA) were fractionated and the cytosolic fractions collected.

Samples were purified using a 2 ml Streptactin^{TM}-affinity column as described in 4.2.1. All column wash and elution fractions were resolved on SDS-PAGE gels and subsequently immunoblotted using antibodies to the *Strep*-II^{TM} tag on TatA (Figure 4.2.3). The immunoblots show that TatA was detected in the cytoplasm (C) and it eluted from the Streptactin^{TM} column over fractions E1-E10. These results therefore confirm the reported cytosolic localisation of TatA in *E. coli* (Berthelmann *et al*., 2008). Interestingly another study showed that the TatA protein is instead localised exclusively to the plasma membrane when expressed at native levels *in vivo* (Leake *et al*., 2008).

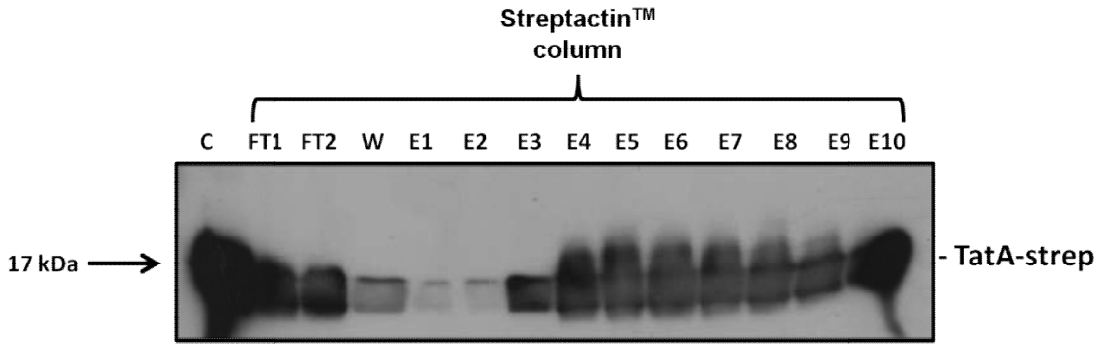

Figure 4.2.3 Purification of TatA complexes from the cytoplasm
E. coli ΔtatAE cells expressing *E. coli* TatA with a C-terminal *Strep*-II™ tag were fractionated. The cytosolic samples were purified by Streptactin™-affinity column. All column fractions were run on SDS-PAGE gels and immunoblotted using antibodies against the *Strep*-II™ tag on TatA. Cytoplasm (C), column flows through (FT1, FT2), wash fraction (W) and elution fractions (E1-E10) are all indicated. Mobility of TatA-strep is indicated on the right. The molecular mass marker is indicated on the left.

4.2.3 Separation of TatE and TatA proteins into soluble and insoluble fractions using the detergent Triton X-114

In order to determine whether the cytosolic TatE protein is a real soluble population of protein it was analysed by phase separation using the detergent Triton X-114.

A solution of the non-ionic detergent Triton X-114 is homogeneous at 0 °C but separates into an aqueous phase and a detergent phase above 20 °C and this temperature is called cloud point. This property of Triton X-114 has been exploited to identify whether proteins are soluble or integral membrane proteins (Bordier, 1981). When a detergent phase separation occurs the soluble proteins are recovered in the aqueous phase whereas integral membrane proteins are found in the detergent phase (Bordier, 1981).

In a control experiment, since *E. coli* TatC has strict membrane localization, purified *E. coli* TatABC was used as a marker. TatC was purified from membranes by affinity chromatography in the presence of 1 % Triton X-114. The sample was incubated at

4 °C for ~ 30 minutes and then warmed to 30 °C to cause the detergent (D) and aqueous (Aq) phases to separate. Phases were collected by centrifugation and run on SDS-PAGE before immunoblotting with antibodies against the *Strep*-II™ tag on TatC.

The Figure 4.2.4 shows that the bulk of the TatC proteins was in the detergent phase as expected. Only a very small amount of the protein was detectable in the aqueous phase confirming that the two phases were cleanly separated.

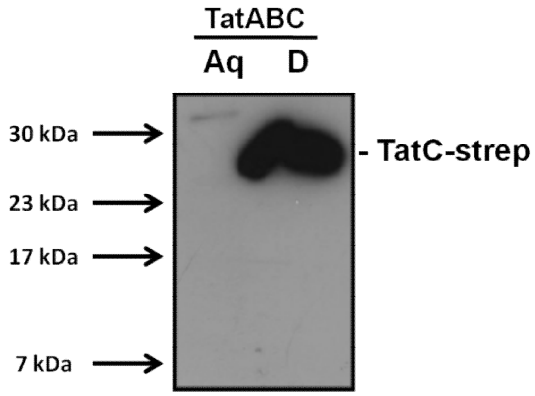

Figure 4.2.4 Separation of a membrane protein using Triton X-114
E. coli TatABC was purified from membranes in 1 % Triton X-114 at 4 °C. The sample was then incubated at 30 °C to separate detergent (D) and aqueous (Aq) phases. Phases were collected by centrifugation and samples subjected to SDS-PAGE. The gel was immunoblotted using antibodies against the *Strep*-II™ tag on TatC. Mobility of TatC-strep is indicated on the right. Molecular mass markers are indicated on the left.

In order to verify whether TatE present in the cytoplasm is a genuinely soluble population of protein, *E. coli ΔtatAE* cells expressing TatE from the plasmid pBAD-E-Strep were fractionated and cytosolic samples collected. For comparison *E. coli ΔtatAE* cells expressing TatA from the plasmid pBAD-A-Strep were also fractionated and the cytosolic fractions collected. The samples were incubated with 1 % Triton X-114 at 4 °C for ~ 30 minutes and then warmed to 30 °C causing the separation of detergent (D) and aqueous (Aq) phases. Phases were collected by centrifugation and run on SDS-PAGE gels before immunoblotting with antibodies against the *Strep*-II™ tag on TatE and TatA.

The Figure 4.2.5 shows that the bulk of TatE and TatA was in the detergent phase even though both proteins were isolated from the cytosolic fractions and a very small amount of the protein was detectable in the aqueous phase.

This result may suggest that both cytosolic TatE and TatA were mis-localized. The localization of cytosolic TatA in the detergent phase was quite unexpected and in contrast with a previous study which showed that TatA was capable of forming homo-multimeric tube-like structures inside the cytoplasm (Berthelmann *et al.,* 2008).

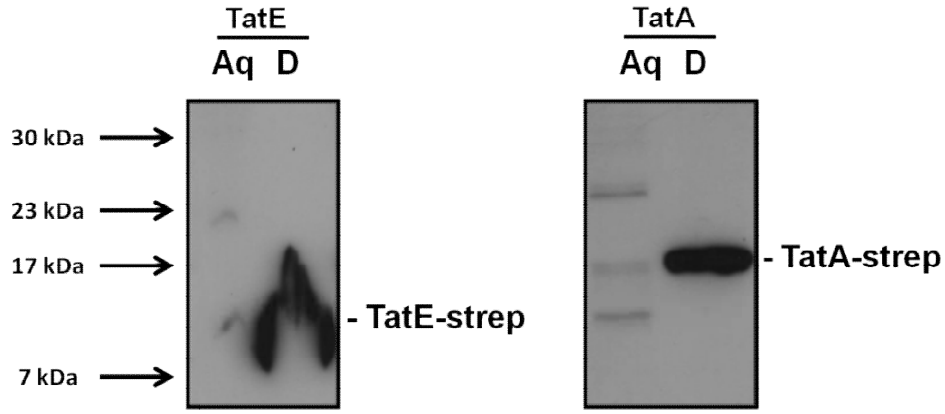

Figure 4.2.5 Determination of cytosolic TatE and TatA solubility by Triton X-114 phase separation
E. coli ΔtatAE cells expressing either TatE (left panel) or TatA (right panel) were fractionated. Cytosolic samples were incubated with 1 % Triton X-114 at 4 °C and separated in detergent (D) and aqueous (Aq) phases as described in chapter 2. Phases were collected by centrifugation and samples subjected to SDS-PAGE. The gels were immunoblotted using antibodies against the *Strep*-II^{TM} tag on TatE or TatA. Mobilities of TatE-strep and TatA-strep are indicated on the right. Molecular mass markers are indicated on the left.

4.2.4 Blue-native polyacrylamide gel electrophoresis (BN-PAGE) of cytosolic TatE and TatA complexes

In order to investigate the dimensions of the cytosolic TatE and TatA complexes, they were analyzed by BN-PAGE.

E. coli ΔtatAE cells expressing TatE or TatA from the plasmid pBAD-E-Strep and pBAD-A-Strep respectively were fractionated. The cytosolic fractions were collected and loaded directly onto BN-gels in absence of any detergent. The gels were then subjected to immunoblotting with antibodies against the *Strep*-II^{TM} tag on TatE and TatA. The Figure 4.2.6 (left panel) shows the presence of a band corresponding to a cytosolic TatE complex that migrated just above the 66 kDa marker. The dimension of this complex was similar of that corresponding to the uppermost band in the BN-gel of solubilised membranes expressing TatE (Figure 3.2.8, chapter 3). In contrast, as shown in the Figure 4.2.6 (right panel), cytosolic TatA ran in the BN-gel as a high molecular weight band corresponding to a complex of ~ 669 kDa. This complex resembles the high molecular weight complexes or aggregates formed by the cytosolic TatAd and TatAy in *B. subtilis* (Barnett *et al*., 2008; Barnett *et al*., 2009).

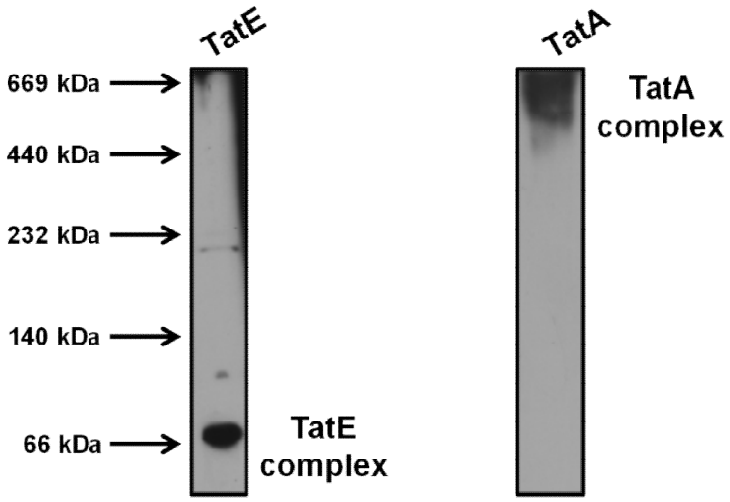

Figure 4.2.6 BN-PAGE of cytosolic TatE and TatA complexes
E. coli ΔtatAE cells expressing either TatE (left panel) or TatA (right panel) were fractionated and the cytosolic samples were subjected to BN-PAGE. The gels were immunoblotted to antibodies to the *Strep*-II^{TM} tag on TatE or TatA. Mobilities of cytosolic TatE and TatA complexes are indicated on the right. Molecular mass markers are indicated on the left.

4.3 Discussion

The functional significance of a soluble population of TatA-type proteins is still a matter of controversy, and its role in the translocation process has not been unequivocally resolved.

In *B. subtilis* TatAd has been found to have a dual localization in the membrane and in the cytoplasm. In this last compartment it has been shown to interact specifically with the prePhoD signal peptide (Pop *et al*., 2003).

Another study has found that soluble TatAd could assemble into micelle-like structures (Westermann *et al*., 2006). The hydrophobic centre of the protein micelles could accommodate the hydrophobic domain of the PhoD signal peptide, whereas the negative charged C-terminal region of TatAd could interact with the twin-arginine motif (Westermann *et al*., 2006). A further study has shown that cytosolic TaAd could serve to target the substrates to the translocase since it binds to cytosolic loops of the membrane protein TatCd (Schreiber *et al*., 2006).

Interestingly in the Gram-positive bacterium *Streptomyces lividans* which is the only Gram-positive bacterium having a TatABC type system, both TatA and TatB are present in the cytoplasm as well as in the membrane (De Keersmaeker *et al*., 2005).

In *E. coli* TatA has been found alongside its membrane localised form in the cytoplasm too, where it forms homo-multimeric tube-like structures inside the cytoplasm (Berthelmann *et al*., 2008). This suggests that the Tat pathways found in Gram-positive and Gram-negative bacteria may operate by a similar mechanism.

Nevertheless another study that used *in vivo* single-molecule imaging showed that the TatA protein is instead localised exclusively to the plasma membrane (Leake *et al*., 2008). This last result is significant as it shows *in vivo* evidence of TatA localisation. It may thus be the case that in many of the *in vitro* studies described above the observed soluble pool of TatA was an artefact of the methods used to isolate the protein complexes. Indeed the results of the Triton-X114 experiments

carried out in this study support the hypothesis that the observed soluble Tat complexes are mis-localised. Still the contradictory results make a meaningful interpretation of the literature difficult and further work is needed to resolve this point.

It remains possible that the cytosolic TatE and TatA proteins, just like Tha4 in plants (Frielingsdorf *et al*., 2008), may form an additional pool of protein that inserts into the membrane, perhaps improving the efficiency of Tat-dependent transport. Obviously further experiments are needed to confirm this hypothesis.

The BN-PAGE data presented in this chapter show that cytosolic TatE and TatA proteins, like their membrane localised counterparts (chapter 3), are organized into complexes of different size. Cytosolic TatE forms a complex of ~ 66 kDa, similar to the largest TatE complex seen in the BN-gel of solubilised membranes expressing TatE (Figure 3.2.8, chapter 3).

In contrast cytosolic TatA, unlike membrane localized TatA (Figure 3.2.7, chapter 3), is not organized into a range of oligomeric complexes but instead it forms a distinct cytosolic complex of ~ 669 kDa which resembles in part the high molecular weight complexes or aggregates formed by the cytosolic TatAd and TatAy in *B. subtilis* (Barnett *et al*., 2009; Barnett *et al*., 2008).

These results show that the TatE complexes have similar features regardless of whether they have a membrane or cytosolic localisation, whilst TatA does not appear to form modular complexes in the cytoplasm. Perhaps this observation suggests that cytosolic TatA has to be present as a discrete cytosolic complex in order to execute its function in the transport mechanism. Further studies are of course needed to address whether cytosolic TatE and TatA proteins are functional or not.

Chapter 5.

Study of the TatE subunit interactions with the other Tat components

5.1 Introduction

Several studies have established that each of the Tat components form stable, defined, multimeric complexes (Leake *et al*., 2008; Behrendt *et al*., 2007; Orriss *et al*., 2007; Oates *et al*., 2005; Porcelli *et al*., 2002; De Leeuw *et al*., 2001). A TatABC complex has been purified from isolated plasma membranes (following overexpression in *E. coli*), and shown to contain equal amounts of TatB and TatC, with small and variable amounts of TatA (Bolhuis *et al.*, 2001). This complex has an apparent molecular mass of approximately 600 kDa as judged by gel filtration chromatography (Bolhuis *et al.*, 2001). A more accurate complex size determination, carried out by using blue-native PAGE, has suggested that the TatABC complexes have a molecular mass of 370 kDa (Oates *et al*., 2005). In contrast the vast majority of *E. coli* TatA is found in separate TatA homo-oligomeric complexes ranging from ~ 50 kDa to over 500 kDa (Oates *et al*., 2005). Apart from the TatABC and separate TatA complexes, TatAB complexes have also been identified (Bolhuis *et al*., 2001; De Leeuw *et al*., 2001) and the role of these TatAB complexes is still not clear. One hypothesis is that they may be either an assembly or disassembly intermediate generated during translocation activity (Oates *et al*., 2005).

Since the TatAB, TatABC and TatA complexes are very much larger than the sum of the molecular masses of the individual Tat subunits, the Tat proteins must be forming homo- and/or hetero-oligomeric interactions; in fact chemical cross-linking studies have indicated that TatA forms at least homo-trimers, and TatB minimally homodimers, in the native membrane environment (De Leeuw *et al*., 2001).

A more recent study that used Bimolecular Fluorescence Complementation (BiFC) has confirmed these findings by showing homo- and hetero-oligomeric complexes of TatA, TatB and TatC (Kostecki *et al*., 2010). The TatBC complex in thylakoid membranes and the TatABC complex in *E. coli* have been shown to have a role in substrate binding (Mori and Cline, 2002; Alami *et al*., 2003). In contrast, the TatA complex appears only to become involved after the initial substrate binding step (Mori and Cline, 2002). Several lines of evidence have suggested that the TatA complex either forms the entire translocation channel, or at the very least, contributes

the bulk of the channel. EM images of *E. coli* TatA complexes show the presence of potential channels large enough to accommodate the largest Tat substrates (Gohlke *et al*., 2005) with a possible lid structure that could serve to seal the channel until the appropriate time. According to this model the heterogeneity of TatA complexes therefore seems to provide a means of transporting Tat substrates of widely varying mass and shape.

Studies on the paralog TatE, reported in chapter 3, are not consistent with this model. In fact the limited range of TatE forms (only two major classes) seems to suggest that one of two alternative models for Tat-dependent translocation are operating. The first model would involve a flexible, but not yet well characterized translocon, whilst the second would involve the presence of multiple TatE complexes that assemble to form the complete translocation pore.

Most studies of the *E. coli* Tat system to date have largely ignored the TatE subunit because it is not essential for translocation activity. Nevertheless, it is constitutively expressed in *E. coli* and can function in place of TatA. *In vivo*, in wild type *E. coli* cells, TatE may form structural or functional interactions with the other Tat subunits, and in this chapter this possibility was examined in detail for the first time.

5.2 Results

5.2.1 Influence of the TatABC subunits on TatE stability in *E. coli*

In order to study whether the stability of TatE is influenced by the other Tat components or not, TatE was expressed from the plasmid pBAD-E-Strep, by induction with arabinose, in *E. coli ΔtatAE*, *ΔtatA*, *ΔtatB*, *ΔtatC*, *ΔtatABCDE* and wild type (WT) *E. coli* MC4100 cells. After 3 hours of induction the cells were fractionated and membrane samples collected. Membranes were solubilised in 1% SDS and run on SDS-PAGE gels before immunoblotting with antibodies against the *Strep*-II™ tag on TatE.

The results are presented in Figure 5.2.1. TatE was clearly present at relatively high levels following expression in the *ΔtatAE* mutant strain. In contrast the level of TatE was lower in *ΔtatA*, *ΔtatB* and WT cells. In *ΔtatC* cells TatE was either expressed at much lower levels or was less stable. In the *ΔtatABCDE* null strain no TatE was detectable after 3 hours of induction, suggesting that either TatE was not expressed at all or it was unstable in the absence of all the other Tat components.

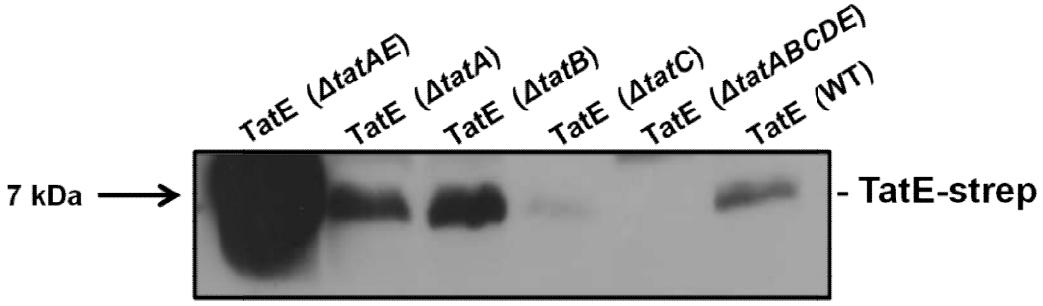

Figure 5.2.1 Expression and stability of TatE proteins in different backgrounds
Plasmid pBAD-E-Strep carried by *E. coli ΔtatAE*, *ΔtatA*, *ΔtatB*, *ΔtatC*, *ΔtatABCDE* and WT *E. coli* MC4100 cells was induced for three hours with 1 mM arabinose. The cells were then fractionated and membrane samples collected. Membrane fractions were analysed by SDS-PAGE and immunoblotted using antibodies against the *Strep*-II™ tag on TatE. Mobility of TatE-strep is indicated on the right. The molecular mass marker is indicated on the left.

5.2.2 TatE is not stable in *ΔtatABCDE* cells

In order to investigate whether the TatE proteins are not expressed at all in *ΔtatABCDE* cells or they are simply unstable in the absence of all the other Tat components a time course experiment has been performed.

TatE was expressed from plasmid pBAD-E-Strep by induction with 1 mM arabinose for 1.5 hours in both *E. coli ΔtatAE* and *ΔtatABCDE* cells. After 1.5 hours of induction the cells were harvested, washed, and then resuspended using growth medium without arabinose present. Cells were then cultured for a further 1 hour. Samples of the cultures were taken every half an hour during the experiment, fractionated and membrane samples collected. Membranes were solubilised in 1% SDS and run on SDS-PAGE gels before immunoblotting with antibodies against the *Strep*-II^{TM} tag on TatE.

As shown in Figure 5.2.2, after 1.5 hours of induction in both backgrounds TatE proteins were detectable in the membranes. After induction was stopped at 1.5 hours, the TatE protein remained largely stable and a significant proportion was still present after the total 2.5 hours of the experiment in *ΔtatAE* cells. In contrast, after induction was stopped in *ΔtatABCDE* cells, TatE was no longer detectable in the membranes suggesting that it was unstable in absence of the other Tat components.

This result is indirect evidence that TatE may be stabilized in the membranes by interacting with the other Tat subunits.

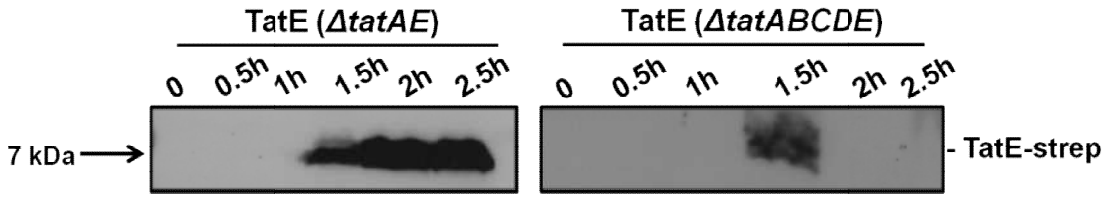

Figure 5.2.2 TatE time course experiment in *E. coli ΔtatAE* and *ΔtatABCDE* cells
Plasmid pBAD-E-Strep carried by *E. coli ΔtatAE* or *ΔtatABCDE* cells was induced for 1.5 hours with 1 mM arabinose before induction was stopped. The cells were then grown for further 1h. Every half an hour during the experiment samples of the culture were taken and cells fractionated. Membrane fractions were analysed by SDS-PAGE and immunoblotted using antibodies against the *Strep*-II^{TM} tag on TatE. Mobility of TatE-strep is indicated on the right. The molecular mass marker is indicated on the left.

5.2.3 TatE does not appear to interact with the TatB and TatC subunits

To test more directly for an interaction between TatE and either TatB or TatC, co-immunoprecipitation experiments were performed. TatE was expressed from the plasmid pBAD-E-Strep in *E. coli ΔtatAE* cells. Membranes were isolated, solubilised with digitonin and immunoprecipitated with anti-TatB or anti-TatC antibodies as described in chapter 2. The samples were run on SDS-PAGE gels before immunoblotting with antibodies against the *Strep*-II^{TM} tag on TatE.

As shown in Figure 5.2.3A TatE cannot be effectively immunoprecipitated using antibodies raised against either TatB (IP α-TatB pellet, panel) or TatC (IP α-TatC pellet, panel) and it was therefore detectable in the supernatant after the centrifugation step in the co-immunoprecipitation experiments (IP α-TatB supernatant and IP α-TatC supernatant, panels). No immunoprecipitation of TatE was observed in a control experiment using an irrelevant antiserum raised against the Green Fluorescent Protein (GFP) (IP α-GFP pellet, panel).

In contrast in positive control experiments (Figure 5.2.3B) using *E. coli ΔtatABCDE* cells expressing *E. coli* TatABC from plasmid pBAD-ABC-Strep, the majority of TatA was immunoprecipitated by anti-TatB antibodies (IP α-TatB pellet, panel) indicating that TatA interacted with TatB as has been already shown by Bolhuis *et al*. (2000). A minor amount of TatA was also present in the supernatant but it was probably due to the large excess of protein produced which cannot be immunoprecipitated (IP α-TatB supernatant, panel). Again no immunoprecipitation was observed using an irrelevant antiserum raised against GFP (IP α-GFP pellet, panel) and all TatA was detected in the supernatant (IP α-GFP supernatant, panel).

Thus TatE appears not to bind to the TatBC complex *in vitro*. Given that TatE can functionally substitute for TatA in *E. coli* this result was surprising, and it may be the case that TatE and TatBC interact *in vivo*, but that this interaction is transient and is not observed in this *in vitro* assay. However this result could be significant; in the plant Tat system, TatA only associates with the TatBC complex in the presence of substrate and ongoing translocation (Mori and Cline, 2002).

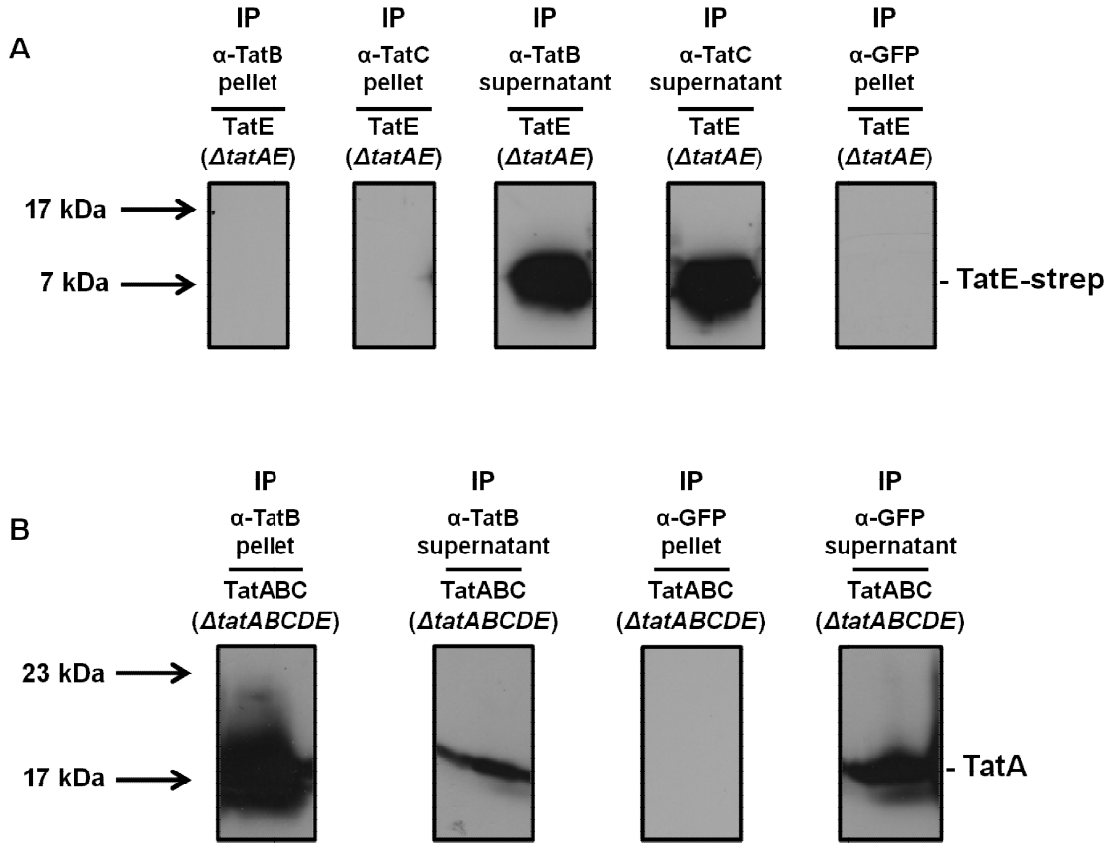

Figure 5.2.3 Co-immunoprecipitation experiments
A. Membranes of *E. coli ΔtatAE* cells expressing TatE were isolated, solubilised with digitonin and immunoprecipitated with anti-TatB, anti-TatC or anti-GFP antibodies (IP α-TatB, IP α-TatC or IP α-GFP respectively). Pellet and supernatant fractions are indicated. The samples were analysed by SDS-PAGE and immunoblotted using antibodies against the *Strep*-II^{TM} tag on TatE. Mobility of TatE-strep is indicated on the right. Molecular mass markers are indicated on the left. Panels were spliced from the same gel (See Appendix A).
B. Membranes of *E. coli ΔtatABCDE* cells expressing TatABC were isolated, solubilised with digitonin and immunoprecipitated with anti-TatB or anti-GFP antibodies (IP α-TatB or IP α-GFP respectively). Pellet and supernatant fractions are indicated. The samples were analysed by SDS-PAGE and immunoblotted using antibodies against TatA. Mobility of TatA is indicated on the right. Molecular mass markers are indicated on the left. Panels were spliced from the same gel (See Appendix A).

5.2.4 Study of the interaction between the TatE and TatA subunits

As mentioned previously, in WT *E. coli* MC4100 cells TatA and TatE are expressed constitutively along with the other Tat components (Jack *et al*., 2001). Moreover these two proteins have overlapping functions in protein transport by the Tat pathway (Sargent *et al*., 1998). In chapter 3 it has been shown that overexpressed TatE, in the absence of TatA, was able to form homo-oligomeric complexes in the membrane. It is thus reasonable to suggest that TatE may interact with TatA during the translocation process forming TatAE mixed complexes. Nevertheless the formation of these complexes has not been reported so far.

In order to investigate the association between TatE and TatA proteins, *tatE* was cloned with a C-terminal *Strep*-II^{TM} tag into the IPTG-inducible vector pEXT22 forming the plasmid pEXT-E-Strep. Next the vectors pEXT-E-Strep and pBAD-A, which expresses TatA, were used to transform *E. coli ΔtatAE* cells. These vectors are compatible which means they can both be maintained within the same *E. coli* cells. However, induction of both promoters by IPTG and arabinose respectively cannot be achieved simultaneously because the two substances appear to inhibit each other (unpublished data). Therefore expression from each plasmid must be separated by time.

First of all the TMAO reductase (TorA) activity assay shown in chapter 3 was used to test whether the simultaneous overexpression of TatE and TatA can complement *E. coli ΔtatAE* cells by restoring export activity. The pBAD-A plasmid was induced first for ~ 2 hours under low oxygen conditions. After the removal of arabinose from the growth medium, the pEXT-E-Strep was induced by IPTG for ~ 2 hours under low oxygen conditions as well. The cells were then fractionated and periplasmic (P), membrane (M), and cytoplasmic (C) fractions prepared. Samples of each were run on a native-PAGE gel which was analyzed for the presence of TorA activity.

As shown in Figure 5.2.4, overexpression of TatE and TatA in *E. coli ΔtatAE* cells (TatE + TatA (*ΔtatAE*), panel) led to efficient export of TorA into the periplasm, suggesting therefore that when TatE and TatA are overexpressed simultaneously, in combination with TatB and TatC components expressed at native levels, they

contribute to the formation of an active translocation system. As shown previously in the *E. coli ΔtatAE* double mutant, no periplasmic activity was detected since Tat export is blocked (*ΔtatAE* panel).

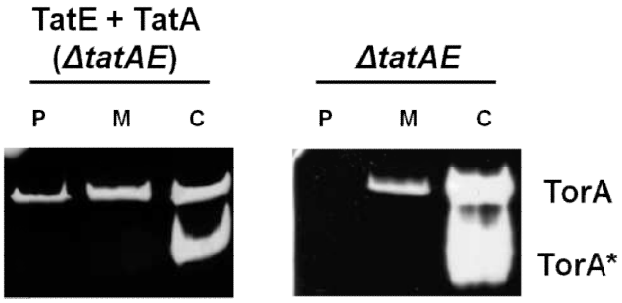

Figure 5.2.4 Traslocation of TMAO reductase by simultaneous overexpression of TatE and TatA
The figure shows native polyacrylamide gels stained for TMAO reductase (TorA) activity. Periplasm, membrane and cytoplasm samples (P, M, and C respectively) were prepared and analyzed from *E. coli ΔtatAE* cells co-expressing *E. coli* TatE and TatA (TatE + TatA (*ΔtatAE*)) and from *E. coli ΔtatAE* cells. The mobility of active TorA is indicated. TorA* indicates a faster migrating form of TorA.

Next, to investigate the ability of TatE and TatA to associate with each other and form hetero-oligomeric complexes in the membranes, affinity chromatography was used. 500 ml of *E. coli ΔtatAE* cells expressing TatE from the plasmid pEXT-E-Strep and TatA from the plasmid pBAD-A were induced first with arabinose and then with IPTG separately. The cells were then fractionated and membranes were isolated as described in chapter 2. Total membranes were solubilized in 2% dodecyl maltoside (DDM) and applied to a 2 ml Streptactin^{TM}-affinity column as described previously.

If the TatA subunit had interacted with TatE which is tagged with a C-terminal *Strep*-II^{TM} tag, TatA should have been detected in the Streptactin^{TM} column elution fractions co-eluting with TatE. Column elution fractions were resolved on SDS-PAGE gels and subsequently immunoblotted using antibodies either to the *Strep*-II^{TM} tag on TatE or against TatA. Figure 5.2.5 shows the presence of Strep-tagged TatE protein and TatA protein in the elution fractions from this column. TatE was eluted

across elution fractions E4-E8 (Figure 5.2.5A), whereas TatA was detectable in almost all the Streptactin™ elution fractions (Figure 5.2.5B). No TatE or TatA was detected in the wash fraction before protein was eluted which suggests the protein was bound in the case of TatE and partially co-eluted in the case of TatA. The presence of TatA in the earlier elution fractions may be due to non specific interactions between the protein and the column. This hypothesis could be tested by purification experiments using TatA alone. Moreover if the TatAE complex was quite transient and the binding constant quite weak then perhaps TatA became free during the elution steps and that is why it may come off the column earlier than TatE. Another explanation could be that the TatAE complexes might be weakened by the detergent used during the purification.

In conclusion this result suggests that TatE and TatA may be associated in the formation of TatAE mixed complexes, even though this cannot be demonstrated unequivocally by the co-purification experiment.

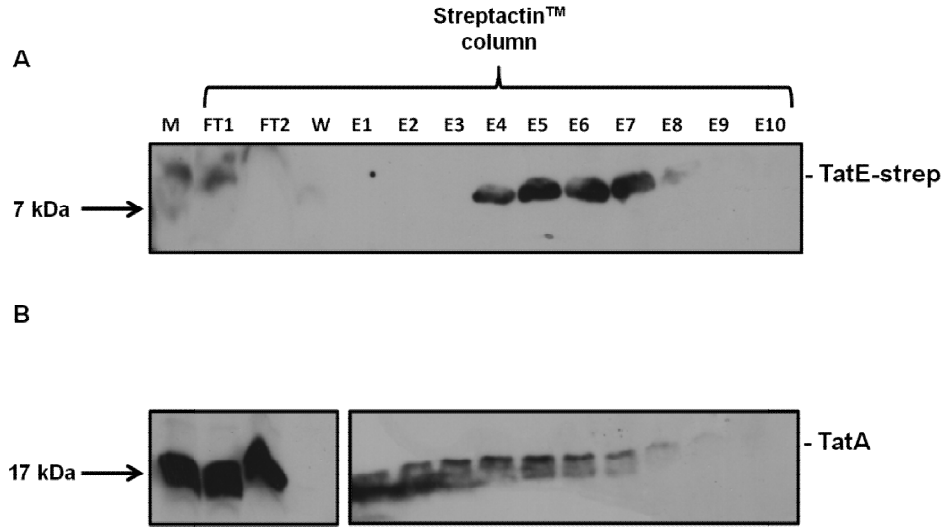

Figure 5.2.5 Co-purification of TatE and TatA by affinity chromatography
Membranes were prepared from *E. coli ΔtatAE* cells co-expressing *E. coli* TatE with a C-terminal *Strep*-II™ tag and *E. coli* TatA. Membranes were solubilised in DDM and applied to a Streptactin™-affinity column. All column fractions were analysed by SDS-PAGE and immunoblotted using antibodies against the *Strep*-II™ tag on TatE (**A**) and against TatA (**B**). Whole membranes (M), column flows through (FT1, FT2), wash fractions (W) and elution fractions (E1-E10) are all indicated. Mobilities of TatE-strep and TatA are indicated on the right. Molecular mass markers are indicated on the left.

5.2.5 Blue-native polyacrylamide gel electrophoresis (BN-PAGE) of TatAE mixed complexes

The possible interaction between TatE and TatA which may indicate the presence of TatAE mixed complexes was further analysed by BN-PAGE. As mentioned previously BN-PAGE is a good tool to study the Tat complexes because the proteins are not denatured therefore the interactions which hold the subunits together can be maintained.

Membranes were prepared from *E. coli ΔtatAE* cells co-expressing TatE from plasmid pEXT-E-Strep and TatA from plasmid pBAD-A and were solubilised in digitonin. The BN-gels were subsequently immunoblotted using antibodies against the *Strep*-II^{TM} tag on TatE and against TatA. As shown in Figure 5.2.6A TatE complexes ran as oligomeric complexes with estimated sizes ranging from over 140 kDa to ~ 669 kDa, whereas TatA complexes, as shown in Figure 5.2.6B, formed the same ladder of bands observed in Figure 3.2.7 of chapter 3. These bands corresponded to separate complexes with estimated sizes ranging from ~ 100 kDa to over 500 kDa which were observed in an earlier study (Oates *et al*., 2005). As reported in chapter 3, BN-PAGE results have shown that TatE proteins when they are expressed in *E. coli ΔtatAE*, in absence of TatA, they were organized in two major complexes with estimated sizes of ~ 66 kDa or just larger. Surprisingly, as shown in Figure 5.2.6A, when TatE was co-expressed along with TatA, the small TatE complexes of ~ 66 kDa were not present anymore. In contrast TatE appears to be organized in high molecular weight oligomeric complexes which migrated in the BN-gel similarly to the higher molecular weight TatA complexes (Figure 5.2.6B).

This result suggests indirectly that TatE, when is co-expressed with TatA, may associate with the larger TatA complexes resulting in the formation of TatAE hetero-oligomeric complexes.

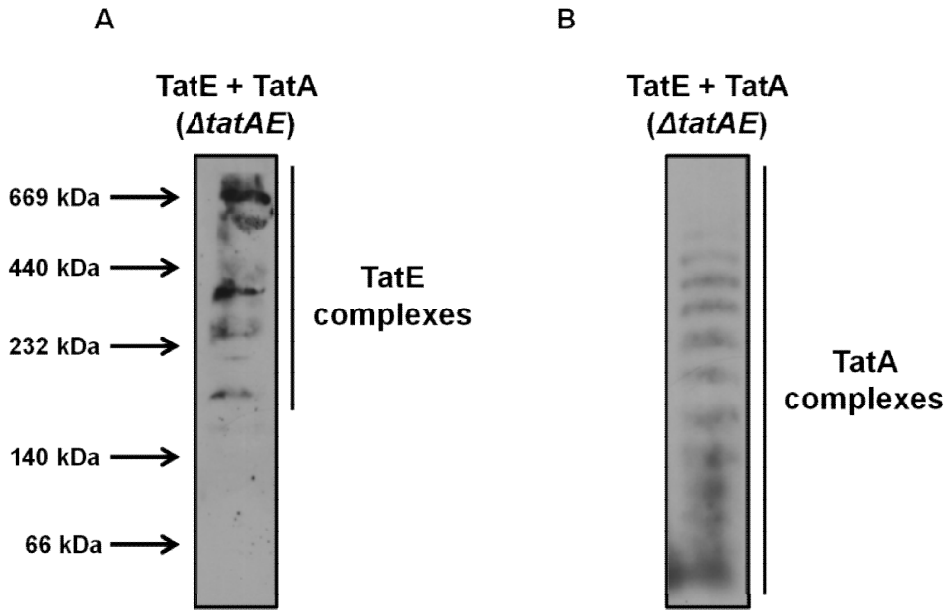

Figure 5.2.6 BN-PAGE of TatAE mixed complexes
Membranes were prepared from *E. coli ΔtatAE* cells co-expressing *E. coli* TatE with a C-terminal *Strep*-II™ tag and *E. coli* TatA. Membranes were solubilised in digitonin and subjected to BN-PAGE. The BN-gels were immunoblotted using antibodies against the *Strep*-II™ tag on TatE (**A**) and against TatA (**B**). Mobilities of TatE and TatA complexes are indicated on the right. Molecular mass markers are indicated on the left.

5.3 Discussion

In chapter 3 alternative models for the Tat-dependent translocation when TatA is absent and TatE overexpressed have been proposed since small sizes of TatE complexes appeared to preclude a role in forming the entire translocation channel. These new models for Tat function were radically different from currently favoured models. One alternative model was consistent with a more discrete form of Tat translocase which is sufficiently flexible to transport a wide range of substrates. Whereas a second alternative model involved a different scenario: multiple TatE complexes may bind to the TatBC complex once substrate has been bound. This would have the advantage of providing flexibility of pore size, with differing numbers of TatE complex generating translocation channels of differing diameters. In a third alternative model proposed the TatBC complex may form the translocation channel and TatE or TatA may activate it.

In this chapter the physical interactions between TatE and the other Tat components have been investigated for the first time, with the aim to gain more insight into the involvement of TatE in the Tat transport mechanism.

The level of TatE, expressed by the arabinose-inducible vector pBAD24, was found to be influenced by the absence or presence of the other Tat subunits. TatE was present at comparably high levels in *E. coli ΔtatAE* cells, whereas the level of TatE was lower in *ΔtatA*, *ΔtatB* and WT cells. These results may suggest that the presence of native TatE could somehow have a negative impact on the stability of the overexpressed TatE. At present it is not clear why this might be the case. The amount of TatE was even lower after expression in the *ΔtatC* strain. TatC therefore may be important in stabilizing TatE in the membrane. This finding is not unexpected since TatC has been shown to drive the assembly of the TatABC complex where it acts as a scaffold for complex assembly (Behrendt *et al.*, 2007; Mangels *et al.*, 2005). Surprisingly in the *ΔtatABCDE* null strain overexpressed TatE was not detectable at all suggesting that TatE was either not expressed or was unstable in cells lacking all the other Tat components.

A time course experiment performed on the *ΔtatABCDE* cells overexpressing TatE has shown that TatE was indeed expressed in this strain, but that it was unstable. This result therefore provides some indirect evidence that TatE may be stabilized in the membranes by interactions with the other Tat subunits.

Nevertheless immunoprecipitation studies have shown that TatE does not seem to stably bind either TatB or TatC subunits even though as shown in chapter 3 it took part in the substrate translocation process. In contrast the paralog TatA was found to interact with TatB (Bolhuis *et al*., 2000) and to be present in the TatABC substrate binding complex (Bolhuis *et al*., 2001) where it may have a role in stabilizing TatB (Mangels *et al*., 2005). TatE may just interact transiently with the other Tat components during the substrate transport. Similar findings were reported for the thylakoid TatA homologue Tha4 which was found to cross-link to the Hfc106 in the presence of a proton gradient and substrate, but no cross-link was detected under resting conditions (Mori and Cline 2002).

In this chapter an interaction between TatE and TatA paralogous proteins has been investigated for the first time. TatE Strep-tagged and TatA proteins were co-expressed by using the compatible vectors pEXT22 and pBAD24 in *E. coli ΔtatAE* cells. Firstly TMAO reductase (TorA) activity assay showed that simultaneous overexpression of TatE and TatA proteins contributes to the formation of an active translocation system. Next, co-purification of TatE and TatA by affinity chromatography has suggested that the two subunits may be associated in the formation of TatAE mixed complexes. The features of those possible complexes were further analysed by BN-PAGE and these results have shown that TatA complexes, even in the presence of overexpressed TatE proteins, form the same ladder of bands with estimated sizes ranging from ~ 100 kDa to over 500 kDa observed in an earlier study (Oates *et al*., 2005). In contrast TatE seemed to form high molecular weight oligomeric complexes with estimated sizes ranging from over 140 kDa to ~ 669 kDa which differed significantly from the small TatE complexes shown in chapter 3. Those TatE complexes migrated in the BN-gel similarly to the higher molecular weight TatA complexes suggesting indirectly that TatE, when is co-expressed with TatA, may associate with the larger TatA complexes resulting in the formation of TatAE hetero-oligomeric complexes.

In chapter 3 it has been shown that TatE and TatA have overlapping roles in protein export by the Tat pathway; however TatE has been reported to play a distinct role either in biofilms or denitrification (Beloin *et al*., 2004; Heikkilä *et al*., 2001). Therefore it would be interesting to investigate whether the TatAE mixed complexes have a role in the cell growth under specific conditions as in the biofilm formation.

Further studies are of course required to confirm the results presented in this chapter. Perhaps using cross-linking approaches would provide a better understanding of the interactions between TatE and the other Tat components.

Chapter 6.

The TatAc protein of Bacillus subtilis forms active Tat systems with TatCd and TatCy

6.1 Introduction

Unlike Gram-negative bacteria, most Gram-positive bacteria, except for *Streptomyces lividans* (De Keersmaeker *et al*., 2005), possess a simpler 'minimalist' Tat system that lacks a TatB component (Jongbloed *et al*., 2004). The Gram-positive bacterium *Bacillus subtilis* contains at least two minimal Tat translocases, each consisting of one specific TatA and one specific TatC subunit and named TatAdCd and TatAyCy (Jongbloed *et al*., 2004). These two TatAC-type systems operate in parallel with apparently different substrate specificities (Jongbloed *et al*., 2006). PhoD is the only identified substrate of the TatAdCd pathway and it is encoded along with the *tatAd* and *tatCd* genes in an operon and expressed under conditions of phosphate limitation (Pop *et al*., 2002). PhoD has both phoshodiesterase and alkaline phosphatase activity and is required for acquisition of inorganic phosphate (Jongbloed *et al*., 2000).

YwbN, a DyP-dependent (dye decolourising) peroxidase that is thought to be important for Fe acquisition, is translocated by the TatAyCy translocase and it is the only identified substrate that is transported by the TatAyCy pathway (Jongbloed *et al*., 2004). The *ywbN* gene is encoded along with the *tatAy* and *tatCy* genes and interestingly, unlike the TatAdCd translocase, the TatAyCy pathway is expressed under all tested conditions (Nicolas *et al*., 2012; Jongbloed *et al*., 2000).

A recent study has also shown that TatAy can be functionally replaced by TatAd when the latter is present in excess amounts (Eijlander *et al*., 2009). Furthermore it has been observed that under conditions of overproduction, TatAdCd was able to accept various Tat substrates (Eijlander *et al*., 2009). This is in contrast to the TatAyCy pathway that did not exhibit the same ability to translocate a wide-range of tested substrates (Eijlander *et al*., 2009).

Two novel Tat substrates have also been identified in *B. subtilis*, YkuE and QcrA (Widdick *et al*., 2008), but it remains to be determined which of the Tat subunits is required for the translocation of these proteins. Given that the TatAyCy pathway is constitutively expressed in *B. subtilis*, the current hypothesis is that this pathway

constitutes a general Tat export pathway, whilst TatAdCd is specifically involved in the cellular response to phosphate limitation.

The absence of any TatB component in most Gram-positive bacteria has suggested that the TatA component in these systems is bifunctional, performing the roles of both *E. coli* TatA and TatB (Jongbloed *et al*., 2006). In support to this idea the TatAdCd pathway has been shown to function in *E. coli* and to transport a number of *E. coli* Tat-substrates (Barnett *et al*., 2008). Recently the presence of an N-terminal TatB-type domain within TatAd, along with a separate domain that seems to be universally conserved among TatA/TatB proteins has been reported (Barnett *et al*., 2011a). In addition, a study performed in *E. coli*, using a chimeric Tat-substrate, has demonstrated that suppressor mutations mapping in the extreme N-terminal domain of TatA can compensate strongly for the absence of TatB (Blaudeck *et al*., 2005). In support of these data a study by Barrett *et al*. (2007) found that bifunctional mutant TatA variants can translocate TorA in the absence of TatB. Similarly Ize *et al*. (2002b) showed that a TatAC system can be partially functional in *E. coli* and taken together these observations suggest that TatA may be a bifunctional component of the Tat machinery, not only in Gram-positive bacteria but also in *E. coli*.

Like the TatABC systems of Gram-negative bacteria, the *B. subtilis* TatAC systems are present at steady state in two separate Tat complexes within the membrane; nevertheless the sizes of the *B. subtilis* complexes are different from their *E. coli* counterparts. The TatAdCd system involves a ~ 230 kDa TatAdCd complex (as judged by BN-PAGE) together with a ~ 160 kDa homo-oligomeric TatAd complex (as judged by gel filtration chromatography) (Barnett *et al*., 2008). Similarly a discrete TatAyCy complex of ~ 200 kDa was found together with a separate ~ 200 kDa TatAy complex following expression in *E. coli* (Barnett *et al*., 2009).

Cross-linking studies have shown that the *E. coli* TatC and TatB components play a critical role in substrate binding (Alami *et al*., 2003; Holzapfel *et al*., 2007). Since the *B. subtilis* Tat pathway is functional in *E. coli* and is able to translocate a number of *E. coli* Tat substrates (Barnett *et al*., 2008; Barnett *et al*., 2009), it is reasonable to hypothesise that the TatAdCd and TatAyCy complexes are similarly functioning in substrate recognition and binding. However an alternative model has been presented

in the literature, where a soluble population of TatA protein is proposed to act as the initial receptor for Tat substrates, with TatA-substrate complexes targeted to membrane localised TatCd (Schreiber *et al*., 2006). This model has been discussed at length in chapter 4 of this manuscript. Both TatAd and TatAy have been observed alongside their expected membrane location in the cytoplasm, where they form very large complexes or aggregates (Barnett *et al*., 2008; Barnett *et al*., 2009).

Overall the *B. subtilis* TatAdCd and TatAyCy complexes were found to be considerably smaller than the *E. coli* TatABC complex. Moreover the TatAd and TatAy complexes appeared to lack the heterogeneity observed with the *E. coli* TatA complex in the membrane. This suggests a different model for Tat-dependent protein transport to the one already described, involving a single defined translocon rather than several size variants. This model has been discussed previously in chapter 3 for *E. coli*, where a limited range of TatE forms is consistent either with the presence of a single flexible translocon, or with multiple TatE complexes coming together to form the translocation channel.

A recent study has shown that certain TatAC translocases from Gram-positive bacteria are intrinsically salt-sensitive, suggesting critical roles for electrostatic interactions in the substrate translocation process (van der Ploeg *et al*., 2011). Interestingly, *B. subtilis* produces a third putative TatA subunit named TatAc, the *tatAc* gene is monocistronic and has no TatC counterpart (Jongbloed *et al*., 2000). The function of TatAc has remained enigmatic due to the fact that no phenotype was so far detectable for *tatAc* mutant *B. subtilis* cells (Jongbloed *et al*., 2000; Jongbloed *et al*., 2004; Tjalsma *et al*., 2000).

Figure 6.1 shows a sequence alignment of *B. subtilis* TatAd, TatAy and TatAc and reveals a high degree of sequence conservation between these three proteins. Only the first 60 amino acids are shown in the figure since the conserved residues are all within this region. The TatAc protein shares a completely conserved FGP motif with TatAd and TatAy. This motif forms a flexible ‘hinge’ region between the transmembrane and amphipathic helix. Mutation of these residues in TatAd have been shown to block the translocation of TorA after expression of the TatAdCd pathway in *E. coli* (Barnett *et al*., 2011a). Similarly the highly conserved ‘hinge’

regions of *E. coli* TatA and TatB have been shown to be important for Tat transport (Greene *et al*., 2007; Lee *et al*., 2006). Another conserved motif within the *B. subtilis* TatAd and TatAy proteins is a KLP motif which is located at the N-terminal end of the amphipathic helix. Again these residues are completely conserved in the TatAc protein too. Substitution of these three residues in TatAd to Ala revealed that the K25A variant can partially translocate TorA in *E. coli*, whereas the L26A variant blocked TorA transport completely. The P27A substitution showed no effect on TorA export (Barnett *et al*., 2011a).

In summary, the constitutive expression of *tatAc* in *B. subtilis* and the high degree of sequence homology between TatAc and TatAd and TatAy suggests that TatAc may also function in the *B. subtilis* Tat pathway.

Figure 6.1 Sequence alignment of *B. subtilis* TatAd, TatAy and TatAc
The TatAd, TatAy and TatAc proteins were aligned using the ClustalW program. Only the first 60 amino acids are shown. Conserved residues are indicated with black boxes and conserved substitutions with red boxes. The predicted transmembrane domain (TM) and the amphipathic helix (APH) are indicated above the alignment.

In this chapter the ability of TatAc to complement *E. coli ΔtatAE* and *ΔtatB* strains and to form active translocases in combination with *B. subtilis* TatCd or TatCy was investigated for the first time.

6.2 Results

6.2.1 TMAO reductase translocation by *B. subtilis* TatAc in *E. coli* strains

The ability of TatAc to complement *E. coli ΔtatAE, ΔtatB* and *ΔtatC* cells in the translocation of the *E. coli* Tat substrate TMAO reductase (TorA) was determined.

The *tatAc* gene was expressed with a C-terminal *Strep*-II tag from plasmid pBAD-Ac-Strep (courtesy of Carmine Monteferrante, University of Groningen) in *E. coli ΔtatAE*, *ΔtatB*, *ΔtatC* and wild type (WT) *E. coli* MC4100 cells. All strains were cultured under low oxygen conditions in order to promote the expression of TorA. These cells were then subjected to sub-cellular fractionation. The periplasmic (P), membrane (M), and cytoplasmic (C) fractions obtained were separated on a 10% native polyacrylamide gel that was subsequently assayed for trimethylamine-*N*-oxide (TMAO) reductase activity as described in chapter 2.

As shown in Figure 6.2.1 expression of TatAc was sufficient to restore translocation activity in the presence of native levels of TatB and TatC (*ΔtatAE* + TatAc panel) as a white band can be visualised in the periplasmic fraction, whereas expressed TatAc was not able to complement either the *E. coli ΔtatB* or *ΔtatC* mutants (*ΔtatB* + TatAc and *ΔtatC* + TatAc, panels). The inability of TatAc to complement *ΔtatB* for the translocation of TorA was in contrast with previous finding that *B. subtilis* TatAd can complement either *ΔtatAE* or *ΔtatB* cells (Barnett *et al*., 2008).

In negative control experiments, as expected, no activity was detectable in the periplasmic fractions of *ΔtatAE*, *ΔtatB* and *ΔtatC* mutants (*ΔtatAE*, *ΔtatB* and *ΔtatC*, panels) thus indicating that no translocation has occurred. In a positive control experiment WT *E. coli* MC4100 cells were able to export efficiently TorA into the periplasm (WT panel). Finally expression of TatAc in WT *E. coli* MC4100 cells (WT + TatAc panel) did not affect the TorA export, confirming that overexpression of *B. subtilis* TatAc was well tolerated in *E. coli* cells.

This data shows for the first time that expression of *B. subtilis* TatAc in *ΔtatAE* cells resulted in efficient export of TorA, thus suggesting that a functional interaction must occur between TatAc and the *E. coli* TatB and TatC components. The TatAc is thus effectively substituting for TatA/E, but not TatB.

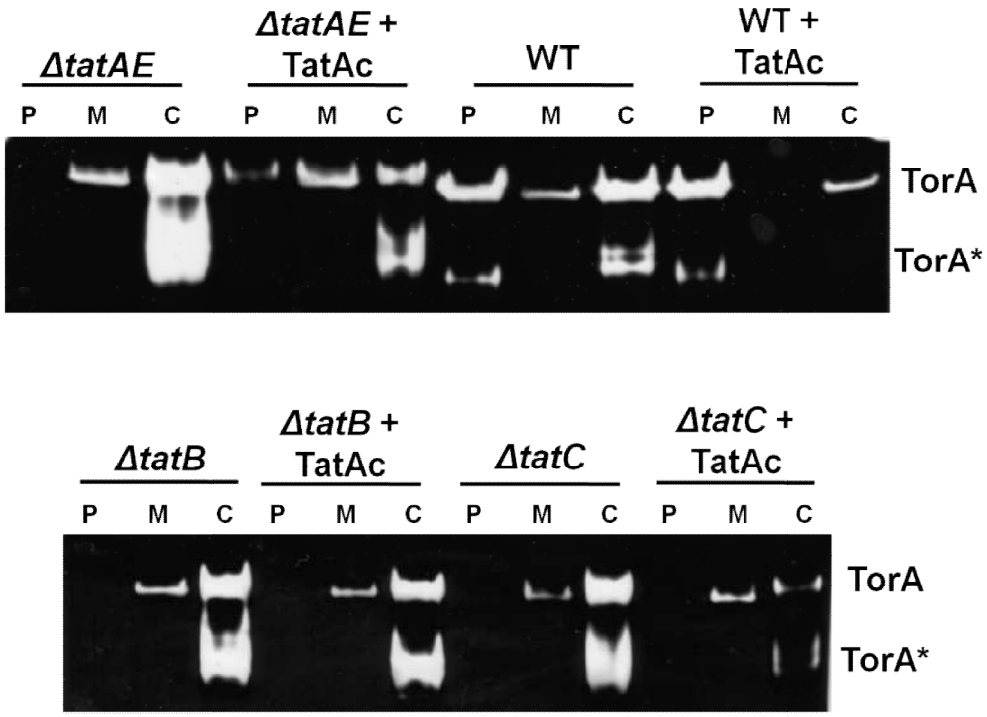

Figure 6.2.1 Traslocation of TMAO reductase by expression of *B. subtilis* TatAc in *E. coli* strains

The figure shows a native polyacrylamide gel stained for TMAO reductase (TorA) activity. Periplasm, membrane and cytoplasm samples (P, M, and C respectively) were prepared and analyzed. Strains used in this analysis were: WT *E. coli* MC4100 (WT panel), *E. coli ΔtatAE*, *ΔtatB* and *ΔtatC* cells or WT *E. coli* MC4100, *ΔtatAE*, *ΔtatB* and *ΔtatC* cells expressing *B. subtilis* TatAc from plasmid pBAD-Ac-Strep (WT + TatAc, *ΔtatAE* + TatAc, *ΔtatB* + TatAc and *ΔtatC* + TatAc, panels respectively). The mobility of active TorA is indicated. TorA* indicates a faster migrating form of TorA.

6.2.2 Translocation of ssDmsA-GFP, ssAmiA-GFP and ssMdoD-GFP in *ΔtatAE* cells expressing TatAc

The ability of *B. subtilis* TatAc to complement *E. coli ΔtatAE* cells in the transport of other substrates was tested. For this purpose substrates comprised of the signal peptide sequences of dimethyl sulfoxide reductase (ssDmsA), N-acetylmuramoyl-L-alanine amidase A (ssAmiA) or Glucans biosynthesis protein D (ssMdoD) linked to GFP were used. DmsA is a cofactor-containing Tat substrate which contains a molybdopterin cofactor and is used in anaerobic respiration (Méjean *et al*., 1994; Weiner *et al*., 1988). ssDmsA-GFP was previously shown to be translocated by Tat (Ray *et al*., 2003). AmiA and MdoD have both been identified as Tat substrates in *E. coli* (Ize *et al*., 2003; Lequette *et al*., 2004). AmiA, as described in chapter 3, is a cell wall amidase required in cytokinesis. MdoD is instead involved in the formation of periplasmic glucan backbone structures. All three heterologous substrates have been shown to be transported by TatAdCd and TatAyCy pathways in *E. coli ΔtatABCDE* cells (Barnett *et al*., 2009). Here, we tested whether a combination of TatAc plus native *E. coli* TatB and TatC could transport them.

Plasmids pBAD-ssDmsA-GFP or pBAD-ssAmiA-GFP or pBAD-ssMdoD-GFP were expressed in WT *E. coli* MC4100 cells, in *E. coli ΔtatAE* cells and in *E. coli ΔtatAE* cells expressing the *B. subtilis tatAc* gene from compatible plasmid pEXT-Ac-Strep with a C-terminal *Strep*-II^{TM} tag (courtesy of Carmine Monteferrante, University of Groningen). Following expression from both plasmids, cells were fractionated into periplasm (P), membrane (M) and cytoplasm (C) fractions which were subjected to SDS-PAGE and gels immunoblotted with anti-GFP antibodies.

As shown in Figure 6.2.2A, in *E. coli ΔtatAE* cells expressing both TatAc and ssDmsA-GFP, ssAmiA-GFP or ssMdoD-GFP a mature size GFP band (mGFP) was present in the immunoblot of the periplasmic fractions suggesting that expressed TatAc was able to form an active translocase in combination with native levels of *E. coli* TatB and TatC. Nevertheless precursor size GFP band (pGFP) was also detectable in all immunoblots of the periplasmic fractions. The meaning of this band is unknown; it may be due to contamination of the periplasm with membrane fraction

during the cells fractionation process. A third band of unknown meaning is also present in the periplasmic fraction when TatAc was coexpressed with ssAmiA-GFP (indicated with a red arrow in Figure 6.2.2A). Some protein was observed in the cytoplasmic and membrane fractions; they may represent precursor and processed form of the substrate. Proteolytic cleavage of the precursor protein in the cytoplasm and accumulation of precursor protein in the membrane, often running as a smear on immunoblots (indicated with arrow heads in Figure 6.2.2), have been already observed in other studies (Barnett *et al*., 2009; Mendel *et al*., 2008). The presence of a mature size GFP band in the membrane fraction was unexpected; it could be due to non-specific clipping of the protein to a size that was very similar to mGFP. An alternative hypothesis is that, since some clipping of the pGFP was apparent in the cytoplasmic fraction, the mGFP band in the membrane fraction may correspond to untranslocated protein that was non-specifically clipped in the cytoplasm and was stuck in the translocon.

As shown in Figure 6.2.2B, no GFP bands were present in the periplasmic fractions of *ΔtatAE* cells as expected, proving the ssDmsA-GFP, ssAmiA-GFP and ssMdoD-GFP export is Tat-dependent. Two faint bands were present in the periplasm when ssAmiA-GFP was expressed; it may again be due to contamination of the periplasmic fraction by the membrane or cytoplasmic fractions during the fractionation process. Again a smear of bands is present in the membrane and cytosolic fractions of ssAmiA-GFP.

As shown in Figure 6.2.2C, in WT *E. coli* MC4100 cells expressing the heterologous substrates the similar pattern of mature and precursor sized GFP bands, observed in Figure 6.2.2A, was here detectable; indicating therefore translocation as expected in these control samples.

These results thus demonstrate that *B. subtilis* TatAc can translocate ssDmsA-GFP, ssAmiA-GFP and ssMdoD-GFP forming an active translocase with *E. coli* TatB and TatC subunits, although the presence of contaminating precursor bands in the periplasm made drawing a firm conclusion difficult.

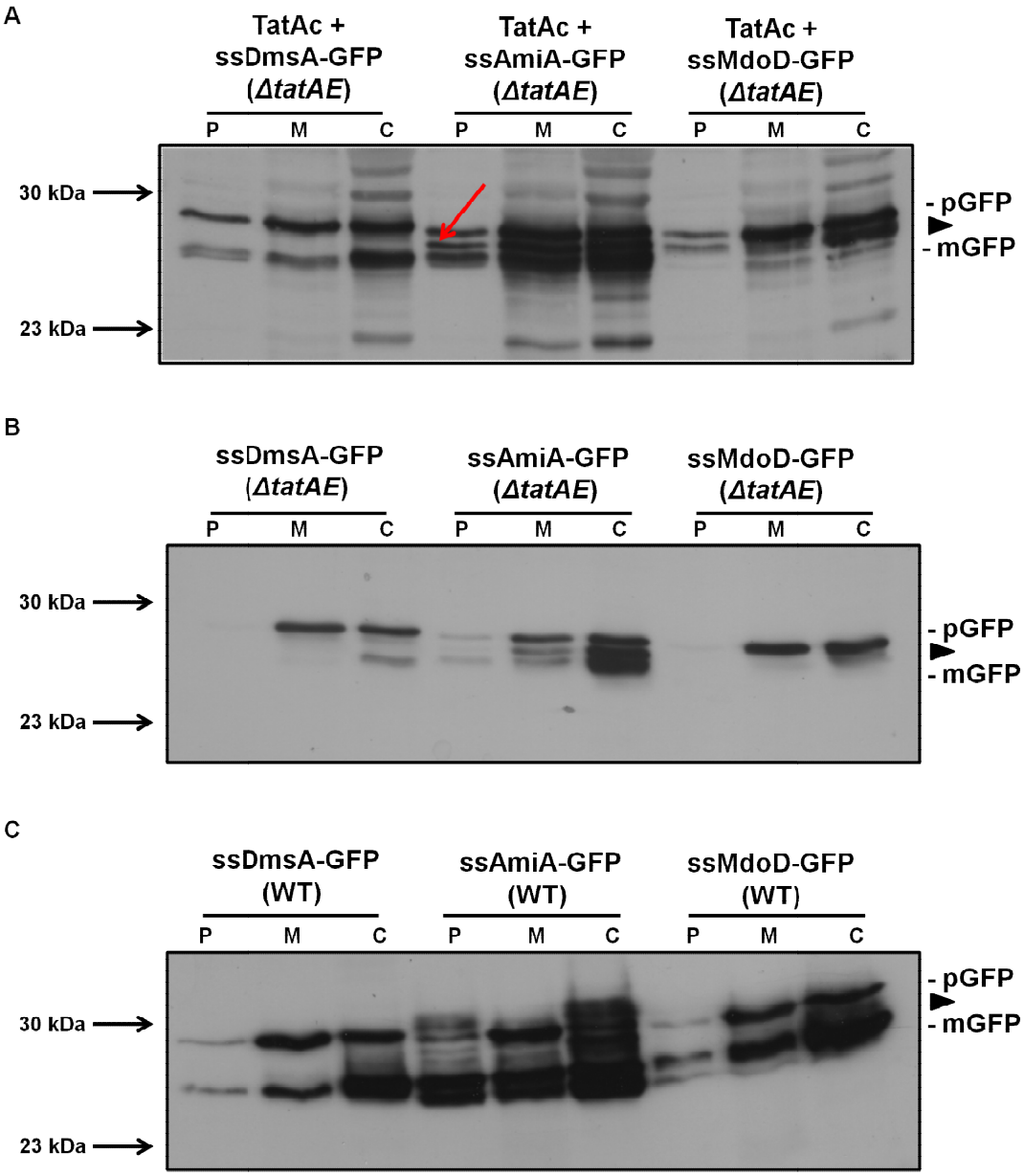

Figure 6.2.2 Translocation of ssDmsA-GFP, ssAmiA-GFP and ssMdoD-GFP in *ΔtatAE* cells expressing TatAc

ssDmsA-GFP, ssAmiA-GFP and ssMdoD-GFP were expressed using pBAD24 plasmids in either *ΔtatAE* cells expressing TatAc (**A**) or *ΔtatAE* cells (**B**) or WT *E. coli* MC4100 cells (**C**). Periplasm, membrane and cytoplasm samples (P, M, and C respectively) were isolated. Samples from each fraction were analysed by SDS-PAGE followed by immunoblotting with antibodies to GFP. The mobilities of precursor (pGFP) and mature (mGFP) GFP forms are indicated on the right. Arrow heads indicate bands of difficult interpretation running as a smear on immunoblots. The red arrow indicates a band of unknown meaning. Molecular mass markers are indicated on the left.

6.2.3 Blue-native polyacrylamide gel electrophoresis (BN-PAGE) of TatAc complex

As just shown *B. subtilis* TatAc was able to promote the export of TorA and heterologous substrates in combination with *E. coli* TatB and TatC components. Next the formation of TatAc complex in the membrane of *E. coli* strains was tested by using BN-PAGE.

Membranes were prepared either from *E. coli ΔtatAE* or *ΔtatABCDE* or *ΔtatB* cells expressing TatAc from plasmid pBAD-Ac-Strep and from *E. coli ΔtatAE* cells expressing TatA from plasmid pBAD-A-Strep as control. All membranes were then solubilised in digitonin and subjected to BN-PAGE analysis. The BN-gel was immunoblotted using antibodies against the *Strep*-II^{TM} tag on TatAc and TatA.

The data in Figure 6.2.3 shows that TatAc formed a small complex of ~ 100 kDa in all the *E. coli* strains tested which was similar to the larger *E. coli* TatE complex observed by BN-PAGE in chapter 3. This result shows therefore that *B. subtilis* TatAc was able to form small complexes in *E. coli* and its ability was neither affected by native expression levels of other *E. coli* Tat components nor their absence. In contrast, as shown in chapter 3, TatA was found organized in heterogeneous complexes with estimated sizes ranging from ~ 100 kDa to over 500 kDa.

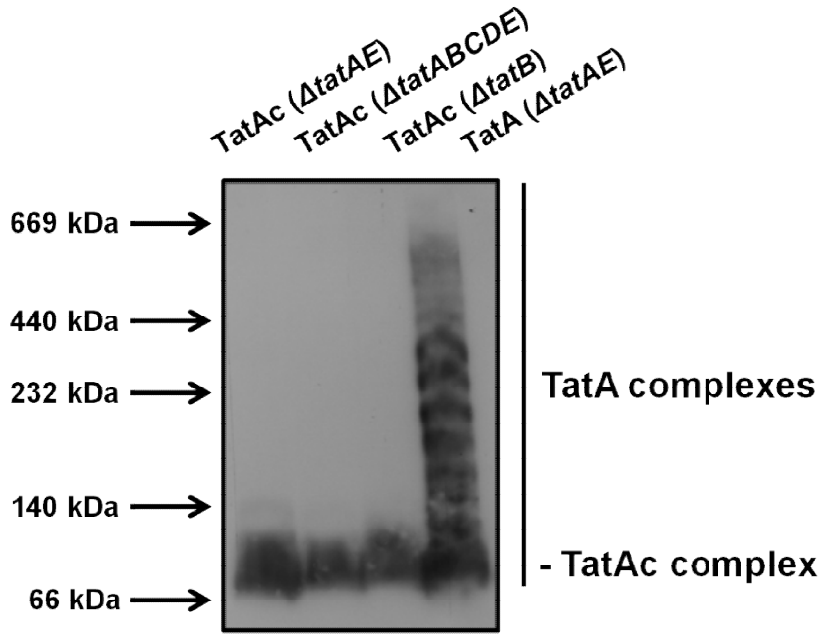

Figure 6.2.3 BN-PAGE of TatAc complexes
Membranes were prepared from either *E. coli ΔtatAE* or *ΔtatABCDE* or *ΔtatB* cells expressing *B. subtilis* TatAc with a C-terminal *Strep*-II^{TM} tag and and from *E. coli ΔtatAE* cells expressing *E. coli* TatA with a C-terminal *Strep*-II^{TM} tag. Membranes were then solubilised in digitonin and subjected to BN-PAGE. The BN-gel was immunoblotted using antibodies against the *Strep*-II^{TM} tag on TatAc and TatA. Mobilities of TatAc and TatA complexes are indicated on the right. Molecular mass markers are indicated on the left.

6.2.4 Translocation of TMAO reductase by TatAcCd and TatAcCy mixed translocases

As mentioned previously the *B. subtilis tatAc* gene is not associated with any *tatC* gene on the chromosome (Jongbloed *et al*., 2000), nevertheless a recent array analysis across 104 conditions has shown that *tatAc* was expressed under most conditions (Nicolas *et al*., 2012) thus raising the possibility that active TatAcCd and/or TatAcCy mixed translocases may be functional. This possibility was tested by expressing the respective *B. subtilis tat* genes in *E. coli*, since the activity and assembly of *Bacillus* Tat translocases can be assayed more readily in this organism than in *B. subtilis* (Barnett *et al*., 2009; Barnett *et al*., 2008).

B. subtilis tatAcCd and *tatAcCy*, bearing a *Strep*-II^{TM} tag at the C-terminal of *tatCd* or *tatCy*, were cloned into pBAD24 vectors resulting in the formation of pBAD-AcCd-Strep and pBAD-AcCy-Strep respectively (courtesy of Carmine Monteferrante, University of Groningen). These vectors were subsequently used to transform *E. coli ΔtatABCDE* cells and the ability of the TatAcCd and TatAcCy proteins to support translocation of TMAO reductase tested. All strains were cultured, and these cells were then subjected to sub-cellular fractionation. The periplasmic (P), membrane (M), and cytoplasmic (C) fractions thus obtained were separated on a 10% native polyacrylamide gel that was subsequently assayed for TMAO reductase activity as described previously.

The results are shown in Figure 6.2.4. As a positive control WT *E. coli* MC4100 cells were used and, as expected, the cells were able to export TorA efficiently into the periplasm (WT panel). As negative controls *ΔtatABCDE* (*Δtat* panel) cells and *ΔtatABCDE* cells expressing either TatAc from plasmid pBAD-Ac-Strep (*Δtat* + TatAc panel) or TatCd from plasmid pBAD-Cd-Strep (*Δtat* + TatCd panel) or TatCy from plasmid pBAD-Cy-Strep (*Δtat* + TatCy panel) were tested. As expected the cells were not capable of transporting active TorA to the periplasm. Interestingly *ΔtatABCDE* cells expressing TatAcCd (*Δtat* + TatAcCd panel) or TatAcCy (*Δtat* + TatAcCy panel) were able to translocate TorA efficiently to the periplasm.

This result shows for the first time that TatAc was able to form active translocases in combination with TatCd or TatCy, at least when expressed in *E. coli*.

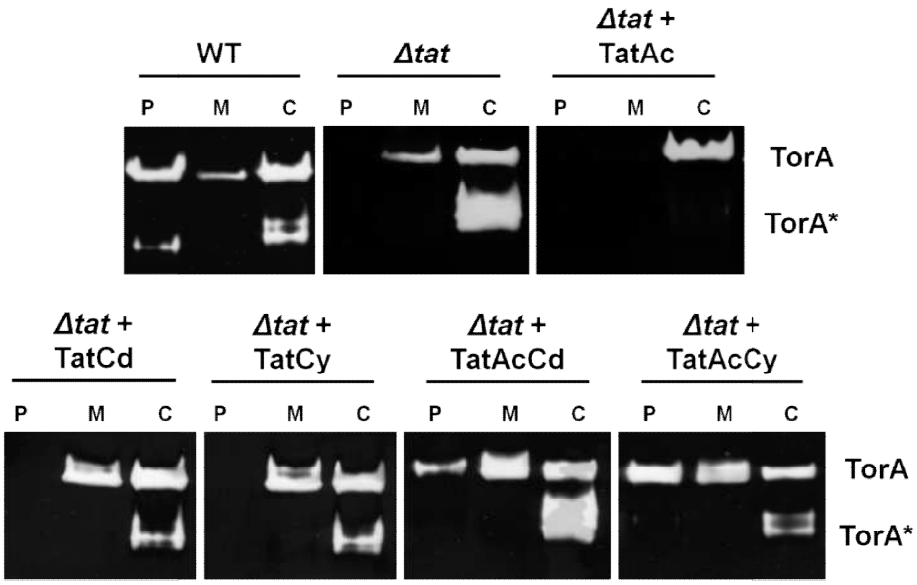

Figure 6.2.4 Traslocation of TMAO reductase by expression of *B. subtilis* TatAcCd and TatAcCy in *E. coli*
The figure shows native polyacrylamide gels stained for TMAO reductase (TorA) activity. Periplasm, membrane and cytoplasm samples (P, M, and C respectively) were prepared. Strains used in this analysis were WT *E. coli* MC4100 (WT), *E. coli* Δ*tatABCDE* (*Δtat*), or *E. coli* Δ*tatABCDE* expressing: *B. subtilis* TatAc from plasmid pBAD-Ac-Strep (*Δtat* + TatAc), *B. subtilis* TatCd from plasmid pBAD-Cd-Strep (*Δtat* + TatCd), *B. subtilis* TatCy from plasmid pBAD-Cy-Strep (*Δtat* + TatCy), *B. subtilis* TatAcCd from plasmid pBAD-AcCd-Strep (*Δtat* + TatAcCd) and *B. subtilis* TatAcCy from plasmid pBAD-AcCy-Strep (*Δtat* + TatAcCy). The position of active TorA is indicated. TorA* indicates a faster migrating form of TorA.

6.2.5 Translocation of the cell wall amidases, AmiA and AmiC by TatAcCd and TatAcCy

The activity of TatAcCd and TatAcCy mixed translocases was further investigated by testing the export of AmiA and AmiC, which, as mentioned in chapter 3, are both required for cell wall biosynthesis in *E. coli* (Bernhardt *et al*., 2003; Ize *et al*., 2003). Cells that do not export these molecules to the periplasm grow in long chains (Ize *et al*., 2003).

As shown in Figure 6.2.5A by phase contrast microscopy (carried out by Carmine Monteferrante, University of Groningen) WT *E. coli* MC4100 cells can be seen as single cells, as expected. In contrast *E. coli ΔtatABCDE* formed long chains due to the mis-localization of AmiA and AmiC (Figure 6.2.5B). *E. coli ΔtatABCDE* cells producing TatAcCd from plasmid pBAD-AcCd-Strep (Figure 6.2.5C) and TatAcCy from plasmid pBAD-AcCy-Strep (Figure 6.2.5D) showed the wild type phenotype although some slightly longer chains were still detectable.

These results suggest therefore that the export of AmiA and AmiC in *E. coli ΔtatABCDE* cells was at least partially restored by the production of TatAcCd or TatAcCy.

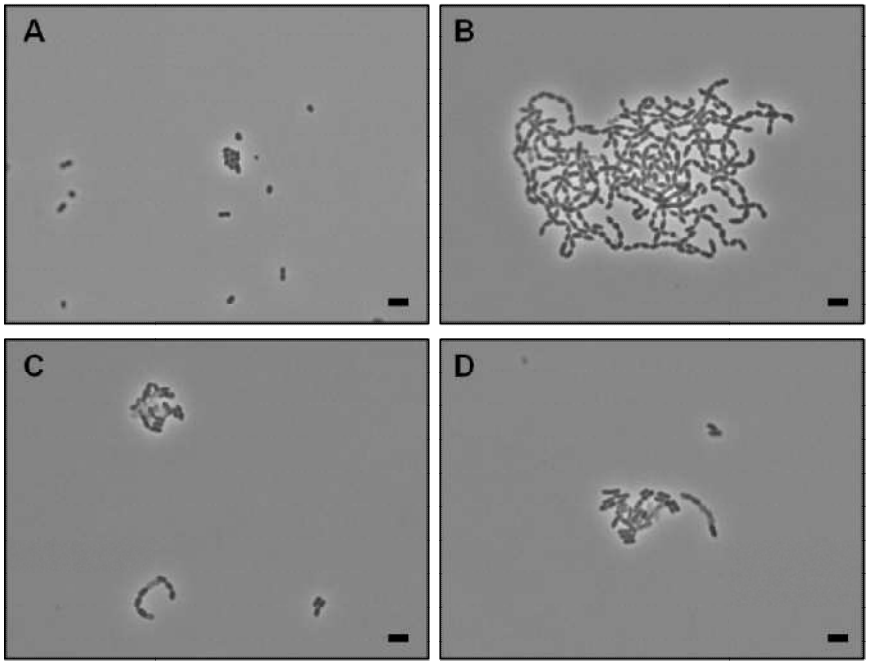

Figure 6.2.5 *B. subtilis* TatAcCd and TatAcCy facilitate AmiA and AmiC export in *E. coli*
Phase contrast microscopy images of: **A.** WT *E. coli* MC4100 cells; **B.** *E. coli* Δ*tatABCDE* cells; **C.** *E. coli* Δ*tatABCDE* cells producing TatAcCd from plasmid pBAD-AcCd-Strep; **D.** *E. coli* Δ*tatABCDE* cells producing TatAcCy from plasmid pBAD-AcCy-Strep. The scale bar is 1.5 μm. (Images provided by Carmine Monteferrante, University of Groningen).

6.2.6 Blue-native polyacrylamide gel electrophoresis (BN-PAGE) of TatAcCd and TatAcCy complexes

In order to investigate the formation of TatAcCd and TatAcCy complexes and to provide an estimate of their sizes a BN-PAGE analysis was performed. For this purpose membranes were isolated from *E. coli ΔtatABCDE* cells expressing either *B. subtilis* TatCd from pBAD-Cd-Strep or TatCy from pBAD-TatCy-Strep or TatAc from pBAD-Ac-Strep or TatAcCd from pBAD-AcCd-Strep or TatAcCy from pBAD-AcCy-Strep. Upon solubilization in 2 % digitonin, membrane proteins were separated by BN-PAGE, followed by immunoblotting with antibodies against the *Strep*-II^{TM} tag.

As shown in Figure 6.2.6, TatCd and TatCy alone formed bands of ~ 66 kDa. In addition, TatCd formed a minor band of ~ 100 kDa. As shown previously TatAc expressed on its own formed a small homogeneous complex of ~ 100 kDa. Importantly, when TatAc was co-expressed with either TatCd or TatCy, bands of ~ 232 kDa and ~ 200 kDa were observed respectively.

This showed that, indeed, TatAc formed membrane-embedded complexes with TatCd and TatCy similar in size to the *B. subtilis* TatAdCd and TatAyCy complexes which have been already described (Barnett *et al*., 2009; Barnett *et al*., 2008).

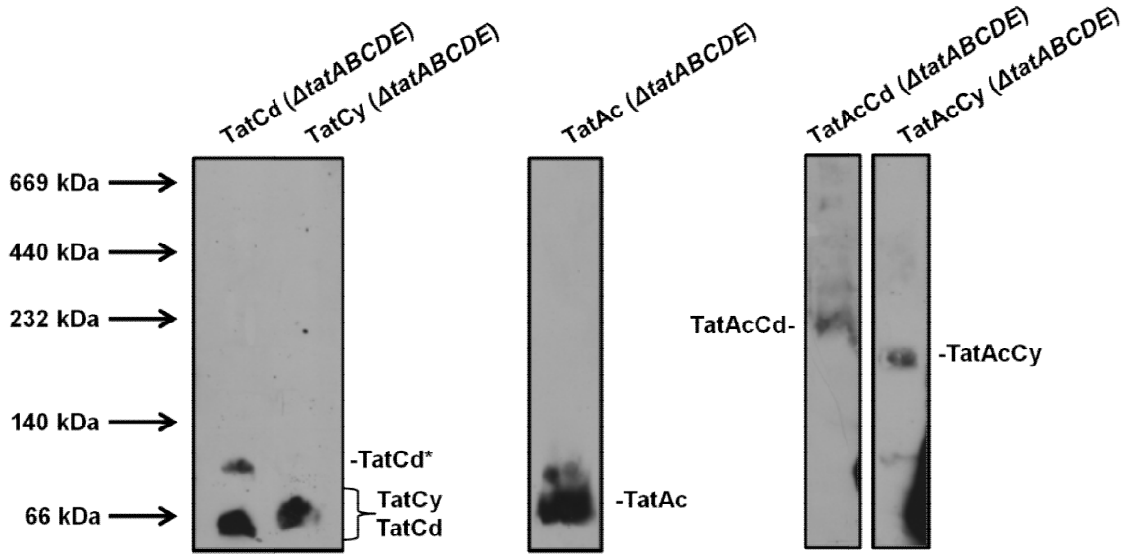

Figure 6.2.6 BN-PAGE of TatAcCd and TatAcCy complexes
Membranes were prepared from *E. coli ΔtatABCDE* cells expressing either *B. subtilis* TatCd or TatCy or TatAc or TatAcCd or TatAcCy. Membranes were then solubilised in digitonin and subjected to BN-PAGE. The BN-gels were immunoblotted using antibodies against the *Strep*-II™ tag. Mobilities of Strep-tagged proteins and complexes are indicated. TatCd* indicates a TatCd complex with higher molecular weight. Molecular mass markers are indicated on the left.

6.2.7 Affinity and gel filtration chromatography of TatAc, TatAcCd and TatAcCy complexes

In order to confirm the BN-PAGE results and to obtain an estimate of the TatAc, TatAcCd and TatAcCy complex sizes by using a different technique, affinity and gel filtration chromatography was used.

500 ml of *E. coli ΔtatABCDE* cells expressing either TatAc from the plasmid pBAD-Ac-Strep or TatAcCd from the plasmid pBAD-AcCd-Strep or TatAcCy from plasmid pBAD-AcCy-Strep were fractionated and membranes were isolated. Total membranes were solubilized in 2% dodecyl maltoside (DDM) and subjected to affinity chromatography using a 2 ml Streptactin™ column. The C-terminal *Strep*-

II^{TM} tag fused to TatAc, TatCd or TatCy binds specifically to the Streptactin^{TM} resin. After sample application the columns were subjected to washing with 16 ml of equilibration buffer before tightly bound proteins were finally eluted with 10 x 0.5 ml of buffer supplemented with desthiobiotin. All column wash and elution fractions were resolved on SDS-PAGE gels and subsequently immunoblotted using antibodies to the *Strep*-II^{TM} tag on TatAc or TatCd or TatCy. The Figure 6.2.7 shows that a small proportion of TatCd and TatCy was detectable in the column wash fractions (W), whereas no TatAc was detected. Higher molecular weight bands were also present (indicated by *). In all three cases most of the protein bound to the affinity column and was specifically eluted across elution fractions E4-E10.

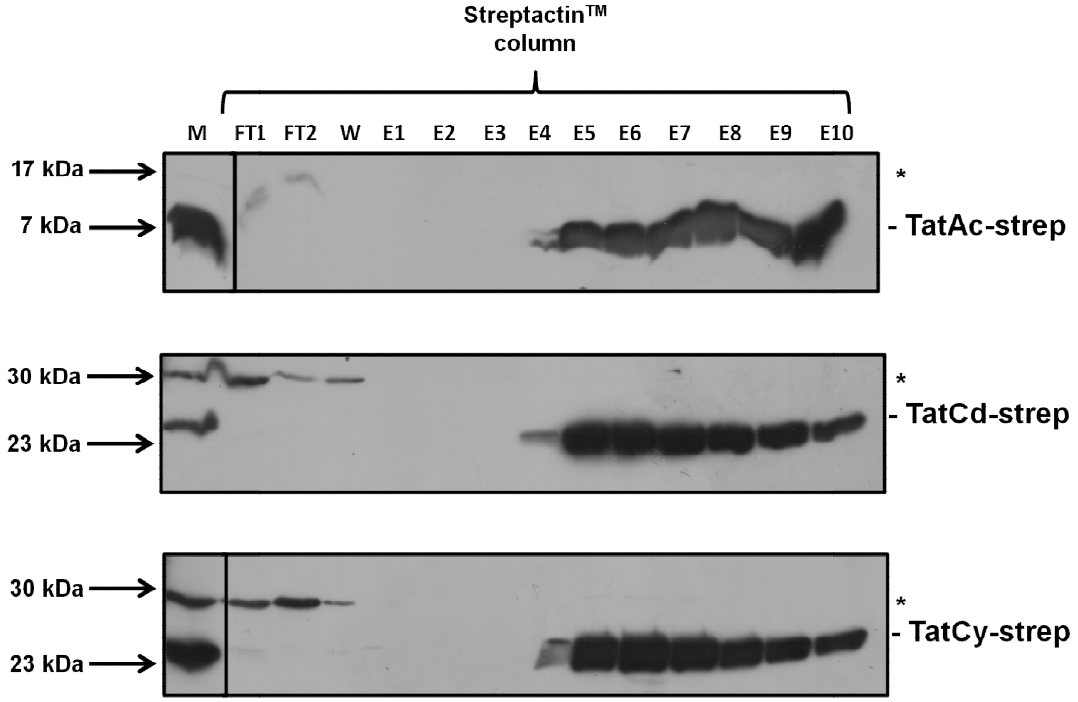

Figure 6.2.7 Affinity chromatography of *B. subtilis* TatAc, TatAcCd and TatAcCy
Membranes were prepared from *E. coli ΔtatABCDE* cells expressing either *B. subtilis* TatAc from the plasmid pBAD-Ac-Strep or TatAcCd from the plasmid pBAD-AcCd-Strep or TatAcCy from the plasmid pBAD-AcCy-Strep. The membranes were solubilised in DDM and applied to a Streptactin^{TM}-affinity column. All column fractions were analysed by SDS-PAGE and immunoblotted using antibodies against the *Strep*-II^{TM} tag on TatAc or TatCd or TatCy. Whole membranes (M), column flows through (FT1, FT2), wash fractions (W) and Streptactin^{TM} elution fractions (E1-E10) are all indicated. Mobilities of TatAc-strep, TatCd-strep and TatCy-strep are indicated on the right. (*) indicates slower migrating forms of TatAc, TatCd and TatCy. Molecular mass markers are indicated on the left.

Unfortunately in the absence of a specific anti-TatAc antibody it was not possible to prove unequivocally that TatAc was co-purified either with TatCd or TatCy in the Streptactin™ elution fractions. Nevertheless the BN-PAGE approach showed positively the formation of TatAcCd and TatAcCy complexes of ~ 232 kDa and ~ 200 kDa respectively, therefore it is reasonable to assume that TatAcCd and TatAcCy have been correctly purified by affinity chromatography.

Gel filtration chromatography was further used to estimate the sizes of the affinity-purified TatAc, TatAcCd and TatAcCy complexes. The samples were applied separately to a calibrated Superdex™-200 gel filtration column as described in chapter 3. The proteins were eluted from the column in 0.5 ml fractions with a single column volume of equilibration buffer. All eluted fractions were analysed by SDS-PAGE and the gels subjected to immunoblotting with *Strep*-II™ tag antibodies.

As shown in Figure 6.2.8A TatAc eluted across fractions 24-27 and according to the protein standards used to calibrate the column this gave a complex size range from ~ 50 kDa to ~ 100 kDa. In contrast TatCd (Figure 6.2.8B) and TatCy (Figure 6.2.8C) eluted from the column across fractions 21-27 and 20-27 respectively corresponding to complexes ranging in size from ~ 50 kDa to ~ 300 kDa. They are presumably the TatAcCd and TatAcCy complexes that were identified earlier by BN-PAGE analysis even though again the co-localization of TatAc with either TatCd or TatCy cannot be demonstrated unequivocally by gel filtration chromatography.

These results whilst less accurate than the BN-PAGE data (because of the influence of the detergent on the migration of the protein complexes through the column), confirm that TatAcCd and TatAcCy formed complexes larger in size than the homo-oligomeric TatAc complex.

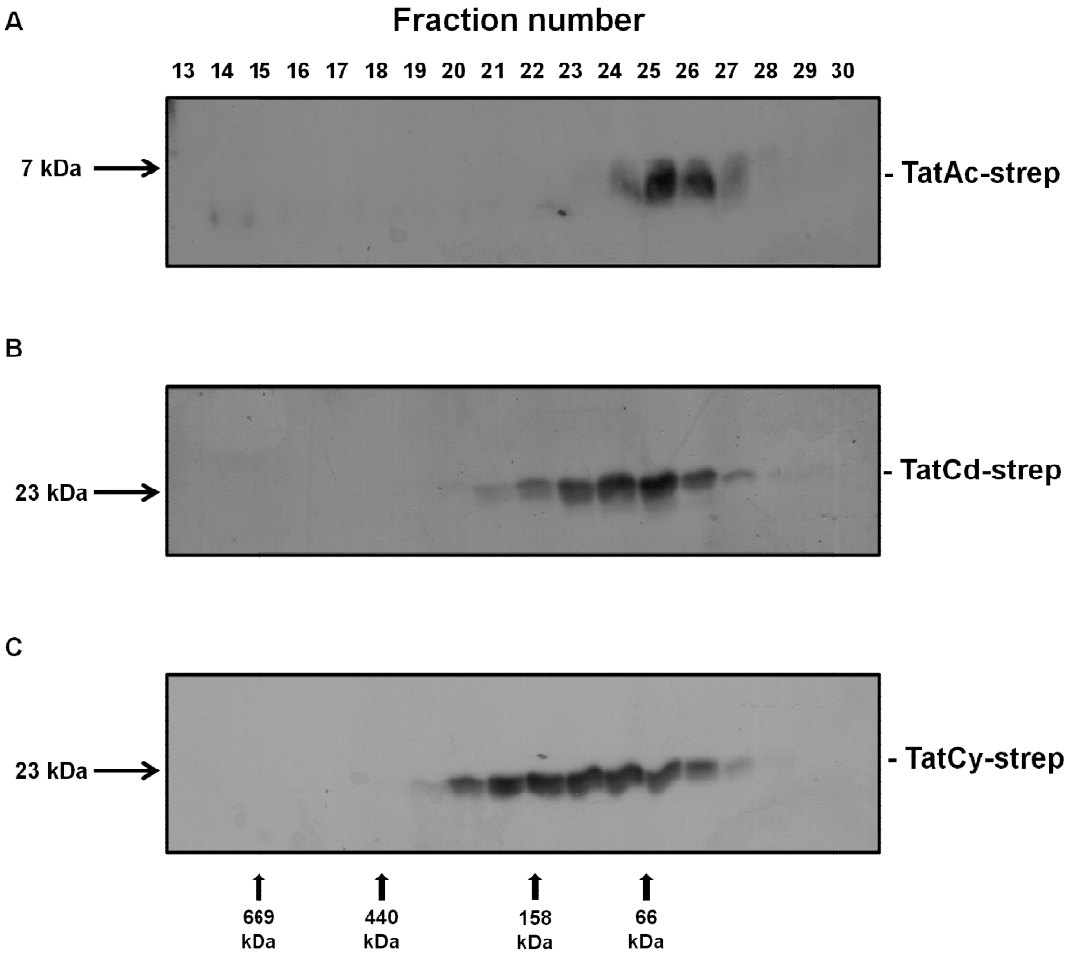

Figure 6.2.8 Gel filtration chromatography of *B. subtilis* TatAc, TatAcCd and TatAcCy complexes

Affinity purified TatAc (**A**), TatAcCd (**B**) and TatAcCy (**C**) complexes were applied to an equilibrated Superdex^{TM}-200 gel filtration column. Elution fractions were analyzed by SDS-PAGE and immunoblotted using antibodies to the *Strep*-II^{TM} tag on TatAc or TatCd or TatCy. Mobilities of TatAc-strep, TatCd-strep and TatCy-strep are indicated on the right. Molecular mass markers are indicated on the left. The peak elution of molecular mass markers is indicated with filled triangles and their molecular masses are shown.

6.3 Discussion

The Gram-positive *Bacillus subtilis* has two *tatC*-like genes denoted *tatCd* and *tatCy* and three TatA paralogues: TatAd, TatAy and TatAc (Jongbloed *et al*., 2000). In contrast to *E. coli*, in which the *tatA*, *tatB*, and *tatC* genes form one operon and the *tatE* gene is monocistronic (Sargent *et al*., 1998), the *tat* genes of *B. subtilis* are located at three distinct chromosomal regions (Jongbloed *et al*., 2000). The *tatAd* and *tatAy* genes have been found to be located upstream of the *tatCd* and *tatCy* genes respectively (Jongbloed *et al*., 2000). In contrast, the *tatAc* gene was found downstream of the *cotC* gene that encodes a spore coat protein (Donovan *et al*., 1987), and unlike *tatAd* and *tatAy* it was not genetically linked to the *tatC* genes (Jongbloed *et al*., 2000).

PhoD is the only identified substrate of the TatAdCd pathway and it is encoded along with the *tatAd* and *tatCd* genes in an operon which is only expressed under conditions of phosphate starvation (Pop *et al*., 2002). The *ywbN* gene, which encodes a DyP-dependent peroxidase, is instead expressed along with the *tatAy* and *tatCy* genes and it is the only identified substrate that is transported by the TatAyCy pathway (Jongbloed *et al*., 2004). Interestingly, even though the *tatAc* gene was found to be expressed under most conditions (Nicolas *et al*., 2012), its involvement in Tat-transport had not been addressed unequivocally until now.

In this chapter the ability of *B. subtilis* TatAc to complement *E. coli* strains was investigated for the first time. It has been shown previously that TatAdCd and TatAyCy can function in *E. coli* and transport both native *E. coli* Tat substrates as well as heterologous substrate proteins (Barnett *et al*., 2008; Barnett *et al*., 2009). As shown in the results section of this chapter, TatAc expressed in *E. coli ΔtatAE* cells was able to efficiently translocate TorA, demonstrating for the first time that a functional interaction must occur between TatAc and the *E. coli* TatB and TatC components. As expected TatAc was not able to complement *ΔtatC* cells since the presence of TatC has been shown to be essential for Tat-dependent translocation (Sargent *et al*., 1998). Interestingly TatAc was not able to complement *ΔtatB* cells, even though it shows a high degree of sequence similarity to the *E. coli* TatB protein

(53% identical residues and conservative replacements) (Jongbloed *et al*., 2000) and even higher sequence identity with TatAd. *B. subtilis* TatAd has been shown to complement both *ΔtatAE* or *ΔtatB E. coli* strains (Barnett *et al*., 2008). Furthermore a recent mutagenesis study has demonstrated that residues in the C-terminal half of the transmembrane span and in the 'hinge' region of TatAd were required for complementation of either *tatA* or *tatB* mutants in *E. coli* (Barnett *et al*., 2011a). In contrast, substitution of residues at the TatAd N-terminus specifically blocked the ability of the subunit to substitute for *E. coli* TatB (Barnett *et al*., 2011a). It would be interesting to use the same approach for studying which residues of TatAc are important for the complementation of *E. coli ΔtatAE* cells.

The ability of *B. subtilis* TatAc to complement *E. coli ΔtatAE* cells was further tested by using heterologous substrates consisting of the signal peptide of either DmsA, AmiA or MdoD linked with GFP. The results showed that besides TorA, TatAc was also able to translocate DmsA-GFP, AmiA-GFP and MdoD-GFP therefore forming an active translocase with *E. coli* TatB and TatC subunits.

The formation of TatAc complexes in the membrane of *E. coli* strains was tested by using BN-PAGE analysis. The results showed for the first time that TatAc formed a small complex of ~ 100 kDa in all the *E. coli* strains tested, and its formation was neither affected by native expression levels of other *E. coli* Tat components nor their absence. The TatAc complex was similar to the bigger *E. coli* TatE complex observed by BN-PAGE in chapter 3. Obviously more studies are required to fully characterise the TatAc complex. Structural studies on purified TatAc could provide an important contribution in understanding the role of TatAc in the formation of mixed translocases with *E. coli* TatB and TatC.

Since the *tatAc* gene is constitutively transcribed in *B. subtilis* (Jongbloed *et al*., 2004), it is reasonable to suggest that TatAc may form active translocases in combination with TatCd or TatCy. Interestingly, the TatAcCd and TatAcCy pathways were able to translocate TorA, AmiA and AmiC to the periplasm of *E. coli ΔtatABCDE* cells efficiently. These results showed for the first time that TatAc is able to form active translocases in combination with TatCd or TatCy. Interestingly, previous studies in *B. subtilis* have shown that the co-expression of TatAc and TatCd

or TatAc and TatCy did not facilitate export of the known Tat substrate PhoD and YwbN (Eijlander *et al*., 2009).

One question that comes out of these studies is why these combinations are not functional in their original host *B. subtilis*. A possible explanation for this is that there are different regulation mechanisms that make the system more selective in respect to the choice of the substrates and proteins needed to form a functional translocase. Such a system might be absent in the Gram-negative bacterium *E. coli* therefore allowing the formation of an even more minimal translocases, in terms of number of genes and dimension.

Finally BN-PAGE analysis showed for the first time that the TatAcCd and TatAcCy mixed translocases form membrane-embedded complexes of ~ 232 kDa and ~ 200 kDa respectively. The sizes of these complexes were similar respectively to the *B. subtilis* TatAdCd and TatAyCy complexes which have been described previously (Barnett *et al*., 2008; Barnett *et al*., 2009). Furthermore the BN-PAGE results were partially confirmed by gel filtration chromatography of purified TatAcCd and TatAcCy complexes.

The work presented in this chapter shows that the *B. subtilis* TatAc protein can form functional Tat systems with both TatCd and TatCy. The TatAcCd and TatAcCy complexes, (similar to the TatAdCd and TatAyCy complexes), are found to be considerably smaller than the previously described *E. coli* TatABC complex (Oates *et al*., 2005). This could just be due to the absence of TatB in TatAC complexes. However, it could also be due to the presence of a different number of TatAC subunits in these complexes and if it is the case this mass difference could have important implications in the translocation mechanism. Moreover, similar to the TatAd and TatAy complexes that have been previously characterised (Barnett *et al*., 2008; Barnett *et al*., 2009), the TatAc protein forms complexes that appear to lack the heterogeneity observed with the *E. coli* TatA complex. Thus, when taken together the data presented in this chapter further support the currently favoured model of *B. subtilis* Tat-dependent translocation that involves separate TatAC and TatA complexes.

As a final consideration: The Tat system with its peculiarity to transport fully folded proteins has the potential to be exploited for biotechnological purposes as shown by Branston *et al*. (2012), Matos *et al*. (2012) and reviewed in Brüser (2003). In this context the results presented in this chapter may prove particularly useful, and the possibility of developing mixed translocases, such as TatAcCd or TatAcCy for the efficient translocation of heterologous protein products might be useful in developing an optimized system for biotechnological applications.

Chapter 7.
Final Discussion

The twin-arginine translocation (Tat) system is one of the most intriguing export pathways which has been found in bacteria, archaea and plant chloroplasts. Tat substrates bear an almost invariant twin-arginine motif in their signal peptide which lends the pathway its name. Since it was discovered in chloroplasts (Cline *et al*., 1992; Klösgen *et al*., 1992; Mould and Robinson, 1991), the Tat pathway has raised great interest in the scientific community because of its peculiar ability to export fully folded proteins across lipid bilayers using only the proton motive force (PMF). These features distinguish it from other protein translocation systems such as the Sec pathway and highlight the potential commercial application of the Tat system for the production of heterologous proteins which are not compatible with the Sec pathway (Brüser, 2007; Kim *et al*., 2005; Branston *et al*., 2012; Matos *et al*., 2012). Additionally, since the Tat system is involved in bacterial pathogenesis (De Buck *et al*., 2008), but is absent from mammalian cells, it may represent an important new target for novel antimicrobial compounds (Ochsner *et al*., 2002).

In *Escherichia coli* three integral membrane proteins: TatA, TatB and TatC are essential for the Tat-dependent translocation (Bogsch *et al*., 1998; Sargent *et al*., 1998; Sargent *et al*., 1999). They were found to be organized in two types of complexes within the plasma membrane: a TatABC complex of ~ 370 kDa and separate TatA homo-oligomeric complexes ranging from ~ 50 kDa to over 500 kDa (Bolhuis *et al*., 2001; Oates *et al*., 2003; Oates *et al*., 2005). According to the current model of Tat-dependent translocation, the TatABC complex acts as the substrate-binding receptor (Alami *et al*., 2003); the substrate-TatABC interaction may be followed by the recruitment of separate TatA complexes (Mori and Cline, 2002) which according to electron microscopy studies may form channels of variable diameter (Gohlke *et al*., 2005), and it was suggested that this TatA organization could facilitate the transport of the wide range of Tat substrates.

Unlike Gram-negative bacteria, most Gram-positive bacteria, possess a simpler Tat system that lacks a TatB component (Jongbloed *et al*., 2004). In *Bacillus subtilis* two TatAC-type systems have been identified operating in parallel with apparently different substrate specificities: the TatAdCd and TatAyCy pathways (Jongbloed *et al*., 2006). Like the TatABC systems of Gram-negative bacteria, the *B. subtilis* TatAC systems are present at steady state in two separate Tat complexes within the

membrane (Barnett *et al*., 2008; Barnett *et al*., 2009). In contrast however the TatA complexes lack the heterogeneity observed with the *E. coli* TatA complex in the membrane.

The mechanism by which the *E. coli* and *B. subtilis* Tat systems export substrates whilst preventing ion leakage during the transport process is still poorly understood. The work presented in this thesis used a number of biochemical approaches to gain further understanding into the assembly and mechanism of the *E. coli* and *B. subtilis* Tat pathways focusing on the study of two previously uncharacterized components: the *E. coli* TatA paralog TatE subunit and the *B. subtilis* TatAc subunit. Four basic questions have been addressed with each forming a chapter of the thesis:

- *Are alternative models for the E. coli Tat-dependent translocation which differ from the current one possible?*

- *Does TatE have a dual localization in both membrane and cytosolic compartments?*

- *Does TatE interact with the other Tat components?*

- *Does B. subtilis TatAc form active systems with TatCd and TatCy?*

The most significant findings are highlighted in this chapter.

7.1 An alternative model of Tat-dependent transport in *E. coli*

Although the TatABC subunits appear to form the primary translocation system, *E. coli* also contains a separate TatA paralog, TatE, that is encoded by a separate, monocistronic *tatE* gene. TatE is a predicted single span membrane protein of 67 amino acids and it exhibits greater than 50 % sequence identity with TatA (Sargent *et al*., 1998). Interestingly TatE and TatA are functionally interchangeable since each can complement the phenotype of *ΔtatAE* mutants (Sargent *et al*., 1999). This

evidence suggests that TatE is an active member of the Tat translocase in *E. coli*, but its complex organization and role in the Tat-dependent translocation had not been addressed in detail. In this study (chapter 3), work was undertaken to investigate the ability of TatE to function in the translocation of a number of different Tat substrates. In addition the assembly of TatE into membrane complexes was investigated for the first time and the nature of these complexes studied using both biochemical and biophysical techniques.

First of all TatE was overexpressed in an *E. coli ΔtatAE* strain (where the *tatA* and *tatE* genes are deleted and TatB, TatC components are present at native levels) and facilitated the efficient transport of Tat substrates including TorA, AmiA and AmiC. These data confirmed that TatE was able to effectively substitute for TatA and form an active translocon when expressed in this strain.

Analytical gel filtration chromatography and blue-native polyacrylamide gel electrophoresis of affinity-purified TatE complexes revealed that these complexes have sizes between ca. 50 and 110 kDa. This result was in marked contrast to previous findings of the *E. coli* TatA complexes, which were found to be very heterogeneous and range in size from ~ 50 kDa to over 500 kDa (Gohlke *et al*., 2005; Oates *et al*., 2005). Moreover, the three-dimensional models obtained by electron microscopy of the two principal TatE complexes, showed single-ring complexes with estimated diameters of 6-8 nm with potential clefts or channels of 2.5 nm in diameter that are accessible from one side of the membrane. Overall the TatE complexes were even smaller than the smallest class of TatA complex analyzed by electron microscopy which had diameter of 8.5-9 nm and a potential channel diameter of 3-3.5 nm (Gohlke *et al*., 2005). Remarkably, the TatE complexes lacked the typical TatA complex heterogeneity which, according to the current Tat translocation model, appeared to provide a means of transporting Tat substrate of widely varying mass and shape (Gohlke *et al*., 2005). The small sizes of TatE complexes seemed to preclude a role in forming the entire translocation channel. Despite this difference, TatE was still able to transport substrates of different sizes from AmiA (~ 30 kDa) and AmiC (~ 45 kDa) to the 90-kDa TorA protein which is one of the largest Tat substrates. Interestingly, the narrowest diameter for TorA, according to its crystal structure from *Shewanella massilia* (Czjzek *et al*., 1998), was estimated at about 5

nm (Wu *et al*., 2000). Thus a single TorA molecule cannot fit in a TatE channel of 2.5 nm. In conclusion the data presented in chapter 3 suggested a different model for Tat-dependent protein transport to the one already described, involving a single defined translocon rather than several size variants. This model may be consistent either with the presence of a single flexible translocon, or with multiple TatE complexes coming together to form the translocation channel (Figure 3.3B and 3.3C, chapter 3).

Interestingly this model may be similar to the *B. subtilis* Tat translocation model, since, as TatE, the *B. subtilis* TatAd and TatAy complexes appeared to lack the heterogeneity observed with the *E. coli* TatA complex in the membrane (Barnett *et al*., 2008; Barnett *et al*., 2009). The Tat systems from Gram-positive and Gram-negative bacteria may thus be more similar than previously thought.

7.2 TatE is present in the cytoplasm and forms TatAE mixed complexes in the membrane

In order to gain further insight into the involvement of TatE in the Tat transport mechanism, further experiments were undertaken with the aim of investigating if TatE has a cytosolic as well as membrane localization, and if physical interactions between TatE and the other Tat components occur.

In *B. subtilis* TatAd and TatAy have been observed alongside their expected membrane location in the cytoplasm, where they form very large complexes or aggregates (Barnett *et al*., 2008; Barnett *et al*., 2009). This soluble population of TatA protein has been proposed to act as the initial receptor for Tat substrates, with TatA-substrate complexes targeted to membrane-localised TatCd (Schreiber *et al*., 2006).

As shown in chapter 4, TatE was found in both the membrane and cytoplasm of *E. coli ΔtatAE* cells after expression from a pBAD vector. For comparison the presence of soluble TatA was also assessed in *E. coli ΔtatAE* cells expressing TatA, and

similar to TatE, it was found to have a cytosolic as well as a membrane localization. The presence of *E. coli* TatA in the cytoplasm is still debated and two independent studies examining TatA *in vivo* showed contradictory results. One study showed that TatA formed homo-multimeric tube-like structures inside the cytoplasm (Berthelmann *et al*., 2008), in contrast another study found that TatA is instead localised exclusively to the plasma membrane (Leake *et al*., 2008). Importantly the study by Leake *et al*. (2008) examined TatA at native levels of expression. In contrast in the study by Berthlemann *et al*. (2008), TatA was expressed at ca. 15 x native levels of expression. Interestingly phase separation experiments using the detergent Triton X-114 suggested that both cytosolic TatE and TatA were mis-localized, lending support to the conclusions of Leake *et al*. (2008).

A soluble form of the chloroplast TatA homologue (Tha4) has been found in the chloroplast stroma, but is not required for precursor targeting to the thylakoid membrane (Frielingsdorf *et al*., 2008). It may thus be possible that the cytosolic TatE and TatA observed, like Tha4, act as an additional pool of protein that inserts into the membrane perhaps improving the efficiency of Tat-dependent transport.

BN-PAGE analysis of cytosolic TatE revealed a complex of ~ 66 kDa In contrast cytosolic TatA forms a distinct complex of ~ 669 kDa which resembles in part the high molecular weight complexes or aggregates formed by the cytosolic TatAd and TatAy in *B. subtilis* (Barnett *et al*., 2009; Barnett *et al*., 2008). These results showed that the TatE complexes have similar size regardless of whether they have a membrane or cytosolic localisation, whilst TatA does not appear to form modular complexes in the cytoplasm. Perhaps this observation suggests that cytosolic TatA has to be present as a discrete cytosolic complex in order to execute its function in the transport mechanism.

Obviously further experiments, perhaps based on *in vivo* methods, are needed to determine whether soluble TatE and TatA are physiological and have a role in the transport mechanism.

As shown in chapter 3, *E. coli ΔtatAE* cells expressing TatE possess an active translocation system, therefore TatE must interact with either the TatB and/or TatC

subunits in order to facilitate the transport of TorA, AmiA and AmiC. Moreover TatE is constitutively expressed in *E. coli* MC400 cells (Jack *et al*., 2001) suggesting that also in wild type cells it may form structural or functional interactions with the other Tat components. The experiments undertaken in chapter 5 showed that the level of TatE expressed by the arabinose-inducible vector pBAD24, was influenced by the absence or presence of the other Tat subunits. In particular the data suggested that TatC may have a role in stabilizing TatE in the membrane. This result was not completely unexpected since TatC has been shown to act as a scaffold driving the assembly of the TatABC complex (Behrendt *et al*., 2007; Mangels *et al*., 2005). Interestingly TatE was not detectable after expression in *ΔtatABCDE* cells suggesting that it was either not expressed or was unstable in cells lacking all the other Tat components. A further time course experiment gave some indirect evidence that TatE may be stabilized in the membranes by interactions with the other Tat subunits. Nevertheless this interaction maybe only transient given that co-immunoprecipitation experiments showed that TatE did not stably bind to either TatB or TatC subunits. This result was not completely unexpected since the thylakoid TatA homologue Tha4 was found to bind Hfc106 only in the presence of a proton gradient and substrate, and no binding was observed under resting conditions (Mori and Cline 2002).

In the same chapter studies were undertaken to investigate the possible interaction between the TatE and TatA subunits. As mentioned previously these two proteins have overlapping function (Sargent *et al*., 1998) and are constitutively expressed in wild type *E. coli* MC4100 cells, it is thus reasonable to suggest that they may interact with each other to form TatAE mixed complexes in the membrane. Co-purification and BN-PAGE experiments following co-expression of *tatA* and *tatE* in *E. coli ΔtatAE* cells pointed to the formation of TatAE hetero-oligomeric complexes with estimated sizes ranging from over 140 kDa to ~ 669 kDa. This is thus a completely novel form of Tat complex that might be functionally significant under specific growth conditions, such as in the biofilm formation, or for handling specific substrates.

Further more direct studies, including cross-linking experiments, would be useful to obtain a better understanding of the interactions between TatE and the other Tat

components. It would be also important to examine TatA and TatE interactions under native levels of expression.

7.3 The *B. subtilis* TatAcCd and TatAcCy mixed translocases are active in *E. coli*

Similar to *E. coli* TatE, the *B. subtilis* TatAc protein is encoded by a monocistronic gene. This gene, unlike the other genes encoding *B. subtilis* TatA-paralogues has no TatC counterpart (Jongbloed *et al*., 2000). Moreover its function has remained enigmatic due to the fact that no phenotype was so far detectable for *tatAc* mutant *B. subtilis* cells (Jongbloed *et al*., 2000; Jongbloed *et al*., 2004; Tjalsma *et al*., 2000). Nevertheless, the constitutive expression of *tatAc* in *B. subtilis* and the high degree of sequence homology between TatAc, TatAd, and TatAy suggests that TatAc may also function in the Tat pathway.

In chapter 6 TatAc was expressed either alone or in combination with *B. subtilis* TatCd and TatCy in different *E. coli* strains, in order to study in detail its structural and functional features. Interestingly TatAc expressed in *E. coli ΔtatAE* was found to translocate the *E. coli* Tat substrate TMAO reductase (TorA), and heterologous substrates consisting of the signal peptide of either DmsA, AmiA or MdoD linked with GFP, showing that TatAc can complement *E. coli ΔtatAE* and that a functional interaction must occur between TatAc and the *E. coli* TatB and TatC components. A similar result was obtained in an earlier study that showed *B. subtilis* TatAd was able to complement *E. coli ΔtatAE* cells (Barnett *et al*., 2008; Barnett *et al*., 2011a). Interestingly and in contrast to TatAd, TatAc was not able to complement *E. coli ΔtatB* cells, even though it shows a high degree of sequence similarity to the *E. coli* TatB protein (Jongbloed *et al*., 2000). This result suggested that *B. subtilis* TatAc does not share the bifunctional nature of the TatAd protein. Since the C-terminal half of the transmembrane span and the hinge region of TatAd had been shown to be essential for complementation of *E. coli ΔtatAE* cells (Barnett *et al*., 2011a), it would be interesting to investigate if the same regions of TatAc are similarly required for complementation in this subunit too.

In an additional experiment, TatAc was expressed alongside either TatCd or TatCy in *E. coli ΔtatABCDE* cells. Both TatAcCd and TatAcCy translocases were found to export TorA, AmiA and AmiC showing for the first time that TatAc was able to form active translocases in combination with TatCd or TatCy in *E. coli*. In contrast a previous study has shown that the co-expression of TatAc and TatCd or TatAc and TatCy in *B. subtilis* itself did not facilitate export of the known Tat substrates PhoD and YwbN (Eijlander *et al*., 2009). These contradictory results may be due to the presence in *E. coli* and *B. subtilis* of different regulation mechanisms which make *B. subtilis* more selective in respect to the choice of the substrates.

Finally BN-PAGE analysis showed for the first time that TatAc formed a small complex of ~ 100 kDa which, like TatE (chapter 3), TatAd (Barnett *et al*., 2008) and TatAy (Barnett *et al*., 2009), lacked the heterogeneity observed with the *E. coli* TatA complexes (Oates *et al*., 2005). Whereas TatAcCd and TatAcCy mixed translocases formed membrane-embedded complexes of ~ 232 kDa and ~ 200 kDa respectively which were similar to the *B. subtilis* TatAdCd and TatAyCy complexes described previously (Barnett *et al*., 2008; Barnett *et al*., 2009). Thus again these data support the currently favoured model of *B. subtilis* Tat-dependent translocation that involves separate TatAC and relatively homogeneous TatA complexes.

In summary, the work presented in this thesis has focused on the study of two previously uncharacterized components: the *E. coli* TatE, and *B. subtilis* TatAc subunits, and has led to an increased understanding of the bacterial Tat pathway. Despite many years of research into this fascinating transport system, there still remains much to be determined, particularly in relation to the translocation mechanism. By examining two largely unstudied components of this system, this thesis has made an important contribution to this field of study, not least in the presentation of an alternative model of Tat-function in *E. coli*. The use of *in vivo* approaches in future studies is likely to prove valuable in elucidating a full knowledge of the Tat system in bacteria. This understanding may yield many rewards, with significant potential for the exploitation of the Tat pathway in biotechnology.

Chapter 8.
References

Akimaru, J., Matsuyama, S., Tokuda, H. and Mizushima, S. (1991). Reconstitution of a protein translocation system containing purified SecY, SecE, and SecA from *Escherichia coli*. *Proc. Natl. Acad. Sci. U S A* **88**, 6545-6549.

Akiyama, Y. and Ito, K. (1987). Topology analysis of the SecY protein, an integral membrane protein involved in protein export in *Escherichia coli*. *EMBO J.* **6**, 3465-3470.

Alami, M., Lüke, I., Deitermann, S., Eisner, G., Koch, H. G., Brunner, J. and Müller, M. (2003). Differential interactions between a twin-arginine signal peptide and its translocase in *Escherichia coli*. *Mol. Cell.* **12**, 937-946.

Alami, M., Trescher, D., Wu, L. F. and Muller, M. (2002). Separate analysis of twin-arginine translocation (Tat)-specific membrane binding and translocation in *Escherichia coli*. *J. Biol. Chem.* **277**, 20499-20503.

Aldridge, C., Cain, P. and Robinson, C. (2009). Protein transport in organelles: Protein transport into and across the thylakoid membrane. *FEBS J.* **276**, 1177-1186.

Aldridge, C., Spence, E., Kirkilionis, M. A., Frigerio, L. and Robinson, C. (2008). Tat-dependent targeting of Rieske iron-sulphur proteins to both the plasma and thylakoid membranes in the cyanobacterium *Synechocystis* PCC6803. *Mol. Microbiol.* **70**, 140-150.

Allen, S. C., Barrett, C. M.,, Ray, N. and Robinson, C. (2002). Essential cytoplasmic domains in the *Escherichia coli* TatC protein. *J. Biol. Chem*. **277**, 10362-10366.

Angelini, S., Deitermann, S. and Koch, H. G. (2005). FtsY, the bacterial signal-recognition particle receptor, interacts functionally and physically with the SecYEG translocon. *EMBO Rep*. **6**, 476-481.

Bachmann, J., Bauer, B., Zwicker, K., Ludwig, B. and Anderka, O. (2006). The Rieske protein from *Paracoccus denitrificans* is inserted into the cytoplasmic membrane by the twin-arginine translocase. *FEBS J.* **273**, 4817-4830.

Bageshwar, U. K. and Musser, S. M. (2007). Two electrical potential-dependent steps are required for transport by the *Escherichia coli* Tat machinery. *J. Cell. Biol.* **179**, 87-99.

Baglieri, J., Beck, D., Vasisht, N., Smith, C. J. and Robinson, C. (2012). Structure of TatA paralog, TatE, suggests a structurally homogeneous form of Tat protein translocase that transports folded proteins of differing diameter. *J. Biol. Chem.* **287**, 7335-7344.

Barnett, J. P., Eijlander, R. T., Kuipers, O. P. and Robinson, C. (2008). A minimal Tat system from a Gram-positive organism: A bifunctional TatA subunit participates in discrete TatAC and TatA complexes. *J. Biol. Chem*. **283**, 2534-42.

Barnett, J. P., Lawrence, J., Mendel, S. and Robinson, C. (2011a). Expression of the bifunctional *Bacillus subtilis* TatAd protein in *Escherichia coli* reveals distinct TatA/B-family and TatB-specific domains. *Arch. Microbiol.* **193**, 583-94.

Barnett, J. P., Robinson C, Scanlan, D. J. and Blindauer, C. A. (2011b). The Tat protein export pathway and its role in cyanobacterial metalloprotein biosynthesis. *FEMS Microbiol. Lett.* **325**, 1-9.

Barnett, J.P., van der Ploeg, R., Eijlander, R. T., Nenninger, A., Mendel, S., Rozeboom, R., Kuipers, O. P., van Dijl, J. M. and Robinson, C. (2009). The twin-arginine translocation (Tat) systems from *Bacillus subtilis* display a conserved mode of complex organization and similar substrate recognition requirements. *FEBS J*. **276**, 232-43.

Barrett, C. M., Freudl, R. and Robinson, C. (2007). Twin arginine translocation (Tat)-dependent export in the apparent absence of TatABC or TatA complexes using modified *Escherichia coli* TatA subunits that substitute for TatB. *J. Biol. Chem*. **282**, 36206-13.

Barrett, C. M., Mangels, D. and Robinson, C. (2005a). Mutations in subunits of the *Escherichia coli* twin-arginine translocase block function via differing effects on translocation activity or tat complex structure. *J. Mol. Biol*. **347**, 453-63.

Barrett, C. M., Mathers, J. E. and Robinson, C. (2003). Identification of key regions within the *Escherichia coli* TatAB subunits. *FEBS Lett.* **537**, 42-6.

Barrett, C. M. and Robinson, C. (2005b). Evidence for interactions between domains of TatA and TatB from mutagenesis of the TatABC subunits of the twin arginine translocase. *FEBS J.* **272**, 2261-75.

Behrendt, J., Lindenstrauss, U. and Brüser, T. (2007). The TatBC complex formation suppresses a modular TatB-multimerization in *Escherichia coli. FEBS Lett*. **581**, 4085-90.

Behrendt, J., Standar, K., Lindenstrauss, U. and Bruser, T. (2004). Topological studies on the twin-arginine translocase component TatC. *FEMS Microbiol. Lett.* **234**, 303-8.

Beloin, C., Valle, J., Latour-Lambert, P., Faure, P., Kzreminski, M., Balestrino, D., Haagensen, J. A., Molin, S., Prensier, G., Arbeille, B. and Ghigo, J. M. (2004). Global impact of mature biofilm lifestyle on *Escherichia coli* K-12 gene expression. *Mol. Microbiol.* **51**, 659-674.

Berks, B. C. (1996). A common export pathway for proteins binding complex redox factors? *Mol. Microbiol.* **22**, 393-404.

Berks, B. C., Palmer, T. and Sargent, F. (2003). The Tat protein translocation pathway and its role in microbial physiology. *Adv. Microb. Physiol.* **47**, 187-254.

Berks, B., Palmer, T. and Sargent, F. (2005) Protein targeting by the bacterial twin arginine translocation (Tat) pathway. *Curr. Opin. Microbiol*. **8**, 174- 181.

Berks, B. C., Sargent, F. and Palmer, T. (2000). The Tat protein export pathway. *Mol. Microbiol.* **35**, 260-274.

Bernhardt, T. G. and de Boer, P.A. (2003). The *Escherichia coli* amidase AmiC is a periplasmic septal ring component exported *via* the twin-arginine transport pathway. *Mol. Microbiol*. **48**, 1171-82.

Bernstein, H. D., Poritz, M. A., Strub, K., Hoben, P. J., Brenner, S. and Walter, P. (1989). Model for signal sequence recognition from amino-acid sequence of 54K subunit of signal recognition particle. *Nature.* **340**, 482-486.

Berthelmann, F. and Brüser, T. (2004). Localization of the Tat translocon components in *Escherichia coli. FEBS Lett.* **569**, 82-8.

Berthelmann, F., Mehner, D., Richter, S., Lindenstrauss, U., Lünsdorf, H., Hause, G. and Brüser, T. (2008). Recombinant expression of tatABC and tatAC results in the formation of interacting cytoplasmic TatA tubes in *Escherichia coli*. *J. Biol. Chem*. **283**, 25281-9.

Blaudeck, N., Kreutzenbeck, P., Freudl, R. and Sprenger, G. A. (2003). Genetic analysis of pathway specificity during posttranslational protein translocation across the *Escherichia coli* plasma membrane. *J. Bacteriol.* **185**, 2811-9.

Blaudeck, N., Kreutzenbeck, P., Muller, M., Sprenger, G. A. and Freudl, R. (2005). Isolation and characterisation of bifunctional *Escherichia coli* TatA mutant proteins that allow efficient tat-dependent protein translocation in the absence of TatB. *J. Biol. Chem.* **280**, 3426-32.

Bochkareva, E. S., Solovieva, M. E. and Girshovich, A. S. (1998) Targeting of GroEL to SecA on the cytoplasmic membrane of *Escherichia coli*. *Proc. Natl. Acad. Sci. U S A* **95,** 478-483.

Bogsch, E., Brink, S. and Robinson, C. (1997). Pathway specificity for a ΔpH-dependent precursor thylakoid lumen protein is governed by a 'Sec-avoidance' motif in the transfer peptide and a 'Sec-incompatible' mature protein. *EMBO J.* **16**, 3851-9.

Bogsch, E. G., Sargent, F., Stanley, N. R., Berks, B. C., Robinson, C. and Palmer, T. (1998). An essential component of a novel bacterial protein export system with homologues in plastids and mitochondria. *J. Biol. Chem*. **273**, 18003-18006.

Bolhuis, A., Bogsch E. G. and Robinson, C. (2000). Subunit interactions in the twin-arginine translocase complex of *Escherichia coli*. *FEBS Lett.* **472**, 88-92.

Bolhuis, A., Mathers, J. E., Thomas, J. D., Barrett, C. M. and Robinson, C. (2001). TatB and TatC form a functional and structural unit of the twin-arginine translocase from *Escherichia coli*. *J. Biol. Chem.* **276**, 20213-9.

Bolhuis, A. (2004). The archaeal Sec-dependent protein translocation pathway. *Philos. Trans. R. Soc. Lond. B. Biol. Sci.* **359**, 919-927.

Bordier C. (1981). Phase separation of integral membrane proteins in Triton X-114 solution. *J. Biol. Chem*. **256,** 1604-1607.

Breyton, C., Haase, W., Rapoport, T. A., Kuhlbrandt, W. and Collinson, I. (2002). Three-dimensional structure of the bacterial protein-translocation complex SecYEG. *Nature*. **418**, 662-5.

Branston, S. D., Matos, C. F., Freedman, R. B., Robinson, C. and Keshavarz-Moore, E. (2012). Investigation of the impact of Tat export pathway enhancement on *E. coli* culture, protein production and early stage recovery. *Biotechnol. Bioeng.* **109**, 983-991.

Brundage, L., Hendrick, J. P., Schiebel, E., Driessen, A. J. and Wickner, W. (1990). The purified *E. coli* integral membrane protein SecY/E is sufficient for reconstitution of SecA-dependent precursor protein translocation. *Cell*. **62**, 649-57.

Brüser, T. (2007). The twin-arginine translocation system and its capability for protein secretion in biotechnological protein production. *Appl. Microbiol. Biotechnol*. **76**, 35-45.

Buchanan, G., Leeuw, E., Stanley, N. R., Wexler, M., Berks, B. C., Sargent, F. and Palmer, T. (2002). Functional complexity of the twin-arginine translocase TatC component revealed by site-directed mutagenesis. *Mol. Microbiol.* **43**, 1457-70.

Buchanan, G., Sargent, F., Berks, B. C. and Palmer, T. (2001). A genetic screen for suppressors of *Escherichia coli* Tat signal peptide mutations establishes a critical role for the second arginine within the twin-arginine motif. *Arch. Microbiol.* **177**, 107-112.

Cabelli, R. J., Dolan, K. M., Qian, L. P. and Oliver, D. B. (1991). Characterization of membrane-associated and soluble states of SecA protein from wild-type and SecA51(TS) mutant strains of *Escherichia coli. J. Biol. Chem.* **266**, 24420-7.

Casadaban, M. J. and Cohen, S. N. (1980). Analysis of gene control signals by DNA fusion and cloning in *Escherichia coli*. *J. Mol. Biol.* **138**, 179-207.

Celebi, N., Yi, L., Facey, S. J., Kuhn, A. and Dalbey, R. E. (2006) Membrane biogenesis of subunit II of cytochrome bo oxidase: contrasting requirements for insertion of N-terminal and C-terminal domains. *J. Mol. Biol.* **357**, 1428-1436.

Chaddock, A. M., Mant, A., Karnauchov, I., Brink, S., Herrmann, R. G., Klosgen, R. B. and Robinson, C. (1995). A new type of signal peptide: central role of a twin-arginine motif in transfer signals for the ΔpH-dependent thylakoidal protein translocase. *EMBO J.* **14**, 2715-2722.

Chan, C. S., Haney, E. F., Vogel, H. J. and Turner R. J. (2011). Towards understanding the Tat translocation mechanism through structural and biophysical studies of the amphipathic region of TatA from *Escherichia coli*. *Biochim. Biophys. Acta* **1808**, 2289-96.

Chan, C. S., Zlomislic, M. R., Tieleman, D. P. and Turner, R. J. (2007). The TatA subunit of *Escherichia coli* twin-arginine translocase has an N-in topology. *Biochemistry*. **46**, 7396-404.

Chun, S. Y. and Randall, L. L. (1994). In vivo studies of the role of SecA during protein export in *Escherichia coli. J. Bacteriol*. **176**, 4197-203.

Clark, S.A. and Theg S. M. (1997). A folded protein can be transported across the chloroplast envelope and thylakoid membranes. *Mol. Biol. Cell* **8**, 923- 934.

Cline, K., Ettinger, W. F. and Theg, S. M. (1992). Protein-specific energy requirements for protein transport across or into thylakoid membranes. Two lumenal proteins are transported in the absence of ATP. *J. Biol. Chem.* **267**, 2688-2696.

Cline, K. and Mori, H. (2001). Thylakoid ΔpH-dependent precursor proteins bind to a cpTatC-Hcf106 complex before Tha4-dependent transport. *J. Cell. Biol.* **154**, 719-29.

Cristóbal, S., de Gier, J. W., Nielsen, H. and von Heijne, G. (1999). Competition between Sec- and TAT-dependent protein translocation in *Escherichia coli*. *EMBO J.* **18**, 2982-90.

Cross, B. C., Sinning, I., Luirink, J. and High, S. (2009). Delivering proteins for export from the cytosol. *Nat. Rev. Mol. Cell. Biol.* **10**, 255-264.

Czjzek, M., Dos Santos, J. P., Pommier, J., Giordano, G., Méjean, V. and Haser, R. (1998). Crystal structure of oxidized trimethylamine N-oxide reductase from *Shewanella massilia* at 2.5 A resolution. *J. Mol. Biol*. **284**, 435-447.

Dabney-Smith, C., Mori, H. and Cline, K. (2006). Oligomers of Tha4 organize at the thylakoid Tat translocase during protein transport. *J. Biol. Chem*. **281**, 5476-5483.

Dalbey, R. E. and Chen, M. (2004). Sec-translocase mediated membrane protein biogenesis. *Biochim. Biophys. Acta* **1694,** 37-53.

Dalbey, R. E. and Kuhn, A. (2000). Evolutionarily related insertion pathways of bacterial, mitochondrial, and thylakoid membrane proteins. *Annu. Rev. Cell Dev. Biol*. **16**, 51-87.

Dalbey, R. E., Wang, P. and Kuhn, A. (2011). Assembly of bacterial inner membrane proteins. *Annu. Rev. Biochem.* **80,** 161-187.

Dalbey, R. E. and Wickner, W. (1985). Leader peptidase catalyzes the release of exported proteins from the outer surface of the *Escherichia coli* plasma membrane. *J. Biol. Chem.* **260**, 15925-15931.

De Buck, E., Lammertyn, E. and Anné, J. (2008). The importance of the twinarginine translocation pathway for bacterial virulence. *Trends Microbiol*. **16**, 442-53.

De Buck, E., Maes, L., Meyen, E., Van Mellaert, L., Geukens, N., Anne, J. and Lammertyn, E. (2005). *Legionella pneumophila* Philadelphia-1 *tatB* and *tatC* affect intracellular replication and biofilm formation. *Biochem. Biophys. Res. Commun.* **331**, 1413-1420.

De Buck, E., Vranckx, L., Meyen, E., Maes, L., Vandersmissen, L., Anné, J. and Lammertyn, E. (2007). The twin-arginine translocation pathway is necessary for correct membrane insertion of the Rieske Fe/S protein in *Legionella pneumophila*. *FEBS Lett.* **581**, 259-64.

De Keersmaeker, S., Van Mellaert, L., Schaerlaekens, K., Van Dessel, W., Vrancken, K., Lammertyn, E., Anné, J. and Geukens, N. (2005). Structural organization of the twin-arginine translocation system in *Streptomyces lividans*. *FEBS Lett.* **579**, 797-802.

De Keersmaeker, S., Vrancken, K., Van Mellaert, L., Anné, J. and Geukens, N. (2007). The Tat pathway in *Streptomyces lividans*: interaction of Tat subunits and their role in translocation. *Microbiology* **153**, 1087-1094.

De Leeuw, E., Porcelli, I., Sargent, F., Palmer, T. and Berks, B. C. (2001). Membrane interactions and self-association of the TatA and TatB components of the twin-arginine translocation pathway. *FEBS Lett.* **506**, 143-8.

DeLisa, M. P., Samuelson, P., Palmer, T. and Georgiou, G. (2002). Genetic analysis of the twin arginine translocator secretion pathway in bacteria. *J. Biol. Chem.* **277**, 29825-31.

DeLisa, M. P., Tullman, D. and Georgiou, G. (2003). Folding quality control in the export of proteins by the bacterial twin-arginine translocation pathway. *Proc. Natl. Acad. Sci. U S A* **100**, 6115-6120.

De Marais, D. J. (2000). Evolution. When did photosynthesis emerge on Earth? *Science* **289**, 1703-1705.

Di Cola, A. and Robinson, C. (2005). Large-scale translocation reversal within the thylakoid Tat system in vivo. *J. Cell. Biol.* **171**, 281-289.

Dilks, K., Rose, R. W., Hartmann, E. and Pohlschroder, M. (2003). Prokaryotic utilization of the twin-arginine translocation pathway: a genomic survey. *J. Bacteriol.* **185**, 1478-83.

Ding, Z. and Christie, P. J. (2003). *Agrobacterium tumefaciens* twin-arginine dependent translocation is important for virulence, flagellation, and chemotaxis but not type IV secretion. *J. Bacteriol.* **185**, 760-71.

Donovan, W., Zheng, L. B., Sandman, K. and Losick, R. (1987). Genes encoding spore coat polypeptides from *Bacillus subtilis*. *J. Mol. Biol.* **196**, 1-10.

Driessen, A. J. (1992). Precursor protein translocation by the *Escherichia coli* translocase is directed by the proton motive force. *EMBO J.* **11**, 847-53.

Driessen, A. J. (2001). SecB, a molecular chaperone with two faces. *Trends Microbiol.* **9**, 193-196.

Driessen, A. J. M. and Nouwen, N. (2008). Protein translocation across the bacterial cytoplasmic membrane. *Annu. Rev. Biochem.* **77**, 643-667.

du Plessis, D. J., Nouwen, N. and Driessen, A. J. (2006). Subunit a of cytochrome o oxidase requires both YidC and SecYEG for membrane insertion. *J. Biol. Chem.* **281**, 12248-12252.

Duong, F. and Wickner, W. (1997). Distinct catalytic roles of the SecYE, SecG and SecDFyajC subunits of preprotein translocase haloenzyme. *EMBO J.* **16**, 2756-68.

Duong, F. and Wickner, W. (1998). Sec-dependent membrane protein biogenesis: SecYEG, preprotein hydrophobicity and translocation kinetics control the stoptransfer function. *EMBO J.* **17**, 696-705.

Dykxhoorn, D. M., St Pierre, R. and Linn, T. (1996). A set of compatible tac promoter expression vectors. *Gene.* **177**, 133-136.

Eijlander, R. T., Jongbloed, J. D. and Kuipers, O. P. (2009). Relaxed specificity of the *Bacillus subtilis* TatAdCd translocase in Tat-dependent protein secretion. *J. Bacteriol*. **191**, 196-202.

Finazzi, G., Chasen, C., Wollman, F. and de Vitry, C. (2003). Thylakoid targeting of Tat passenger proteins shows no Delta pH dependence in *vivo*. *EMBO J.* **22**, 807-815.

Frielingsdorf, S., Jakob, M. and Klösgen, R. B. (2008). A stromal pool of TatA promotes Tat-dependent protein transport across the thylakoid membrane. *J. Biol. Chem*. **283**, 33838-45.

Fulda, S., Huang, F., Nilsson, F., Hagemann, M. and Norling, B. (2000). Proteomics of *Synechocystis* sp. strain PCC 6803. *Eur. J. Biochem.* **267**, 5900-5907.

Genest, O., Seduk, F., Ilbert, M., Méjean, V. and Iobbi-Nivol, C. (2006). Signal peptide protection by specific chaperone. *Biochem. Biophys. Res. Commun*. **339**, 991- 995.

Gerard, F. and Cline, K. (2006). Efficient twin arginine translocation (Tat) pathway transport of a precursor protein covalently anchored to its initial cpTatC binding site. *J. Biol. Chem.* **281**, 6130-6135.

Gerard, F. and Cline, K. (2007). The thylakoid proton gradient promotes an advanced stage of signal peptide binding deep within the Tat pathway receptor complex. *J. Biol. Chem.* **282**, 5263-5272.

Gohlke, U., Pullan, L., McDevitt, C. A., Porcelli, I., de Leeuw, E., Palmer, T., Saibil, H. R. and Berks, B. C. (2005). The TatA component of the twin-arginine protein transport system forms channel complexes of variable diameter. *Proc. Natl. Acad. Sci. U S A.***102,** 10482-10486.

Gouffi, K., Gerard, F., Santini, C. L. and Wu, L. F. (2004). Dual topology of the *Escherichia coli* TatA protein. *J. Biol. Chem.* **279**, 11608-15.

Grahl, S., Maillard, J., Spronk, C. A., Vuister, G. W. and Sargent, F. (2012). Overlapping transport and chaperone-binding functions within a bacterial twin-arginine signal peptide. *Mol. Microbiol.* **83**: 1254-1267.

Greene, N. P., Porcelli, I., Buchanan, G., Hicks, M. G., Schermann, S. M., Palmer, T. and Berks, B. C. (2007). Cysteine scanning mutagenesis and disulfide mapping studies of the TatA component of the bacterial twin arginine translocase. *J. Biol. Chem.* **282**, 23937-45.

Grudnik, P., Bange, G. and Sinning, I. (2009). Protein targeting by the signal recognition particle. *Biol. Chem.* **390**, 775-782.

Guzman, L. M., Barondess, J. J. and Beckwith, J. (1992). FtsL, an essential cytoplasmic membrane protein involved in cell division in *Escherichia coli*. *J. Bacteriol.* **174**, 7716-7728.

Hanada, M., Nishiyama, K. I., Mizushima, S. and Tokuda, H. (1994). Reconstitution of an efficient protein translocation machinery comprising SecA and the three membrane proteins, SecY, SecE, and SecG (p12). *J. Biol. Chem.* **269**, 23625-31.

Harris, C. R. and Silhavy, T. J. (1999). Mapping an interface of SecY (PrlA) and SecE (PrlG) by using synthetic phenotypes and *in vivo* cross-linking. *J. Bacteriol.* **181**, 3438-3444.

Hatzixanthis, K., Clarke, T. A., Oubrie, A., Richardson, D. J., Turner, R. J. and Sargent, F. (2005). Signal peptide-chaperone interactions on the twin-arginine protein transport pathway. *Proc. Natl. Acad. Sci. U S A.* **102**, 8460-5.

Hatzixanthis, K., Palmer, T. and Sargent, F. (2003). A subset of bacterial inner membrane proteins integrated by the twin-arginine translocase. *Mol. Microbiol.* **49**, 1377-90.

Haward, S. R., Napier, J. A. and Gray, J. C. (1997). Chloroplast SecA functions as a membrane-associated component of the Sec-like protein translocase of pea chloroplasts. *Eur. J. Biochem.* **248**, 724-730.

Heikkilä, M. P., Honisch, U., Wunsch, P. and Zumft, W. G. (2001). Role of the Tat transport system in nitrous oxide reductase translocation and cytochrome cd1 biosynthesis in *Pseudomonas stutzeri*. *J. Bacteriol*. **183** 1663-1671.

Hicks, M. G., de Leeuw, E., Porcelli, I., Buchanan, G., Berks, B. C. and Palmer, T. (2003). The *Escherichia coli* twin-arginine translocase: conserved residues of TatA and TatB family components involved in protein transport. *FEBS Lett.* **539**, 61-7.

Hicks, M. G., Lee, P. A., Georgiou, G., Berks, B. C. and Palmer, T. (2005). Positive selection for loss-of-function tat mutations identifies critical residues required for TatA activity. *J. Bacteriol.* **187**, 2920-2925.

Holzapfel, E., Eisner, G., Alami, M., Barrett, C. M., Buchanan, G., Lüke, I., Betton, J., Robinson, C., Palmer, T., Moser, M. and Müller, M. (2007). The entire N-terminal half of TatC is involved in twin-arginine precursor binding. *Biochemistry*. **46**, 2892-2898.

Hu, Y., Zhao, E., Li, H., Xia, B. and Jin, C. (2010). Solution NMR structure of the TatA component of the twin-arginine protein transport system from Gram-Positive bacterium *Bacillus subtilis*. *J. American. Chem. Soci*. **132**, 15942-15944.

Hulford, A., Hazell, L., Mould, R. M. and Robinson C. (1994). Two distinct mechanisms for the translocation of proteins across the thylakoid membrane, one requiring the presence of a stromal protein factor and nucleotide triphosphates. *J. Biol. Chem*. **269**, 3251-3256.

Hunt, J. F., Weinkauf, S., Henry, L., Fak, J. J., McNicholas, P., Oliver, D. B. and Deisenhofer, J. (2002). Nucleotide control of interdomain interactions in the conformational reaction cycle of SecA. *Science.* **297**, 2018-2026.

Hynds, P. J., Robinson, D. and Robinson, C. (1998). The sec-independent twinarginine translocation system can transport both tightly folded and malfolded proteins across the thylakoid membrane. *J. Biol. Chem.* **273**, 34868-74.

Ikeda, M. and Nakagawa, S. (2003). The Corynebacterium glutamicum genome: features and impacts on biotechnological processes. *Appl. Microbiol. Biotechnol.* **62**, 99-109.

Ilbert, M., Méjean, V., Giudici-Orticoni, M. T., Samama, J. P. and Iobbi-Nivol, C. (2003). Involvement of a mate chaperone (TorD) in the maturing pathway of molybdoenzyme TorA. *J. Biol. Chem.* **278**, 28787-28792.

Ize, B., Gerard, F. and Wu, L. F. (2002a). *In vivo* assessment of the Tat signal peptide specificity in *Escherichia coli*. *Arch. Microbiol.* **178**, 548-53.

Ize, B., Gérard, F., Zhang, M., Chanal, A., Voulhoux, R., Palmer, T., Filloux, A. and Wu, L. F. (2002b). In vivo dissection of the Tat translocation pathway in *Escherichia coli*. *J. Mol. Biol*. **317**, 327-35.

Ize, B., Stanley, N. R., Buchanan, G. and Palmer, T. (2003). Role of the *Escherichia coli* Tat pathway in outer membrane integrity. *Mol. Microbiol.* **48**, 1183 -93.

Jack, R. L., Buchanan, G., Dubini, A., Hatzixanthis, K., Palmer, T. and Sargent, F. (2004). Coordinating assembly and export of complex bacterial proteins. *EMBO J.* **23**, 3962-3972.

Jack, R. L., Sargent, F., Berks, B. C., Sawers, G. and Palmer, T. (2001). Constitutive expression of *Escherichia coli* tat genes indicates an important role for the twin-arginine translocase during aerobic and anaerobic growth. *J. Bacteriol.* **183**, 1801-4.

Jarvis, P. and Robinson, C. (2004). Mechanisms of protein import and routing in chloroplasts. *Curr. Biol.* **14**, R1064-R1077.

Jones, D. T. (1999). Protein secondary structure prediction based on position-specific scoring matrices. *J. Mol. Biol.* **292**, 195-202.

Jongbloed, J. D., Grieger, U., Antelmann, H., Hecker, M., Nijland, R., Bron, S. and van Dijl, J. M. (2004). Two minimal Tat translocases in *Bacillus*. *Mol. Microbiol.* **54**, 1319-1325.

Jongbloed, J. D., Martin, U., Antelmann, H., Hecker, M., Tjalsma, H., Venema, G., Bron, S., van Dijl, J. M. and Müller, J. P. (2000). TatC is a specificity determinant for protein secretion via the twin-arginine translocation pathway. *J. Biol. Chem*. **275**, 41350-41357.

Jongbloed, J. D., van der Ploeg, R. and van Dijl, J. M. (2006). Bifunctional TatA subunits in minimal Tat protein translocases. *Trends Microbiol*. **14**, 2-4.

Kedrov, A., Kusters, I., Krasnikov, V. V. and Driessen, A. J. (2011). A single copy of SecYEG is sufficient for preprotein translocation. *EMBO J.* **30**, 4387-97.

Kim, J. Y., Fogarty, E. A., Lu, F. J., Zhu, H., Wheelock, G. D., Henderson, L. A. and DeLisa, M. P. (2005). Twin-arginine translocation of active human tissue plasminogen activator in *Escherichia coli*. *Appl. Environ. Microbiol.* **71**, 8451-8459.

Klösgen, R. B., Brock, I. W., Herrmann, R. G. and Robinson, C. (1992). Proton gradient-driven import of the 16 kDa oxygen-evolving complex protein as the full precursor protein by isolated thylakoids. *Plant. Mol. Biol.* **18**, 1031-1034.

Koch, S., Fritsch, M. J., Buchanan, G. and Palmer ,T. (2012). *Escherichia coli* TatA and TatB proteins have N-out, C-in Topology in intact cells. *J. Biol. Chem.* **287**, 14420-14431.

Kostakioti, M., Newman, C. L., Thanassi, D. G. and Stathopoulos, C. (2005). Mechanisms of protein export across the bacterial outer membrane. *J. Bacteriol.* **187**, 4306-4314.

Kostecki, J. S., Li, H., Turner, R. J. and DeLisa, M. P. (2010). Visualizing interactions along the *Escherichia coli* twin-arginine translocation pathway using protein fragment complementation. *PLoS One* **5**, e9225.

Laemmli, U. K. (1970). Cleavage of structural proteins during the assembly of the head of bacteriophage T4. *Nature* **227**, 680-685.

Laidler, V., Chaddock, A. M., Knott, T. G., Walker, D. and Robinson, C. (1995). A SecY Homolog in *Arabidopsis thaliana*. *J. Biol. Chem.* **270**, 17664-17667.

Lavander, M., Ericsson, S. K., Bröms, J. E. and Forsberg, A. (2006). The twin arginine translocation system is essential for virulence of *Yersinia pseudotuberculosis*. *Infect. Immun.* **74**, 1768-76.

Leake, M. C., Greene, N. P., Godun, R. M., Granjon, T., Buchanan, G., Chen, S., Berry, R. M., Palmer, T. and Berks, B. C. (2008). Variable stoichiometry of the TatA component of the twin-arginine protein transport system observed by in vivo single-molecule imaging. *Proc. Natl. Acad. Sci. U S A.* **105**, 15376-81.

Lecker, S., Lill, R., Ziegelhoffer, T., Georgopoulos, C., Bassford, P. J., Kumamoto C. A. and Wickner, W. (1989). Three pure chaperone proteins of *Escherichia coli*--SecB, trigger factor and GroEL--form soluble complexes with precursor proteins in vitro. *EMBO J.* **8**, 2703-2709.

Lee, P. A., Buchanan, G., Stanley, N. R., Berks, B. C. and Palmer, T. (2002). Truncation analysis of TatA and TatB defines the minimal functional units required for protein translocation. *J. Bacteriol.* **184**, 5871–9.

Lee, P. A., Orriss, G. L., Buchanan, G., Greene, N. P., Bond, P. J., Punginelli, C., Jack, R. L., Sansom, M. S., Berks, B. C. and Palmer, T. (2006). Cysteine-scanning mutagenesis and disulfide mapping studies of the conserved domain of the twin- arginine translocase TatB component. *J. Biol. Chem.* **281**, 34072-85.

Lequette, Y., Odberg-Ferragut, C., Bohin, J. P. and Lacroix, J. M. (2004). Identification of mdoD, an mdoG paralog which encodes a twin-arginine-dependent periplasmic protein that controls osmoregulated periplasmic glucan backbone structures. *J. Bacteriol.* **186**, 3695-3702.

Lim, H. K., Mansell, T. J., Linderman, S. W., Fisher, A. C., Dyson, M. R., and DeLisa M. P. (2009). Mining mammalian genomes for folding competent proteins using Tat-dependent genetic selection in *Escherichia coli*. *Protein Sci.* **18**, 2537-2549.

Liu, D., Gong, Q., Ma, Y., Li, P., Li, J., Yang, S., Yuan, L., Yu, Y., Pan, D., Xu, F. and Wang, N. N. (2010). cpSecA, a thylakoid protein translocase subunit, is essential for photosynthetic development in *Arabidopsis*. *J. Exp. Bot.* **61**, 1655-1669.

Luirink, J., and Sinning, I. (2004). SRP-mediated protein targeting: structure and function revisited. *Biochim. Biophys. Acta* **1694**, 17-35.

Ma, X. and Cline, K. (2000). Precursors bind to specific sites on thylakoid membranes prior to transport on the delta pH protein translocation system. *J. Biol. Chem.* **275**, 10016-10022.

Ma, X. and Cline, K. (2010). Multiple precursor proteins bind individual Tat receptor complexes and are collectively transported. *EMBO J.* **29**, 1477-1488.

Maldonado, B., Buchanan, G., Müller, M., Berks, B. C. and Palmer, T. (2011a). Genetic evidence for a TatC dimer at the core of the *Escherichia coli* twin arginine (Tat) protein translocase. *J. Mol. Microbiol. Biotechnol.* **20**, 168-175.

Maldonado, B., Kneuper, H., Buchanan, G., Hatzixanthis, K., Sargent, F., Berks, B. C. and Palmer, T. (2011b). Characterisation of the membrane-extrinsic domain of the TatB component of the twin arginine protein translocase. *FEBS Lett.* **585**, 478-484.

Mangels, D., Mathers, J., Bolhuis, A. and Robinson, C. (2005). The core TatABC complex of the twin-arginine translocase in *Escherichia coli*: TatC drives assembly whereas TatA is essential for stability. *J. Mol. Biol*. **354**, 415-23.

Marques, J. P., Schattat, M. H., Hause, G., Dudeck, I. and Klösgen R. B. (2004). In vivo transport of folded EGFP by the DeltapH/TAT-dependent pathway in chloroplasts of *Arabidopsis thaliana*. *J. Exp. Bot*. **55**, 1697-1706.

Matos, C. F., Branston, S. D., Albiniak, A., Dhanoya, A., Freedman, R. B., Keshavarz-Moore, E. and Robinson, C. (2012). High-yield export of a native heterologous protein to the periplasm by the tat translocation pathway in *Escherichia coli*. *Biotechnol. Bioeng.* (in Press).

Matos, C. F., Robinson, C. and Di Cola, A. (2008). The Tat system proofreads FeS protein substrates and directly initiates the disposal of rejected molecules. *EMBO J*. **27**, 2055-63.

Maurer, C., Panahandeh, S., Jungkamp, A. C., Moser, M. and Müller, M. (2010). TatB functions as an oligomeric binding site for folded Tat precursor proteins. *Mol. Biol. Cell.* **21**, 4151-4161.

McDonough, J. A., Hacker, K. E., Flores, A. R., Pavelka, M. S. and Braunstein, M. (2005). The twin-arginine translocation pathway of *Mycobacterium smegmatis* is functional and required for the export of mycobacterial beta-lactamases. *J. Bacteriol.* **187**, 7667-7679.

McGuffin, L. J., Bryson, K. and Jones, D. T. (2000). The PSIPRED protein structure prediction server. *Bioinformatics* **16**, 404-405.

Meloni, S., Rey, L., Sidler, S., Imperial, J., Ruiz-Argüeso, T. and Palacios J. M. (2003). The twin-arginine translocation (Tat) system is essential for Rhizobium-legume symbiosis. *Mol. Microbiol.* **48**, 1195-1207.

Méjean, V., Iobbi-Nivol, C., Lepelletier, M., Giordano, G., Chippaux, M. and Pascal, M. C. (1994). TMAO anaerobic respiration in *Escherichia coli*: involvement of the tor operon. *Mol. Microbiol.* **11**, 1169-79.

Mendel, S., McCarthy, A., Barnett, J. P., Eijlander, R. T., Nenninger, A., Kuipers, O. P. and Robinson, C. (2008). The *Escherichia coli* TatABC and a *Bacillus subtilis* TatAC-type system recognise three distinct targeting determinants in Twin-arginine signal peptides. *J. Mol. Biol*. **375**, 661-72.

Mitra, K., Schaffitzel, C., Shaikh, T., Tama, F., Jenni, S., Brooks, C. L., Ban, N. and Frank, J. (2005). Structure of the *E. coli* protein-conducting channel bound to a translating ribosome. *Nature*. **438**, 318-24.

Monteferrante, C. G., Baglieri, J., Robinson, C. and van Dijl, J. M. (2012). The third TatA subunit TatAc of *Bacillus subtilis* can form active twin-arginine translocases with the TatCd and TatCy subunits. *Appl. Environ. Microbiol*. **78**, 4999-5001.

Mori, H. and Cline, K. (2002). A twin arginine signal peptide and the pH gradient trigger reversible assembly of the thylakoid [Delta]pH/Tat translocase. *J. Cell. Biol*. **157**, 205-210.

Mori, H., Summer, E. J., Ma, X. and Cline, K. (1999). Component specificity for the thylakoidal Sec and Delta pH-dependent protein transport pathways. *J. Cell. Biol.* **146**, 45-56.

Mould, R. M. and Robinson, C. (1991). A proton gradient is required for the transport of two lumenal oxygen-evolving proteins across the thylakoid membrane. *J. Biol. Chem.* **266**, 12189-93.

Müller, J. P., Bron, S., Venema, G. and van Dijl J. M. (2000). Chaperone-like activities of the CsaA protein of *Bacillus subtilis*. *Microbiol.* **146**, 77-88.

Müller, M. and Klösgen, R. B. (2005). The Tat pathway in bacteria and chloroplasts (Review). *Mol. Membr. Biol*. **22**, 113-21.

Nakai, M., Nohara, T., Sugita, D. and Endo, T. (1994). Identification and characterization of the SecA protein homologue in the cyanobacterium *Synechococcus* PCC7942. *Biochem. Biophys. Res. Commun.* **200**, 844-851.

Nakai, M., Sugita, D., Omata, T. and Endo, T. (1993). Sec-Y protein is localized in both the cytoplasmic and thylakoid membranes in the cyanobacterium *Synechococcus* PCC7942. *Biochem. Biophys. Res. Commun.* **193**, 228-234.

Nicolas, P., Mäder, U., Dervyn, E. and other authors. (2012). Condition-dependent transcriptome reveals high-level regulatory architecture in *Bacillus subtilis*. *Science.* **335**, 1103-1106.

Nishiyama, K., Hanada, M. and Tokuda, H. (1994). Disruption of the gene encoding p12 (SecG) reveals the direct involvement and important function of SecG in the protein translocation of *Escherichia coli* at low temperature. *EMBO J.* **13**, 3272-7.

Nouwen, N., Piwowarek, M., Berrelkamp, G. and Driessen A. J. (2005). The large first periplasmic loop of SecD and SecF plays an important role in SecDF functioning. *J. Bacteriol*. **187**, 5857-5860.

Oates, J., Barrett, C. M., Barnett, J. P., Byrne, K., Bolhuis, A. and Robinson, C. (2005). The *Escherichia coli* twin-arginine translocation apparatus incorporates a distinct form of TatABC complex, spectrum of modular TatA complexes and minor TatAB complex. *J. Mol. Biol*. **346**, 295-305.

Oates, J., Mathers, J., Mangels, D., Kuhlbrandt, W., Robinson, C. and Model, K. (2003). Consensus structural features of purified bacterial TatABC complexes. *J. Mol. Biol.* **330**, 277-86.

Ochsner, U. A., Snyder, A., Vasil, A. I. and Vasil, M. L. (2002). Effects of the twin-arginine translocase on secretion of virulence factors, stress response, and pathogenesis. *Proc. Natl. Acad. Sci. U S A.* **99**, 8312-7.

Oresnik, I. J., Ladner, C. L. and Turner, R. J. (2001). Identification of a twinarginine leader-binding protein. *Mol. Microbiol.* **40**, 323-331.

Orriss, G. L., Tarry, M. J., Ize, B., Sargent, F., Lea, S. M., Palmer, T. and Berks, B. C. (2007). TatBC, TatB, and TatC form structurally autonomous units within the twin arginine protein transport system of *Escherichia coli*. *FEBS. Lett*. **581**, 4091-7.

Osborne, A. R., Clemons, W. M. and Rapoport T. A. (2004). A large conformational change of the translocation ATPase SecA. *Proc. Natl. Acad. Sci. U S A* **101**, 10937-10942.

Osborne, A., Rapoport, T. and van den Berg, B. (2005). Protein translocation by the Sec61/SecY channel. *Annu. Rev. Cell. Develop. Biol.* **21**, 529-550.

Paetzel, M., Karla, A., Strynadka, N. C. J. and Dalbey, R. E. (2002). Signal Peptidases. *Chem. Rev.* **102**, 4549-4580.

Palmer, T., Sargent, F. and Berks, B. C. (2005). Export of complex cofactor containing proteins by the bacterial Tat pathway. *Trends Microbiol*. **13**, 175-80.

Papanikolau, Y., Papadovasilaki, M., Ravelli, R. B., McCarthy, A. A., Cusack, S., Economou, A. and Petratos, K. (2007). Structure of dimeric SecA, the *Escherichia coli* preprotein translocase motor. *J. Mol. Biol.* **366**, 1545-1557.

Peschek, G. A. (1996). Structure-function relationships in the dual-function photosynthetic-respiratory electron-transport assembly of cyanobacteria (blue-green algae). *Biochem. Soc. Trans.* **24**, 729-733.

Phillips, G.J. and Silhavy, T. J. (1992). The *E. coli* ffh gene is necessary for viability and efficient protein export. *Nature*. **359**, 744-6.

Pommier, J., Méjean, V., Giordano, G. and Iobbi-Nivol, C. (1998). TorD, a cytoplasmic chaperone that interacts with the unfolded trimethylamine N-oxide reductase enzyme (TorA) in *Escherichia coli*. *J. Biol. Chem.* **273**, 16615-16620.

Pool, M. R. (2005). Signal recognition particles in chloroplasts, bacteria, yeast and mammals (review). *Mol. Membr. Biol.* **22**, 3-15.

Pop, O., Martin, U., Abel, C. and Muller, J. P. (2002). The Twin-arginine signal peptide of PhoD and the TatAd/Cd proteins of *Bacillus subtilis* form an autonomous Tat translocation system. *J. Biol. Chem.* **277**, 3268-3273.

Pop, O. I., Westermann, M., Volkmer-Engert, R., Schulz, D., Lemke, C., Schreiber, S., Gerlach, R., Wetzker, R. and Muller, J. P. (2003). Sequence specific binding of prePhoD to soluble TatAd indicates protein mediated targeting of the Tat export in *Bacillus subtilis*. *J. Biol. Chem.* **278**, 38428-36.

Porcelli, I., De Leeuw, E., Wallis, R., Van Den Brink-Van Der Laan, E., De Kruijff, B., Wallace, B. A., Palmer, T. and Berks, B. C. (2002). Characterization and membrane assembly of the TatA component of the *Escherichia coli* twin-arginine protein transport system. *Biochemistry.* **41**, 13690-13697.

Pradel, N., Ye, C., Livrelli, V., Xu, J., Joly, B. and Wu, L. F. (2003). Contribution of the twin arginine translocation system to the virulence of enterohemorrhagic *Escherichia coli* O157:H7. *Infect. Immun.* **71**, 4908-4916.

Price, C. E. and Driessen, A. J. (2010). Biogenesis of membrane bound respiratory complexes in *Escherichia coli*. *Biochim. Biophys. Acta* **1803**, 748-766.

Pugsley, A. P. (1993). The complete general secretory pathway in Gram-negative bacteria. *Microbiol. Rev.* **57**, 50-108.

Punginelli, C., Maldonado, B., Grahl, S., Jack, R., Alami, M., Schröder, J., Berks, B. C. and Palmer T. (2007). Cysteine scanning mutagenesis and topological mapping of the *Escherichia coli* twin-arginine translocase TatC Component. *J. Bacteriol*. **189**, 5482-94.

Randall, L. L. and Hardy, S. J. (1986). Correlation of competence for export withlack of tertiary structure of the mature species: a study *in vivo* of maltose-binding protein in *E. coli*. *Cell.* **46**, 921-8.

Ray, N., Nenninger, A., Mullineaux, C. and Robinson, C. (2005). Location and mobility of twin arginine translocase subunits in the *Escherichia coli* plasma membrane. *J. Biol. Chem.* **280**, 17961-17968.

Ray, N., Oates, J., Turner, R. J. and Robinson, C. (2003). DmsD is required for the biogenesis of DMSO reductase in *Escherichia coli* but not for the interaction of the DmsA signal peptide with the Tat apparatus. *FEBS Lett.* **534**, 156-60.

Richter, S. and Bruser, T. (2005). Targeting of Unfolded PhoA to the Tat Translocon of *Escherichia coli*. *J. Biol. Chem.* **280**, 42723-42730.

Richter, S., Lindenstrauss, U., Lucke, C., Bayliss, R. and Brüser, T. (2007). Functional Tat transport of unstructured, small, hydrophilic proteins. *J. Biol. Chem.* **282**, 33257-33264.

Robinson, C., Matos, C., Beck, D., Ren, C., Lawrence, J., Vasisht, N. and Mendel, S. (2011). Transport and proofreading of proteins by the twin-arginine translocation (Tat) system in bacteria. *Biochim. Biophy. Acta Biomembr.* **1808**, 876-884.

Rodrigue, A., Chanal, A., Beck, K., Muller, M. and Wu, L. F. (1999). Cotranslocation of a periplasmic enzyme complex by a hitchhiker mechanism through the bacterial tat pathway. *J. Biol. Chem.* **274**, 13223-13228.

Roy, L. M. and Barkan, A. (1998). A SecY homologue is required for the elaboration of the chloroplast thylakoid membrane and for normal chloroplast gene expression. *J. Cell. Biol.* **141**, 385-395.

Saier, M. H. (2006). Protein secretion and membrane insertion systems in Gram-negative bacteria. *J. Membr. Biol*. **214**, 75-90.

Saint-Joanis, B., Demangel, C., Jackson, M., Brodin, P., Marsollier, L., Boshoff, H. and Cole, S. T. (2006). Inactivation of Rv2525c, a substrate of the twin arginine translocation (Tat) system of Mycobacterium tuberculosis, increases beta-lactam susceptibility and virulence. *J. Bacteriol.* **188**, 6669-6679.

Sambrook, J., Fritsch, E. F. and Maniatis, T. (1989). *Molecular Cloning: A Laboratory Manual*, New York: Cold Spring Harbour Laboratory Press.

Samuelson, J. C., Chen, M., Jiang, F., Möller, I., Wiedmann, M., Kuhn, A., Phillips, G. J. and Dalbey, R. E. (2000). YidC mediates membrane protein insertion in bacteria. *Nature*. **406**, 637-41.

Sanders, C., Wethkamp, N. and Lill, H. (2001). Transport of cytochrome c derivatives by the bacterial Tat protein translocation system. *Mol. Microbiol.* **41**, 241-246.

Santini, C., Bernadac, A., Zhang, M., Chanal, A., Ize, B., Blanco, C. and Wu, L. (2001). Translocation of jellyfish green fluorescent protein via the Tat system of *Escherichia coli* and change of its periplasmic localization in response to osmotic up-shock. *J. Biol. Chem.* **276**, 8159-8164.

Santini, C. L., Ize, B., Chanal, A., Muller, M., Giordano, G. and Wu, L. F. (1998). A novel sec-independent periplasmic protein translocation pathway in *Escherichia coli*. *EMBO J.* **17**, 101-12.

Sardis, M. F. and Economou, A. (2010). SecA: a tale of two protomers. *Mol. Microbiol.* **76**, 1070-1081.

Sargent, F. (2007). The twin-arginine transport system: moving folded proteins across membranes. *Biochem. Soc. Trans.* **35**, 835-847.

Sargent, F., Berks, B. C. and Palmer, T. (2002). Assembly of membrane-bound respiratory complexes by the Tat protein-transport system. *Arch. Microbiol.* **178**, 77-84.

Sargent, F., Bogsch, E. G., Stanley, N. R., Wexler, M., Robinson, C., Berks, B. C. and Palmer, T. (1998). Overlapping functions of components of a bacterial Sec-independent protein export pathway. *EMBO J.* **17,** 3640-3650.

Sargent, F., Gohlke, U., De Leeuw, E., Stanley, N. R., Palmer, T., Saibil, H. R. and Berks, B. C. (2001). Purified components of the *Escherichia coli* Tat protein transport system form a double-layered ring structure. *Eur. J. Biochem.* **268**, 3361-7.

Sargent, F., Stanley, N. R., Berks, B. C. and Palmer, T. (1999). Sec-independent protein translocation in *Escherichia coli*. A distinct and pivotal role for the TatB protein. *J. Biol. Chem*. **274**, 36073-36082.

Schägger, H., Cramer, W. A. and von Jagow, G. (1994). Analysis of molecular masses and oligomeric states of protein complexes by blue native electrophoresis and isolation of membrane protein complexes by two-dimensional native electrophoresis. *Anal. Biochem.* **217**, 220-30.

Schägger, H. and von Jagow, G. (1991). Blue native electrophoresis for isolation of membrane protein complexes in enzymatically active form. *Anal. Biochem.* **199**, 223- 31.

Shanmugham, A., Bakayan, A., Völler, P., Grosveld, J., Lill, H. and Bollen, Y. J. (2012) The hydrophobic core of twin-arginine signal sequences orchestrates specific binding to tat-pathway related chaperones. *PLoS One* **7**, e34159.

Schatz, P. J., Riggs, P. D., Jacq, A., Fath, M. J. and Beckwith, J. (1989). The secE gene encodes an integral membrane protein required for protein export in *Escherichia coli*. *Genes Dev*. **3**, 1035-44.

Schreiber S., Stengel R., Westermann M., Volkmer-Engert R., Pop O. I. and Muller J. P. (2006). Affinity of TatCd for TatAd elucidates its receptor function in the *Bacillus subtilis* Twin-srginine trasnslocation (Tat) translocase system. *J. Biol. Chem.* **281**, 19977-19984.

Schuenemann, D., Amin, P., Hartmann, E. and Hoffman, N. E. (1999). Chloroplast SecY is complexed to SecE and involved in the translocation of the 33-kDa but not the 23-kDa subunit of the oxygen-evolving complex. *J. Biol. Chem.* **274**, 12177-12182.

Schünemann, D. (2007). Mechanisms of protein import into thylakoids of chloroplasts. *Biol. Chem.* **388**, 907-915.

Settles, A. M., Yonetani, A., Baron, A., Bush, D. R., Cline, K. and Martienssen, R. (1997). Sec-independent protein translocation by the maize Hcf106 protein. *Science.* **278**, 1467-70.

Sharma, V., Arockiasamy, A., Ronning, D. R., Savva, C. G., Holzenburg, A., Braunstein, M., Jacobs, W. R. and Sacchettini, J. C. (2003). Crystal structure of *Mycobacterium tuberculosis* SecA, a preprotein translocating ATPase. *Proc. Natl. Acad. Sci. U S A* **100**, 2243-2248.

Silvestro, A., Pommier, J., Pascal, M. C. and Giordano, G. (1989). The inducible trimethylamine N-oxide reductase of *Escherichia coli* K12: its localization and inducers. *Biochim. Biophys. Acta.* **999**, 208-16.

Spence, E., Sarcina, M., Ray, N., Moller, S. G., Mullineaux, C. W. and Robinson, C. (2003). Membrane-specific targeting of green fluorescent protein by the Tat pathway in the cyanobacterium Synechocystis PCC6803. *Mol. Microbiol.* **48**, 1481- 1489.

Srivastava, R., Pisareva, T. and Norling, B. (2005). Proteomic studies of the thylakoid membrane of *Synechocystis* sp. PCC 6803. *Proteomics* **5**, 4905-4916.

Stanley, N. R., Findlay, K., Berks, B. C. and Palmer, T. (2001). *Escherichia coli* strains blocked in Tat-dependent protein export exhibit pleiotropic defects in the cell envelope. *J. Bacteriol.* **183**, 139-144.

Stanley, N. R., Palmer, T. and Berks, B. C. (2000). The twin arginine consensus motif of Tat signal peptides is involved in Sec-independent protein targeting in *Escherichia coli*. *J. Biol. Chem.* **275**, 11591-6.

Stengel, K. F., Holdermann, I., Cain, P., Robinson, C., Wild, K. and Sinning, I. (2008). Structural basis for specific substrate recognition by the chloroplast signal recognition particle protein cpSRP43. *Science* **321**, 253-256.

Summer, E. J., Mori, H., Settles, A. M. and Cline, K. (2000). The thylakoid delta pH-dependent pathway machinery facilitates RR-independent N-tail protein integration. *J. Biol. Chem.* **275**, 23483-23490.

Sun, C., Rusch, S. L., Kim, J. and Kendall, D. A. (2007). Chloroplast SecA and *Escherichia coli* SecA have distinct lipid and signal peptide preferences. *J. Bacteriol.* **189**, 1171-1175.

Tarry, M., Schafer, E., Chen, S., Buchanan, G., Greene, N., Lea, S., Palmer, T., Saibil, H. and Berks, B. (2009). Structural analysis of substrate binding by the TatBC component of the twin-arginine protein transport system. *Proc. Natl. Acad. Sci. U S A.* **106**, 13284-13289.

Thomas, J. D., Daniel, R. A., Errington, J. and Robinson, C. (2001). Export of active green fluorescent protein to the periplasm by the twin-arginine translocase (Tat) pathway in *Escherichia coli*. *Mol. Microbiol.* **39**, 47-53.

Tjalsma, H., Bolhuis, A., Jongbloed, J. D. H., Bron, S. and van Dijl, J. M. (2000). Signal peptide-dependent protein transport in *Bacillus subtilis*: a genome-based Survey of the Secretome. *Microbiol. and Mol. Biol. Rev* **64**, 515-547.

Tottey, S., Waldron, K. J., Firbank, S. J., Reale, B., Bessant, C., Sato, K., Cheek, T. R., Gray, J., Banfield, M. J., Dennison, C. and Robinson, N. J. (2008). Protein-folding location can regulate manganese-binding versus copper- or zinc-binding. *Nature.* **455**, 1138-1142.

Towbin, H., Staehelin, T. and Gordon, J. (1979). Electrophoretic transfer of proteins from polyacrylamide gels to nitrocellulose sheets: procedure and some applications. *Proc. Natl. Acad. Sci. U S A* **76**, 4350-4354.

Tsukazaki, T., Mori, H., Echizen, Y., Ishitani, R., Fukai, S., Tanaka, T., Perederina, A., Vassylyev, D.G., Kohno, T., Maturana, A.D., Ito, K. and Nureki, O. (2011). Structure and function of a membrane component SecDF that enhances protein export. *Nature*. **474**, 235-238.

van Bloois, E., Haan, G. J., de Gier, J. W., Oudega, B. and Luirink, J. (2006). Distinct requirements for translocation of the N-tail and C-tail of the *Escherichia coli* inner membrane protein CyoA. *J. Biol. Chem.* **281**, 10002-10009.

van Dalen, A., Killian, A. and de Kruijff, B. (1999). $\Delta\phi$ stimulates membrane translocation of the C-terminal part of a signal sequence. *J. Biol. Chem.* **274**, 19913-19918.

van den Berg, B., Clemons, W. M., Collinson, I., Modis, Y., Hartmann, E., Harrison, S. C. and Rapoport, T. A. (2004). X-ray structure of a protein-conducting channel. *Nature.* **427**, 36-44.

van der Ploeg, R., Barnett, J. P., Vasisht, N., Goosens, V. J., Pöther, D. C., Robinson, C. and van Dijl, J. M. (2011). Salt sensitivity of minimal twin arginine translocases. *J. Biol. Chem.* **286**, 43759-43770.

van Wely, K. H., Swaving, J., Freudl, R. and Driessen, A. J. (2001). Translocation of proteins across the cell envelope of Gram-positive bacteria. *FEMS Microbiol. Rev.* **25**, 437-454.

Vassylyev, D. G., Mori, H., Vassylyeva, M. N., Tsukazaki, T., Kimura, Y., Tahirov, T. H. and Ito, K. (2006). Crystal structure of the translocation ATPase SecA from *Thermus thermophilus* reveals a parallel, head-to-head dimer. *J. Mol. Biol.* **364**, 248-258.

Veenendaal, A. K., van der Does, C. and Driessen, A. J. (2004). The protein-conducting channel SecYEG. *Biochim. Biophys. Acta.* **1694**, 81-95.

Voelker, R. and Barkan, A. (1995). Two nuclear mutations disrupt distinct pathways for targeting proteins to the chloroplast thylakoid. *EMBO J.* **14**, 3905-3914.

von Heijne, G. (1995). Signal sequences: the limits of variation. *J. Mol. Biol.* **184**, 99-105.

Voulhoux, R., Ball, G., Ize, B., Vasil, M. L., Lazdunski, A., Wu, L. F. and Filloux, A. (2001). Involvement of the twin-arginine translocation system in protein secretion via the type II pathway. *EMBO J.* **20**, 6735-6741.

Vrontou, E. and Economou, A. (2004). Structure and function of SecA, the preprotein translocase nanomotor. *Biochim. Biophys. Acta.* **1694**, 67-80.

Walker, M. B., Roy, L. M., Coleman, E., Voelker, R. and Barkan, A. (1999). The maize tha4 gene functions in sec-independent protein transport in chloroplasts and is related to hcf106, tatA, and tatB. *J. Cell. Biol.* **147**, 267-76.

Walther, T. H., Grage, S. L., Roth, N. and Ulrich, A. S. (2010). Membrane alignment of the pore-forming component TatA(d) of the twin-arginine translocase from *Bacillus subtilis* resolved by solid-state NMR spectroscopy. *J. Am. Chem. Soc.* **132**, 15945-15956.

Wang, P. and Dalbey, R. E. (2011). Inserting membrane proteins: the YidC/Oxa1/Alb3 machinery in bacteria, mitochondria, and chloroplasts. *Biochim. Biophys. Acta.* **1808**, 866-875.

Warren, G., Oates, J., Robinson, C. and Dixon, A. M. (2009). Contributions of the transmembrane domain and a key acidic motif to assembly and function of the TatA complex. *J. Mol. Biol*. **388**, 122-32.

Weiner, J. H., Bilous, P. T., Shaw, G. M., Lubitz, S. P., Frost, L., Thomas, G. H., Cole, J. A. and Turner, R. J. (1998). A novel and ubiquitous system for membrane targeting and secretion of cofactor-containing proteins. *Cell.* **93**, 93-101.

Weiner, J. H., MacIssac, D. P., Bishop, R. E. and Bilous, P. T. (1988). Purification and properties of *Escherichia coli* dimethyl sulfoxide, an iron-sulfur molybdoenzyme with broad substrate specificity. *J. Bacteriol.* **170**, 1505-1510.

Westerman M., Pop I. O., Gerlach G., Appel T. R., Schlormann W., Schreiber S. and Muller J. P. (2006). The TatAd component of the *Bacillus subtilis* twin-arginine protein transport system forms homo-multimeric complexes in its cytosolic and membrane embedded localisation. *Biochim. Biophys. Acta*. **1758**, 443-451.

Wexler, M., Sargent, F., Jack, R. L., Stanley, N. R., Bogsch, E. G., Robinson, C., Berks, B. C. and Palmer, T. (2000). TatD is a cytoplasmic protein with DNase activity. No requirement for TatD family proteins in sec-independent protein export. *J. Biol. Chem.* **275**, 16717-22.

Widdick, D. A., Eijlander, R. T., van Dijl, J. M., Kuipers, O. P. and Palmer, T. (2008). A facile reporter system for the experimental identification of twin-arginine translocation (Tat) signal peptides from all kingdoms of life. *J. Mol. Biol*. **375**, 595-603.

Wu, L. F., Ize, B., Chanal, A., Quentin, Y. and Fichant, G. (2000). Bacterial twin-arginine signal peptide-dependent protein translocation pathway: evolution and mechanism. *J. Mol. Microbiol. Biotechnol.* **2**, 179-189.

Xie, K. and Dalbey, R. E. (2008). Inserting proteins into the bacterial cytoplasmic membrane using the Sec and YidC translocases. *Nat. Rev. Micro.* **6**, 234-244.

Yahr, T. L. and Wickner, W. T. (2001). Functional reconstitution of bacterial Tat translocation *in vitro*. *EMBO J.* **20**, 2472-9.

Yen, M. R., Tseng, Y. H., Nguyen, E. H., Wu, L. F. and Jr Saier, M. H. (2002). Sequence and phylogenetic analyses of the twin-arginine targeting (Tat) protein exportsystem. *Arch. Microbiol.* **177**, 441-50.

Yuan, J., Dalbey, R. E. and Kuhn, A. (2010). Membrane protein insertion in *E. coli*. *Meth. Mol. Biol.* **619**, 63-77.

Yuan, J., Henry, R., McCaffery, M. and Cline, K. (1994). SecA homolog in protein transport within chloroplasts: evidence for endosymbiont-derived sorting. *Science.* **266**, 796-798.

Zimmer, J., Li, W. and Rapoport, T. A. (2009). A novel dimer interface and conformational changes revealed by an X-ray structure of *B. subtilis* SecA. *J. Mol. Biol.* **364**, 259-265.

Zoufaly, S., Fröbel, J., Rose, P., Flecken, T., Maurer, C., Moser, M. and Müller, M. (2012). Mapping precursor-binding site on TatC subunit of twin arginine-specific protein translocase by site-specific photo cross-linking. *J. Biol. Chem.* **287**, 13430-13441.

Appendix A

Co-immunoprecipitation images

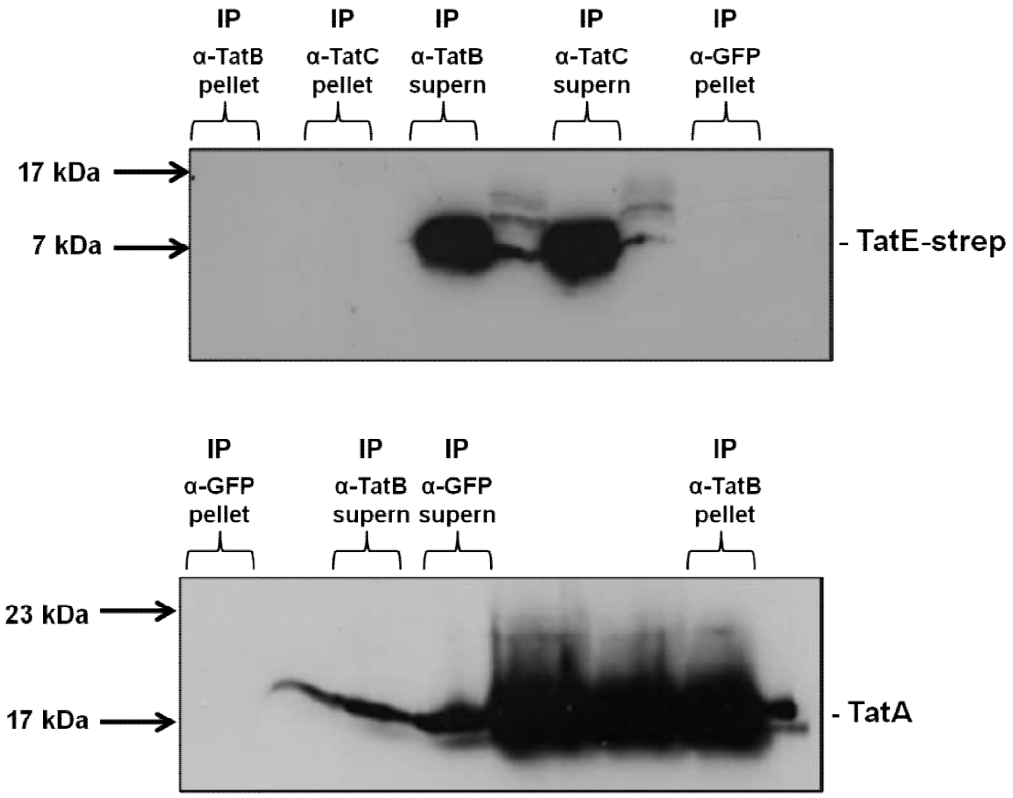

Co-immunoprecipitation experiments
Original images spliced in Figure 5.2.5 chapter 5. The cut-out is indicated.

Appendix B

Published work

THE JOURNAL OF BIOLOGICAL CHEMISTRY VOL. 287, NO. 10, pp. 7335–7344, March 2, 2012

Structure of TatA Paralog, TatE, Suggests a Structurally Homogeneous Form of Tat Protein Translocase That Transports Folded Proteins of Differing Diameter[S]

Received for publication, November 22, 2011, and in revised form, December 20, 2011 Published, JBC Papers in Press, December 21, 2011, DOI 10.1074/jbc.M111.326355

Jacopo Baglieri[1], **Daniel Beck, Nishi Vasisht, Corinne J. Smith, and Colin Robinson**[2]

From the School of Life Sciences, University of Warwick, Coventry CV4 7AL, United Kingdom

Background: The Tat system transports folded proteins in bacteria.
Results: Unlike TatA, the paralogous TatE is found as small, homogeneous complexes.
Conclusion: TatE cannot form a variable translocation channel as suggested for TatA.
Significance: This work suggests a new model in which a structurally homogeneous form of translocase uses a flexible channel.

The twin-arginine translocation (Tat) system transports folded proteins across bacterial and plant thylakoid membranes. Most current models for the translocation mechanism propose the coalescence of a substrate-binding TatABC complex with a separate TatA complex. In *Escherichia coli,* TatA complexes are widely believed to form the translocation pore, and the size variation of TatA has been linked to the transport of differently sized substrates. Here, we show that the TatA paralog TatE can substitute for TatA and support translocation of Tat substrates including AmiA, AmiC, and TorA. However, TatE is found as much smaller, discrete complexes. Gel filtration and blue native electrophoresis suggest sizes between ~50 and 110 kDa, and single-particle processing of electron micrographs gives size estimates of 70–90 kDa. Three-dimensional models of the two principal TatE complexes show estimated diameters of 6–8 nm and potential clefts or channels of up to 2.5 nm diameter. The ability of TatE to support translocation of the 90-kDa TorA protein suggests alternative translocation models in which single TatA/E complexes do not contribute the bulk of the translocation channel. The homogeneity of both the TatABC and the TatE complexes further suggests that a discrete Tat translocase can translocate a variety of substrates, presumably through the use of a flexible channel. The presence and possible significance of double- or triple-ring TatE forms is discussed.

The twin-arginine translocation (Tat)[3] pathway system transports folded proteins across the chloroplast thylakoid membrane and the plasma membranes of many bacteria (reviewed in Refs. 1 and 2). Tat substrates bear cleavable N-terminal signal peptides containing a critical and highly conserved twin-arginine motif within the consensus sequence (3, 4). In *Escherichia coli*, the minimal set of components required for Tat-dependent translocation are three integral membrane proteins, TatA, TatB, and TatC, encoded by the *tatABC* operon, with molecular masses of 10, 18 and 30 kDa, respectively (5–7). At the steady state, these subunits are found in two types of complex within the plasma membrane: a substrate-binding TatABC complex of ~370 kDa and separate TatA homo-oligomeric complexes ranging from ~50 kDa to over 500 kDa (8–10). There is good evidence that the TatABC complex is responsible for the initial binding of substrate molecules, and the TatBC subunits appear to be particularly important in this respect (9). It is also believed that TatA complexes assemble with the TatABC complex to form a transient "supercomplex," with TatA forming the translocation channel. It has been proposed that the variable size of the TatA complex could be a key feature that enables the system to generate a channel of appropriate diameter for a given substrate (10, 11), and electron microscopy studies have shown that TatA complexes do indeed contain potential pores of widely differing diameter (11). Accordingly, TatA is generally considered to form the bulk of the translocation pore. Studies on the Tat system in thylakoids suggest a similar mechanism in which the binding of substrate to the TatBC subunits (denoted Hcf106-cpTatC in plants) initiates assembly with the separate TatA complex (Tha4 in plants) to form the active translocon (12).

Although the TatABC subunits appear to form the primary translocation system, *E. coli* also contains a separate TatA paralog, TatE, that is encoded by a monocistronic *tatE* gene. The *tatE* gene is found only in enterobacteria (13) with the exception of the Gram-positive bacteria *Corynebacterium glutamicum* and *Corynebacterium efficiens*, which also have a Tat system containing the *tatE* gene in addition to *tatA*, *tatB*, and *tatC* (14). The *E. coli tatE* gene encodes a 67-amino acid predicted membrane protein that exhibits greater than 50% sequence identity with TatA (5). Overexpression of TatE results in complementation of a *tatA* mutant, indicating a similar role (15), but TatE is normally produced at levels that are much lower than those of TatA (16). Nevertheless, there is evidence that TatE plays a distinct role. In *E. coli*, tatE is induced in biofilms, and *Pseudomonas stutzeri tatE* expression is associated with denitrification, perhaps pointing to an important role for TatE proteins under specific growth conditions or possibly as an adaptation for handling specific substrates (17, 18).

[S] This article contains supplemental Fig. 1.
[1] Funded by Transys ITN (Marie Curie Initial Training Network, Project 215524).
[2] To whom correspondence should be addressed. Tel.: 44-2476-523558; Fax: 44-2476-523568; E-mail: colin.robinson@warwick.ac.uk.
[3] The abbreviations used are: Tat, twin-arginine translocation; TMAO, trimethylamine *N*-oxide; TorA, TMAO reductase; DDM, dodecyl maltoside; BN, blue native.

TABLE 1
Plasmids and strains used in this work

	Relevant properties	Reference/source
Plasmids		
pBAD-E-Strep	pBAD24 derivative containing the *E. coli tatE* gene with a C-terminal *Strep*-II^{TM} tag; Amp^r	This study
pBAD-A-Strep	pBAD24 derivative containing the *E. coli tatA* gene with a C-terminal *Strep*-II^{TM} tag; Amp^r	(21)
pBAD-ABC-Strep	pBAD24 derivative containing the *E. coli tatABC* operon; with a C-terminal *Strep*-II^{TM} tag; Amp^r	(8)
pRD8	pING1 derivative containing the *E. coli Lep* gene; Amp^r	(22)
Strains of *E. coli*		
MC4100	F$^-$ ΔlacU169 araD139 rpsL150 relA1 ptsF rbs flbB5301	(19)
MC4100 Δ*tatABCDE*	*tat* deletion strain	(5)
MC4100 Δ*tatAE*	*tatA* and *tatE* deletion strain	(5)
MC4100 Δ*tatA*	*tatA* deletion strain	(5)

In this study, we report for the first time the purification and characterization of *E. coli* TatE complexes following expression in the presence of native levels of the TatB and TatC components. TatE supports efficient translocation of Tat substrates, but the data reveal major differences between TatA and TatE complexes. Most importantly, the TatE complexes are far smaller and more homogeneous than TatA complexes. Indeed, single TatE complexes are smaller than one of the best studied Tat substrates. The results are consistent with a different model for Tat action in which a limited number of discrete Tat complexes are sufficiently flexible to transport a wide range of substrates. In this model, single TatE/TatA complexes would not provide the bulk of the translocation pore.

EXPERIMENTAL PROCEDURES

Bacterial Strains, Plasmids, and Growth Conditions—All of the strains and plasmids used are listed in Table 1. *E. coli* MC4100 was used as the parental strain (19). Δ*tatABCDE*, Δ*tatAE*, and Δ*tatA* (5, 20) have been described previously. Arabinose-resistant derivatives were used as described (8). *E. coli* was grown aerobically in Luria broth (LB). *E. coli* was grown anaerobically in Luria broth supplemented with 0.5% glycerol, 0.5% trimethylamine *N*-oxide (TMAO), and 1 μM ammonium molybdate. The media were supplemented with ampicillin to a final concentration of 100 μg/ml and arabinose to 1 mM when required.

DNA Techniques—All of the enzymes used were from Roche Applied Science or Fermentas Life Sciences. The polymerase chain reaction (PCR) was performed using Expand DNA polymerase (Roche Applied Science). For arabinose-inducible overproduction of *E. coli* TatE, plasmid pBAD-E-Strep was constructed as follows. The *tatE* gene was amplified from *E. coli* MC4100 chromosomal DNA with primers tatE_NcoI_for (ataccATGGGTGAGATTAGTATTAC; nucleotides identical to genomic DNA are capitalized, and restriction sites are underlined) and tatEs_PstI_rev (tatccagtctgcagcctccttta**ttttttcaaactgtgggtgcgaccacgccga**CTCTTTATGAGAGAG; nucleotides in bold specify the *Strep*-II^{TM} tag peptide). The resulting product was digested with NcoI and PstI and ligated into plasmid pBAD24, generating pBAD-E-Strep.

Expression and Purification of the TatE complex and TatA Complex—E. coli Δ*tatAE* cells containing plasmid pBAD-E-Strep or pBAD-A-Strep were grown aerobically to mid-exponential phase with the induction of *tatE* on plasmid pBAD-E-Strep and *tatA* on plasmid pBAD-A-Strep using 1 mM arabinose. The membranes were isolated as described previously (8) and solubilized in 2% dodecyl maltoside (DDM). The solubilized membranes were loaded on a Q-Sepharose column, and the proteins were eluted as described in Ref. 8. Avidin (2 μg/ml) was added to the sample to block any biotin-containing proteins, and the sample was loaded on a 2-ml *Strep*-Tactin-Sepharose (Institut für Bioanalytik). The column was washed with 8 column volumes of equilibration buffer containing Tris-HCl, pH 8.0, 150 mM NaCl, and 0.1% DDM. Bound protein was eluted from the column in 10 0.5-ml fractions using the same buffer as above but containing 2.5 mM desthiobiotin (Institut für Bioanalytik). The eluted peak fraction was loaded onto a Superdex^{TM} 200 HR 10/30 gel filtration column (Amersham Biosciences) and was eluted with the same equilibration buffer as described above but containing 0.02% DDM.

SDS-PAGE and Western Blotting—The proteins were separated using SDS-polyacrylamide gel electrophoresis and immunoblotted using specific antibodies to TatA and TatB (8) and goat anti-rabbit IgG horseradish peroxidase conjugate. The *Strep*-II^{TM} tag on TatE and TatA was detected directly using a *Strep*-Tactin-horseradish peroxidase conjugate (Institut für Bioanalytik). An ECL detection kit (Amersham Biosciences) was used to visualize the proteins.

Blue Native Polyacrylamide Gel Electrophoresis—Blue native polyacrylamide gel electrophoresis of Tat complexes was performed as described previously (10). Solubilized membranes and purified protein were loaded and separated on a polyacrylamide gradient gel (5–13.5%). The proteins were detected by immunoblotting as described above.

TMAO Reductase Activity Assay—TMAO reductase activity assay was performed as described previously (8, 23). *E. coli* cells were grown anaerobically until mid-exponential growth phase prior to fractionation into periplasmic, cytoplasmic, and membrane fractions. The cell fractions were loaded and separated on a 10% native polyacrylamide gel that was subsequently assayed for TMAO reductase activity as described previously.

Protease Accessibility Experiments—For the protease accessibility experiments, *E. coli* Δ*tatAE* cells containing plasmid pBAD-E-Strep, pBAD-A-Strep (21), and pRD8 (22) were used to express TatE, TatA, and leader peptidase, respectively. Spheroplasts were prepared by resuspending the cell pellet in 2.5 ml of 33 mM Tris-HCl (pH 8.0), 40% sucrose, and 5 mM Na_2EDTA (0.1 mg/ml). Cells were incubated at 4 °C for 30 min and then harvested at 4000 × *g* for 15 min. The resulting spheroplast pellet was resuspended in 1 ml of ice-cold 33 mM Tris-HCl and 40% sucrose. Aliquots (50 μl) of the spheroplast

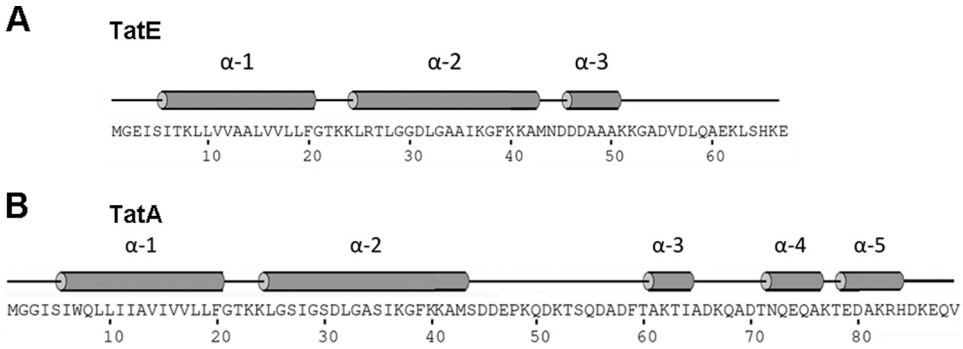

FIGURE 1. **Predicted secondary structure elements of the *E. coli* TatE (*A*) and TatA (*B*) protein.** The prediction is that of the program PSIPRED (29). α-Helices are represented as cylinders, and they are denoted as *α-1*, *α-2*, *α-3*, *α-4*, and *α-5*.

preparations were incubated at 25 °C for 30 min in the presence of 0.5 mg/ml proteinase K (Invitrogen) and/or 2% (v/v) Triton X-100 (BDH Laboratory Supplies).

Microscopy—Images were recorded with a Leica DMRE microscope equipped with a Leica TCS SP2 confocal unit and an argon laser. The natural light was selected, and the images were recorded with a photomultiplier using the Leica confocal software. The samples were visualized with a 63× oil immersion objective (numerical aperture, 1.4; Leica). The image size is 512 × 512 pixels, and the images were averaged from four successive scans.

Electron Microscopy—A sample of the TatE complex taken from the peak fraction of the gel filtration run was diluted 1:2 with the gel filtration sample buffer + 0.02% DDM. 4 μl of this sample was applied to freshly glow discharged (negatively) carbon-coated copper grids (300 mesh). The grid was then washed and stained following the touching drop method (40) 1 × 10-s washes in gel filtration buffer minus detergent and 2 × 10-s washes in water followed by 2 × 10-s stains with 2% uranyl acetate. After blotting, the grid was then left to air-dry. Micrographs were taken on a 200-kV JEOL 2011 FEG TEM operating a 4k Gatan UltraScan CCD camera with a pixel size of 15 μm. Tilt pairs of images were taken at a magnification of ~86,000× under low dose conditions, with the first at an angle of 45° and the second at 0°. The average defocus of the 10 (40) selected tilt pairs was 1.8 μm.

Image Processing—Image processing was performed using the SPIDER/WEB software (24) managed through the SPIRE GUI interface (25). Many of the batch files used were adapted from those provided with the SPIDER tutorial package. Micrograph quality and defocus of the untilted images were estimated using both CTFFIND3 and the TF ED SPIDER operation. Particles were then picked from the best micrographs interactively using the JWEB pair-wise picking option. CTFTILT3 (26) was used to verify the tilt angle of the tilted images and calculate the defocus across these images. Particles were normalized and then contrast transfer function-corrected by phase flipping. Clear top-down views of the untilted particles were selected and shift-aligned and then cross-correlated to the whole dataset to find more. They were then assessed for size variation using the approach described previously (27) and classified using a hierarchical ascendant classification multivariate statistical analysis method into two size classes. The remaining particles were separated by the same method into potential side views and multiple-ringed structures. The untilted particles were then aligned both translationally and rotationally using a reference-free approach to provide the in-plane rotation angles needed to align the images. The tilted particles were centered only (no rotational alignment). With the required Euler angles defined (in-plane rotation from the untilted images and out-of-plane tilt from the tilted images), three-dimensional reconstructions were generated by back projection using the Simultaneous Iterative Reconstruction Technique algorithm (28). After refinement of the structures by projection matching, these models were then filtered around the nominal resolution as determined by the 0.5 Fourier shell correlation.

RESULTS

TatE Expression Restores Export of TorA in ΔtatAE Mutant—*E. coli* TatE is a 67-residue membrane protein with predicted secondary structural elements that are shown in Fig. 1*A*. TatE is strongly predicted to contain a single transmembrane α-helix at the amino terminus (helix α-1) followed by a segment containing an amphipathic α-helix (helix α-2) similar to TatA. For comparison, the predicted secondary structure of *E. coli* TatA is illustrated in Fig. 1*B*. In general, the structure of TatE resembles those of *E. coli* TatA and *Bacillus subtilis* TatAd, which have been studied by NMR (30, 31).

Previous experiments performed with Tat proteins expressed at native levels have shown TatA and TatE to have overlapping functions in the Tat pathway (5). We set out to test whether overexpressed TatE can complement the previously characterized *E. coli* Δ*tatAE* cells by restoring export activity in our strains. First, we assessed the activity of TatE in *E. coli* following expression from the multicopy pBAD24 plasmid. The *tatE* gene was expressed in *E. coli* Δ*tatAE* cells, and a TMAO reductase activity assay was conducted as described under "Experimental Procedures." TMAO reductase (TorA) is a periplasmic protein required for growth of *E. coli* on minimal TMAO and glycerol media. It is a known Tat substrate that can be detected using a methyl viologen-linked reduction assay in a native polyacrylamide gel. TatE was overexpressed from plasmid pBAD-E-Strep with a C-terminal *Strep*-II^{TM} tag in *E. coli* Δ*tatAE* cells under anaerobic conditions, after which the cells were fractionated and the localization of TorA was determined (Fig. 2*A*).

In Fig. 2*A*, the *left-hand panels* show control tests in which wild-type *E. coli* MC4100 cells (*WT*) were fractionated into

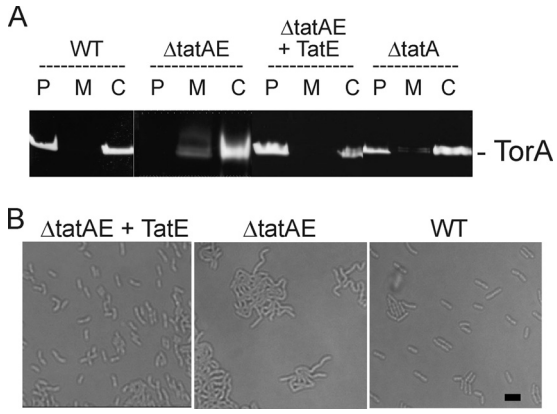

FIGURE 2. ***E. coli* TatE complements Δ*tatAE E. coli* mutant.** *A*, the figure shows a native polyacrylamide gel stained for TorA activity. Periplasm, membrane, and cytoplasm samples (*P*, *M*, and *C*, respectively) were prepared and analyzed from wild-type *E. coli* MC4100 cells (*WT*), from the *E. coli* Δ*tatAE* and Δ*tatA* cells, and from *E. coli* Δ*tatAE* cells expressing *E. coli* TatE from plasmid pBAD-E-Strep (Δ*tatAE* + *TatE*). The mobility of active TorA is indicated. *B*, TatE expression can complement the filamentous phenotype of *E. coli* Δ*tatAE* cells. Confocal microscope images of wild-type *E. coli* MC4100 cells (*WT*), *E. coli* Δ*tatAE* cells, and *E. coli* Δ*tatAE* cells expressing TatE from the pBAD-E-Strep plasmid (Δ*tatAE* + *TatE*) are shown. The *scale bar* is 1.5 μm.

membrane, cytoplasm, and periplasm samples (*lanes M, C,* and *P,* respectively). The data show that the TorA activity is found in the periplasm as expected, with TorA activity also present in the cytoplasm as is often observed (8). As expected in the *E. coli* Δ*tatAE* double mutant, no periplasmic activity is detected because Tat export is blocked. As found previously (5), TorA export proceeds in the *E. coli* Δ*tatA* single mutant because TatE is able to substitute for TatA. Importantly, overexpression of TatE in *E. coli* Δ*tatAE* cells (Δ*tatAE* + *TatE panel*) leads to efficient export of TorA. This experiment confirms that the TatE is active under these conditions and able to function effectively in the absence of TatA, in combination with TatB and TatC components expressed at native levels. The effectiveness of the cell fractionation protocol was positively assayed as shown in supplemental Fig. 1. Expression of TatE was routinely confirmed by immunoblotting in this and subsequent experiments (data not shown).

TatE Restores Export of AmiA and AmiC in ΔtatAE Mutant—*E. coli* amidases AmiA and AmiC are periplasmic proteins that are translocated by the Tat pathway and involved in cytokinesis (32). These substrates are mislocalized in an *E. coli* Δ*tatABCDE* strain causing a distorted cell division phenotype, such that the cells grow in long chain-like filaments (33). This phenotype is shown in Fig. 2*B* by the *E. coli* Δ*tatAE* cells. Overexpression of TatE in *E. coli* Δ*tatAE* cells restores the wild-type cell division phenotype (Δ*tatAE* + *TatE panel*), and the cells resemble wild-type cells, indicating that AmiA and AmiC are being correctly exported by the Tat pathway. The cells appear identical to wild-type cells (*WT*). These data, taken in conjunction with the TorA export data, show that TatE is able to effectively substitute for TatA and form an active translocon in this strain.

Characterization of TatE Complexes Formed after Overexpression of tatE Gene—To study the nature of TatE complexes, *E. coli* Δ*tatAE* cells expressing TatE from the plasmid pBAD-E-Strep (with a *Strep*-II^{TM} tag fused to the C terminus of TatE) were fractionated, and membranes were isolated. Total membranes were solubilized in 2% DDM and first subjected to anion exchange chromatography using a Q-Sepharose resin. Eluted protein was further purified on a *Strep*-Tactin affinity column as described under "Experimental Procedures." All column fractions were immunoblotted using antibodies to the *Strep*-II^{TM} tag on TatE. The data presented in Fig. 3*A* show that a proportion of TatE was detectable in the column wash fractions, but most of the protein bound to the column and was specifically eluted from the column across elution fractions 5–10.

The TatE complexes were then applied to a calibrated Superdex^{TM} 200 HR 10/30 gel filtration column, and elution fractions were immunoblotted using antibodies to the *Strep*-II^{TM} tag on TatE (Fig. 3*B*). The immunoblots show TatE to elute across fractions 20–26 with a peak in fraction 23. This represents a relatively tight peak, suggesting that TatE is rather homogeneous, and calibration of the column shows the complex to be ~130 kDa in mass on average, including the detergent micelle. This result is in marked contrast to previous findings on the *E. coli* TatA complex, which was found to be remarkably heterogeneous and present as complexes ranging in size from ~50 kDa to over 500 kDa (10, 11). To confirm this point under similar experimental conditions, we expressed *E. coli* TatA from the plasmid pBAD-A-Strep, where TatA is likewise tagged with a C-terminal *Strep*-II^{TM} tag, and we purified the protein by Q-Sepharose and *Strep*-Tactin column using the same protocol (data not shown). When subjected to gel filtration chromatography under identical conditions, *E. coli* TatA elutes across a much broader range of fractions (Fig. 3*B*), confirming the large range of size forms for this complex. TatE elutes with a sharper peak, which indicates the presence of a complex that is both smaller and far more homogeneous than the TatA complex.

The purified TatE complexes were further analyzed by blue native (BN) polyacrylamide gel electrophoresis. BN gels have been widely used to study hydrophobic membrane-bound protein complexes because they often provide a higher level of resolution when compared with gel filtration, enabling more accurate determination of molecular mass and complex composition (34, 35). The TatE gel filtration fractions 21–26 from Fig. 3*B* were loaded onto a BN gel, and the gel was subjected to immunoblotting with antibodies against the *Strep*-II^{TM} tag on TatE. Fig. 4 shows the presence of two major bands corresponding to TatE complexes that migrate with, or close to, the 66-kDa marker. A minor third band runs above them. The sizes of these TatE complexes are consistent with those estimated by gel filtration, where the detergent micelle contributes to the apparent size of complexes. Again, we analyzed TatA under identical conditions, and the data are shown in Fig. 4. TatA gel filtration elution fractions 18–25 were subjected to BN gel electrophoresis, and the TatA complexes formed the characteristic ladder of bands observed in an earlier study (10). These bands correspond to separate complexes with estimated sizes ranging from ~100 kDa to over 500 kDa, with the gel filtration fractions containing distinct size classes. Thus, the BN gel results confirm that TatE subunits are organized as relatively small, homogeneous complexes that differ considerably from TatA complexes generated under the same conditions.

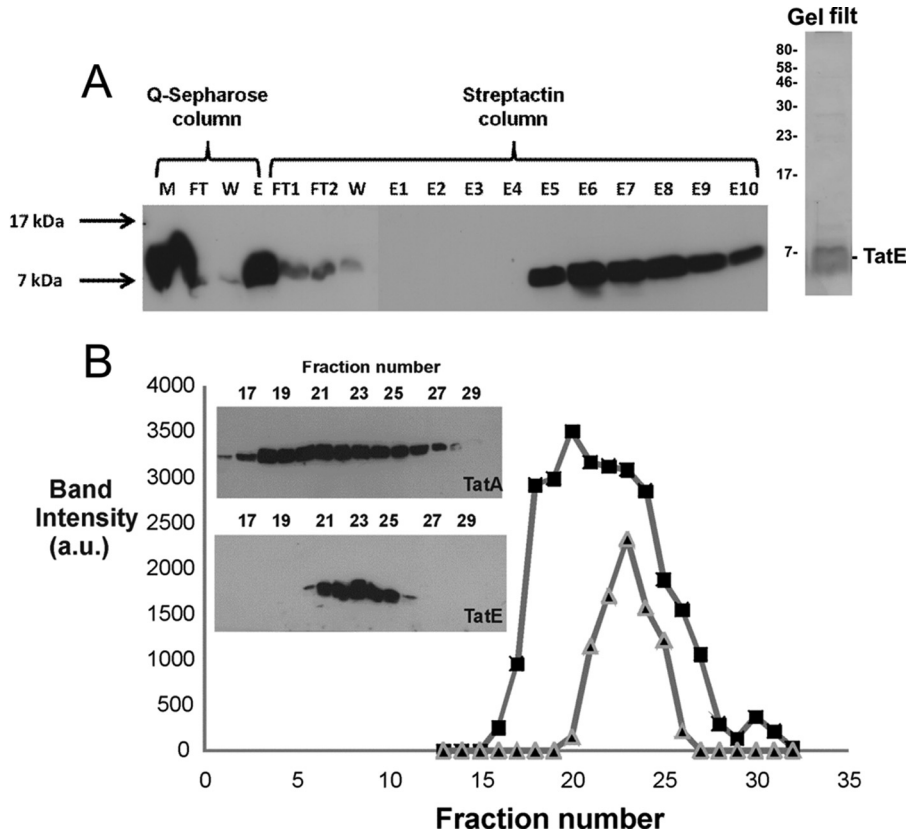

FIGURE 3. **Affinity purification and gel filtration of distinct *E. coli* TatE-containing complexes.** *A*, membranes were prepared from *E. coli* Δ*tatAE* cells expressing *E. coli* TatE with a C-terminal *Strep*-II™ tag, solubilized in DDM, and applied to a Q-Sepharose anion exchange column. The Q-Sepharose peak elution fractions were then loaded on a *Strep*-Tactin affinity column. All column fractions were immunoblotted using antibodies against the *Strep*-II™ tag on TatE. Whole membranes (*M*), flow-through columns (*FT*, *FT1*, *FT2*), wash fractions (*W*), the Q-Sepharose elution fraction (*E*), and *Strep*-Tactin elution fractions (*E1–E10*) are all indicated. Mobility of TatE is indicated on the *right*. Molecular mass markers are indicated on the *left*. Affinity-purified TatE was applied to a calibrated Superdex 200 gel filtration column as described under "Experimental Procedures," and the peak elution fraction was analyzed by silver-stained gel (*gel filt. panel*). *B*, TatA and TatE were expressed in *E. coli* Δ*tatAE* cells under identical conditions and affinity-purified as in *A*, and the peak fractions were run on a Superdex 200 gel filtration column. Peak elution fractions were analyzed by immunoblotting using antibodies to the *Strep*-II™ tag on TatE and TatA, and the intensities of the TatE (*filled triangles*) and TatA (*filled squares*) bands are shown plotted against the fraction number. The column was calibrated using a set of protein standards of known molecular mass, namely thyroglobulin (669 kDa), ferritin (440 kDa), aldolase (158 kDa) and albumin (66 kDa). Mobilities of TatE and TatA are indicated. *a. u.*, arbitrary units.

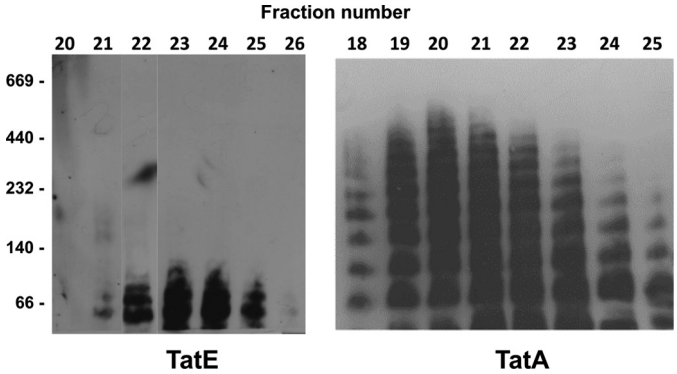

FIGURE 4. **Blue native gel electrophoresis identifies three discrete TatE complexes with an estimated mass of ~66 kDa.** TatE gel filtration elution fractions 21–26 and TatA gel filtration elution fractions 18–25 were subjected to blue native gel electrophoresis as described under "Experimental Procedures." The gels were immunoblotted using antibodies to the *Strep*-II™ tag on the C terminus of TatE and TatA. Mobilities of molecular mass markers (in kDa) are indicated on the *left*.

The properties of TatE complexes were further analyzed as shown in Fig. 5. In Fig. 5*A*, we expressed TatE in Δ*tatAE* cells as above but subjected the solubilized membranes to BN gel analysis without further purification. The results (*TatE lane*) show that TatE complexes run as the same two primary forms as observed in Fig. 4 (~50 and 70 kDa). As a control to confirm that the gel resolved larger complexes, we expressed TatABC in the same cells, with a C-terminal *Strep*-II™ tag present on TatC. The blot (*ABC lane*) shows that TatC is present in the ~400-kDa TatABC complex previously described in Ref. 10. In a second experiment, we expressed TatE in the same manner and solubilized samples of the membranes in digitonin and C12E9 as well as DDM. The solubilized membranes were then subjected to gel filtration as in Fig. 3, and the elution profiles of the TatE complexes are shown in Fig. 5*B*. The data show that TatE complexes elute in a generally similar manner in all three cases, with similarly sharp elution peaks and a relatively small average size (under 150 kDa in all cases, including the micelle). When compared with DDM-solubilized complexes, TatE complexes appear to be slightly smaller in C12E9 and slightly larger in digitonin, but this may reflect the differing sizes of the micelles (digitonin, in particular, forms a relatively large micelle).

Electron Microscopy of TatE Complexes—Examination of TatE complexes using electron microscopy of negatively stained samples confirmed the relatively homogeneous nature

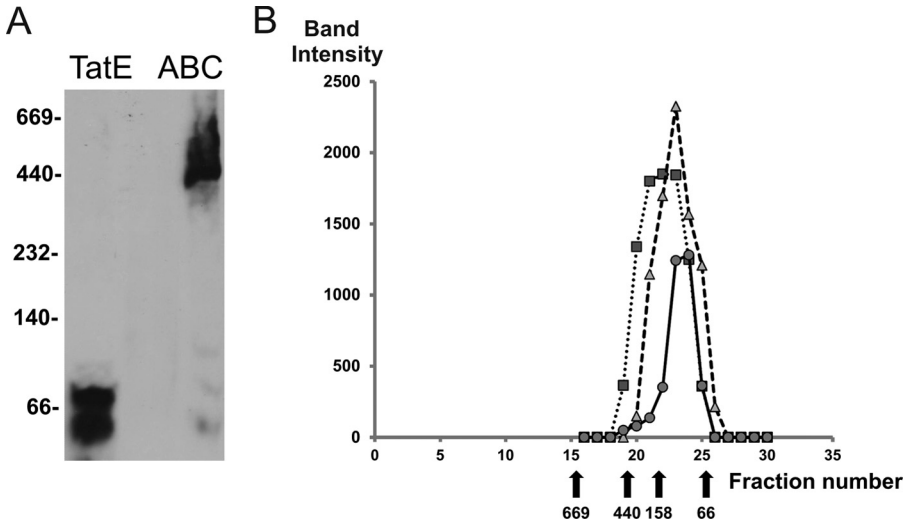

FIGURE 5. **TatE complexes are relatively small and homogeneous in different detergents.** *A*, membranes were prepared from *E. coli* Δ*tatAE* cells expressing TatE or TatABC proteins in which a *Strep*-II™ tag was present on the C terminus of TatE or TatC, respectively. The membranes were solubilized in digitonin and subjected to blue native gel electrophoresis as in Fig. 4. The gel was immunoblotted to antibodies to the *Strep*-II™ tag. *B*, membranes were prepared from *E. coli* Δ*tatAE* cells expressing TatE and solubilized in 1% (v/v) digitonin (*filled squares*), 2% dodecyl maltoside (*filled triangles*), or 2% C12E9 (*filled circles*). The samples were run on a calibrated Superdex 200 gel filtration column as described in the legend for Fig. 3 in the presence of the same detergents, with digitonin present at 0.1% (v/v) and C12E9 at 0.1%. Fractions were immunoblotted with antibodies to the *Strep*-II™ tag on TatE, and the intensities of the bands are shown plotted against fraction number. The peak elutions of molecular mass markers (as detailed in the legend for Fig. 3) are indicated with *filled triangles*, and their molecular masses are shown in kDa.

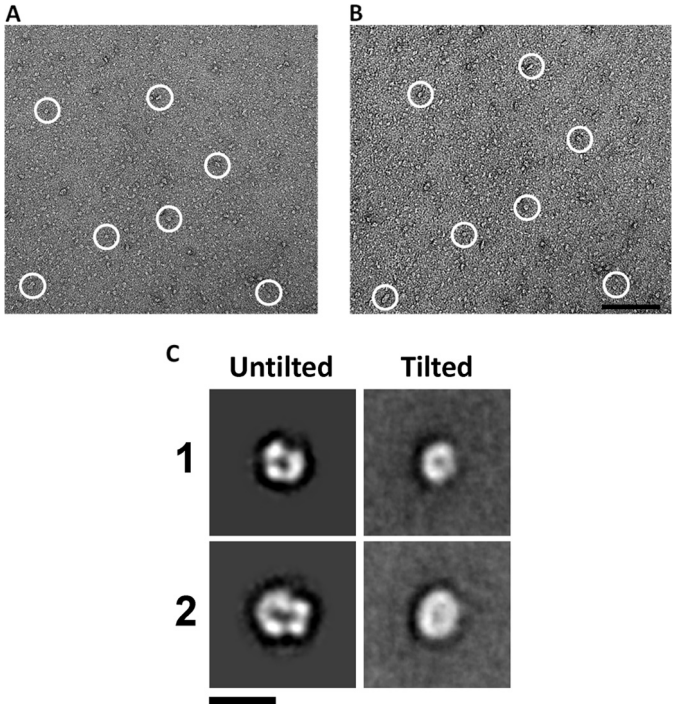

FIGURE 6. **Micrographs of TatE tilt pair and class averages of TatE complexes.** *A* and *B*, area of micrograph untilted (*A*) and tilted to 45° (*B*). Corresponding particle pairs in both images are *circled*. The *scale bar* is 100 nm. *C*, the two principal size classes of round TatE complexes are shown. Aligned class averages of the untilted particles and centered tilted particles are shown. Class 1 consists of 226 particles, and class 2 contains 288. The *scale bar* is 10 nm.

of the sample in comparison with reported images of TatA. We observed small ring-shaped structures lying in a preferred orientation on the grid. In addition, we observed larger structures composed of two or more rings, which appeared to adopt a wider array of orientations. We analyzed these structures using single-particle image processing techniques and obtained a three-dimensional reconstruction using a random conical tilt strategy. Fig. 6 shows an area of a micrograph untilted (*A*) and tilted to ~45° (*B*).

The raw micrographs and class averages both revealed that most of the complexes formed small ring-shaped structures with a maximum diameter of ~8 nm and a dark central area indicating the possibility of a pore or well in the center. Approximately 1000 initial particles were picked from 10 tilt pairs of images, and clear top-down views of the untilted particles were selected for further analysis. Multivariate statistical analysis of the untilted particles revealed a moderate variation in particle size of around 2 nm. The particles were separated into two size classes (containing 226 and 288 particles, respectively) using the strategy described in Ref. 27 and aligned using a reference-free method (28) to generate the class averages shown in Fig. 6*C*. Using the in-plane orientations from the untilted particles, a three-dimensional electron density map, with an estimated resolution of 29 Å, was generated for both classes using the tilted particles, and these are shown in Fig. 7. As indicated by the original images, these maps show ring-shaped structures. The dark central area observed in the micrographs was revealed to result from a central cleft or well within the ring, occluded on one side. The shape of the three-dimensional volume obtained is similar to previous structures shown for TatA complexes but much smaller in diameter (6–8 nm when compared with 9–13 nm in the case of TatA (11)). The diameter of the observed cleft for both three-dimensional volumes obtained was ~2.5 nm.

As well as the single-ring structures described above, a number of particles contained multiple rings and appear as potential dimers or trimers of the single-ringed structures. These multimers were picked separately from the single-ringed particles as the obvious difference in structure made them easily distinguishable; they were then processed and aligned using a refer-

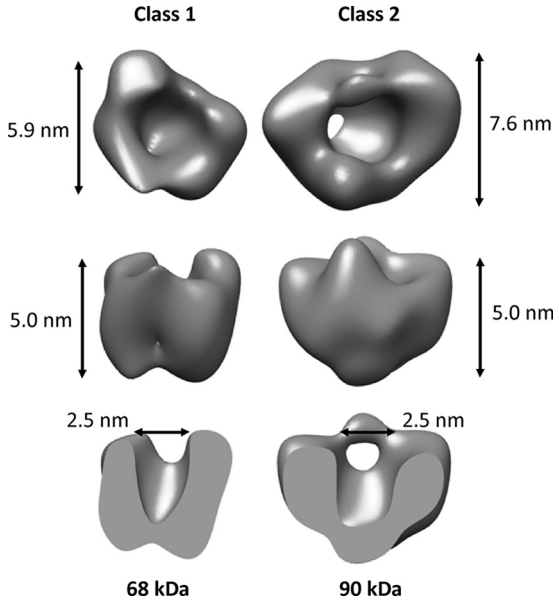

FIGURE 7. **Three-dimensional density maps of TatE complex assemblies.** The small and large TatE complexes are shown filtered to 29 Å and contoured at ~5 σ (S.D. above mean density). Dimensions shown from top to bottom are: complex diameter, complex height, and pore width. Molecular masses were estimated based on a protein density of 0.844 Da/Å^3. The figure was produced using the program UCSF Chimera.

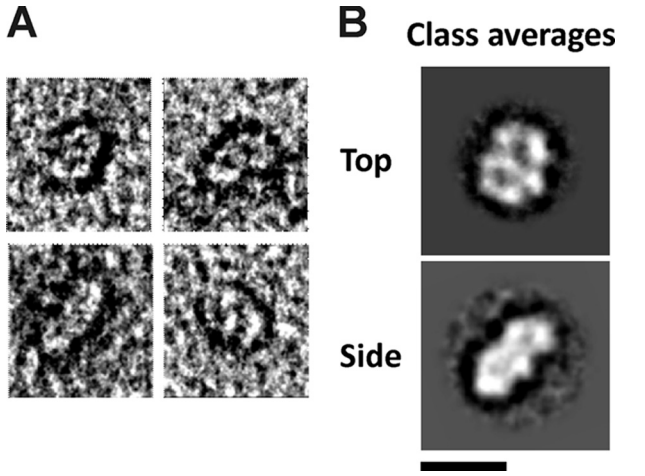

FIGURE 8. **Montage and class averages of multiringed TatE complex structures.** A range of multiringed structures was observed across multiple grids, and the majority of these structures consisted of two rings. Representative raw images are shown in *A*. Of these, the most homogeneous particles were averaged (*B*) to provide a top-down view (132 particles) and potential side view (95 particles). In the top-down view, two small but distinct pores are present, and these are occluded in the side view. The top-down view is ~6 nm wide, reduced to 5 nm for the side view. Both averages measure 10.5 nm in their longest dimension. The *scale bar* is 10 nm.

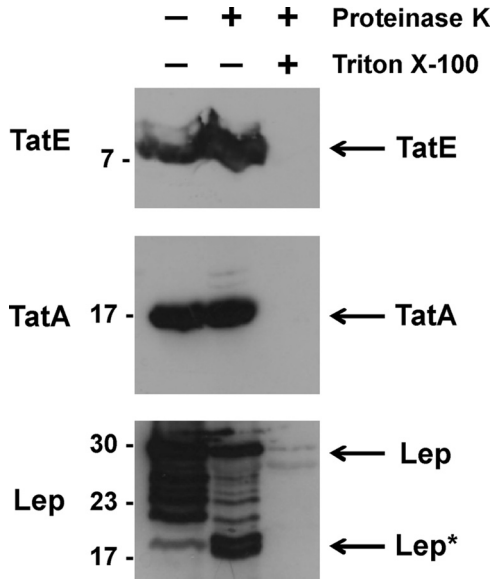

FIGURE 9. **Topological organization of TatE probed by protease accessibility assay.** Spheroplasts were prepared from *E. coli* Δ*tatAE* cells expressing TatE and TatA (from pBAD-E-Strep and pBAD-A-Strep plasmid, respectively) and leader peptidase (*Lep*) from (pRD8 plasmid) and subjected to proteinase K accessibility assay as described under "Experimental Procedures." Spheroplasts were incubated in presence of proteinase K and/or Triton X-100 where indicated. Samples were subjected to precipitation with trichloroacetic acid and then analyzed by immunoblotting using antibodies to the *Strep*-tag II™ on TatE and TatA (*panels TatE and TatA*) or an antiserum directed against the leader peptidase (*Lep panel*). *Lep** indicates the characteristic degradation product formed by digestion of the periplasmic domain of membrane-embedded leader peptidase by proteinase K. Mobilities of molecular mass markers (in kDa) are indicated on the *left*. Mobilities of TatE, TatA, and leader peptidase are also indicated.

ence-free alignment. This alignment was then refined using the class average as a final reference.

These larger particles appear to sit in two preferred orientations, a clear top-down view (as seen for the single-ringed particles) and a potential side view where the central pore or cleft is occluded. These larger structures were observed across a range of samples and grids and appear to represent a significant subset of the particles (~20% of the initial particle set). The majority of this set consisted of two rings with a small number showing three potential rings. Dilution of the sample (1:2 and 1:5) did not remove these multiple-ringed structures, suggesting that they are not attributable to crowding on the grid. The class average of the most homogeneous set of particles with two-ringed structures shows a complex of 6 by 10.5 nm, as shown in Fig. 8. Crude size estimations based on a low resolution three-dimensional model of this class, contoured to the dimensions of the two-dimensional average, give a molecular mass of ~120 kDa. This correlates with the uppermost band seen using BN gel electrophoresis (Fig. 4) and is approximately twice the size of the single-ring structures (68–90 kDa). The existence of multiringed forms of TatE may be relevant for the mechanism of pore formation because they show that the purified TatE complexes are capable of associating to form larger structures (see below). Interestingly, these larger structures still show two small and distinct pores. The cellular relevance of this phenomenon remains to be established in future studies.

Topological Orientation of TatE—As mentioned above, the TatE three-dimensional density map shows a cylindrical ring with additional protein density forming a potential lid covering the central channel at one end only. To assess whether the lid is located at the cytoplasmic or periplasmic side of the membrane, we attempted to determine the topological organization of TatE using protease accessibility measurements. Spheroplasts were prepared from *E. coli* Δ*tatAE* cells expressing TatE from the plasmid pBAD-E-Strep and were subjected to proteinase K treatment. The fate of TatE was assessed by immunoblotting. TatE was insensitive to proteinase K treatment (Fig. 9), which suggests that TatE is not accessible from the periplasmic side of

the membrane. As has been shown previously (36), TatA is not accessible from the periplasmic side of the membrane either (Fig. 9, *center panel*). Control experiments demonstrate that permeabilization of the spheroplast membrane with the detergent Triton X-100 renders both TatE and TatA susceptible to digestion by proteinase K. As a control for the efficacy of the proteinase K treatment, we tested for degradation of the periplasmic loop of leader peptidase as demonstrated previously (37). The data in Fig. 9 show the appearance of characteristic degradation products when proteinase K is incubated with the spheroplasts. These results suggest that the bulk of TatE is present in the cytoplasm, as shown for TatA, which would place a potential lid in the TatE structure on the cytoplasmic side of the membrane. However, this point requires further analysis because we cannot be certain that TatE does not contain a periplasmic domain that is insensitive to proteinase K in the absence of Triton.

DISCUSSION

The mechanism of the Tat system is still poorly understood in many respects, but a series of studies indicates the possibility of distinct roles for the separate TatABC and TatA complexes that are found at the steady state. There is clear evidence that, in both plant thylakoid and *E. coli* systems, the TatABC complex has a role in substrate binding. These subunits have been shown to cross-link to *in vitro*-synthesized substrates under conditions that promote binding but not translocation (9), and a TatBC complex has been purified with one or two substrate molecules bound to it after overexpression of substrates in the absence of TatA (38). In contrast, the TatA complex appears only to become involved after this initial substrate binding step (12).

Several lines of evidence have suggested that the TatA complex either forms the entire translocation channel, or at the very least, contributes the bulk of the channel. EM images of *E. coli* TatA complexes show the presence of potential channels (11) with a possible lid structure that could serve to seal the channel until the appropriate time. *E. coli* TatA complexes are furthermore present in a large range of sizes when purified (10, 11), and it was suggested that this could facilitate the transport of a wide range of substrate sizes. On the basis of these data, it has become widely accepted that the function of TatA is to generate the translocation pore for folded proteins, and this general model has been discussed in several reviews (*e.g.* Ref. 2). Key factors in the above model are the size and heterogeneity of the apparent channels in the EM images. The largest class of TatA complex had a diameter of 13.5 nm and a potential channel diameter of 6.5–7 nm, large enough to accommodate the largest Tat substrates, including TorA. The heterogeneity, on the other hand, appeared to provide a means of transporting Tat substrates of widely varying mass and shape. Thus, at the point of translocation, the full Tat translocase would exist in a series of size forms, dictated by the size of the TatA complex that was involved.

Our studies on TatE complexes are not consistent with this model. Previous studies have shown that TatE can complement the Δ*tatA* mutant (15), and in this study, we have confirmed that overexpressed TatE facilitates the efficient transport of several Tat substrates, including TorA, in the absence of TatA. However, the physicochemical/structural properties of isolated TatE complexes are very different from those of TatA complexes. Gel filtration studies show that TatE elutes as a smaller, more homogeneous set of complexes with an average size of ~130 kDa. However, this includes the detergent micelle, and more accurate BN studies suggest the presence of 2–3 complex types with sizes in the 50–110-kDa range. EM analysis has enabled us to derive three-dimensional models for the two primary TatE forms, although we stress that the small size of the complexes places them on the lower limit for accurate characterization by EM. Overall, single-ring TatE complexes are even smaller than the very smallest class of TatA complex analyzed to date (class 1 in Ref. 11), which had a diameter of 8.5–9 nm and a potential channel diameter of 3–3.5 nm. It should be emphasized that although TatE is overexpressed in this study, the pBAD vector directs only a moderate level of overexpression, and exactly the same expression system was previously used to characterize the large range of TatA complexes under essentially identical conditions (10). Moreover, the TatE complexes have exhibited the same characteristics after expression for short times or after purification in a range of different detergents. There has been no evidence for the presence of larger TatE complexes under any of these conditions, and we have therefore concluded that the smaller size of solubilized/purified TatE is likely to reflect the natural state of the complex.

TatE complexes do resemble smaller TatA complexes in some respects, and they likewise appear to possess a central cavity that is accessed from one side of the membrane. The N-terminal periplasmic region of TatA (and TatE) comprises only a few residues, and it is therefore highly likely that the potential lid is on the cytoplasmic face of the complex, where it may function to prevent leakage of small molecules. Proteinase K digestion studies support this idea. Overall, however, two important points emerge from the combined biochemical/structural studies.

The first is that the small sizes of TatE complexes appear to preclude a role in forming the entire translocation channel, or even the bulk thereof. One alternative possibility is that the TatABC complex forms the primary translocation channel and that TatA/E serves to activate it. The size of the TatABC complex, ~370 kDa in *E. coli* (10), is such that combination with even a small TatE complex could generate an active supercomplex of over 400 kDa, which may be more capable of forming a translocation channel for substrates of 90 kDa or more. Moreover, there is evidence from the thylakoid Tat system that TatC is actively involved in the actual translocation event because substrate molecules that are covalently cross-linked to TatC on the stromal side can be subsequently transported to the lumenal side (39).

More generally, the data are consistent with a model for Tat function that is radically different from currently favored models. The observed heterogeneity of TatA has prompted models that involve recruitment of one variant of TatA complex, from a spectrum of size classes, to match the size of the substrate being translocated. In contrast, the observation of such a limited range of TatE forms (only two major classes) is consistent with a model in which a much more discrete form of Tat trans-

locase is sufficiently flexible to transport a wide range of substrates. Further study is of course required to test this model.

A second model involves a different scenario; multiple TatA/E complexes bind to the TatABC complex once substrate has been bound. This would have the advantage of providing flexibility of pore size, with differing numbers of TatA/E complex generating translocation channels of differing diameters (the same role proposed for the variability of TatA complexes). The multiringed structures of TatE that we have observed would support this modular interaction of smaller rings to produce a larger superstructure. The simpler scenario, involving the assembly of only one or two defined translocases, may be more logical, but this model again deserves further consideration.

Acknowledgments—We are grateful to Ian Portman for technical help with electron microscopy and to the Wellcome Trust for generous support (Grant 055663/Z/98/Z) to the Imaging Suite at the University of Warwick. We thank Dr. James P Barnett for advice and useful discussions and Professor Gunner Von Heijne for providing the leader peptidase expression plasmid and anti-leader peptidase antiserum.

REFERENCES

1. Robinson, C., Matos, C. F., Beck, D., Ren, C., Lawrence, J., Vasisht, N., and Mendel, S. (2011) Transport and proofreading of proteins by the twin-arginine translocation (Tat) system in bacteria. *Biochim. Biophys. Acta* **1808,** 876–884
2. Müller, M., and Klösgen, R. B. (2005) The Tat pathway in bacteria and chloroplasts (review). *Mol. Membr. Biol.* **22,** 113–121
3. Chaddock, A. M., Mant, A., Karnauchov, I., Brink, S., Herrmann, R. G., Klösgen, R. B., and Robinson, C. (1995) A new type of signal peptide: central role of a twin-arginine motif in transfer signals for the delta pH-dependent thylakoidal protein translocase. *EMBO J.* **14,** 2715–2722
4. Stanley, N. R., Palmer, T., and Berks, B. C. (2000) The twin-arginine consensus motif of Tat signal peptides is involved in Sec-independent protein targeting in *Escherichia coli*. *J. Biol. Chem.* **275,** 11591–11596
5. Sargent, F., Bogsch, E. G., Stanley, N. R., Wexler, M., Robinson, C., Berks, B. C., and Palmer, T. (1998) Overlapping functions of components of a bacterial Sec-independent protein export pathway. *EMBO J.* **17,** 3640–3650
6. Bogsch, E. G., Sargent, F., Stanley, N. R., Berks, B. C., Robinson, C., and Palmer, T. (1998) An essential component of a novel bacterial protein export system with homologues in plastids and mitochondria. *J. Biol. Chem.* **273,** 18003–18006
7. Weiner, J. H., Bilous, P. T., Shaw, G. M., Lubitz, S. P., Frost, L., Thomas, G. H., Cole, J. A., and Turner, R. J. (1998) A novel and ubiquitous system for membrane targeting and secretion of cofactor-containing proteins. *Cell* **93,** 93–101
8. Bolhuis, A., Mathers, J. E., Thomas, J. D., Barrett, C. M., and Robinson, C. (2001) TatB and TatC form a functional and structural unit of the twin-arginine translocase from *Escherichia coli*. *J. Biol. Chem.* **276,** 20213–20219
9. Alami, M., Lüke, I., Deitermann, S., Eisner, G., Koch, H. G., Brunner, J., and Müller, M. (2003) Differential interactions between a twin-arginine signal peptide and its translocase in *Escherichia coli*. *Mol. Cell* **12,** 937–946
10. Oates, J., Barrett, C. M., Barnett, J. P., Byrne, K. G., Bolhuis, A., and Robinson, C. (2005) The *Escherichia coli* twin-arginine translocation apparatus incorporates a distinct form of TatABC complex, spectrum of modular TatA complexes and minor TatAB complex. *J. Mol. Biol.* **346,** 295–305
11. Gohlke, U., Pullan, L., McDevitt, C. A., Porcelli, I., de Leeuw, E., Palmer, T., Saibil, H. R., and Berks, B. C. (2005) The TatA component of the twin-arginine protein transport system forms channel complexes of variable diameter. *Proc. Natl. Acad. Sci. U.S.A.* **102,** 10482–10486
12. Mori, H., and Cline, K. (2002) A twin-arginine signal peptide and the pH gradient trigger reversible assembly of the thylakoid ΔpH/Tat translocase. *J. Cell Biol.* **157,** 205–210
13. Yen, M. R., Tseng, Y. H., Nguyen, E. H., Wu, L. F., and Saier, M. H., Jr. (2002) Sequence and phylogenetic analyses of the twin-arginine targeting (Tat) protein export system. *Arch. Microbiol.* **177,** 441–450
14. Ikeda, M., and Nakagawa, S. (2003) The *Corynebacterium glutamicum* genome: features and impacts on biotechnological processes. *Appl. Microbiol. Biotechnol.* **62,** 99–109
15. Sargent, F., Stanley, N. R., Berks, B. C., and Palmer, T. (1999) Sec-independent protein translocation in *Escherichia coli*: a distinct and pivotal role for the TatB protein. *J. Biol. Chem.* **274,** 36073–36082
16. Jack, R. L., Sargent, F., Berks, B. C., Sawers, G., and Palmer, T. (2001) Constitutive expression of *Escherichia coli* tat genes indicates an important role for the twin-arginine translocase during aerobic and anaerobic growth. *J. Bacteriol.* **183,** 1801–1804
17. Heikkilä, M. P., Honisch, U., Wunsch, P., and Zumft, W. G. (2001) Role of the Tat transport system in nitrous oxide reductase translocation and cytochrome cd1 biosynthesis in *Pseudomonas stutzeri*. *J. Bacteriol.* **183,** 1663–1671
18. Beloin, C., Valle, J., Latour-Lambert, P., Faure, P., Kzreminski, M., Balestrino, D., Haagensen, J. A., Molin, S., Prensier, G., Arbeille, B., and Ghigo, J. M. (2004) Global impact of mature biofilm lifestyle on *Escherichia coli* K-12 gene expression. *Mol. Microbiol.* **51,** 659–674
19. Casadaban, M. J., and Cohen, S. N. (1979) Lactose genes fused to exogenous promoters in one step using a Mu-lac bacteriophage: *in vivo* probe for transcriptional control sequences. *Proc. Natl. Acad. Sci. U.S.A.* **76,** 4530–4533
20. Wexler, M., Sargent, F., Jack, R. L., Stanley, N. R., Bogsch, E. G., Robinson, C., Berks, B. C., and Palmer, T. (2000) TatD is a cytoplasmic protein with DNase activity: no requirement for TatD family proteins in sec-independent protein export. *J. Biol. Chem.* **275,** 16717–16722
21. Warren, G., Oates, J., Robinson, C., and Dixon, A. M. (2009) Contributions of the transmembrane domain and a key acidic motif to assembly and function of the TatA complex. *J. Mol. Biol.* **388,** 122–132
22. Dalbey, R. E., and Wickner, W. (1985) Leader peptidase catalyzes the release of exported proteins from the outer surface of the *Escherichia coli* plasma membrane. *J. Biol. Chem.* **260,** 15925–15931
23. Silvestro, A., Pommier, J., Pascal, M. C., and Giordano, G. (1989) The inducible trimethylamine *N*-oxide reductase of *Escherichia coli* K12: its localization and inducers. *Biochim. Biophys. Acta* **999,** 208–216
24. Frank, J., Radermacher, M., Penczek, P., Zhu, J., Li, Y., Ladjadj, M., and Leith, A. (1996) SPIDER and WEB: processing and visualization of images in three-dimensional electron microscopy and related fields. *J. Struct. Biol.* **116,** 190–199
25. Shaikh, T. R., Gao, H., Baxter, W. T., Asturias, F. J., Boisset, N., Leith, A., and Frank, J. (2008) SPIDER image processing for single-particle reconstruction of biological macromolecules from electron micrographs. *Nat. Protoc.* **3,** 1941–1974
26. Mindell, J. A., and Grigorieff, N. (2003) Accurate determination of local defocus and specimen tilt in electron microscopy. *J. Struct. Biol.* **142,** 334–347
27. White, H. E., Saibil, H. R., Ignatiou, A., and Orlova, E. V. (2004) Recognition and separation of single particles with size variation by statistical analysis of their images. *J. Mol. Biol.* **336,** 453–460
28. Penczek, P., Radermacher, M., and Frank, J. (1992) Three-dimensional reconstruction of single particles embedded in ice. *Ultramicroscopy* **40,** 33–53
29. Jones, D. T. (1999) Protein secondary structure prediction based on position-specific scoring matrices. *J. Mol. Biol.* **292,** 195–202
30. Hu, Y., Zhao, E., Li, H., Xia, B., and Jin, C. (2010) Solution NMR structure of the TatA component of the twin-arginine protein transport system from gram-positive bacterium *Bacillus subtilis*. *J. Am. Chem. Soc.* **132,** 15942–15944
31. Walther, T. H., Grage, S. L., Roth, N., and Ulrich, A. S. (2010) Membrane alignment of the pore-forming component TatA(d) of the twin-arginine translocase from *Bacillus subtilis* resolved by solid-state NMR spectros-

copy. *J. Am. Chem. Soc.* **132,** 15945–15956
32. Bernhardt, T. G., and de Boer, P. A. (2003) The *Escherichia coli* amidase AmiC is a periplasmic septal ring component exported via the twin-arginine transport pathway. *Mol. Microbiol.* **48,** 1171–1182
33. Ize, B., Stanley, N. R., Buchanan, G., and Palmer, T. (2003) Role of the *Escherichia coli* Tat pathway in outer membrane integrity. *Mol. Microbiol.* **48,** 1183–1193
34. Schägger, H., and von Jagow, G. (1991) Blue native electrophoresis for isolation of membrane protein complexes in enzymatically active form. *Anal. Biochem.* **199,** 223–231
35. Schägger, H., Cramer, W. A., and von Jagow, G. (1994) Analysis of molecular masses and oligomeric states of protein complexes by blue native electrophoresis and isolation of membrane protein complexes by two-dimensional native electrophoresis. *Anal. Biochem.* **217,** 220–230
36. Porcelli, I., de Leeuw, E., Wallis, R., van den Brink-van der Laan, E., de Kruijff, B., Wallace, B. A., Palmer, T., and Berks, B. C. (2002) Characterization and membrane assembly of the TatA component of the *Escherichia coli* twin-arginine protein transport system. *Biochemistry* **41,** 13690–13697
37. de Gier, J. W., Mansournia, P., Valent, Q. A., Phillips, G. J., Luirink, J., and von Heijne, G. (1996) Assembly of a cytoplasmic membrane protein in *Escherichia coli* is dependent on the signal recognition particle. *FEBS Lett.* **399,** 307–309
38. Tarry, M. J., Schäfer, E., Chen, S., Buchanan, G., Greene, N. P., Lea, S. M., Palmer, T., Saibil, H. R., and Berks, B. C. (2009) Structural analysis of substrate binding by the TatBC component of the twin-arginine protein transport system. *Proc. Natl. Acad. Sci. U.S.A.* **106,** 13284–13289
39. Gérard, F., and Cline, K. (2006) Efficient twin-arginine translocation (Tat) pathway transport of a precursor protein covalently anchored to its initial cpTatC-binding site. *J. Biol. Chem.* **281,** 6130–6135
40. Rubinstein, J. L. (2007) Structural analysis of membrane protein complexes by single particle electron microscopy. *Methods* **41,** 409–416

Applied and Environmental Microbiology

TatAc, the Third TatA Subunit of *Bacillus subtilis* , Can Form Active Twin-Arginine Translocases with the TatCd and TatCy Subunits

Carmine G. Monteferrante, Jacopo Baglieri, Colin Robinson and Jan Maarten van Dijl

Appl. Environ. Microbiol. **2012, 78(14):4999. DOI: 10.1128/AEM.01108-12.**
Published Ahead of Print 27 April 2012.

AEM
Journals.ASM.org

TatAc, the Third TatA Subunit of *Bacillus subtilis*, Can Form Active Twin-Arginine Translocases with the TatCd and TatCy Subunits

Carmine G. Monteferrante,[a] Jacopo Baglieri,[b] Colin Robinson,[b] and Jan Maarten van Dijl[a]

Department of Medical Microbiology, University of Groningen and University Medical Center Groningen, Groningen, the Netherlands,[a] and School of Life Sciences, University of Warwick, Coventry, United Kingdom[b]

Two independent twin-arginine translocases (Tat) for protein secretion were previously identified in the Gram-positive bacterium *Bacillus subtilis*. These consist of the TatAd-TatCd and TatAy-TatCy subunits. The function of a third TatA subunit named TatAc was unknown. Here, we show that TatAc can form active protein translocases with TatCd and TatCy.

Protein transport from the cytoplasm to different bacterial compartments or the external milieu is facilitated by dedicated molecular machines (6). Among these protein translocases, the twin-arginine translocases (Tat) stand out because they permit the passage of tightly folded proteins across the cytoplasmic membrane. The proteins translocated by Tat are synthesized with signal peptides that contain a well-conserved twin-arginine (RR) motif for specific targeting to a membrane-embedded Tat translocase (13, 17, 23). The Tat translocases of Gram-negative bacteria, such as *Escherichia coli*, are composed of three subunits named TatA, TatB, and TatC (4, 18). The formation of an active protein-conducting channel is believed to require the formation of a supercomplex composed of a TatABC heterotrimeric complex and homo-oligomeric TatA complexes (1, 8). In contrast, most Gram-positive bacteria possess minimized Tat translocases that contain only TatA and TatC subunits. Nevertheless, various studies indicate that these TatAC translocases employ a mechanism similar to that of the TatABC translocases of Gram-negative bacteria (10, 17).

The Gram-positive bacterium *Bacillus subtilis* is a well-known "cell factory" for secretory protein production (20, 21). In this organism, two Tat translocases are known to operate in parallel. The TatAdCd translocase consists of the TatAd and TatCd subunits, and the TatAyCy translocase consists of the TatAy and TatCy subunits (11, 12, 15). While the TatAdCd translocase is produced mainly under conditions of phosphate starvation (12, 14, 15), the TatAyCy translocase is expressed under all conditions tested (12, 14). Interestingly, *B. subtilis* produces a third TatA subunit named TatAc (12). The function of TatAc has remained enigmatic due to the fact that no phenotype was so far detectable for *tatAc* mutant *B. subtilis* cells (11, 12, 20). Therefore, the present studies were aimed at determining whether TatAc can actually form active translocases in combination with TatCd or TatCy. This possibility was tested by expressing the respective *tat* genes in *E. coli*, because the activity and assembly of *Bacillus* Tat translocases can be assayed more readily in this organism than in *B. subtilis* (2). For this purpose, the *tatAc* gene was amplified from the *B. subtilis* genome (GenBank/EMBL/DDBJ accession number AL009126) and cloned into plasmid pBAD24, resulting in pBAD-Ac. Next, the *tatCd* and *tatCy* genes were PCR amplified such that the respective proteins contain a C-terminal StrepII tag. The amplified *tatCd*-StrepII and *tatCy*-StrepII genes were cloned into pBAD-Ac, resulting in pBAD-AcCd-Strep and pBAD-AcCy-Strep, respectively. These vectors were subsequently used to transform *E. coli* Δ*tatABCDE* cells, which lack all *E. coli tat* genes. Next, the resulting strains were tested for their ability to transport the previously identified *E. coli* Tat substrates TorA, AmiA, and AmiC (3, 5, 9). To monitor TorA export to the periplasm, *E. coli* cells were grown anaerobically until mid-exponential growth phase, and these cells were then subjected to subcellular fractionation as previously described (16). The periplasmic, cytoplasmic, and membrane fractions thus obtained were separated on a 10% native polyacrylamide gel that was subsequently assayed for trimethylamine *N*-oxide (TMAO) reductase activity as described previously (5, 19). The results in Fig. 1 show that the Δ*tatABCDE* cells producing TatAc plus TatCd or TatAc plus TatCy were capable of transporting active TorA to the periplasm. In contrast, Δ*tatABCDE* cells expressing only *tatAc*, *tatCy*, or *tatCd* were not able to export active TorA to this subcellular location. This showed for the first time that TatAc was able to form active translocases in combination with TatCd or TatCy. To further investigate the activity of these translocases, we tested the export of AmiA and AmiC, which are both required for cell wall biosynthesis in *E. coli* (3, 9). Cells that do not export these molecules to the periplasm grow in long chains, as is observed for the *E. coli* Δ*tatABCDE* strain (Fig. 2A and B) (9). As shown by phase-contrast microscopy, the bacteria producing TatAc plus TatCd or TatAc plus TatCy showed the wild-type phenotype, although some slightly longer chains were still detectable (Fig. 2C and D). This is indicative of active export of AmiA and/or AmiC to the periplasm, providing further support for the idea that active TatAcCd and TatAcCy complexes can be formed in *E. coli*.

To demonstrate the formation of TatAcCd and TatAcCy complexes, a blue native (BN) PAGE analysis was performed. For this purpose, membranes were isolated from cells expressing TatCd-StrepII, TatCy-StrepII, TatAc-TatCd-StrepII, or TatAc-TatCy-StrepII. In addition, cells producing TatAc-StrepII from plasmid pBAD24 were included in the analyses. Upon solubilization in 2% digitonin, membrane proteins were separated by BN PAGE, fol-

Received 4 April 2012 **Accepted** 19 April 2012
Published ahead of print 27 April 2012
Address correspondence to Jan Maarten van Dijl, j.m.van.dijl01@umcg.nl.
C.G.M. and J.B. contributed equally to this work.

doi:10.1128/AEM.01108-12

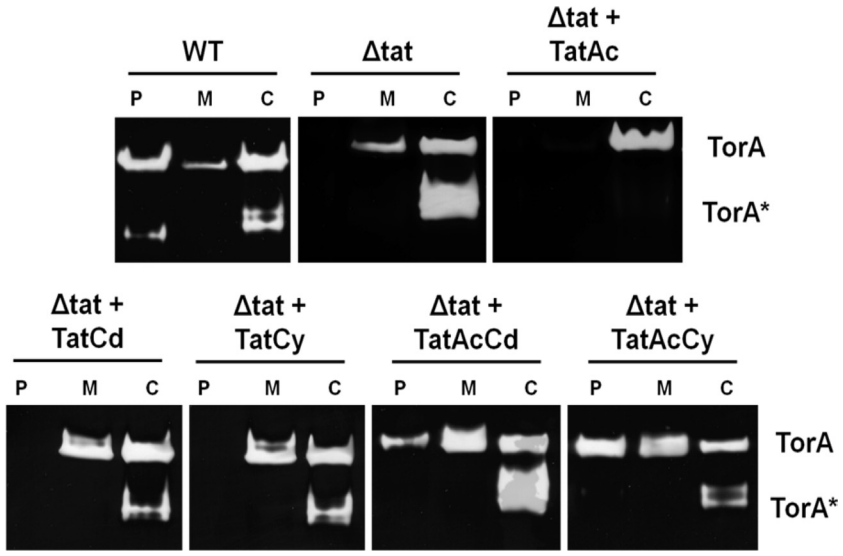

FIG 1 *B. subtilis* TatAcCd and TatAcCy facilitate TorA export in *E. coli*. Cells of *E. coli* Δ*tatABCDE* were subjected to subcellular fractionation. Proteins in the periplasmic (P), membrane (M), and cytoplasmic (C) fractions obtained were separated by native PAGE, and the gels were subsequently analyzed for TMAO reductase (TorA) activity. Strains used in this analysis were *E. coli* MC4100 (WT), *E. coli* Δ*tatABCDE* (Δtat), or *E. coli* Δ*tatABCDE* expressing *B. subtilis* TatAc from plasmid pBAD-Ac-Strep (Δtat + TatAc), *B. subtilis* TatCd from plasmid pBAD-Cd-Strep (Δtat + TatCd), *B. subtilis* TatCy from plasmid pBAD-Cy-Strep (Δtat + TatCy), *B. subtilis* TatAcCd from plasmid pBAD-AcCd-Strep (Δtat + TatAcCd), or *B. subtilis* TatAcCy from plasmid pBAD-AcCy-Strep (Δtat + TatAcCy). The position of active full-length TorA is indicated. TorA* indicates a faster-migrating form of TorA (22).

lowed by immunoblotting with antibodies against the StrepII tag. As shown in Fig. 3, TatCd-StrepII and TatCy-StrepII alone formed bands of ~66 kDa. In addition, TatCd-StrepII formed a minor band of ~100 kDa. TatAc-StrepII expressed by itself formed a small homogeneous complex of ~100 kDa. Importantly, when TatAc (nontagged) was coexpressed with either TatCd-StrepII or TatCy-StrepII, bands of ~230 kDa or ~200 kDa, respectively, were observed. This showed that TatAc does indeed form membrane-embedded complexes with TatCd and TatCy.

In conclusion, our present studies document for the first time that the hitherto enigmatic third TatA subunit of *B. subtilis* known as TatAc can engage in the formation of active TatAC-type trans-

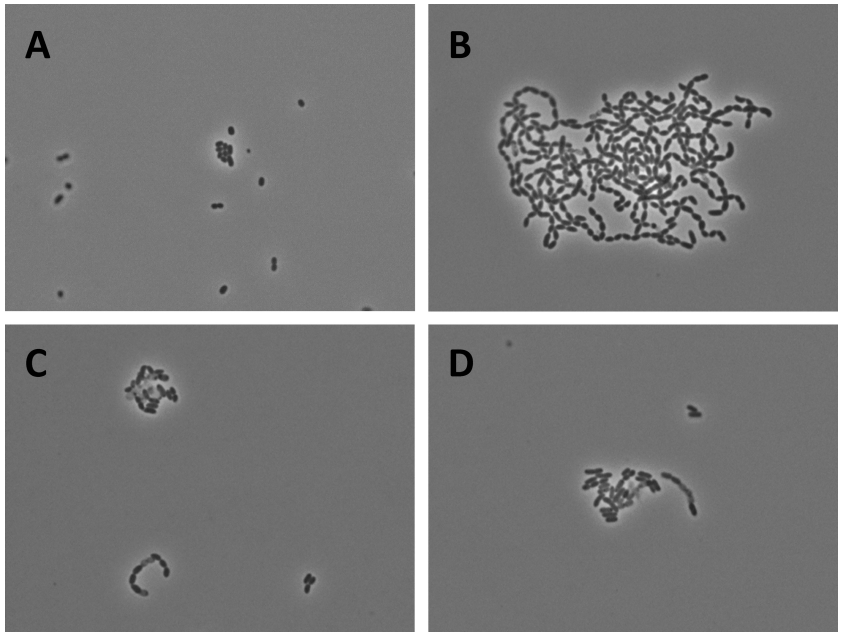

FIG 2 *B. subtilis* TatAcCd and TatAcCy facilitate AmiA and AmiC export in *E. coli*. The export of AmiA and AmiC in *E. coli* was assayed indirectly by assessing the chain length of exponentially growing cells. (A) *E. coli* MC4100 (WT); (B) *E. coli* Δ*tatABCDE* forms long chains due to the mislocalization of AmiA and AmiC (9); (C) *E. coli* Δ*tatABCDE* producing TatAcCd from plasmid pBAD-AcCd-Strep; (D) *E. coli* Δ*tatABCDE* producing TatAcCy from plasmid pBAD-AcCy-Strep. As evidenced by the significantly reduced chain length, the export of AmiA and AmiC in *E. coli* Δ*tatABCDE* is at least partially restored by the production of TatAcCd or TatAcCy.

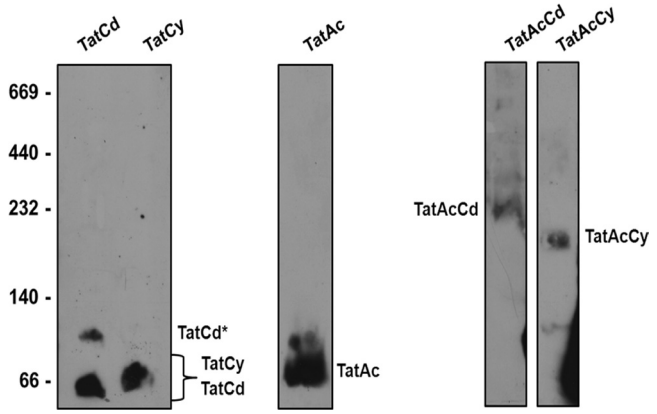

FIG 3 TatAcCd and TatAcCy form discrete complexes. To investigate complex formation, TatCd-StrepII, TatCy-StrepII, TatAc-StrepII, TatAc-TatCd-StrepII, or TatAc-TatCy-StrepII were expressed in *E. coli* Δ*tatABCDE*. Next, membranes from the respective cells were isolated. Membrane proteins were then solubilized in 2% digitonin and separated by blue native PAGE. The gels were immunoblotted using StrepII-specific antibodies and a secondary anti-mouse IgG-horseradish peroxidase conjugate. The EZ-ECL detection kit was used to visualize bound antibodies. The mobility of molecular mass markers (left panel) and StrepII-tagged proteins and complexes is indicated (kDa). TatCd* indicates a TatCd complex with higher molecular weight.

locases. The results also show that TatAc has no particular preference for partnering with TatCd or TatCy. It is noteworthy that the identified TatAcCd and TatAcCy complexes appear to be homogeneous and relatively small (~230 to 200 kDa). Interestingly, previous studies in *B. subtilis* have shown that the coexpression of TatAc and TatCd or TatAc and TatCy does not facilitate the export of the known Tat substrates PhoD and YwbN (7). Furthermore, a recent tiling array analysis across 104 conditions has shown that *tatAc* is expressed under most conditions (14). These previous observations together with our present findings suggest that TatAcCd and TatAcCy translocases could be involved in the specific export of as-yet-unidentified Tat substrates in *B. subtilis*. However, it has to be noted here that our present observations on TatAc function were made upon heterologous expression in *E. coli* and that it remains to be assessed whether TatAc fulfills the same functions in *B. subtilis*.

ACKNOWLEDGMENTS

We acknowledge Ewoud Reilman for his help with the microscopy.

C.G.M., J.B., C.R., and J.M.V.D. were supported through the CEU projects PITN-GA-2008-215524 and -244093 and the transnational SysMO projects BACELL SysMO 1 and 2 through the Research Council for Earth and Life Sciences of the Netherlands Organization for Scientific Research.

REFERENCES

1. **Baglieri J, Beck D, Vasisht N, Smith CJ, Robinson C.** 2012. Structure of the TatA paralog, TatE, suggests a structurally homogeneous form of Tat protein translocase that transports folded proteins of differing diameter. J. Biol. Chem. **287**:7335–7344.
2. **Barnett JP, et al.** 2009. The twin-arginine translocation (Tat) systems from *Bacillus subtilis* display a conserved mode of complex organization and similar substrate recognition requirements. FEBS J. **276**:232–243.
3. **Bernhardt TG, de Boer PA.** 2003. The *Escherichia coli* amidase AmiC is a periplasmic septal ring component exported via the twin-arginine transport pathway. Mol. Microbiol. **48**:1171–1182.
4. **Bogsch EG, et al.** 1998. An essential component of a novel bacterial protein export system with homologues in plastids and mitochondria. J. Biol. Chem. **273**:18003–18006.
5. **Bolhuis A, Mathers JE, Thomas JD, Barrett CML, Robinson C.** 2001. TatB and TatC form a functional and structural unit of the twin-arginine translocase from *Escherichia coli*. J. Biol. Chem. **276**:20213–20219.
6. **Desvaux M, Hébraud M, Talon R, Henderson IR.** 2009. Secretion and subcellular localizations of bacterial proteins: a semantic awareness issue. Trends Microbiol. **17**:139–145.
7. **Eijlander RT, Jongbloed JD, Kuipers OP.** 2009. Relaxed specificity of the *Bacillus subtilis* TatAdCd translocase in Tat-dependent protein secretion. J. Bacteriol. **191**:196–202.
8. **Gohlke U, et al.** 2005. The TatA component of the twin-arginine protein transport system forms channel complexes of variable diameter. Proc. Natl. Acad. Sci. U. S. A. **102**:10482–10486.
9. **Ize B, Stanley NR, Buchanan G, Palmer T.** 2003. Role of the *Escherichia coli* Tat pathway in outer membrane integrity. Mol. Microbiol. **48**:1183–1193.
10. **Jongbloed JDH, van der Ploeg R, van Dijl JM.** 2006. Bifunctional TatA subunits in minimal Tat protein translocases. Trends Microbiol. **14**:2–4.
11. **Jongbloed JDH, et al.** 2004. Two minimal Tat translocases in *Bacillus*. Mol. Microbiol. **54**:1319–1325.
12. **Jongbloed JDH, et al.** 2000. TatC is a specificity determinant for protein secretion via the twin-arginine translocation pathway. J. Biol. Chem. **275**:41350–41357.
13. **Jongbloed JDH, et al.** 2002. Selective contribution of the twin-arginine translocation pathway to protein secretion in *Bacillus subtilis*. J. Biol. Chem. **277**:44068–44078.
14. **Nicolas P, et al.** 2012. Condition-dependent transcriptome reveals high-level regulatory architecture in *Bacillus subtilis*. Science **335**:1103–1106.
15. **Pop O, Martin U, Abel C, Müller JP.** 2002. The twin-arginine signal peptide of PhoD and the TatAd/Cd proteins of *Bacillus subtilis* form an autonomous Tat translocation system. J. Biol. Chem. **277**:3268–3273.
16. **Randall LL, Hardy SJ.** 1986. Correlation of competence for export with lack of tertiary structure of the mature species: a study *in vivo* of maltose-binding protein in *E. coli*. Cell **46**:921–928.
17. **Robinson C, et al.** 2011. Transport and proofreading of proteins by the twin-arginine translocation (Tat) system in bacteria. Biochim. Biophys. Acta **1808**:876–884.
18. **Sargent F, et al.** 1998. Overlapping functions of components of a bacterial Sec-independent protein export pathway. EMBO J. **17**:3640–3650.
19. **Silvestro A, Pommier J, Pascal MC, Giordano G.** 1989. The inducible trimethylamine N-oxide reductase of *Escherichia coli* K12: its localization and inducers. Biochim. Biophys. Acta **999**:208–216.
20. **Tjalsma H, Bolhuis A, Jongbloed JD, Bron S, van Dijl JM.** 2000. Signal peptide-dependent protein transport in *Bacillus subtilis*: a genome-based survey of the secretome. Microbiol. Mol. Biol. Rev. **64**:515–547.
21. **Tjalsma H, et al.** 2004. Proteomics of protein secretion by *Bacillus subtilis*: separating the "secrets" of the secretome. Microbiol. Mol. Biol. Rev. **68**:207–233.
22. **Warren G, Oates J, Robinson C, Dixon AM.** 2009. Contributions of the transmembrane domain and a key acidic motif to assembly and function of the TatA complex. J. Mol. Biol. **388**:122–132.
23. **Yuan J, Zweers JC, van Dijl JM, Dalbey RE.** 2010. Protein transport across and into cell membranes in bacteria and archaea. Cell. Mol. Life Sci. **67**:179–199.

Journal of Experimental Botany, Vol. 63, No. 4, pp. 1689–1698, 2012
doi:10.1093/jxb/err444 Advance Access publication 24 January, 2012

Journal of Experimental Botany
www.jxb.oxfordjournals.org

REVIEW PAPER

Targeting of lumenal proteins across the thylakoid membrane

Anna M. Albiniak*, Jacopo Baglieri* and Colin Robinson†

School of Life Sciences, University of Warwick, Coventry CV4 7AL, UK

* These authors contributed equally to this work.
† To whom correspondence should be addressed. E-mail: colin.robinson@warwick.ac.uk

Received 28 August 2011; Revised 6 December 2011; Accepted 9 December 2011

Abstract

The biogenesis of the plant thylakoid network is an enormously complex process in terms of protein targeting. The membrane system contains a large number of proteins, some of which are synthesized within the organelle, while many others are imported from the cytosol. Studies in recent years have shown that the targeting of imported proteins into and across the thylakoid membrane is particularly complex, with four different targeting pathways identified to date. Two of these are used to target membrane proteins: a signal recognition particle (SRP)-dependent pathway and a highly unusual pathway that appears to require none of the known targeting apparatus. Two further pathways are used to translocate lumenal proteins across the thylakoid membrane from the stroma and, again, the two pathways differ dramatically from each other. One is a Sec-type pathway, in which ATP hydrolysis by SecA drives the transport of the substrate protein through the membrane in an unfolded conformation. The other is the twin-arginine translocation (Tat) pathway, where substrate proteins are transported in a folded state using a unique mechanism that harnesses the proton motive force across the thylakoid membrane. This article reviews progress in studies on the targeting of lumenal proteins, with reference to the mechanisms involved, their evolution from endosymbiotic progenitors of the chloroplast, and possible elements of regulation.

Key words: Protein targeting, Sec, signal peptide, Tat, thylakoid.

Introduction

Chloroplasts are organelles that are best known as the site of photosynthesis and other important biochemical processes in plant cells. They are believed to originate from photosynthetic bacteria and they have a complex structure. In addition to the inner and outer membranes of the envelope, chloroplasts contain an abundant internal thylakoid membrane system which carries out, for example, the critical processes of light capture, electron transport, and photophosphorylation. These membranes enclose three internal compartments: the intermembrane space, stroma, and thylakoid lumen.

Although the chloroplast has its own genome, the majority of chloroplast proteins is encoded by the nuclear genome and post-translationally transported into chloroplasts by a common import apparatus, namely the TOC/TIC (translocon at the outer/inner envelope membrane of chloroplasts) complex (reviewed in Schnell *et al.*, 1997; Abdallah *et al.*, 2000; Soll and Schleiff, 2004; Aronsson and Jarvis, 2009). This system imports proteins in an unfolded state at so-called 'contact sites' between the two membranes (Jarvis and Soll, 2001), after which the substrates refold in the stroma. Many imported proteins function in the stroma, and their biogenesis is thus essentially complete at that point. However, a large number of proteins are further targeted into the thylakoid network—either into the membrane, or across the membrane into the lumenal space. In recent years, it has become clear that this protein trafficking is highly organized, with at least four separate pathways operating for the targeting of thylakoid proteins.

To date, it seems that integral membrane proteins are inserted into thylakoids by two very different pathways. A subset of proteins, namely the abundant light-harvesting

chlorophyll-binding proteins (LHCPs) are inserted by a pathway that requires the action of a chloroplast signal recognition particle (cpSRP) and FtsY in the stroma, together with a protein termed Alb3 in the thylakoid membrane (Bals *et al.*, 2010). This pathway is related to the SRP pathway of bacteria, which is used for the insertion of almost all inner membrane proteins (at least in the best studied example, *Escherichia coli*). The similarity is perhaps unsurprising, given the endosymbiotic origin of chloroplasts, yet the biogenesis of thylakoid membrane proteins differs in one key respect because most of the remaining thylakoid membrane proteins are inserted by a completely different pathway that does not involve SRP or Alb3, or indeed any known targeting apparatus (Woolhead *et al.*, 2001).

Two further pathways are used for the targeting of soluble proteins into the lumenal space, and this review will focus on these topics. These substrates are invariably synthesized in the cytosol with bipartite N-terminal presequences which contain two targeting signals in tandem. Once in the stroma, the first envelope transit domain of the presequence is removed by stromal processing peptidase (SPP). This leads to the exposure of a thylakoid signal peptide, forming a stromal intermediate which is transported across the thylakoid membrane and processed by the thylakoid processing peptidase (TPP). The generalized system for the targeting of lumenal proteins is summarized in Fig. 1.

It is the thylakoid signal peptide that largely dictates which route is followed. A subset of lumenal proteins is transported in an unfolded state by a Sec-type pathway (cpSec), whereas others are transported by the Tat pathway (cpTat) that appears to function primarily in the transport of fully-folded proteins. This unusual trait has been in the centre of much interest since its discovery.

Tat systems have now been characterized in a wide variety of bacterial species. Interestingly, unlike the Sec pathway, Tat system transports proteins by a mechanism that does not require nucleoside triphosphatases (NTPs), but which relies totally on the ΔpH across the thylakoid membrane (Cline *et al.*, 1992; Mould and Robinson, 1991). The aim of this review is to present recent progress on thylakoid Sec and Tat systems in plants and bacteria, highlighting new discoveries about their structure, function and regulation. Particular emphasis will be placed on the Tat pathway.

The Sec pathway

Sec systems are evolutionarily conserved protein translocation machineries that are present in the eukaryotic endoplasmic reticulum (Osborne *et al.*, 2005), the archaeal plasma membrane (Bolhuis, 2004), the eubacterial plasma membrane (Dalbey and Chen, 2004; Veenendaal *et al.*, 2004; Vrontou and Economou, 2004), and the thylakoid membranes of plant and algal chloroplasts. A common mechanistic feature of all Sec systems is that the substrates are transported in an unfolded conformation through a protein-conducting channel. In bacteria, much work has been performed in order to characterize the Sec pathway, whereas our knowledge of the cpSec pathway is limited, with current models being mainly based on homology to the bacterial general secretory pathway. In *E. coli*, the Sec translocon consists minimally of SecA, SecE, and SecY (Akimaru *et al.*, 1991). The signal peptide of the preprotein substrate binds post-translationally to the SecA ATPase in the cytoplasm. The SecA-preprotein complex couples with the Sec core components consisting of the integral membrane proteins SecY and SecE which are thought to form the key parts of the Sec protein conducting channel, and SecG is also part of a well-characterized SecYEG translocon. A SecDF ancillary complex is found associated with the SecYEG complex in the membrane, although its precise function is rather unclear (Nouwen *et al.*, 2005). SecA, through a cycle of ATP binding hydrolysis and release, drives the translocation of the precursor trough the SecYEG pore (Dalbey and Chen, 2004). In chloroplasts, homologues to SecA (cpSecA), SecY (cpSecY), and SecE (cpSecE) have been identified (Nakai *et al.*, 1994; Yuan *et al.*, 1994; Laidler *et al.*, 1995; Roy and Barkan, 1998; Schuenemann *et al.*, 1999) but several components of the bacterial Sec pathway (SecB, SecG, and SecD/F) have not been identified. Studies show that thylakoid cpSecA/cpSecYE works similarly to the *E. coli* system, for example, the translocation step across thylakoid membranes is dependent on ATP and it is inhibited by the SecA inhibitor azide (Hulford *et al.*, 1994; Yuan *et al.*, 1994; Haward *et al.*, 1997). Moreover antibodies against cpSecY prevent cpSecA-dependent protein translocation, suggesting that, as the bacterial counterparts, cpSecY and cpSecA work in concert (Mori *et al.*, 1999).

Interestingly it has been shown that cpSecA ATPase activity is stimulated by cpSec-dependent thylakoid signal peptides, but not by *E. coli* signal peptides, and that stimulation of cpSecA ATPase activity exhibits specific lipid requirements that differ from those of *E. coli* SecA (Sun *et al.*, 2007). Recently, it has been shown that cpSecA is essential for photosynthetic development in *Arabidopsis,* because its absence can lead to severe defects in chloroplast sub-organelle structure and function (Liu *et al.*, 2010). The inability of the cpSec translocon to transport dihydrofolate reductase (DHFR), in a methotrexate-stabilized folded conformation, demonstrates that the cpSec pathway, similar to bacteria, requires protein substrates to be in an unfolded state for transport (Hynds *et al.*, 1998; Marques *et al.*, 2004). In chloroplasts, there is no homologue of the bacterial cytosolic chaperone SecB, which is dedicated to preventing folding of Sec substrates, thus the stromal factors necessary to maintain cpSec pre-proteins in an unfolded state remain unknown.

In summary, it appears that the cpSec system is something of a slimmed-down, 'minimal' Sec-type system that lacks many of the non-essential components found in *E. coli*. In general, however, the available evidence suggests that it operates by a broadly similar mechanism. These similarities and differences are shown in Fig. 2, which

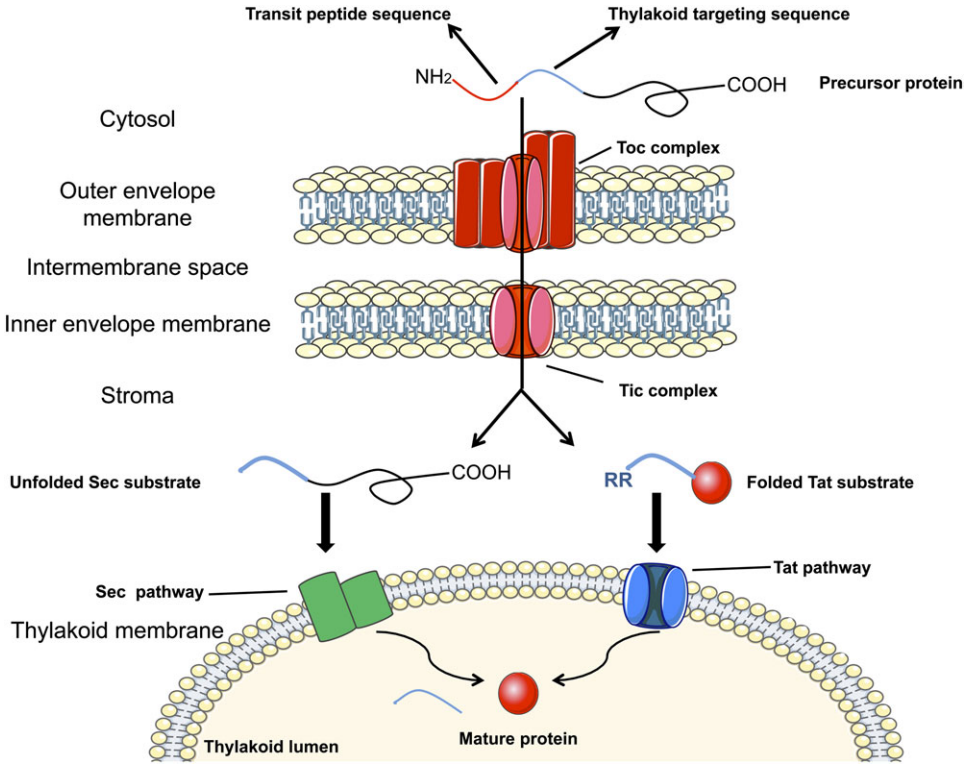

Fig. 1. Targeting of proteins to the chloroplast thylakoid lumen. The diagram illustrates the basic features of the pathways used for transporting proteins from the cytosol to the thylakoid lumen. Lumenal proteins are synthesized with bipartite N-terminal signal peptides, depicted as red and blue lines. The precursor protein is transported into the stroma in an unfolded conformation by the Toc and Tic complexes in the outer and inner membranes, respectively. Following import, the N-terminal stroma-targeting sequence (red line) is removed by a stromal processing peptidase; this exposes the second, thylakoid-targeting signal peptide (blue line) with its distinctive twin arginine motif (RR). Tat substrates are translocated in a fully folded form and following the translocation via thylakoid membrane, the signal peptide is removed by the thylakoid processing peptidase.

reviews the basic structures of the *E. coli* and cpSec systems.

The Tat system in bacteria

While the primary focus of this article is on the thylakoid Tat system, it is useful and interesting to discuss Tat systems in bacteria. The bacterial Tat system is responsible for the export of a number of proteins to the periplasm, outer membrane or growth medium. As with thylakoidal Tat substrates, bacterial Tat substrates bear cleavable N-terminal signal peptides containing a critical and highly conserved twin-arginine motif within the consensus sequence (Chaddock *et al.*, 1995; Stanley *et al.*, 2000). The systems's most notable attribute is an ability to transport large folded proteins across the tightly sealed plasma membrane (reviewed in Müller and Klösgen, 2005; Robinson *et al.*, 2011) and many Tat substrates are cofactor-containing redox enzymes involved in anaerobic respiratory pathways.

In *E. coli* and many other Gram-negative bacteria, the minimal set of components required for Tat-dependent translocation are three integral membrane proteins, TatA, TatB, and TatC, encoded by the *tatABC* operon, with molecular masses of 10, 18, and 30 kDa, respectively (Bogsch *et al.*, 1998; Sargent *et al.*, 1998; Weiner *et al.*, 1998). These subunits are found in two types of complex within the plasma membrane: a substrate-binding TatABC complex of ~ 370 kDa, and separate TatA homo-oligomeric complexes ranging from ~ 50 kDa to over 500 kDa (Bolhuis *et al.*, 2001; Alami *et al.*, 2003; Oates *et al.*, 2005). It has been suggested that these TatA complexes may form pores of different sizes which match the varying dimensions of Tat substrates (Gohlke *et al.*, 2005; Oates *et al.*, 2005). Several studies favour a model in which these complexes transiently coalesce to generate the full translocase (Mori and Cline, 2002). In a recent study, using a genetic fusion approach, it has been suggested that the functional unit of TatC is a dimer and that only one functional TatC within the dimeric unit is sufficient for Tat transport activity, thus supporting the idea that there is an even number of TatC protomers in the TatBC complex (Maldonado *et al.*, 2011).

Interestingly, most Gram-positive organisms possess a simpler 'minimalist' Tat system which lacks a TatB component (Jongbloed *et al.*, 2004) and contains instead a bifunctional TatA component (Jongbloed *et al.*, 2006). In *Bacillus subtilis*, two TatAC-type systems, TatAdCd and TatAyCy, operate in parallel with different substrate specificity (Jongbloed *et al.*, 2006). Again, two complexes

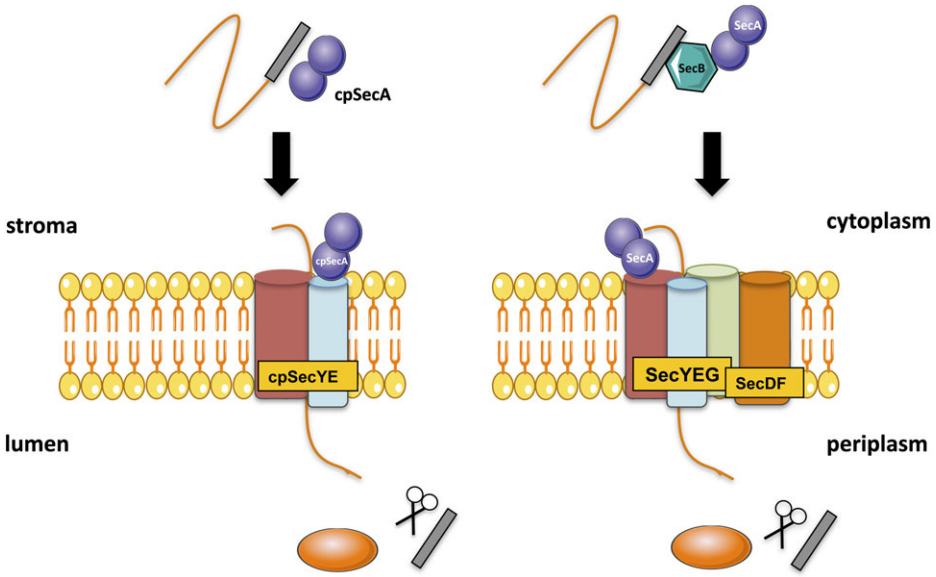

Fig. 2. Basic structures of the *E. coli* and thylakoid Sec systems. A common mechanistic feature of all Sec systems is that the substrates are transported in an unfolded conformation through a protein-conducting channel. In thylakoids (left panel), the Sec transport minimally involves cpSecA ATPase (a dimer) and the membrane-bound cpSecE and cpSecY subunits. cpSecA ATPase activity provides the energy to drive the translocation of proteins through the SecE/Y pore. In *E. coli* (right panel) additional components include the chaperone SecB and the membrane proteins SecG (part of a SecYEG complex) and an associated SecDF complex. The substrate is targeted to the SecYEG complex through the interactions of SecB with the SecYEG associated SecA protein. The signal peptide of the substrate binds to SecA triggering the release of SecB. As in thylakoids, the substrate is then translocated through the SecYGE pore in a mechanism that is driven by ATP hydrolysis. After translocation, the signal peptides (represented as grey rectangles) of both thylakoid and *E. coli* Sec substrates are removed by processing peptidases (represented as scissors).

are present at steady-state: for example, the TatAdCd system involves a ~230 kDa TatAdCd complex together with a ~160 kDa homo-oligomeric TatAd complex (Barnett *et al.*, 2008) and the TatAyCy, is broadly similar (Barnett *et al.*, 2009). These complexes therefore seem to be different to their *E. coli* counterparts in terms of size and composition, with the TatAd complex also appearing to lack the heterogeneity observed with the *E. coli* TatA complex. This suggests a new model for Tat-dependent protein transport, involving a single defined translocon rather than a spectrum of size variants. Recently it has been demonstrated the presence of an N-terminal TatB-type domain within TatAd, together with a separate domain that appears to be universally conserved among TatA/TatB proteins (Barnett *et al.*, 2011).

The chloroplast Tat pathway and cpTat components

The chloroplast Tat translocase consists of three membrane proteins termed Tha4, Hcf106, and cpTatC, which are homologues of the bacterial TatA, TatB, and TatC proteins, respectively. The first cpTat component was identified after the isolation of a maize *hcf106* (high chlorophyll fluorescence 106) mutant, defective in a cpSec-independent protein transport pathway (Voelker and Barkan, 1995; Settles *et al.*, 1997). This was followed by the identification of *E. coli* Tat components (Bogsch *et al.*, 1998; Sargent *et al.*, 1998; Weiner *et al.*, 1998). Hcf106 and Tha4 are single-spanning membrane proteins containing an N-terminal transmembrane domain followed by a short amphipathic α-helix and an unstructured C-terminal domain. cpTatC is predicted to contain six transmembrane domains and both N- and C- termini are located in the stroma.

Substrate specificity of the chloroplast Tat pathway

Approximately 50% of thylakoid lumen proteins are translocated either by the cpSec or the cpTat pathway, and the characteristics of their signal peptides have been thoroughly studied in several reports (Peltier *et al.*, 2002; Schubert *et al.*, 2002; Robinson and Bolhuis, 2004). All thylakoid cpTat and cpSec targeting signals are similar in certain respects, resembling classical bacterial 'signal' peptides in overall structure (von Heijne *et al.*, 1989; Robinson *et al.*, 1998). They are characterized by an N-terminal basic region, a hydrophobic central core and a polar C-terminal region ending in an Ala-X-Ala terminal processing site (Aldridge *et al.*, 2009). A twin arginine (RR) motif located in the N-domain of signal peptides is a specific targeting signal for the Tat pathway (Chaddock *et al.*, 1995), and this explains the pathway's nomenclature (twin-arginine translocation). The twin-arginine motif is not the only feature distinguishing the two types of signal peptide, and it is located within a wider consensus motif. In *E. coli* other

determinants within the consensus motif have also been found to be important for translocation. One example is the hydrophilic-1 residue, relative to the twin-arginine motif (typically serine, threonine, aspartate or asparagine). When this serine is mutated to alanine in the signal peptides of *E. coli* TorA and DmsA, it causes a dramatic reduction in translocation activity. Other determinants have also been identified. The residue 2 places after the RR pair is usually either a phenylalanine or a leucine. In the signal peptide of TorA the substitution of this phenylalanine with either alanine or serine had no effect on translocation, whilst substitution by aspartic acid caused a complete block in transport. The signal peptide of DmsA contains leucine at this position, and substitution by either alanine or aspartic acid caused a complete block in transport. Thus it is evident the importance of the residue at this +2 position varies between substrates but an acidic residue at this position cannot be tolerated (Mendel *et al.*, 2008).

These results show that three distinct determinants have important roles in signal peptide recognition by the *B. subtilis* and *E. coli* Tat systems. Plant Tat signal peptides have a shorter consensus sequence (RRXXϕ) compared with the extended bacterial one ((S/T)RRXFLK); where ϕ is typically leucine, phenylalanine, valine or methionine, and X can be any amino acid (Stanley *et al.*, 2000). While the RR motif is essentially invariant there is no tendency for Phe to occur at the +2 position and the presence of a +4 Lys is very rare. Hence plant Tat signals are noticeably different.

Despite the differences between bacterial and cpTat signals, the key functional features of the Tat signal appear to be highly conserved. For example, several *E. coli* Tat signals support very efficient translocation into isolated pea thylakoids, whether or not the +4 Lys is present (Wexler *et al.*, 1998; Halbig *et al.*, 1999). Tat signals also differ from Sec signal peptides in other respects, including a tendency to contain basic residues in the Tat signal peptide C-domain (Bogsch *et al.*, 1997) and they contain a less hydrophobic H-domain when compared with Sec signals. Figure 3 illustrates a range of Sec and Tat signal peptides. As examples, the 23 kDa and 16 kDa proteins of the photosystem II oxygen-evolving complex (OEC) are well-known cpTat substrates, whereas the 33 kDa OEC protein and plastocyanin are cpSec substrates (Kirwin *et al.*, 1989; Bauerle and Keegstra, 1991; Cline *et al.*, 1992; Schubert *et al.*, 2002; Sun *et al.*, 2007).

Thylakoid Tat substrates range in size from around 4 kDa to over 60 kDa, and it is believed that these proteins are probably transported in a folded form, although the folding status of nearly all of these substrates remains unknown at present (Peltier *et al.*, 2002). Analysis of the substrate specificity does suggest interesting differences to the substrate specificity of bacterial systems. In *E. coli*, the majority of Tat substrates are redox proteins that bind cofactors such as FeS, NiFe or molybdopterin centres (among others). The apparent 'rationale' is that these cofactors are inserted only in the cytoplasm, which necessitates partial or full folding of the protein before transport. The Sec pathway could never export such proteins and this explains the presence of the Tat system. In chloroplasts, however, only a very few cpTat substrates contain redox factors (polyphenol oxidase, for example), and it has been suggested that the remaining substrates may simply fold too rapidly, or tightly, for the cpSec system to handle them effectively.

Interestingly, a versatile reporter system for Tat signal peptide identification has been developed for the first time by Widdick *et al.* (2008). The reporter system is based on the *Streptomyces coelicolor* agarase protein, which is secreted into the growth medium by the Tat pathway and whose extracellular activity can be assayed colorimetrically. By replacing the native agarase signal peptide with an uncharacterized one is possible to identify probable Tat substrates from all kingdoms of life.

Thylakoid Tat complexes: structure and mechanism

Chloroplast Tat components are organized into two distinct complexes in the membrane. The first, Hcf106-cpTatC, is a large ~700 kDa complex which has been characterized by BN-PAGE analysis and co-immunoprecipitation of digitonin-solubilized thylakoid membranes (Cline and Mori, 2001). Tha4, on the other hand, has not been detected in the Hcf106-cpTatC complex at resting state, but is present as a separate homo-oligomer (Dabney-Smith *et al.*, 2006). Martin *et al.* (2009) proposed that cpTatC might integrate through one of the unknown thylakoid translocation pathways. Import time-course and chase assays confirmed that cpTatC targets to thylakoids via a stromal intermediate. In addition, the analysis of membranes isolated from *Arabidopsis thaliana* mutants lacking cpSecY or Alb3 showed that neither is necessary for cpTatC membrane integration nor assembly into the cpTat receptor complex. These data suggest the existence of another translocase, possibly one dedicated to the integration of chloroplast translocases. Vladimirou *et al.* (2009) by photobleaching studies, showed that the Hcf106-GFP fusion protein is either immobile within the thylakoid membrane, or its diffusion is tightly restricted within distinct regions. This provides direct evidence for a strict compartmentation of membrane types within the continuous thylakoid membrane layer.

Mechanistic studies strongly suggest that substrates bind first to the Hcf106-cpTatC complex; substrates can be cross-linked to this complex under conditions that prevent full translocation (Ma and Cline, 2000; Cline and Mori, 2001; Mori and Cline, 2002; Gerard and Cline, 2006). According to site-directed cross-linking studies on the bacterial system (Alami *et al.*, 2003), the RR proximal region of the signal peptide is in close contact with TatC, whereas the hydrophobic domain and some parts of the adjacent mature domain are in close contact with TatB (Alami *et al.*, 2003; Gerard and Cline, 2006). It seems likely that thylakoid signal peptides interact with the Tat apparatus in a similar manner, although this has not yet been probed in any detail.

Fig. 3. Thylakoid-targeting signal peptides for imported lumenal proteins. The figure shows signals peptides for representative substrates of the Tat and Sec translocases; note that the first envelope transit peptide domain of the bipartite presequence has been omitted. Tat substrates: PPO, polyphenol oxidase; Hcf106, photosystem II stability/assembly factor; PSBT, photosystem II subunit T; At1g03610, thylakoid lumenal protein; PQL2, photosystem II oxygen-evolving enhancer protein; At1g20810, probable FKBP-type peptidyl-propyl *cis-trans* isomerase 1; PPD4, PsbP domain-containing protein 4; PPL2, PsbP-like protein 2; At2g43560, FKBP-type peptidyl-propyl *cis-trans* isomerase 2; 23K and 16K, oxygen evolving complex proteins; PSI-N, photosystem I subunit N. Important features of Tat substrates include a conserved twin-arginine motif (in bold) immediately upstream of the H-domain together with a highly hydrophobic amino acid two or three residues thereafter (underlined). Sec pathway substrates: 33K, oxygen evolving complex protein; PSI-F, photosystem I reaction centre subunit III; PC, plastocyanin, VDE1, violaxanthin de-epoxidase; PSBO1, oxygen-evolving enhancer protein 1-1; DRT112, plastocyanin major isoform; CYP37, peptidyl-prolyl *cis-trans* isomerase, DEGP1, protease Do-like 1. The alignment shows the hydrophobic core (underlined) and lysine residue preceding it in bold.

Tha4 does cross-link to the cpTatC-Hcf106 complex in the presence of a precursor protein and a thylakoid ΔpH (Mori and Cline, 2002), which suggests that the formation of the full translocon occurs under these conditions. Given the evidence that the Hcf106-cpTatC complex acts as the substrate-binding unit (with the analogous TatBC complex carrying out a similar role in bacteria) it seems likely that the separate Tha4 complex (TatA in bacteria) could form the translocation pore, or at least contribute to it. Analysis of *E. coli* TatA using single particle electron microscopy reveals that TatA forms ring-shaped structures of variable diameter (Gohlke *et al.*, 2005), supporting a model in which Tha4/TatA form a pore-like channel and, furthermore, raising the possibility that Tha4/TatA oligomerization and recruitment might be tailored to the size of the protein to be transported. Thus, one of the primary current models for the overall translocation process involves three main phases: (i) binding of precursor protein to the Hcf106-cpTatC complex (TatBC complex in bacteria), (ii) coalescence of this complex with the Tha4 complex (TatA complex in bacteria), and (iii) translocation of the folded substrate protein through the membrane. This process is depicted in Fig. 4. However, it should be noted that the late stages of translocation are not understood in any real detail, and there is very little information on the nature of the translocation pore.

Cross-linking studies have shown that Tha4 undergoes conformational rearrangements during active protein transport, with the amphipathic helix and C-terminal tail interacting only in response to conditions leading to protein transport (Dabney-Smith *et al.*, 2006). Binding of the precursor can occur in the absence of a ΔpH (Ma and Cline, 2000) but the thylakoid proton gradient induces a tighter interaction between the signal peptide and cpTatC and Hcf106 such that, during transport, the signal peptide is bound deep within the Tat receptor complex (Gerard and Cline, 2007). Recently, it has been reported that multiple precursor proteins can bind to sites in a single translocase, and can be transported across

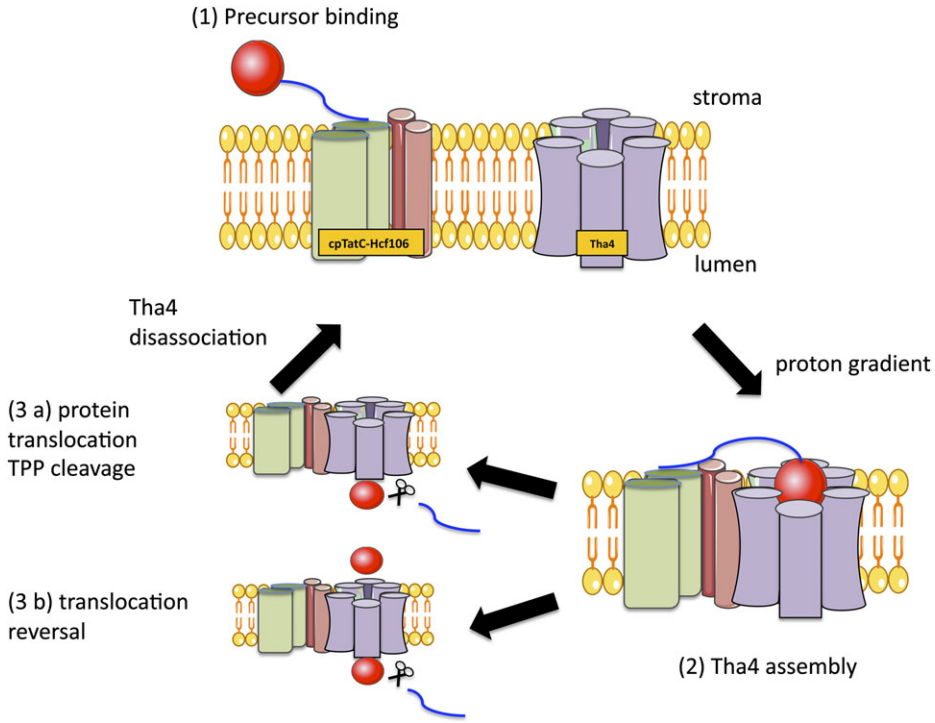

Fig. 4. Current model for the Tat translocation process. (1) The precursor protein binds through the signal peptide to a cpTatC-Hcf106 receptor complex in the thylakoid membrane. (2) Precursor binding in the presence of the proton gradient triggers assembly of Tha4 oligomers with the precursor–receptor complex and the putative translocase is formed. (3a) The precursor protein is then transported across the thylakoid membranes. The signal peptide is cleaved by the TPP and the mature protein is released into the lumen. After protein transport, Tha4 dissociates from the receptor complex and the system is reset. (3b) The 'translocation reversal' process, reported in Di Cola and Robinson (2005) is also represented here, see the text for details.

membrane together by Tat system in isolated pea chloroplasts. Moreover, oligomers as large as tetramers are collectively transported to the lumen with efficiency nearly as great as that of monomers (Ma and Cline, 2010).

Regulation of the chloroplast Tat system

The thylakoidal Tat translocation mechanism has been widely studied *in vitro* using well-established translocation assays. These assays have involved the incubation of intact chloroplasts or isolated thylakoids with *in vitro*-synthesized substrates, and the combined data have shown translocation by the thylakoid Tat system to be efficient, reliant on a ΔpH, and invariably unidirectional. However, a study performed on the green alga *Chlamydomonas reinhardtii* using *in vivo* pulse labelling and analysis of Tat substrates, showed that their maturation did not depend on the thylakoidal ΔpH. The involvement of additional and critical intracellular factors was suggested (Finazzi *et al.*, 2003).

Di Cola and Robinson (2005) investigated the targeting of an authentic Tat substrate (OE23) and several GFP constructs in transfected tobacco protoplasts. They showed that the constructs are targeted to the chloroplasts and processed to the mature size. However unlike the *in vitro* assays, where the cpTat substrates are exclusively found in the lumen, in this *in vivo* study the vast majority of mature GFP and much of the mature OE23 was found in the stroma. Moreover, it was shown that the maturation had been carried out by the thylakoidal processing peptidase (TPP), the active site of which is located on the lumenal face of the thylakoid membrane. Therefore the authors concluded that the translocation within this pathway is reversible to a significant extent, which means that a large proportion of a given substrate could be partially translocated across the thylakoid membrane, processed to the mature size, and returned to the stroma as part of a 'translocation reversal' process (see Fig. 4). Mutations that block cleavage by TPP cause the accumulation of intermediate-size protein that is tightly associated with the thylakoid membrane and largely resistant to proteolysis. It was suggested that these molecules may be delayed in the reverse translocation process and perhaps trapped within the translocation machinery.

Summarizing remarks

The targeting of lumenal proteins has now been studied in some detail and a great deal is known about the overall pathway steps and the components involved. In the case of the cpSec pathway, some elements have yet to be analysed in any detail; currently very little is known about the fates of cpSec substrates in the stroma, and especially whether they are prevented from folding by specific chaperone molecules. It remains possible that the cpSec translocon is able actively to unfold these proteins (at least to an extent)

but these questions remain to be properly addressed. In general, the cpSec system appears to resemble the well-characterized bacterial Sec systems, but it should be emphasized that this is only an impression based on a relatively limited number of studies.

The more recently-discovered cpTat system also appears to be similar in many respects to those operating in Gram-negative bacteria. In particular, the roles of the three core cpTat components appear to be similar, and these components form two distinct complexes of broadly similar characteristics. However, in neither case do we understand the translocation mechanism in genuine detail and this has to be the focus of future research. The available evidence suggests that two distinct complexes come together to form a 'supercomplex' after binding of substrate to one of them and there are tantalizing hints of substantial pores in EM images of bacterial TatA complexes. However, at the moment, we have no idea how these complexes form a relatively huge, transient pore that is capable of allowing passage of folded proteins. In fact, there is not even solid evidence for the existence of such a pore at the stage of translocation. Much needs to be done if this remarkable translocase is to be understood properly.

Acknowledgements

AMA and JB are funded by Transys ITN (Marie Curie Initial Training Network, project number: 215524).

References

Abdallah F, Salamini F, Leister D. 2000. A prediction of the size and evolutionary origin of the proteome of chloroplasts of *Arabidopsis*. *Trends in Plant Science* **5,** 141–142.

Akimaru J, Matsuyama S, Tokuda H, Mizushima S. 1991. Reconstitution of a protein translocation system containing purified SecY, SecE, and SecA from *Escherichia coli*. *Proceedings of the National Academy of Sciences, USA* **88,** 6545–6549.

Alami M, Lüke I, Deitermann S, Eisner G, Koch H-G, Brunner J, Müller M. 2003. Differential interactions between a twin-arginine signal peptide and its translocase in *Escherichia coli*. *Molecular Cell* **12,** 937–946.

Aldridge C, Cain P, Robinson C. 2009. Protein transport in organelles: protein transport into and across the thylakoid membrane. *FEBS Journal* **276,** 1177–1186.

Aronsson H, Jarvis P. 2009. The chloroplast protein import apparatus, its components, and their roles. In: Sandelius AS, Aronsson H, eds. *The chloroplast: interactions with the environment*. Plant Cell Monographs, Vol. 13. Heidelberg, Germany: Springer-Verlag, 89–123.

Bals T, Dünschede B, Funke S, Schünemann D. 2010. Interplay between the cpSRP pathway components, the substrate LHCP and the translocase Alb3: an *in vivo* and *in vitro* study. *FEBS Letters* **584,** 4138–4144.

Barnett JP, Eijlander RT, Kuipers OP, Robinson C. 2008. A minimal Tat system from a Gram-positive organism: a bifunctional TatA subunit participates in discrete TatAC and TatA complexes. *Journal of Biological Chemistry* **283,** 2534–2542.

Barnett JP, Lawrence J, Mendel S, Robinson C. 2011. Expression of the bifunctional *Bacillus subtilis* TatAd protein in *Escherichia coli* reveals distinct TatA/B-family and TatB-specific domains. *Archives of Microbiology* **193,** 583–594.

Barnett JP, van der Ploeg R, Eijlander RT, Nenninger A, Mendel S, Rozeboom R, Kuipers OP, van Dijl JM, Robinson C. 2009. The twin-arginine translocation (Tat) systems from *Bacillus subtilis* display a conserved mode of complex organization and similar substrate recognition requirements. *FEBS Journal* **276,** 232–243.

Bauerle C, Keegstra K. 1991. Full-length plastocyanin precursor is translocated across isolated thylakoid membranes. *Journal of Biological Chemistry* **266,** 5876–5883.

Bogsch E, Brink S, Robinson C. 1997. Pathway specificity for a delta pH-dependent precursor thylakoid lumen protein is governed by a 'Sec-avoidance' motif in the transfer peptide and a 'Sec-incompatible' mature protein. *EMBO Journal* **16,** 3851–3859.

Bogsch EG, Sargent F, Stanley NR, Berks BC, Robinson C, Palmer T. 1998. An essential component of a novel bacterial protein export system with homologues in plastids and mitochondria. *Journal of Biological Chemistry* **273,** 18003–18006.

Bolhuis A. 2004. The archaeal Sec-dependent protein translocation pathway. *Philosophical Transactions of the Royal Society, London B Biological Sciences* **359,** 919–927.

Bolhuis A, Mathers JE, Thomas JD, Barrett CML, Robinson C. 2001. TatB and TatC form a functional and structural unit of the twin-arginine translocase from *Escherichia coli*. *Journal of Biological Chemistry* **276,** 20213–20219.

Chaddock AM, Mant A, Karnauchov I, Brink S, Herrmann RG, Klösgen RB, Robinson C. 1995. A new type of signal peptide: central role of a twin-arginine motif in transfer signals for the delta pH-dependent thylakoidal protein translocase. *EMBO Journal* **14,** 2715–2722.

Cline K, Ettinger WF, Theg SM. 1992. Protein-specific energy requirements for protein transport across or into thylakoid membranes. Two lumenal proteins are transported in the absence of ATP. *Journal of Biological Chemistry* **267,** 2688–2696.

Cline K, Mori H. 2001. Thylakoid {Delta}pH-dependent precursor proteins bind to a cpTatC-Hcf106 complex before Tha4-dependent transport. *Journal of Cell Biology* **154,** 719–730.

Dabney-Smith C, Mori H, Cline K. 2006. Oligomers of Tha4 organize at the thylakoid Tat translocase during protein transport. *Journal of Biological Chemistry* **281,** 5476–5483.

Dalbey RE, Chen M. 2004. Sec-translocase mediated membrane protein biogenesis. *Biochimica et Biophysica Acta* **1694,** 37–53.

Di Cola A, Robinson C. 2005. Large-scale translocation reversal within the thylakoid Tat system *in vivo*. *Journal of Cell Biology* **171,** 281–289.

Finazzi G, Chasen C, Wollman F-A, de Vitry C. 2003. Thylakoid targeting of Tat passenger proteins shows no Delta pH dependence *in vivo*. *EMBO Journal* **22,** 807–815.

Gerard F, Cline K. 2006. Efficient twin arginine translocation (Tat) pathway transport of a precursor protein covalently anchored to its

initial cpTatC binding site. *Journal of Biological Chemistry* **281,** 6130–6135.

Gerard F, Cline K. 2007. The thylakoid proton gradient promotes an advanced stage of signal peptide binding deep within the Tat pathway receptor complex. *Journal of Biological Chemistry* **282,** 5263–5272.

Gohlke U, Pullan L, McDevitt CA, Porcelli I, de Leeuw E, Palmer T, Saibil HR, Berks BC. 2005. The TatA component of the twin-arginine protein transport system forms channel complexes of variable diameter. *Proceedings of the National Academy of Sciences, USA* **102,** 10482–10486.

Halbig D, Hou B, Freudl R, Sprenger GA, Klösgen RB. 1999. Bacterial proteins carrying twin-R signal peptides are specifically targeted by the [Delta]pH-dependent transport machinery of the thylakoid membrane system. *FEBS Letters* **447,** 95–98.

Haward SR, Napier JA, Gray JC. 1997. Chloroplast SecA functions as a membrane-associated component of the Sec-like protein translocase of pea chloroplasts. *European Journal of Biochemistry* **248,** 724–730.

Hulford A, Hazell L, Mould RM, Robinson C. 1994. Two distinct mechanisms for the translocation of proteins across the thylakoid membrane, one requiring the presence of a stromal protein factor and nucleotide triphosphates. *Journal of Biological Chemistry* **269,** 3251–3256.

Hynds PJ, Robinson D, Robinson C. 1998. The sec-independent twin-arginine translocation system can transport both tightly folded and malfolded proteins across the thylakoid membrane. *Journal of Biological Chemistry* **273,** 34868–34874.

Jarvis P, Soll J. 2001. Toc, Tic, and chloroplast protein import. *Biochimica et Biophysica Acta* **1541,** 64–79.

Jongbloed JD, Grieger U, Antelman H, Hecker M, Najland R, Bron S, van Dijl JM. 2004. Two minimal Tat translocases in *Bacillus*. *Molecular Microbiology* **54,** 1319–1325.

Jongbloed JDH, van der Ploeg R, van Dijl JM. 2006. Bifunctional TatA subunits in minimal Tat protein translocases. *Trends in Microbiology* **14,** 2–4.

Kirwin PM, Meadows JW, Shackleton JB, Musgrove JE, Elderfield PD, Mould R, Hay NA, Robinson C. 1989. ATP-dependent import of a lumenal protein by isolated thylakoid vesicles. *EMBO Journal* **8,** 2251–2255.

Laidler V, Chaddock AM, Knott TG, Walker D, Robinson C. 1995. A SecY homolog in *Arabidopsis thaliana*. Sequence of a full-length cDNA clone and import of the precursor protein into chloroplasts. *Journal of Biological Chemistry* **270,** 17664–17667.

Liu D, Gong Q, Ma Y, *et al*. 2010. cpSecA, a thylakoid protein translocase subunit, is essential for photosynthetic development in *Arabidopsis*. *Journal of Experimental Botany* **61,** 1655–1669.

Ma X, Cline K. 2000. Precursors bind to specific sites on thylakoid membranes prior to transport on the delta pH protein translocation system. *Journal of Biological Chemistry* **275,** 10016–10022.

Ma X, Cline K. 2010. Multiple precursor proteins bind individual Tat receptor complexes and are collectively transported. *EMBO Journal* **29,** 1477–1488.

Maldonado B, Buchanan G, Müller M, Berks BC, Palmer T. 2011. Genetic evidence for a TatC dimer at the core of the *Escherichia coli* twin arginine (Tat) protein translocase. *Journal of Molecular Microbiology and Biotechnology* **20,** 168–175.

Martin JR, Harwood JH, McCaffery M, Fernandez DE, Cline K. 2009. Localization and integration of thylakoid protein translocase subunit cpTatC. *The Plant Journal* **58,** 831–842.

Marques JP, Schattat MH, Hause G, Dudeck I, Klösgen RB. 2004. *In vivo* transport of folded EGFP by the DeltapH/TAT-dependent pathway in chloroplasts of *Arabidopsis thaliana*. *Journal of Experimental Botany* **55,** 1697–1706.

Mendel S, McCarthy A, Barnett JP, Eijlander RT, Nenninger A, Kuipers OP, Robinson C. 2008. The *Escherichia coli* TatABC system and a *Bacillus subtilis* TatAC- type system recognize three distinct targeting determinants in twin-arginine signal peptides. *Journal of Molecular Biology* **375,** 661–672.

Mori H, Cline K. 2002. A twin arginine signal peptide and the pH gradient trigger reversible assembly of the thylakoid {Delta}pH/Tat translocase. *Journal of Cell Biology* **157,** 205–210.

Mori H, Summer EJ, Ma X, Cline K. 1999. Component specificity for the thylakoidal Sec and Delta pH-dependent protein transport pathways. *Journal of Cell Biology* **146,** 45–56.

Mould RM, Robinson C. 1991. A proton gradient is required for the transport of two lumenal oxygen-evolving proteins across the thylakoid membrane. *Journal of Biological Chemistry* **266,** 12189–12193.

Müller M, Klösgen RB. 2005. The Tat pathway in bacteria and chloroplasts (review). *Molecular Membrane Biology* **22,** 113–121.

Nakai M, Goto A, Nohara T, Sugita D, Endo T. 1994. Identification of the SecA protein homolog in pea chloroplasts and its possible involvement in thylakoidal protein transport. *Journal of Biological Chemistry* **269,** 31338–31341.

Nouwen N, Piwowarek M, Berrelkamp G, Driessen AJ. 2005. The large first periplasmic loop of SecD and SecF plays an important role in SecDF functioning. *Journal of Bacteriology* **187,** 5857–5860.

Oates J, Barrett CML, Barnett JP, Byrne KG, Bolhuis A, Robinson C. 2005. The *Escherichia coli* twin-arginine translocation apparatus incorporates a distinct form of TatABC complex, spectrum of modular TatA complexes and minor TatAB complex. *Journal of Molecular Biology* **346,** 295–305.

Osborne AR, Rapoport TA, van den Berg B. 2005. Protein translocation by the Sec61/SecY channel. *Annual Review of Cell and Development Biology* **21,** 529–550.

Peltier J-B, Emanuelsson O, Kalume DE, *et al*. 2002. Central functions of the lumenal and peripheral thylakoid proteome of *Arabidopsis* determined by experimentation and genome-wide prediction. *The Plant Cell* **14,** 211–236.

Robinson C, Bolhuis A. 2004. Tat-dependent protein targeting in prokaryotes and chloroplasts. *Biochimica et Biophysica Acta* **1694,** 135–147.

Robinson C, Hynds PJ, Robinson D, Mant A. 1998. Multiple pathways for the targeting of thylakoid proteins in chloroplasts. *Plant Molecular Biology* **38,** 209–221.

Robinson C, Matos CF, Beck D, Ren C, Lawrence J, Vasisht N, Mendel S. 2011. Transport and proofreading of proteins by the twin-arginine translocation (Tat) system in bacteria. *Biochimica et Biophysica Acta* **1808,** 876–884.

Roy LM, Barkan A. 1998. A SecY homologue is required for the elaboration of the chloroplast thylakoid membrane and for normal chloroplast gene expression. *Journal of Cell Biology* **141,** 385–395.

Sargent F, Bogsch EG, Stanley NR, Wexler M, Robinson C, Berks BC, Palmer T. 1998. Overlapping functions of components of a bacterial Sec-independent protein export pathway. *EMBO Journal* **17,** 3640–3650.

Schnell DJ, Blobel G, Keegstra K, Kessler F, Ko K, Soll J. 1997. A consensus nomenclature for the protein-import components of the chloroplast envelope. *Trends in Cell Biology* **7,** 303–304.

Schubert M, Petersson UA, Haas BJ, Funk C, Schroder WP, Kieselbach T. 2002. Proteome map of the chloroplast lumen of *Arabidopsis thaliana*. *Journal of Biological Chemistry* **277,** 8354–8365.

Schuenemann D, Amin P, Hartmann E, Hoffman NE. 1999. Chloroplast SecY is complexed to SecE and involved in the translocation of the 33-kDa but not the 23-kDa subunit of the oxygen-evolving complex. *Journal of Biological Chemistry* **274,** 12177–12182.

Settles AM, Yonetani A, Baron A, Bush DR, Cline K, Martienssen R. 1997. Sec-independent protein translocation by the maize Hcf106 protein. *Science* **278,** 1467–1470.

Soll J, Schleiff E. 2004. Protein import into chloroplasts. *Nature Reviews Molecular Cell Biology* **5,** 198–208.

Stanley NR, Palmer T, Berks BC. 2000. The twin arginine consensus motif of Tat signal peptides is involved in Sec-independent protein targeting in *Escherichia coli*. *Journal of Biological Chemistry* **275,** 11591–11596.

Sun C, Rusch SL, Kim J, Kendall DA. 2007. Chloroplast SecA and *Escherichia coli* SecA have distinct lipid and signal peptide preferences. *Journal of Bacteriology* **189,** 1171–1175.

Veenendaal AK, van der Does C, Driessen AJ. 2004. The protein-conducting channel SecYEG. *Biochimica et Biophysica Acta* **1694,** 81–95.

Vladimirou E, Li M, Aldridge CP, Frigerio L, Kirkilionis M, Robinson C. 2009. Diffusion of a membrane protein, Tat subunit Hcf106, is highly restricted within the chloroplast thylakoid network. *FEBS Letters* **583,** 3690–3696.

von Heijne G, Steppuhn J, Herrmann RG. 1989. Domain structure of mitochondrial and chloroplast targeting peptides. *European Journal of Biochemistry* **180,** 535–545.

Voelker R, Barkan A. 1995. Two nuclear mutations disrupt distinct pathways for targeting proteins to the chloroplast thylakoid. *EMBO Journal* **14,** 3905–3914.

Vrontou E, Economou A. 2004. Structure and function of SecA, the preprotein translocase nanomotor. *Biochimica et Biophysica Acta* **1694,** 67–80.

Weiner JH, Bilous PT, Shaw GM, Lubitz SP, Frost L, Thomas GH, Cole JA, Turner RJ. 1998. A novel and ubiquitous system for membrane targeting and secretion of cofactor-containing proteins. *Cell* **93,** 93–101.

Wexler M, Bogsch EG, Klösgen RB, Palmer T, Robinson C, Berks BC. 1998. Targeting signals for a bacterial Sec-independent export system direct plant thylakoid import by the [Delta]pH pathway. *FEBS Letters* **431,** 339–342.

Widdick DA, Eijlander RT, van Dijl JM, Kupers OP, Palmer T. 2008. A facile reporter system for the experimental identification of twin- arginine translocation (Tat) signal peptides from all kingdoms of life. *Journal of Molecular Biology* **375,** 595–603.

Woolhead CA, Thompson SJ, Moore M, Tissier C, Mant A, Rodger A, Henry R, Robinson C. 2001. Distinct Albino3-dependent and -independent pathways for thylakoid membrane protein insertion. *Journal of Biological Chemistry* **276,** 40841–40846.

Yuan J, Henry R, McCaffery M, Cline K. 1994. SecA homolog in protein transport within chloroplasts: evidence for endosymbiont-derived sorting. *Science* **266,** 796–798.